# GEOCHEMICAL EVALUATION OF SOURCE ROCK POTENTIAL AND CHARACTERIZATION OF HYDROCARBON OCCURRENCES IN THE EASTERN DAHOMEY BASIN, NIGERIA

## BY

### SAEED MOHAMMED
**B. Tech (Hons); M.Sc.**

**Student number: 3776487**

**A thesis submitted in fulfillment of the requirements for the**

**Degree of Doctor of Philosophy in Applied Geology
(Petroleum Option)**

**DEPARTMENT OF EARTH SCIENCES, UNIVERSITY OF THE WESTERN CAPE, BELLVILLE, SOUTH AFRICA**

**Supervisor: Dr. Mimonitu Opuwari**

**Co-Supervisor: Prof. Salam Titinchi**

**August 2020**

## DECLARATION

I make the declaration that the research titled "**Geochemical Evaluation of Source Rock Potential and Characterization of Hydrocarbon Occurrences in the Eastern Dahomey Basin, Nigeria.**" is my work. The work was never used for the award of any degree in any other university. All the sources that I quoted have been indicated and duly acknowledged utilizing complete references.

**Saeed Mohammed**                                                    August, 2020

S.Moh'd

Signature

# ACKNOWLEDGMENTS

When I set out to write the acknowledgments for this thesis, it started me thinking of my late parents, Alhaji Mohammed Odawn and Hajia Habiba Mohammed, who instilled in me the moral code that defines my life. They taught me forbearance, gratitude, and goal setting. To their credit, I embarked on this journey after a hiatus of more than 25 years from academics. I am eternally grateful to God for having good parents. I thank Him for my late grandparents, Aguiye Oma Ejibo (Aguiye, the daughter of Ejibo), and Mallam Mohammed Umodu, from whom I learned virtue, character, ordinariness, and simplicity. I am thankful to my uncle, Alhaji Halilu Mohammed.

I am immensely grateful to my dear wife, Dr. Ramatu, and our children, Saeeda, Salma, Habiba, and Sakeena. I thank them for their sacrifice, patience, encouragement, and support. They endured and prevailed even though we had to use our savings to fund over 95 % of this project. I thank Ramatu for her love and dedication to the family.

From my supervisors, Dr. Mimonitu Opuwari and Prof. Salam Titinchi, I learned many lessons on collaboration, resourcefulness, and principles necessary for research. They encouraged and worked with me to establish partnerships with research agencies, publish papers, and attend conferences. From a grateful heart, I want to thank you for all the help and interests you have shown. The entire journey would not have been possible without the assistance of good-natured and highly dedicated people like you.

I am indebted to the Departments of Earth Sciences and Chemistry, University of the Western Cape, and I am grateful to my Head of Department, Prof. Dirk Frei. I am thankful for the assistance that I received from Mr. Lilburne Cyster, Mr. Andrea Williams, Mr. Evan Swartbooi, Dr. Abdi Siad, Mrs. Wasielah Davids, Mr. Shamiel Davids, and Ms. Janine Beconey. I am grateful to Mr. Earl Mc Donald, Christiana Bamigboye, and Moses Ubong.

To my colleagues at the Theology Guest House, where I spent the more significant part of the time working on the thesis, may I say thank you. I am grateful to Kelfiwe Rasedie, Luis Manuel Joao, Ivete Tembe, Ellen E. Klutsy, Beatrice Bella Johnson (BBJ), Abosede Ajibare for their supports, encouragement, and convivial conversations, which lightened the moods during the coronavirus pandemic lockdown. I am also thankful for the heritage of learning of those that preceded me and of my contemporaries.

To Prof. Henry Amosi, Prof. Timothy Bata, Prof. Taofik Adedosu, Prof. Mohammed B. Abubakar, Prof. Aliyu Jauro, Dr. Abu Momoh, Prof. Aminu Bello, Dr. Sadiya Bello, Mall. Issa Bala, Dr. Adam, Dr. Umar Ahmadu Ali, Dr. Comfort Agada, Dr. Marcus Edino, Hajia Hafsat Onatade, Mr. Raimi Salhu, Mr. and Mrs. Flomo, Mr. Solomon Eromosele, Ms. Isabele Cunha, Mrs. Saadetu Ataojoko, Alh. Idris Yamusa, Mrs. Chide Ogenyi Robert, Mallam Lawal Namanu, Ms. Atule Lentina, Raimi Salhu, John Onwuegbuzie, and Francis Yappis, I give you kudos for your encouragement. I am grateful to Ms. Christelle Onana for her assistance in proofreading my manuscripts.

I am indebted to my late mentors, Prof. Maduka Orazulike and Mallam Zakariyau Allarama, for a lifetime of study and scholarship. I am also thankful to Prof. E.F.C. Dike for his training and mentorship throughout my time as an undergraduate. Prof. Dike stimulated my interest in Geology, and it is to his credit that I went into Petroleum Geology, a career that showered me with many blessings.

I am grateful to my family for a lifetime of love and understanding. I am thankful to my late brothers, Alhaji Ibrahim Mohammed, Yahaya Mohammed, Tijani (World Man) Mohammed, Yakubu Mohammed, Muktar Yahaya, Alhaji Dogwo Yahaya, and my beloved nephew, Lawal Dodo Abubakar.

I am thankful to Ramatu Ojoagefu, Ummy, Mero, Rekiya, Safiya, and Bilkis for their prayers. I am indebted to Hajia Fatima Jibrin and Late Alhaji Jibrin Yunusa for their supports.

Finally, to all those mentioned and those not mentioned because they are numerous, I cannot thank you well enough, but God will.
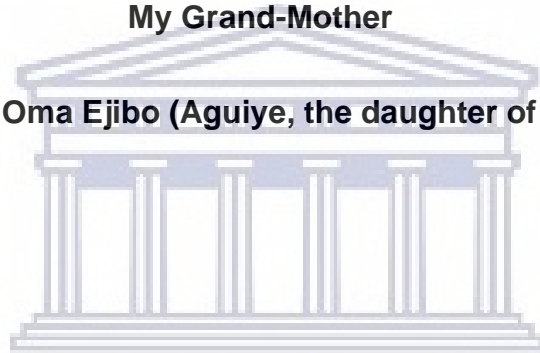
# DEDICATION

**In Memory of my Dearly Beloved Parents**

**Alhaji Mohammed Odawn and Hajia Habiba Mohammed (MY HEROES, MY FRIENDS)**

**And**

**My Grand-Mother**

**Aguiye Oma Ejibo (Aguiye, the daughter of Ejibo)**

# OUTCOME OF RESEARCH

**Mohammed, S., Opuwari, M., and Titinchi, S. (2020)**. Source rock evaluation of Afowo clay type from the Eastern Dahomey Basin, Nigeria: Insights from different measurements. Sci. Rep. 1–13 (2020). https://www.nature.com/articles/s41598-020-68918-y

**Mohammed, S., Opuwari, M., Titinchi, S., Bata, T., and Mohammed, B.A. (2019)**. Evaluation of source rock potential and hydrocarbon composition of oil sand and associated clay deposits from the Eastern Dahomey Basin, Nigeria. J. African Earth, Sci. 160, 1 – 8.

https://www.sciencedirect.com/science/article/pii/S1464343X19302584

**Mohammed, S., Opuwari, M., and Titinchi, S. (Undergoing Review by Scientific Reports).** Petroleum Biodegradation and Enrichment of Heavy Metals in Associated Economic Crops: A Case Study from the Eastern Dahomey Basin, Nigeria.

**Mohammed, S., Opuwari, M., Titinchi, S., Bata, T., and Mohammed, B.A., (2018).** Source to Reservoir Correlation and Hydrocarbon Compositions of Oil Sand Deposits in Dahomey Basin, Nigeria. AAPG International Conference and Exhibition, Cape Town, South Africa.

**Mohammed, S., Opuwari, M., Titinchi, S., Bata, T., and Mohammed, B.A., (2018).** Source Rock Thermal Maturity Evaluation: Insight from Different Measurements. Nigerian Association of Petroleum Explorationists Conference, Lagos, Nigeria**.**

**Geochemical Evaluation of Source Rock Potential and Characterization of Hydrocarbon Occurrences in the Eastern Dahomey Basin, Southwestern, Nigeria**

**Saeed Mohammed**

**Key Words:**

Eastern Dahomey Basin

Afowo Formation

Oil Sands

Source Rocks

Rock Evaluation Pyrolysis

Total Organic Carbon

Thermal Maturity

Carbon Isotopes

Metal Distribution

Biomarkers

Kerogen

Organic Petrography

## ABBREVIATIONS

HAWK*       = Hydrocarbon Analyzer with Kinetic

ICP-MS      = Inductively Coupled Plasma- Mass Spectrometry

TGA         = Thermogravimetric Analysis

CHNS        = Carbon, Hydrogen, Nitrogen, and Sulfur Analyzer

TD-GC       = Thermal Desorption-Gas Chromatography

TD-GC       = Thermal Desorption–Gas Chromatography

GC-MS       = Gas Chromatography-Mass Spectrometry

LOI         = Loss on Ignition

TOC         = Total Organic Carbon

TOM         = Total Organic Matter

PI          = Production Index

S1          = Thermally Free Hydrocarbon

S2          = Volume of hydrocarbon that was generated during the thermal breakdown of kerogen

Tmax        = Temperature at which maximum generation of hydrocarbon occurred during the pyrolysis of kerogen

# ABSTRACT

Nigeria is endowed with significant oil sand and heavy oil reserves. These reserves are found within the Cretaceous Afowo Formation in the Eastern Dahomey Basin. The petroleum systems and quality of these reserves are poorly understood. Harnessing these resources necessitate comprehensive deposit evaluation and characterization.

This research focuses on the geochemical evaluation of source rock potential and characterization of oil sands and heavy oil from the Eastern Dahomey Basin. Surface and subsurface samples of potential source rocks underlying the oil sands, oil sands, and heavy oils from different parts of the basin were collected and analyzed to evaluate hydrocarbon generating potential, composition, and quality. Potential source rock samples were analyzed with a multi-parameter approach using Rock-Eval Pyrolysis, Organic Petrography, Gas Chromatography, Thermogravimetric Analysis, and Loss on Ignition. The oil sands and heavy oils samples were analyzed using gas chromatography (GC), Gas Chromatography-Mass Spectrometry (GC-MS), Hydrocarbon Analyzer with Kinetic – Petroleum Assessment Method (HAWK-PAM), Inductively Coupled Plasma-Mass Spectrometry (ICP-MS), Carbon Isotopes, CHNS, and ASTM. Rock-Eval results showed that total organic carbon (TOC, wt. %) ranged from 0.51 weight % to 21.36 weight %, while total organic matter contents from loss on ignition varied from 9.41 wt.% to 38.75 wt. %, indicating rich source rocks. Kerogen typing ranged between Types II and III, indicating oil to gas generating potentials. In the analysis of thermal maturation, organic maturation temperature (Tmax) was found to be below 435 °C from rock-eval and thermogravimetric analysis. Maceral analysis indicated the abundance of liptinites with reflectance measurements ranging from 0.34 %$R_o$ and 0.56 %$R_o$, while Gas chromatography

indicated a bimodal distribution of n-alkanes of an odd carbon number predominance in the C25 to C33 range. The various complementary maturation analysis all showed the source rocks to be thermally immature.

In the analysis of the oil sand and heavy oil samples, GC and GC-MS showed the absence of lightweight molecular components and complete absence of pristane and phytane; it was not possible to identify and quantify the biomarkers. This is interpreted to suggest the predominance of heavy oil and severe widespread biodegradation. The Vanadium/Nickel ratio (V/Ni) from ICP-MS ranged from 0.44 to 2.36, indicating that the petroleum was generated by source rocks deposited in suboxic to anoxic conditions. Carbon Isotopes measurements on the whole oil ranged from -27.7 ‰ to -25.4 ‰, suggesting that source rocks of terrigenous and marine organic matter inputs generated the petroleum. The sulfur contents ranged from 0.18 wt. % to 1.83 wt. %, with a total acid number (TAN) of 5.5 mg KOH/g, indicating sour crude oil. The oils' API gravities ranged from 5.12 °API to 14.31 °API with a viscosity of 73560 cPs at 50 °C, and boiling point distribution of middle and heavy distillates suggesting heavy oil.

This study added to the body of knowledge and included approaches that characterized the source rock and oil sands/heavy oil of the Eastern Dahomey Basin.
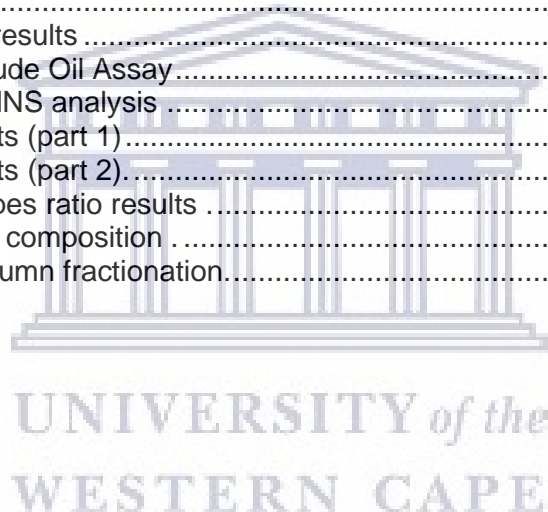
# TABLE OF CONTENTS

# LIST OF TABLES

# LIST OF FIGURES

## LIST OF APPENDICES

Appendix 1:Source rock evaluation of Afowo clay type from the Eastern Dahomey Basin, Nigeria: Insights from different measurements.

Appendix 2: Evaluation of source rock potential and hydrocarbon composition of oil sand and associated clay deposits from the Eastern Dahomey Basin, Nigeria.

UNIVERSITY *of the*
WESTERN CAPE
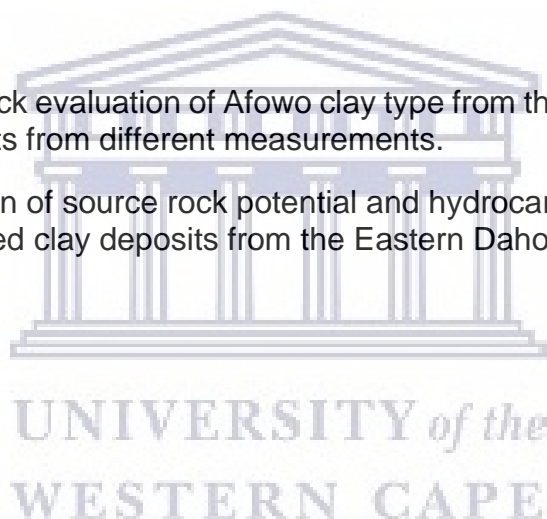
# CHAPTER ONE

# INTRODUCTION

## 1.0:   BACKGROUND INFORMATION

Oil sands are sands rich in heavy oil that are bereft of lightweight molecular components due to biodegradation and water washing. The crude bitumen contained in the unconsolidated sands is a viscous mixture of hydrocarbons. In its natural state, the crude bitumen will not flow unless heated or diluted with lighter hydrocarbons. When natural bitumen is mobile in the reservoir, it is generally referred to as extra-heavy oil (Meyer et al.,2007).

World resources of bitumen and heavy oil are estimated to amount to 5.6 trillion barrels, compared to the remaining conventional crude oil reserves of 1.02 trillion barrels (Hein, 2006). Over 80% of the bitumen and heavy oil resources of the world are found in Venezuela, Canada, and the United States of America; the Orinoco Oil Belt of Venezuela is the single most massive heavy oil field in the world (Santos, 1991).  Substantial oil sands and heavy oil reserves are also found in Angola, the Democratic Republic of Congo, Madagascar, and Nigeria. The amalgam of vast oil sand and heavy oil reserves, global energy needs, high oil price, and technological innovations have resulted in their profitable extraction and processing.

Nigeria has a well-developed conventional oil industry and is also endowed with significant oil sand and heavy oil deposits. These deposits are found in the eastern segment of the Dahomey Basin (Fig.1).
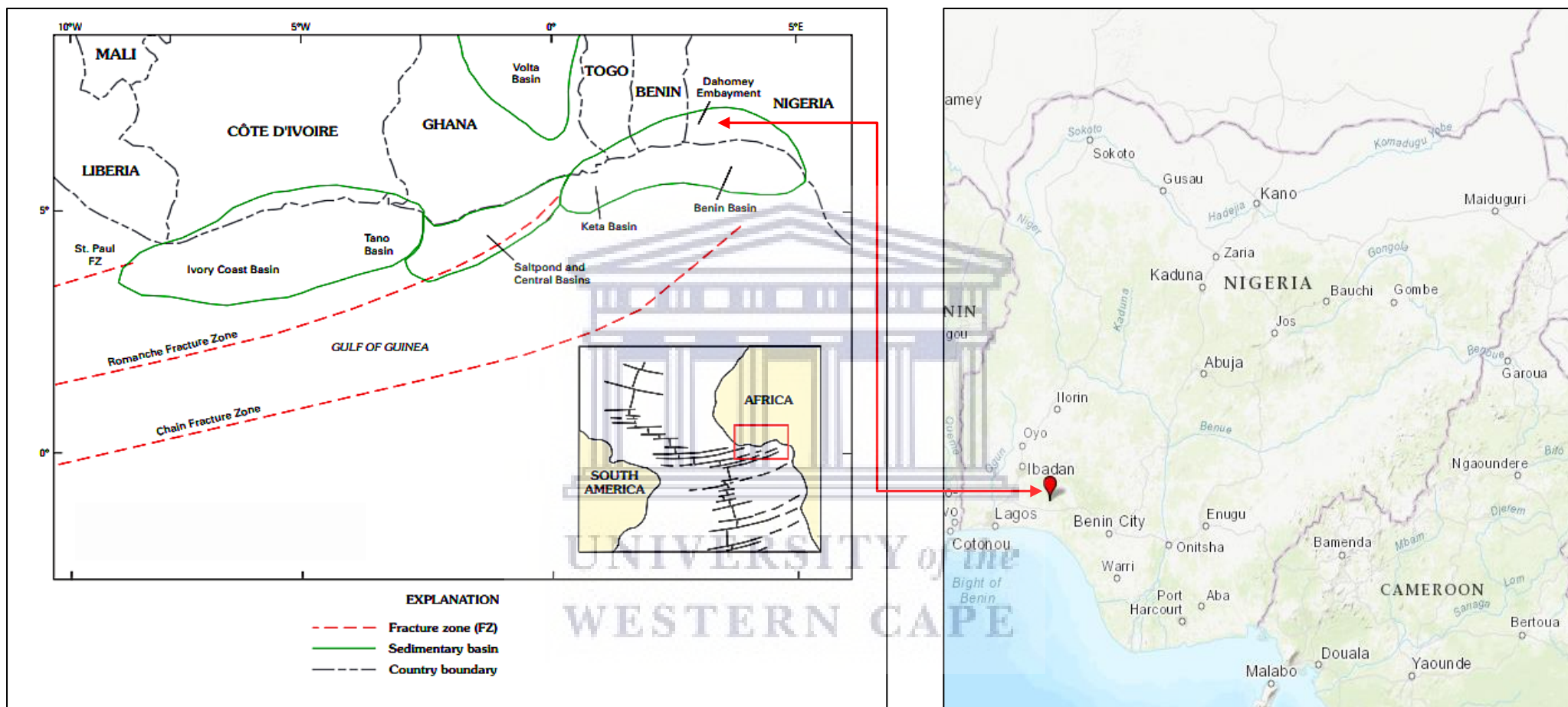
*Figure 1: Map of a part of West Africa, showing the sedimentary basins and main fracture zones within the Gulf of Guinea's Province. The Mid-Atlantic Ridge and fracture zones are shown in the inset map (Modified from Brownfield and Charpentier, 2006). The Red arrows indicate the Eastern Dahomey Basin's location (Dahomey Embayment) in the regional map and a part of the basin in southwestern Nigeria where the study was carried out.*

3

The Dahomey Basin, also known as the Benin Basin, is situated in the Gulf of Guinea province. The Gulf of Guinea comprises wrench-modified (Clifford, 1986) coastal and offshore basins consisting of the Ivory Coast, Tano, Saltpond, Central, Keta, and Benin Basins (Brownfield and Charpentier, 2006). These basins evolved in the Mesozoic era by tectonism that was characterized by block and transform faulting during the breakup of the African and South American paleocontinents.

The Dahomey Basin extends from southeastern Ghana through Togo and the Republic of Benin to southwestern Nigeria. The western limit of the basin is bounded by the Ghana Ridge, an offset extension of the Romanche Fracture Zone. It is separated from the Niger Delta Basin in the east by a subsurface basement high referred to as the Okitipupa Ridge (Obaje,2009; Oli et al., 2019). The basin hosts a large wedge of Cretaceous to Recent sediments of up to 3,000 m (Nton et al., 2009; Ogala et al., 2019; Whiteman, 1982), which thicken toward the offshore. The stratigraphy of the eastern sector of the basin (Eastern Dahomey Basin) in southwestern Nigeria consists of the Cretaceous sediments of the Abeokuta Group (Ise, Afowo, and Araromi Formations) and the Tertiary sediments of Ewekoro, Akinbo, Oshosun, Ilaro, and Benin Formations (Omatsola and Adegoke,1981). The Afowo Formation of the Abeokuta Group, comprising of sandstones, shales, claystones, and siltstones, has been of great interest due to reported occurrences of oil sands (Enu, 1990; Ndukwe et al., 2015; Nton et al., 2009; Omatsola and Adegoke, 1981).

Extensive deposits of oil sands and bituminous seepages abound in the Cretaceous sediments of the Afowo Formation across a belt of about 120 km long and 4 – 6 km wide in southwestern Nigeria (Enu, 1985).

Outcrops of the oil sands and associated source rocks (claystones and shales) are commonly found along road cuts and river banks, while seepages of highly viscous oil are seen in outcrops and farmlands on sunny days. In addition to the outcrop of oil sands and oil seepages, oil sands and heavy oils have been encountered in wells at relatively shallow depths; most of these wells have been abandoned. The oil sands, shales, claystones, and oil seepages suggest direct indicators of a petroleum system in the Eastern Dahomey Basin.

Nigeria's estimate of oil sand and heavy oil reserves is more than 58 billion oil-equivalent (Ministry of Mines and Steel Development, 2009). In the past decades, the Nigerian government and oil companies have focused on exploiting conventional hydrocarbon resources with minimal attention paid to the vast oil sand deposits. The current push and paradigm shift to diversify the economy, increase petroleum production, and create jobs for the teeming population make the exploitation of oil sands and heavy oil an ideal target of high national interest. However, harnessing the vast oil sand and heavy crude necessitates a comprehensive deposit evaluation and characterization.

This study used primary data obtained from outcrop and borehole samples to evaluate the hydrocarbon generating potential of the source rock and characterize the hydrocarbons of the petroliferous Afowo Formation. The samples consisted of claystones, shales, oil sands, cores, and heavy oil.

The research incorporates a multi-parameter method to evaluate the source rock potential and characterize the oil sands and heavy oils of the petroliferous Afowo Formation of the Eastern Dahomey Basin. An integrated approach such as this is necessary to assess the hydrocarbon generating potential of the source rock, identify if the hydrocarbons migrated from a source area that was not covered by

the samples, and evaluate the reservoired hydrocarbons for their composition, quality, and refining characteristics.

## 1.1:   PROBLEM STATEMENT

The Eastern Dahomey Basin in southwestern Nigeria hosts significant oil sand and heavy oil deposits that have remained undeveloped. However, the renewed efforts to diversify the economy, increase petroleum reserves, reduce imports of heavy crude oil for blending purposes, and create jobs have generated interests to develop the basin's untapped hydrocarbon resources.

The scarcity of data on source rock evaluation in the basin and characterization of the oil sand and heavy oil as it relates to its composition, quality, metal contents, refining, and possible origin has made this work to be relevant. The source rock assessment for its hydrocarbon generating potential is necessary to determine the origin of the reservoired oils; this information is key to exploring additional reserves within the basin. Besides, characterizing the oil sands and heavy oil is crucial for its exploitation, transportation, processing, and refining.

The application of an integrated approach involving rock evaluation pyrolysis, organic petrography, thermogravimetry, elemental analysis, carbon isotopes, gas chromatography, and gas chromatography-mass spectrometry will serve as geochemical techniques to assess the source rock and characterize the reservoired hydrocarbons.

## 1.2:   APPROACH AND THESIS OUTLINE

This research adopted a methodology that included fieldwork to acquire source rocks, oil sands, oil seeps, and heavy oil samples from different parts of the basin. A critical aspect of the fieldwork was a seamless interaction with the government agencies and the host communities. This interaction ensured that the fieldwork

went unencumbered; the chiefs of the host communities provided the sites for the boreholes. The Ministry of Solid Minerals, Federal Republic of Nigeria, granted me the access and authority to carry out the fieldwork and provided the core samples from previously drilled wells.

Source rock samples were evaluated for their hydrocarbon generating potential. The oil sand, heavy oil, and oil seep samples were assessed to determine their quality, composition, and refining characteristics. These assessments were carried out using a variety of geochemical techniques in different laboratories. The thesis outline is shown in Figure 2, and it is divided into seven chapters.
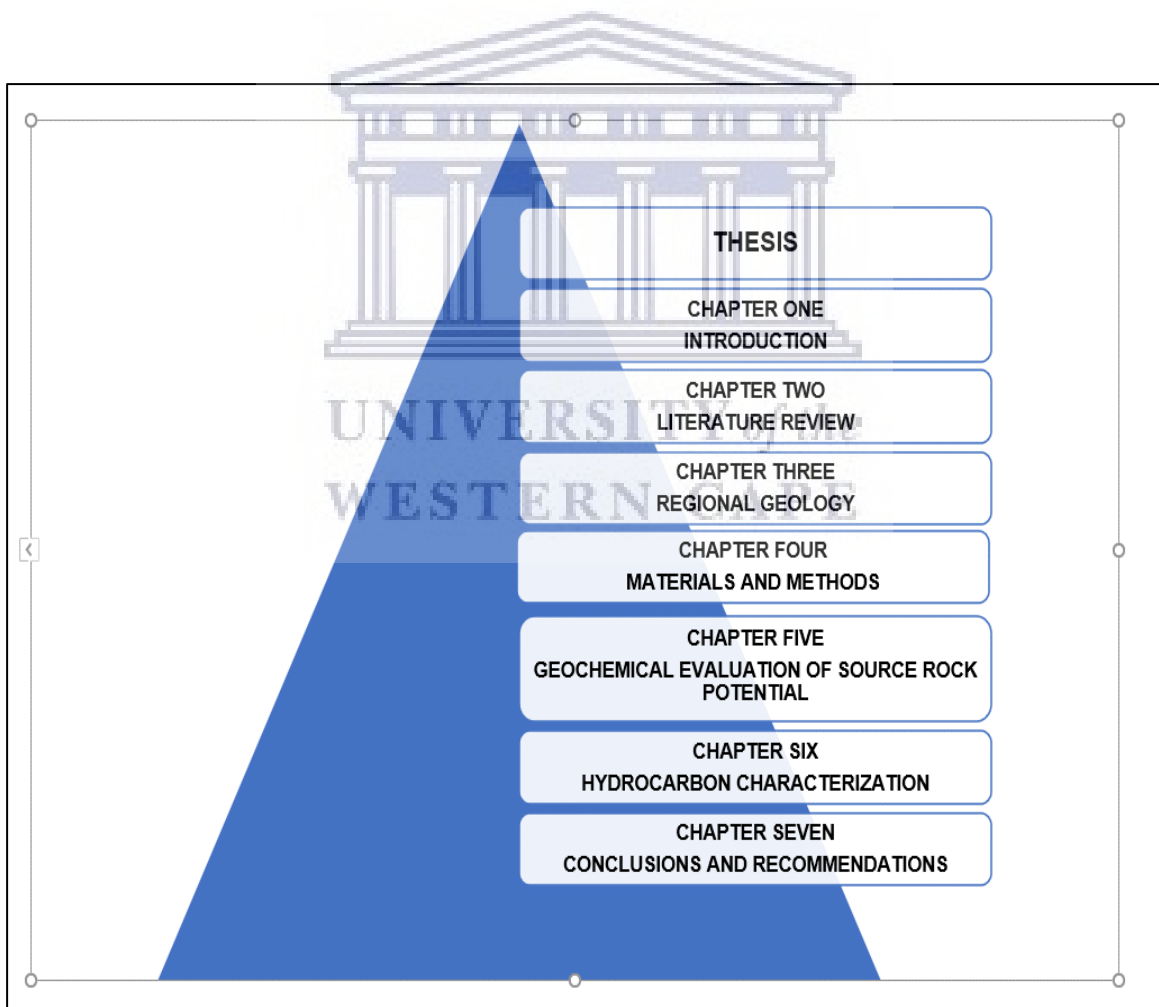


*Figure 2: Thesis outline*

## 1.3:   LOCATION OF AREA OF STUDY

The Eastern Dahomey Basin is located in southwestern Nigeria (Fig.1). The study area and sample locations (Fig. 3) are situated within Ogun and Ondo States. The locations fall within Latitudes 06° 35' 27.0" N to 06° 40' 755" N, and Longitudes 04° 12' 00.6" E to 04° 49' 49.7" E.  The hydrocarbon resources of the basin span Lagos, Ogun, Ondo, and Edo States in the southwest (Fig. 4).
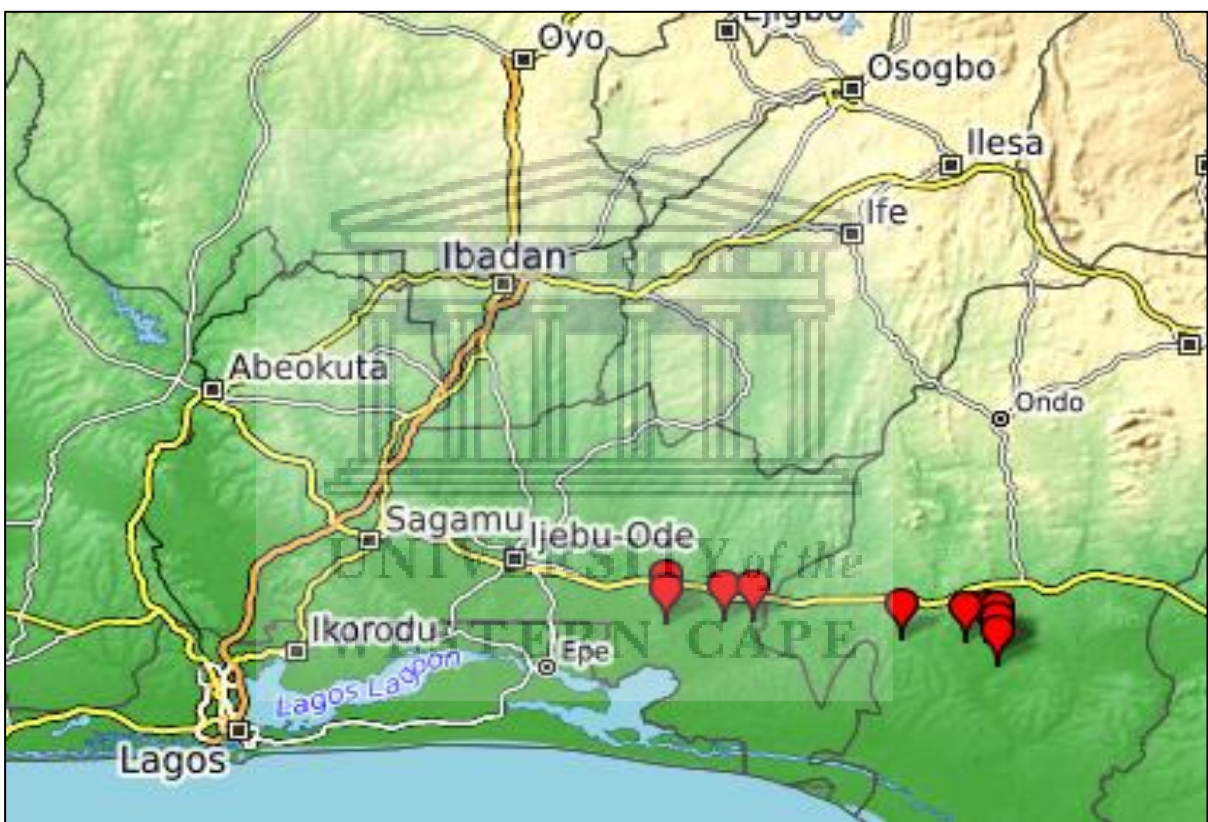


*Figure 3: Map showing the location of the study area (highlighted by the red markers).*

.
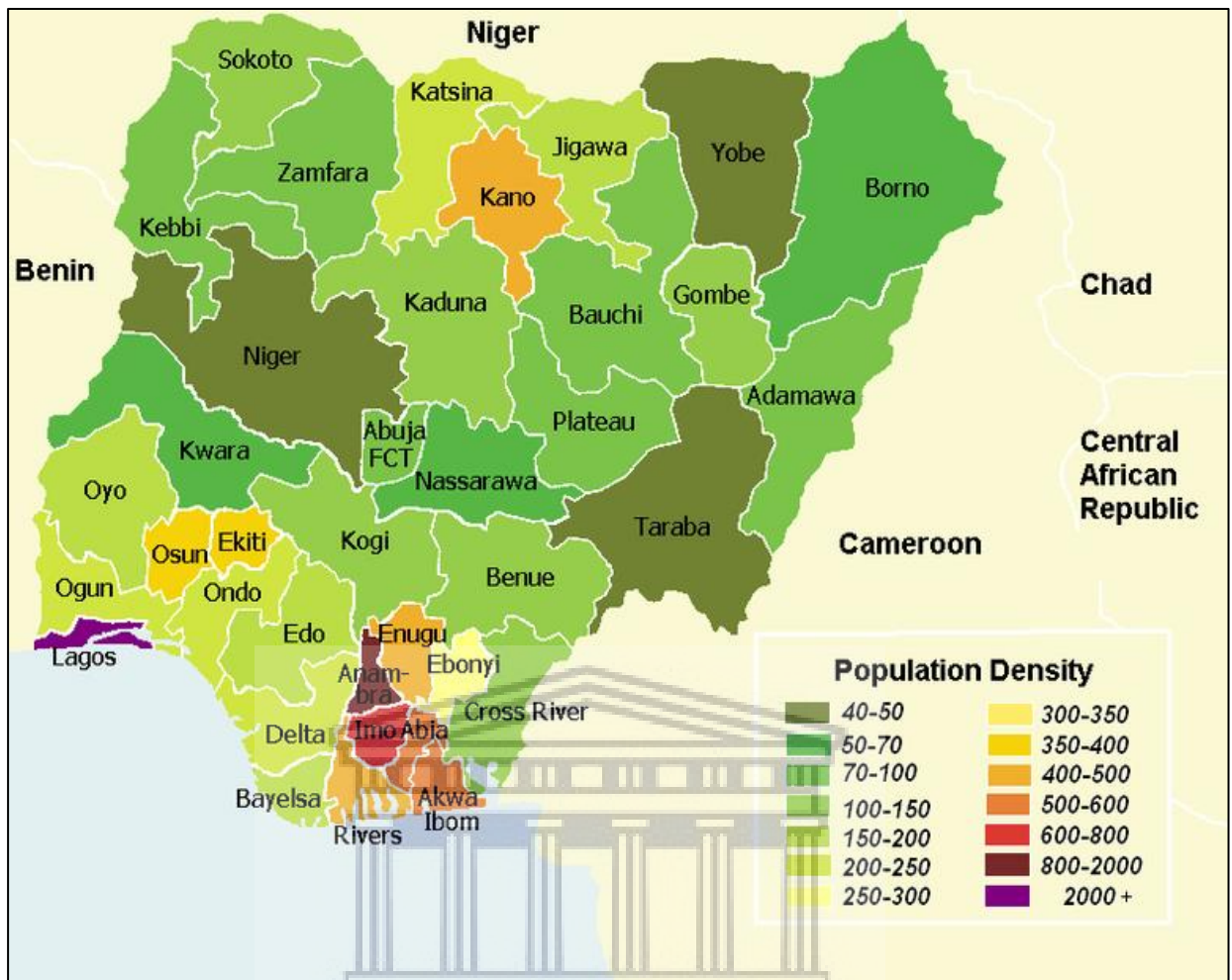
*Figure 4: Geographical map of Nigeria. The oil sand and heavy oil of the Eastern Dahomey Basin are found in Lagos, Ogun, Ondo, and Edo States.*

## 1.4:    RESEARCH AIMS AND OBJECTIVES

This research aims to evaluate the source rock potential and characterize the oil sand and heavy oil deposits of the Eastern Dahomey Basin. These objectives could be achieved by employing a multi-parameter method to assess both the source rocks and the reservoired hydrocarbons.

The specific aims and objectives of this research include the following:

a) Evaluate the source rock and determine its hydrocarbon generating potential.

b) Evaluate the reservoired hydrocarbons for their composition, quality, and refining characteristics.
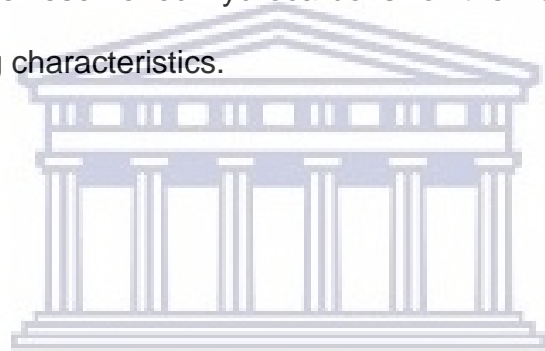
# CHAPTER TWO: LITERATURE REVIEW

## 2.1: SYNOPSIS OF THE CHAPTER

This review examines petroleum source rocks and their geochemical evaluation to assess hydrocarbon generating potential. Also, it reviews oil sands and heavy crude. It concludes with a discussion on the petroliferous Afowo Formation of the Eastern Dahomey Basin.

## 2.2: Source Rock Evaluation

Petroleum originates from the source rock. The viability of a petroleum system depends on its source rock. The present-day geography of petroleum reserves and provinces is controlled mainly by the source rocks (Peters et al., 2005). Without the source rock, all other components (reservoir rock, trap, and seal) and processes needed to exploit hydrocarbon reserves become irrelevant (McCarthy et al., 2011). Hydrocarbon generation from the thermal breakdown of organic matter in the source rock during its burial history is a part of the overall process of thermal metamorphism of organic matter (Tissot and Welte, 1984). The hydrocarbon types generated by petroleum source rocks throughout its evolutionary pathway are influenced by the quantity/quality of organic matter and organic maturation temperature.

Source rocks can be broadly defined as fine-grained organic-rich rocks that could generate (potential source rock) or have already produced (effective or active source rock) significant amounts of petroleum (Peters et al., 2005). Petroleum source rocks have also been defined on the basis that such rocks must have generated and expelled hydrocarbons in quantities sufficient for commercial accumulation (Hunt, 1996). Because of the difficulties in defining the term "commercial," the definition of source rocks by Peters et al. ( 2005) is preferred.

The petroleum generating potential of a source rock largely depends on its organic richness and thermal maturity. Organic richness refers to the quality and quantity of organic matter in the source rock. In contrast, thermal maturity refers to the temperature that the source rock was exposed to over some time. Heat increases as the rocks are buried deeper beneath successive layers of sediments, and it is the thermal transformation of organic matter that causes source rock to generate petroleum (McCarthy et al., 2011). Heat transforms organic matter in the source rock to kerogen (insoluble organic matter), and as heat increases, the kerogen undergoes thermal cracking to generate petroleum.

Based on thermal transformation or evolution of organic matter, source rocks that have not generated petroleum are thermally immature (potential source rock). In contrast, source rocks that are producing petroleum are thermally mature (active source rock), and those that have generated all their hydrocarbons are considered to be post-mature (Hunt, 1996; Peters and Moldowan, 1993; Peters et al., 2005; Tissot and Welte, 1984b).

 The geochemical evaluation of a given source rock is achieved by appraising its source richness, source quality, and thermal maturity. Source richness is a measure of the amount of organic matter in sediment capable of generating hydrocarbons. It indicates the sediment's hydrocarbon generation capacity and not merely a measure of the amount of organic matter present ( Dembicki, 2017). On the other hand, source quality is a measure of the types of organic matter present in the sediment. It indicates the types of hydrocarbons that the sediment can generate. Thermal maturity measures the degree to which the organic matter in the sediments has been altered by the combined effects of time and temperature.

The stages of hydrocarbon generation and classification of a petroleum source rock are gauged by its degree of thermal maturity.

The conventional source rock screening processes include total organic carbon (TOC), rock-evaluation pyrolysis, vitrinite reflectance ($R_o$), petrographic analysis of maceral composition, and elemental analysis. A multi-parameter approach is often recommended since single data types may be in error or affected by contamination (Dembicki, 2017). The multi-parameter method requires that more than one analytical method be used to appraise source rocks to establish a high degree of confidence in the results.

Additional source rock screening can be augmented by gas chromatography (GC) and gas chromatography-mass spectrometry (GC-MS). Geochemical analysis with GC and GC-MS helps identify the organic matter's biological precursors within a given source rock and the depositional environment (Hunt, 1996; Peters and Moldowan, 1993; Tissot and Welte, 1984). Gas chromatography elucidates the distribution of different compound types in the whole extract (bitumen) or the saturated fraction and provides clues to the kerogen type and thermal maturity. Gas chromatography-mass spectrometry provides a means to identify geochemical fossils (Biomarkers) that can be used to determine maturity, geologic age, depositional environment, perform oil – to - oil and source – to -oil correlations. Petroleum systems can be defined with a source–to–oil correlation by establishing the genetic relationship between the generating source rock and resulting oil in the reservoir. Oil–to–oil correlation helps determine the number of oil families in a basin by identifying the number of active source rock (Dembicki, 2017; Faboya et al., 2015; Peters et al., 2005). Some of the parameters that are used to assess source rock potentials are shown in Tables 1, 2, and 3 (Peters and Cassa, 1994).

*Table 1: Generative potential of immature source rock (Peters and Cassa, 1994).*

| | | Rock-Eval (mg/g rock) | | | |
|---|---|---|---|---|---|
| Potential (quantity) | TOC (wt. %) | S1 | S2 | Bitumen (ppm) | Hydrocarbons (ppm) |
| Poor | <0.5 | <0.5 | <2.5 | <500 | <300 |
| Fair | 0.5 – 1 | 0.5 – 1 | 2.5 – 5 | 500-1000 | 300-600 |
| Good | 1 – 2 | 1 – 2 | 5 – 10 | 1000-2000 | 600-1200 |
| Very good | 2 – 4 | 2 - 4 | 10 – 20 | 2000-4000 | 1200-2400 |
| Excellent | >4 | >4 | > 20 | >4000 | >2400 |

TOC = Total organic carbon;

S1 = Hydrocarbons that have already been generated

S2 = Hydrocarbon generating potential remaining in the kerogen.

*Table 2: Kerogen type and expelled products (Peters and Cassa, 1994).*

| Kerogen (quality) | Hydrogen index (mg HC/g TOC) | S2/S3 | Atomic H/C | Main product at peak |
|---|---|---|---|---|
| I | >600 | >15 | >1.5 | Oil |
| II | 300-600 | 10-15 | 1.2-1.5 | Oil |
| II/III | 200-300 | 5-10 | 1.0-1.2 | Oil/gas |
| III | 50-200 | 1-5 | 0.7-1.0 | Gas |
| IV | <50 | <1 | <0.7 | None |

H/C, atomic hydrogen/carbon ratio; S2, hydrocarbon generating potential remaining in the kerogen; S3, an indicator of the amount of oxygen associated with the kerogen

*Table 3: Thermal maturity (Peters and Cassa, 1994).*

| | Maturation | | | | Generation | | |
| --- | --- | --- | --- | --- | --- | --- | --- |
| Maturity | $R_o$ (%) | Tmax (°C) | TAI | | Bitumen/TOC* | Bitumen (mg/g rock) | Production Index (S1/(S1+S2)) |
| **Immature** | 0.20-0.60 | <435 | 1.5-2.6 | | <0.05 | <50 | <0.10 |
| **Mature** | | | | | | | |
| Early | 0.60-0.65 | 435-445 | 2.6-2.7 | | 0.05-0.10 | 50-100 | 0.10-0.15 |
| Peak | 0.65-0.90 | 445-450 | 2.6-2.7 | | 0.15-0.25 | 150-250 | 0.25-0.40 |
| Late | 0.90-1.35 | 450-470 | 2.9-3.3 | | - | - | >0.40 |
| Postmature | >1.35 | >470 | >3.3 | | - | - | - |

Note
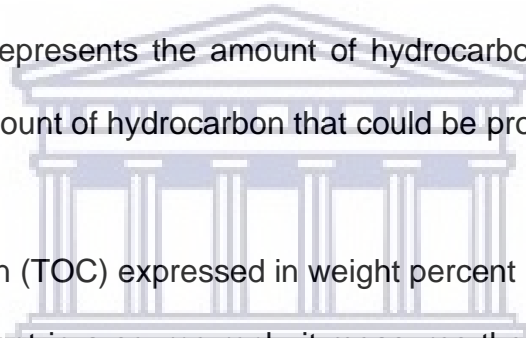
* Many gas-prone coals have high bitumen yields like oil-prone samples, but extract yields normalized to TOC are low (<30 mg HC/g TOC). Bitumen/TOC ratios >0.25 indicate contamination, migrated oil, or artifact caused by ratios of small, inaccurate numbers (Peters et al., 2005).

$R_o$ = Vitrinite reflectance

Tmax=  Temperature at which the maximum rate of hydrocarbon generation occurs during rock evaluation pyrolysis

TAI = Thermal alteration index

Production index = Represents the amount of hydrocarbon already generated relative to the total amount of hydrocarbon that could be produced.

The total organic carbon (TOC) expressed in weight percent (wt. %) is the amount of organic carbon present in a source rock; it measures the quantity and not the quality of organic carbon in rock or sediment samples. Total organic carbon is a proxy for the total amount of organic matter present in the sediment (Ronov, 1958). It is used as an indicator of source richness concerning how much hydrocarbon the sediment may generate. Although TOC is fundamental to source rock evaluation, it should be interpreted cautiously on its own (Dembicki, 2017) as some of the organic matter in the sediment is inert and will not generate petroleum (Tissot et al., 1974). Another constraint with TOC is that it is maturity sensitive, and it decreases with increasing maturation as hydrocarbons are generated and expelled (Daly and Edman, 1987).

The relative inert kerogen content increases throughout organic matter's thermal evolution from immature to the postmature state as the reactive organic matter is pyrolyzed to generate hydrocarbons. Therefore, the TOC is less accurate as an indicator of source richness as the source rock becomes increasingly mature. It is better to use TOC in conjunction with other data to obtain a complete picture of source rock richness (Dembicki, 2017). The interpretation of TOC data can also be impaired by contamination when oil-based drilling muds and organic drilling mud additives are used for drilling as it can increase the apparent TOC content of sediment (Carvajal-Ortiz and Gentzis, 2015).

Elemental analysis of hydrogen, carbon, oxygen, and Rock-Evaluation Pyrolysis data (Hydrogen index, Oxygen index) are used independently or concurrently to appraise the quality of organic matter and the constituent kerogen. Kerogen can be classified based on hydrogen/carbon (H/C) versus oxygen/carbon (O/C) atomic ratios from elemental analysis using a van Krevelen diagram (Fig. 5). The van Krevelen diagram was initially developed to characterize coals during their thermal maturation, or coalification (Krevelen, 1961; Peters et al., 2005; Stach et al., 1982; Taylor et al. 1998), and its use was extended to include the classification of kerogen in sedimentary rocks (Tissot et al., 1974).
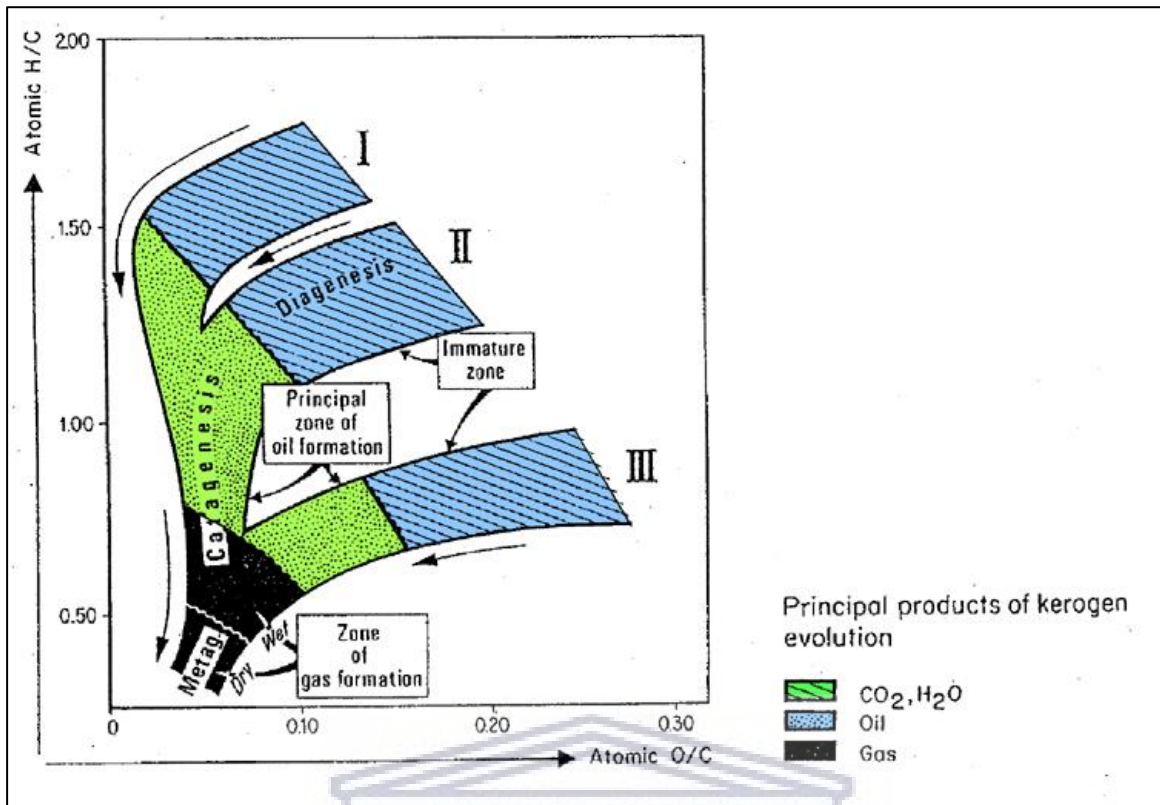
*Figure 5: Cross-plot of H/C and O/C atomic ratios (Van Krevelen diagram) showing kerogen types, evolutionary pathways, and maturation products (From Tissot and Welte, 1978).*

Because of the complexity of analyzing organic oxygen in kerogen (Peters et al., 2005), a modified Van Krevelen diagram is often used. The modified plot (Fig. 6) is based on the cross-plot of hydrogen index (HI) versus oxygen index (OI) rather than on H/C against O/C atomic ratios, and it is applied in the characterization of kerogen.
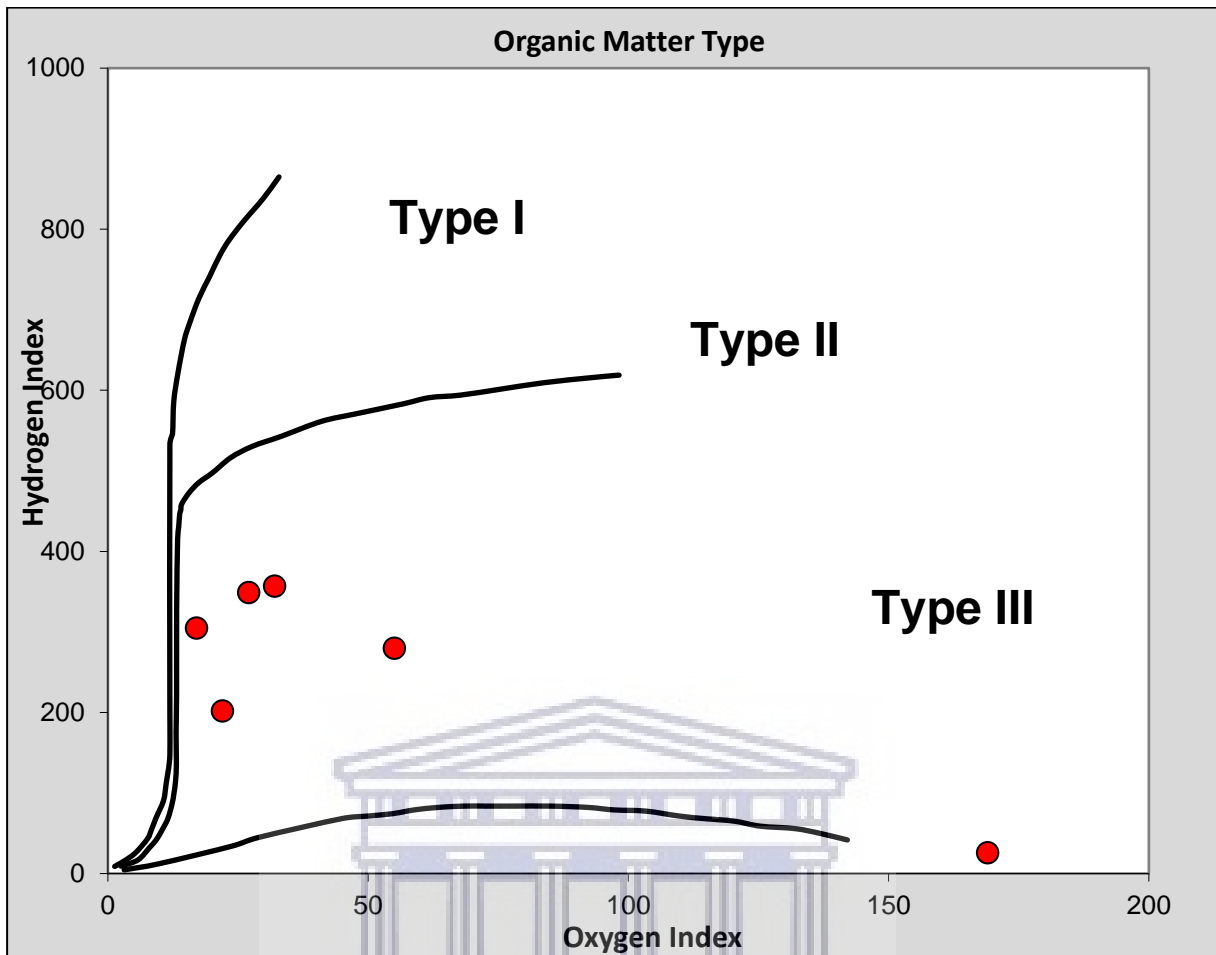
*Figure 6: A modified Van Krevelen diagram using rock evaluation pyrolysis data (Adapted from Mohammed et al., 2019).*

Both indexes (HI and OI) are derived from Rock-Evaluation Pyrolysis; the analysis not only produces similar results to elemental analysis, but it is faster, less expensive, and requires a small mass of sample (approximately < 100 mg). Rock-Evaluation Pyrolysis (Rock-Eval pyrolysis) has evolved to become a petroleum industry-standard analysis for source rock since the early 1980s. It continues to be a mainstay of source rock analysis today (Dembicki, 2017).

The pyrolysis results produce a wide range of data (Tmax, S1, S2, S3, S4, TOC, hydrogen index, oxygen index, production index) that cannot be obtained from elemental analysis; elemental analysis is not only time consuming but expensive.

In addition to using hydrogen index and oxygen index to classify kerogen type, cross-plots of HI versus Tmax (Espitalie et al., 1984) and S2 against TOC (Katz and Elrod, 1983) can be used for a similar application. Even though Rock-Eval pyrolysis has become the industry standard for source rock evaluation, the results' interpretation can be subject to errors ( Dembicki, 2009; Espitalie et al.,1980; Katz and Elrod, 1983). For example, while S2 represents the hydrocarbon generating potential remaining in the sediment's kerogen, there are instances when materials that should be confined to S1 are carried over and included in the S2.  This situation can  occur with contamination of the sediment by organic drilling mud additives (processed asphalt, gilsonite) as well as in cases when a high proportion of the generated material consists mainly of resins and asphaltenes that may not be volatile at 300 °C (Dembicki, 2017). Notwithstanding advances in technology that have resulted in improved source rock analyzers, additional data from other forms of analyses are needed for satisfactory interpretation.

Kerogen has also been classified based on source material and provenance (Table 4).

*Table 4: Classification of kerogen based on source material and provenance (Adapted from McCarthy et al., 2011).*

| Kerogen Type | Source Material | General Environment of Deposition | Hydrocarbon type at maturity |
| --- | --- | --- | --- |
| I | Mainly algae | Lacustrine setting | Waxy oil |
| II | Mainly planktons, some contribution from algae | Marine setting | Oil |
| III | Mainly higher plants | Terrestrial setting | Gas |
| IV | The reworked, oxidized material | Varied setting | Nil |

There are three primary hydrocarbon generating kerogen types (Tissot et al., 1974). Type 1 kerogen has a high initial hydrogen/carbon ratio and low initial oxygen/carbon ratios. It is derived primarily from algal materials deposited mainly in lacustrine environments. Type 1 kerogen can also form in brackish water and lagoonal environments (Revill et al., 1994). The thermal decomposition of Type kerogen 1 produces mainly waxy oil. Type II kerogen has relatively high hydrogen/carbon and moderate oxygen/carbon atomic ratios in its primordial state. Type II kerogen generates mainly naphthenic oil. It can be derived from both autochthonous organic matter deposited under reducing conditions in the marine environment and allochthonous higher plant components such as leaf cuticles, spores, and pollens (Dembicki, 2017). Type III kerogen has low hydrogen/carbon and high oxygen/carbon atomic ratios. Type III kerogen is prone to generate gas, and it is derived from terrestrial high plant debris and or aquatic organic matter deposited in an oxidizing environment. In addition to these main types of kerogens, other brands have also been recognized.

Type IV (Tissot and Welte, 1984) has a deficient hydrogen/carbon and variable oxygen/carbon atomic ratio. Type IV kerogen is inert with no hydrocarbon generating potential. Type II-S is a variant of Type II kerogen and is rich in sulfur (8-14 wt %). Type II-S kerogen is derived from autochthonous organic matter deposited under highly reducing conditions in marine environments most often associated with upwelling conditions (Orr, 1986). Organic sulfur-rich variants (Type 1-S and Type III-S) have also been recognized for Type I and Type III kerogens. In addition to this extended classification of kerogens, mixtures of Type I and Type III or Type II and Type III can also be found.

The organic maturation temperature (Tmax) is the primary Rock-Eval parameter for evaluating source rock's thermal maturity; the kerogen types have different potentials to generate hydrocarbons at varying Tmax. Tmax values generally increase with increasing depth (Espitalie et al., 1977), and it can be related to other maturity indicators such as vitrinite reflectance (Peters et al., 2005). Characteristic Tmax values for the top and bottom of the oil windows (Espitalié, 1986; Peters, 1986) are shown in Table 5. The temperature range for the top of the oil window (Table 5) indicates that the absolute changes in Tmax vary with kerogen type and maturity (Espitalié et al., 1985; Peters, 1986). While the Tmax values for Type I kerogen are about 440 °C at the top of the oil window, Type II and Type III kerogen have Tmax values of approximately 435 °C and 445 °C, respectively (Table 6).

*Table 5: Thermal maturity interpretations from Rock-Eval Tmax (After Espitalie et al., 1986; Peters, 1986)*

| Maturation | Tmax |
|---|---|
| Top oil window | ~435 - 445 |
| Bottom oil window | ~ 470 |

*Table 6: Tmax at the top of the oil window for different kerogen type (Espitalie et al., 1985; Espitalie, 1986; Peters, 1986)*

| Kerogen Type | Tmax at the top of the oil window |
|---|---|
| Type I | ~ 440 |
| Type II | ~ 435 |
| Type III | ~ 445 |

As maturity progresses, the influence of kerogen type diminishes, and all three kerogen types have Tmax values of approximately 470 °C at the bottom of the oil window (Dembicki, 2017).

## 2.3: Oil Sand/Tar Sand/Heavy Oil

Oil sands are sands rich in heavy oil, with the lighter components being absent due to biodegradation and water washing. The sand consists of bitumen (soluble organic matter) and host sediment with associated minerals and insoluble organic matter, excluding any related natural gas (Hein, 2006). Typically, oil sand contains about 75 % inorganic matter, 10 % bitumen, 10 % silt and clay, and 5 % water (National Energy Board, 2004). The crude bitumen contained in the sands is a viscous mixture of hydrocarbons. In its natural state, the crude bitumen will not flow unless heated or diluted with lighter hydrocarbons. The difficulties involved in producing oil sand and heavy oil have hindered their utilization as a resource. Their reserves' estimates triple the amount of combined world reserves of conventional oil and gas (Curtis et al., 2002).

The definition of oil sand and heavy oil has attracted several controversies, and no clear distinction is made between oil sands and heavy oil. While some countries refer to it as oil sand or tar sand, it is called heavy oil by others. For example, many of Venezuela's heavy oils would be considered oil sands in Canada or tar sands in the United States (Hein, 2006).

Heavy oils, ultraheavy oils, and oil sands have been defined based on viscosity and density. Density is defined in terms of degrees of American Petroleum Institute (API) gravity, which is related to specific gravity (Curtis et al., 2002). Specific gravity is the ratio of a body's mass to the mass of an equal volume of

water at a specified temperature (Dembicki, 2017). The denser the oil, the lower is its API gravity.

The formula relating specific gravity to API gravity is given by

$$API\ gravity = \left(\frac{141.5}{Specific\ gravity}\right) - 131.5$$

Viscosity is the internal friction due to molecular cohesion in fluids, which results in resistance to flow. The unit of measurement of viscosity is poise (P), and it is commonly expressed as centipoise (cP). Crude oils have wide-ranging viscosities and densities. Viscosity determines the ease that the oil will flow, and it is more critical to the oil producers. By contrast, density is of prime interest to the refiners as it is a better indicator of the yield from distillation. Viscosity is greatly influenced by temperature, but temperature has a minimal effect on density. Because of the minimal impact of temperature on density, density has become a vital oilfield parameter to classify crude oils. Liquid hydrocarbons exhibit a continuum of API gravities within the range of 4° API to 70° API (Curtis et al., 2002).

Heavy oils have API gravities within the range of 10° API to 20° API at room temperature and viscosities of less than 10,000 cP (Mallakh, 1983), allowing some primary production (Hein, 2006). In contrast, oil sands have in situ viscosities higher than 10,000 cP and API greater or less than 10° API (Kuuskraa et al., 1987). The viscosities and API gravities of liquid hydrocarbons and some liquids are shown in Figure 7.
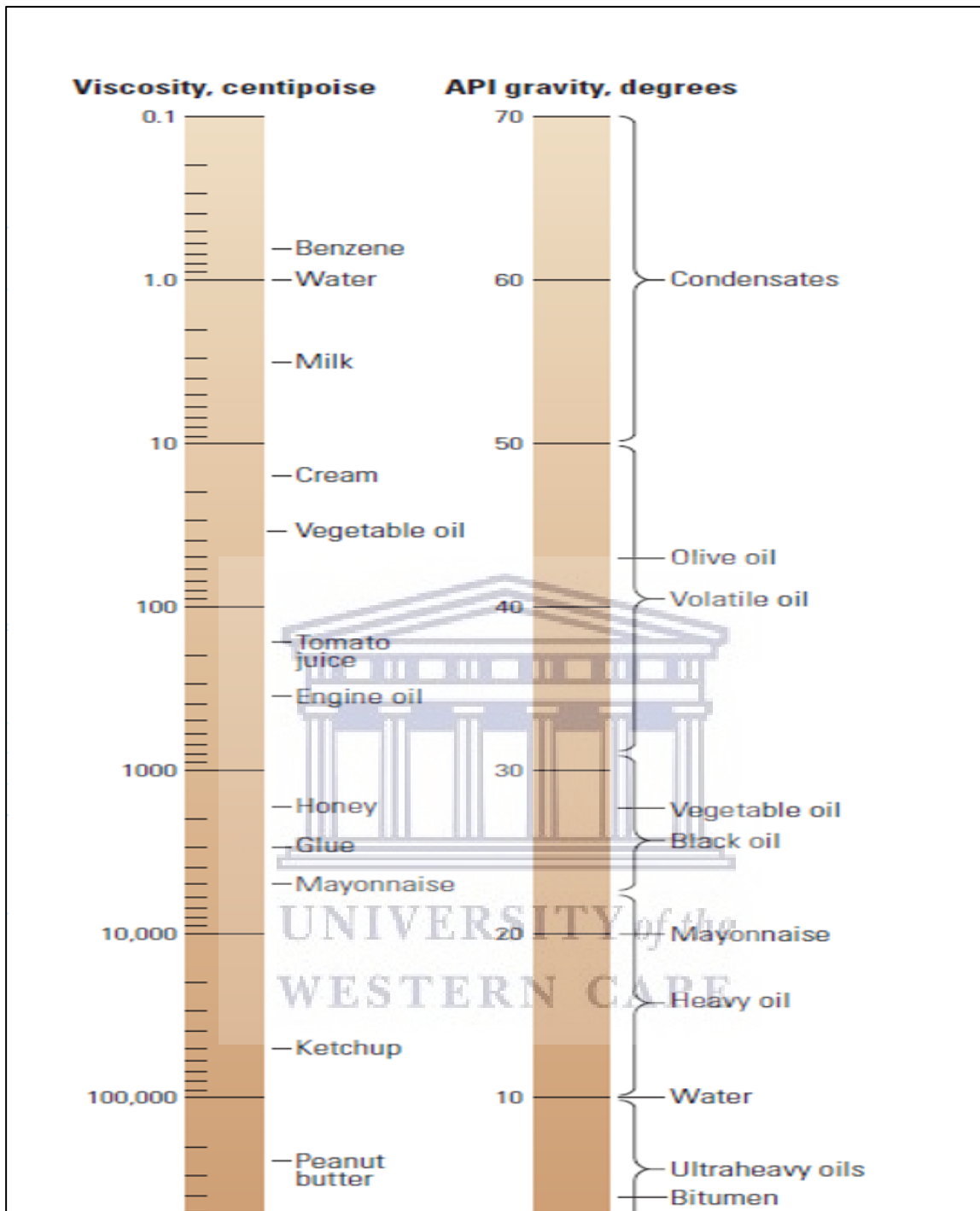
*Figure 7: Viscosities and gravities of hydrocarbons and other liquids (Curtis et al., 2002).*

Both oil sands and ultra-heavy oils are denser than water. The United States Department of Energy (DOE) defines heavy oils as oils with API gravities between 10° API and 20° API, but there is no such clear-cut distinction in nature. Still, in some reservoirs, oil with API gravity as low as 7° or 8° is considered heavy rather than ultraheavy because it can be produced by heavy oil production methods (Curtis et al., 2002). In general, the API gravities of liquid hydrocarbons range from 4° for bitumen-rich sands to 70° for condensates.

The first crude oil that results from the thermal break down of Type I and Type II kerogen is not heavy and has an API gravity of 30° to 40°. Crude oils become heavy after the removal of light end molecular components through biodegradation, water-washing, gas-washing, and evaporation during their migration and entrapment in reservoirs and traps (Alexander et al., 1983; Deroo et al., 1974). The degradation can occur at depths in the subsurface by anaerobic microbes or when they are exposed to an oxidizing zone by aerobic microbes.

The process of biodegradation alters the composition and characters of the oil forever. It is carried out by microbes that are indigenous to the reservoir sediments at the time of deposition of the sediments. These microbes remain inactive until hydrocarbons migrate into the reservoir (Head et al., 2003). They are anaerobic due to the lack of oxygen in the subsurface (Jones et al., 2008). The microbes' biological activity in the reservoir is centered along the oil-water column due to their needs for water-soluble nutrients (Head et al. 2003). Biodegradation is sensitive to reservoir conditions. For it to occur, the temperature, formation water salinity, supplies of water-soluble, and hydrocarbon substrate in the reservoir have to be adequate to promote microbial growth.

Biodegradation is greatly influenced by temperature, and optimal microbial activity occurs at reservoir temperatures between 35° C to 45°C (Larter et al., 2006). The microbial activity begins to diminish as the temperature increases from 45° C to 65° C and within a temperature range of 65° C to 80° C, microbial activity is limited, thus reducing the rate of biodegradation (Dembicki, 2017). The microbes are eliminated or pasteurized at temperatures higher than 80° C ending biodegradation (Head et al., 2003).

Formation water salinity, although not as well understood as temperature, plays a vital role in biodegradation. The rate of biodegradation decreases with an increase in formation water salinity (Larter et al., 2006; Mille et al., 1991). In addition to temperature and salinity controls on biodegradation, there has to be an adequate supply of nutrients. Nutrients such as nitrate, phosphate, iron, potassium support the microbial communities. Besides, there has to be dynamic water mixing to transport the nutrients to the oil-water contact and supply of fresh hydrocarbons to the oil-water contact (Head et al., 2003). These controls can result in compositional gradients in the oil column showing progressively less biodegradation with increasing distance from the oil-water contact in actively biodegrading reservoirs (Larter et al., 2006).

Biodegradation alters the composition of crude oil. The metal concentration, asphaltenes content, weight percent sulfur, and viscosity will increase as the oil is degraded. In contrast, API gravity, light hydrocarbon content, wax content, and pour point will decrease with progressive biodegradation (Dembicki, 2017). Compositional changes and the extent of biodegradation can be recognized from the chromatograms of whole crude oil (Fig. 8).
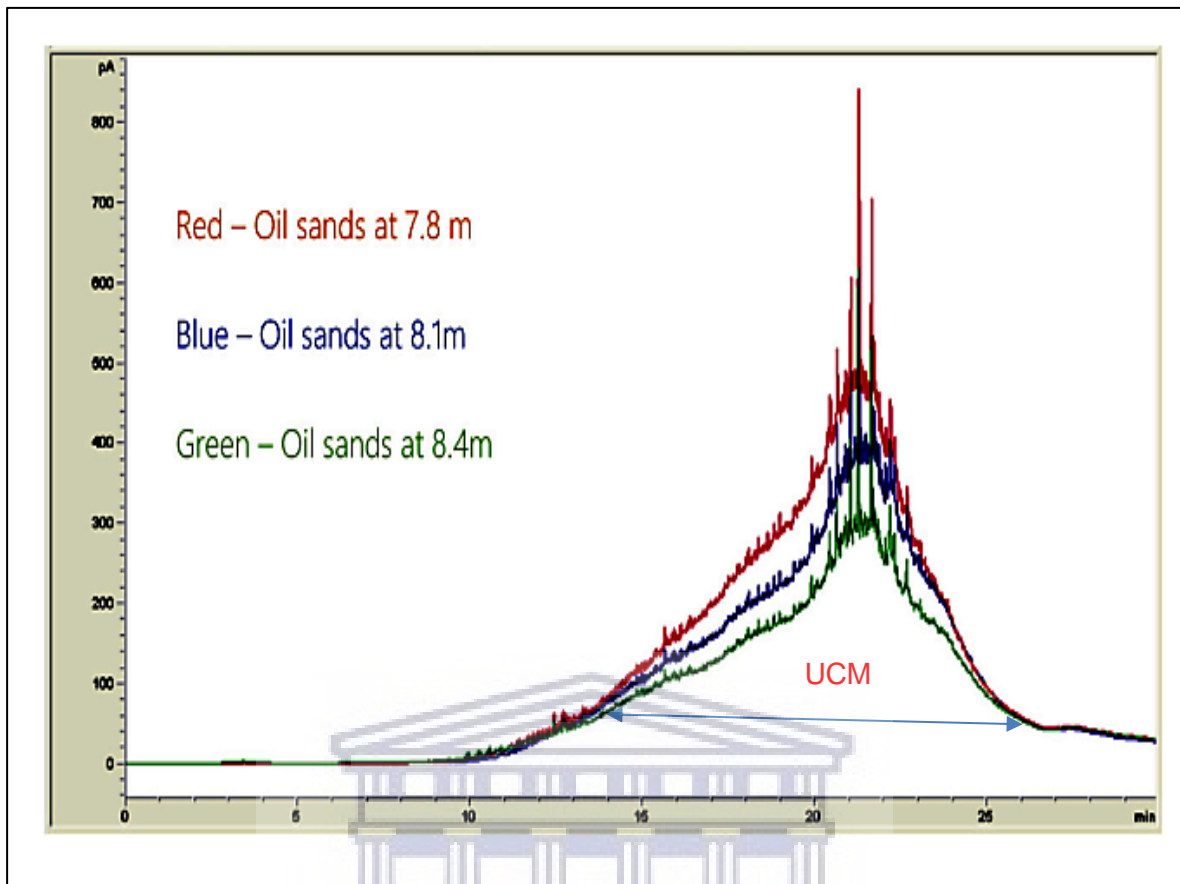
*Figure 8: Chromatograms of oil sands showing the loss of light end molecular components and the development of humps of unresolved complex mixtures (UCM), indicating biodegradation (Adapted from Mohammed et al., 2019).*

The loss of light end molecular components and the appearance of a hump of the unresolved complex mixture (UCM) reflect the compositional changes that indicate biodegradation.

Vast amounts of bitumen (oil sand or tar sand) and heavy oil dominates the world's hydrocarbon resources (Table 7, Fig. 9).

*Table 7: Major Heavy Oil and Bitumen Regions of the World (Adapted from Kashirtsev and Hein, 2013).*

| Region | Heavy Oil (bbl) | Bitumen (bbl) | Total (bbl) |
|---|---|---|---|
| Venezuela | 265.7 | 0.1 | 265.8 |
| Alberta, Canada | 2.71 | 174.5 | 177.21 |
| Middle East | 78.2 | 0 .0 | 78.2 |
| Asia | 29.6 | 42.8 | 72.4 |
| California, USA | 62.85 | 5.34 | 68.19 |
| Africa | 7.2 | 43 | 50.2 |
| Russia | 13.4 | 33.7 | 47.1 |
| Utah, USA | 0.06 | 32.33 | 32.39 |
| Alaska, USA | 0.14 | 19.0 | 19.14 |
| Others, USA | 3.44 | 14.08 | 17.52 |
| Texas, USA | 11.84 | 5.44 | 17.28 |
| Europe | 4.9 | 0.2 | 5.1 |
| Total | 480.04 | 370.49 | 850.53 |
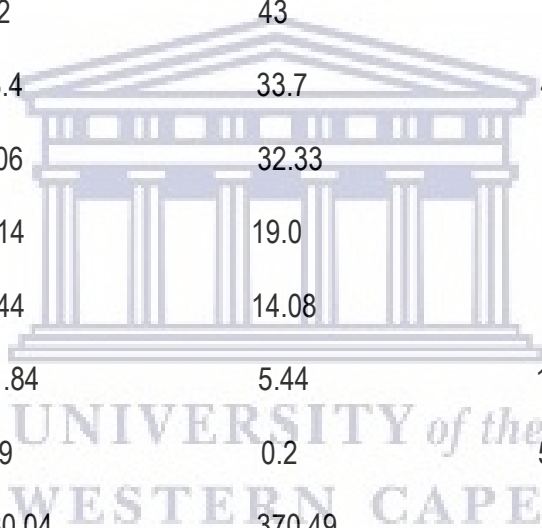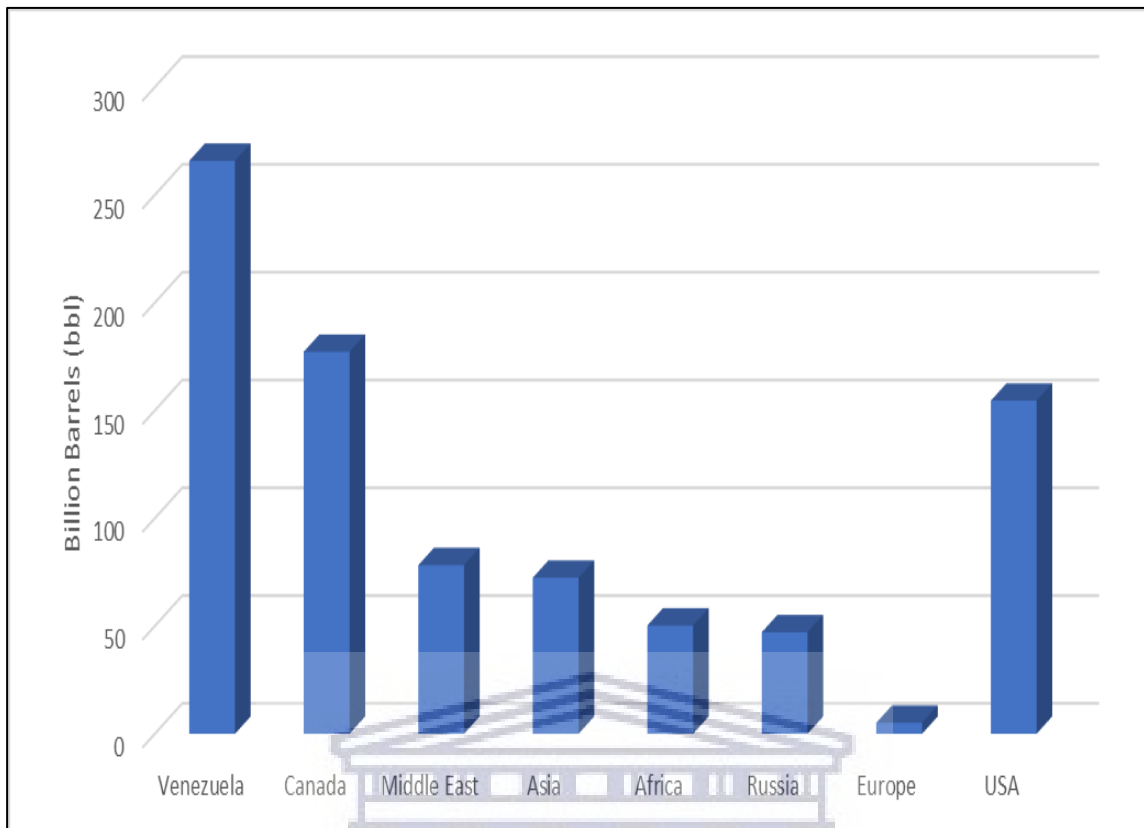
*Figure 9: Major heavy oil and Bitumen Regions of the world (Adapted from Kashirtsev and Hein, 2013).*

These resources are often ignored because of the difficulties in their extraction and associated high costs of production. Compared to the remaining conventional crude oil reserves of 1.02 trillion barrels, bitumen and heavy oil are estimated to amount to 5.6 trillion barrels (Hein, 2006). Despite the global abundance of heavy oil and bitumen, the world's oil and gas supplies are dominated by the more easily produced conventional hydrocarbon reserves, which are predicted to reach their peak as early as 2030. The projected decline and scarcity of energy supplies from conventional hydrocarbon resources make the exploitation of bitumen and heavy oil an ideal target of global interest. Technological advancements such as cyclic steam stimulation (CSS), steam-assisted gravity drainage (SAGD), horizontal well, well placement, logging-while-drilling, and in-situ technologies are improving

recoveries and reducing the cost of production of heavy oil and bitumen (Curtis et al., 2002).

## 2.4: Oil Sand Deposits in the Eastern Dahomey Basin

Marked oil sand deposits have been known to occur in the eastern segment of the Dahomey Basin (Benin Basin) since the 1900s (Ogala et al., 2019). The reserves of oil sands and heavy oil are estimated to be about 58 billion barrels of oil equivalent (Ministry of Mines and Steel Development, 2009). The oil sand occurs along a belt of 6 km wide and more than 120 km long (Enu, 1985). Earlier studies (Coursey et al., 1963; Crocket and Wescott, 1954) were focused on the suitability of the raw material for road construction.

Reviews by the Nigerian Bitumen Corporation from 1904 to 1914 and studies by Durham and Pickett (1966) explored the possibility of producing heavy oil directly or through secondary recovery techniques. Several wells were drilled around Agbabu and Lekki Lagoon, but the projects were deemed uneconomical and abandoned (Enu, 1985).

Previous works on the geology of the oil sand deposits in the Afowo Formation (Enu, 1987; Enu, 1985; Omatsola and Adegoke 1981) indicated that the formation is composed of medium to coarse-grained sandstones with variable but thick interbedded shales, siltstones, and claystones. The lithological profile of the formation by Enu (1987) identified two principal tar bearing sandy horizons (X and Y) that are each about 12 – 15 m thick separated by a greenish to grey shale, an 8 m thick oil shale. Recent studies (Akinmosin et al., 2013; Amigun et al., 2012; Odunaike et al., 2010) which characterized the Afowo Formation based on resistivity profiling revealed that the oil sand occurs at varying depth intervals.

Several organic geochemical studies have been carried out on the source rocks and crude oils of the Niger Delta Basin (Abrakasa and Nwankwoala, 2019; Akaegbobi et al., 2000; Faboya et al., 2015; Ogala and Akaegbobi, 2014; Sonibare et al.,2008; Udo and Ekweozor, 1990). In contrast, there is limited data on source rock assessment and characterization of the oil sand deposits of the Eastern Dahomey Basin. This scarcity of information is directly related to a mix of government policies that have hindered exploration activity in the Eastern Dahomey Basin and other frontier basins. Decades of oil exploration and exploitation in Nigeria have focused on the prolific Niger Delta Basin with its vast reserves of conventional hydrocarbons.

Previous source rock evaluation studies in the Eastern Dahomey Basin include those of Akinmosin et al. (2015), Nton et al. (2009), and Uzoegbu et al. (2016). Nton et al. (2009) evaluated the hydrocarbon generating potential of the shales penetrated by Ibese and Aje-1 wells. They concluded that the source rock has low to adequate organic richness with potential for gas at maturity. A similar study (Akinmosin et al., 2015), which used six core samples from a borehole, indicated Type III and Type IV kerogen with Tmax ranging from 343 °C to 427 °C, suggesting thermal immaturity. Uzoegbu et al. (2016) used Rock-Eval to characterize the oil sands, which revealed Type I, Type II, and Type III kerogen, and the Tmax ranged from 428 °C to 439 °C. The range of kerogen types and Tmax indicated in the study by Uzoegbu et al. (2016) is because the evaluation was carried on bituminous sands, which cannot be classified as a petroleum source rock. These studies (Akinmosin et al., 2015; Nton et al., 2009; Uzoegbu et al., 2016) relied exclusively on Rock-Eval pyrolysis in their assessments and did not take into account a multi-parameter approach.

Ogala et al. (2019), in their study of a geochemical and organic petrological analysis of bituminous sediments from the basin, made use of outcrop samples of bituminous sediments; the samples did not have depth information. They indicated that the indigenous huminite population's random reflectance values ranged between 0.40 %$R_o$ and 0.45 %$R_o$, suggesting thermal immaturity. In contrast, the respective reflectance of the migrabitumens varies from 0.49 %$R_o$ to 0.59 %$R_o$, corresponding to vitrinite equivalent reflectance values of 0.70 %$R_o$ – 0.76 %$R_o$ falling well within the oil window (Ogala et al., 2019). However, the estimation of maturity was based on a single data type, and outcrop samples are prone to oxidation.

A seminal study of source rock potential of the Maastrichtian Araromi Formation in the Eastern Dahomey (Adekeye et al., 2019) made use of Rock-Eval, Organic Petrology, and GC-MS to assess the shales penetrated by the Araromi and Gbekebo wells. The results revealed Type II, Type II/III, Type III, and Type IV kerogen, which are thermally immature (Adekeye et al., 2019). However, no detailed geochemical evaluation of the source rock potential and characterization of the oil sand and heavy oil deposits of the Afowo Formation has been carried out.

The geochemical characterization of the tar sand and heavy oil deposits (Emmanuel and Ajibade, 2014; Ndukwe et al., 2015) from the basin relied mainly on elemental analysis of outcrop samples of oil sand and oil seeps. Emmanuel and Ajibade (2015) used elemental analysis of Carbon, Hydrogen, Oxygen, Nitrogen, and Phosphorous to characterize the deposits, while Ndukwe et al. (2015) categorized the deposits based on Cobalt, Nickel, and Zinc contents. These studies (Emmanuel and Ajibade, 2014; Ndukwe et al., 2015) did not

estimate the degree of biodegradation nor determine hydrocarbon composition and refining characteristics, and neither did they assess the API gravity and total acid number (TAN). The information is critical to exploiting the oil sands and heavy oil.

This present research will use a multi-parameter method to evaluate the hydrocarbon generating potential of the source rock, which underlies the oil sand to determine the origin of the reservoired hydrocarbons. This information is necessary for future exploration activity. Besides, the oil sand and heavy oil will be characterized by different methods to assess their quality, composition, and refining characteristics.

# CHAPTER THREE: REGIONAL GEOLOGY

## 3.1: SYNOPSIS OF THE CHAPTER

The chapter discusses the evolution of the sedimentary basins in the Gulf of Guinea province in West Africa, with particular emphasis on the eastern segment of the Dahomey Basin. The east sector of the Dahomey Basin is referred to as Eastern Dahomey Basin or Dahomey Embayment, and it is situated in southwestern Nigeria. The stratigraphic successions in the basin are discussed.

## 3.2: GEOLOGICAL SETTING

The province of the Gulf of Guinea, as defined by the United States Geological Survey (USGS), consists of the coastal and offshore areas of Côte D'Ivoire, Ghana, Togo, and Benin, and the western part of the coast of Nigeria. It extends from Liberia's eastern border to the west edge of the Niger Delta Basin in Nigeria. The sedimentary basins in the Gulf of Guinea Province consist of Ivory Coast, Tano, Saltpond and Central, Keta, and Benin Basins (Fig. 10). These basins share common structural and stratigraphic characteristics; they are wrench-modified (Clifford, 1986) and host rocks ranging from Ordovician to Holocene (Kjemperud et al., 1992)
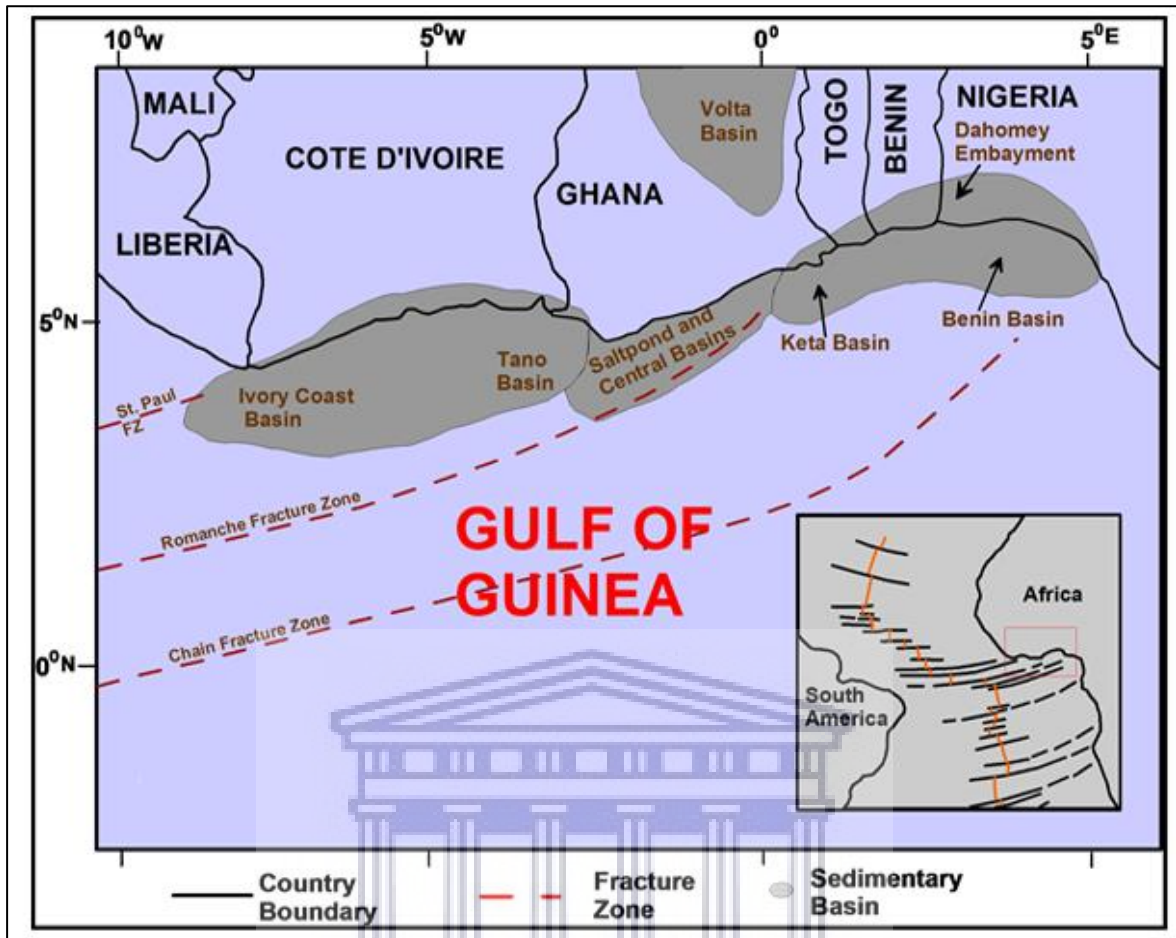
*Figure 10: Sedimentary Basins in the Gulf of Guinea Province, showing major structural features (Kjemperud et al., 1992). The Mid-Atlantic Ridge and fractures are shown in the index map.*

The eastern boundary of the Gulf of Guinea Province is the Niger Delta Province (Klett et al., 1997), and the western border is the Western Coastal Province (Fig. 11).
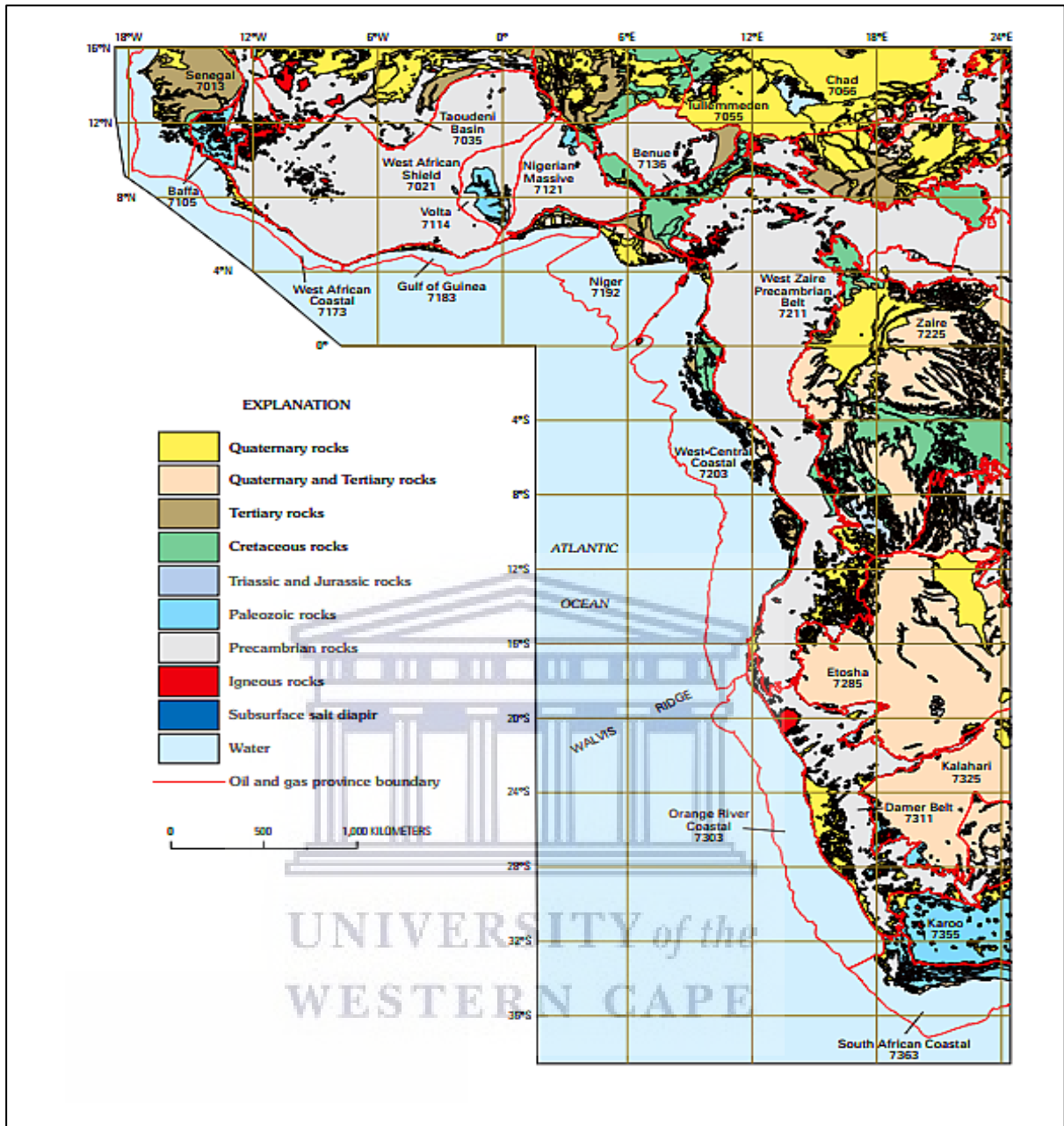
*Figure 11: Generalized geologic map of West Africa* (Brownfield and Charpentier, 2006; Persits et al., 2002)*, showing province boundaries and selected province names and codes as defined by Klett et al. (1997).*

The Gulf of Guinea evolved at the culmination of the Late Jurassic to Early Cretaceous tectonism that was characterized by both block and transform faulting superimposed across an extensive Paleozoic basin during the breakup of the African, North American, and South American paleocontinents

(Brownfield and Charpentier, 2006). The province has undergone complex evolution, which is divided into pre-transform (Late Proterozoic to Late Jurassic), syn-transform (Late Jurassic to Early Cretaceous), and post transform (Late Cretaceous to Holocene) stages of basin development (Brownfield and Charpentier, 2006). The area is marked structurally by three major transform fault zones, the St. Paul Fracture Zone, the Romanche Fracture Zone, and the Chain Fracture. The St. Paul Fracture Zone is situated along the northwestern boundary, while the Romanche Fracture Zone separates the Ivory Coast and Saltpond, and Central Basins from the Keta Basin. The Chain Fracture Zone is along the eastern border. These principal fracture zones defined the basins and acted as dams for the transportation and accumulation of sediments. Sedimentary fill within the Ivory Coast Basin is more than 6,000 m thick (Fig. 12), and the Dahomey Basin contains up to 3000 m thick of sediments (Whiteman, 1982).
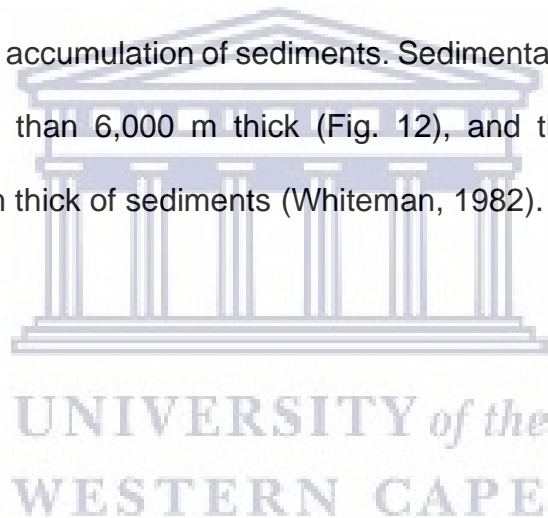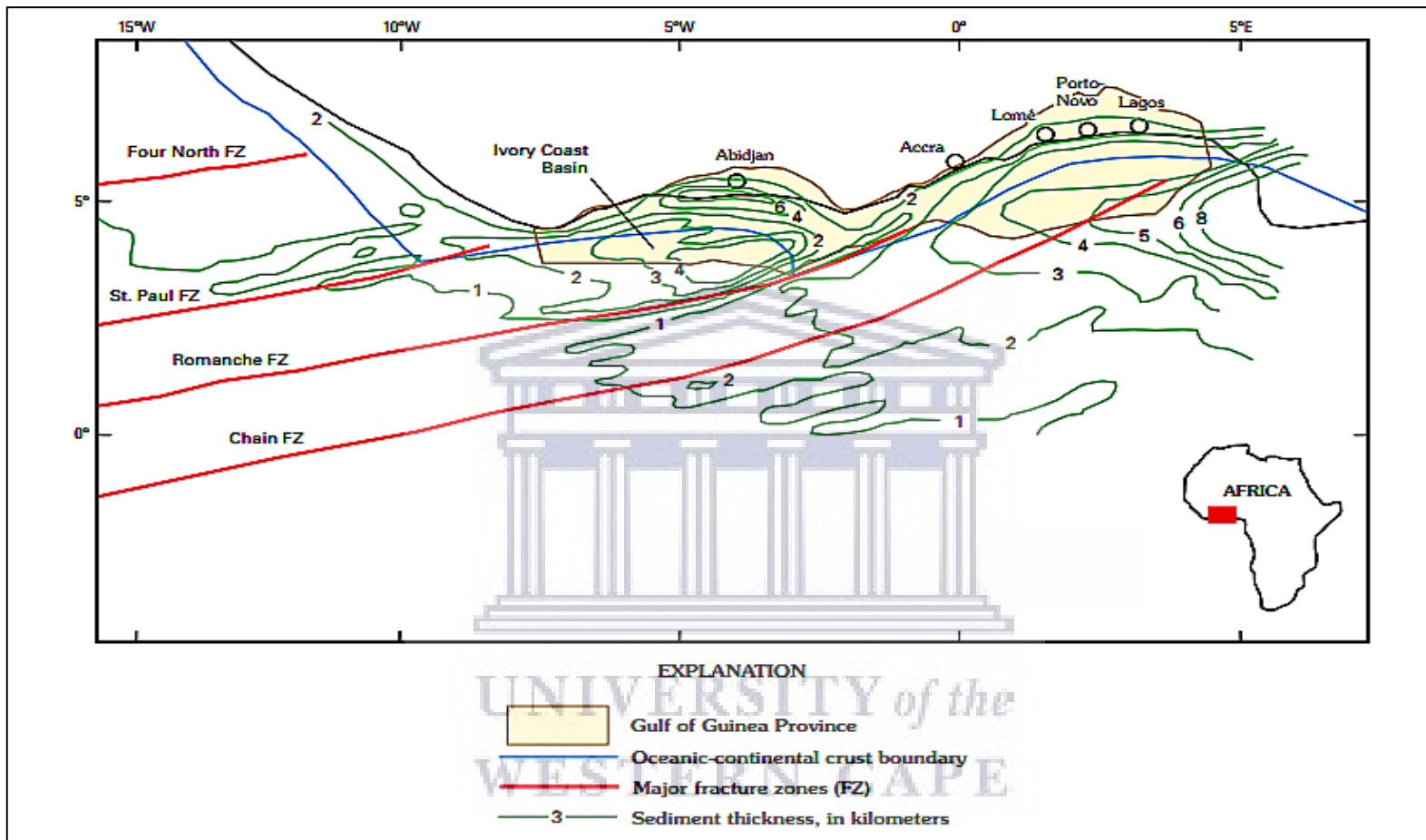
*Figure 12: Map showing major fracture zones (FZ), sediment thickness, and oceanic-continental crust boundary for the Gulf of Guinea (Modified from Brownfield and Charpentier, 2006; Emery and Uchupi, 2012; MacGregor et al., 2003).*

The Dahomey Basin is a blend of inland/coastal/offshore basins in the Gulf of Guinea that extends from southeastern Ghana through Togo and the Republic of Benin to southwestern Nigeria (Obaje, 2009; Oli et al., 2019). It is a marginal pull – apart (Klemme, 1975) or marginal sag basin (Kingston et al., 1983), which evolved during the period of rifting in the Late Jurassic to Early Cretaceous times (Adekeye et al., 2019; Omatsola and Adegoke, 1981; Whiteman, 1982). The tectonism was attended by an extended period of thermally induced basin subsidence from the Middle-Upper Cretaceous to Tertiary times as the South American and African tectonic plates entered a drift phase to accommodate the emerging Atlantic Ocean (Kaki et al., 2013; Storey, 1995). The western limit of the basin is bounded by the Ghana Ridge, an offset extension of the Romanche Fracture Zone (Olabode, 2015). Simultaneously, its eastern boundary is confined by the Benin hinge line, which separates the Okitipupa Structure from the Niger Delta Basin (Akinmosin et al., 2015).

The basin hosts a large wedge of Cretaceous to Recent sediments of up to 3,000 m (Nton et al., 2009; Ogala et al., 2019), which thicken toward the offshore. The interplay of sedimentation, eustatic sea-level fluctuation of normal faulted graben, and horst structure of the basin floor have produced thick accumulations of sediments within the grabens. These accumulations were accompanied by sediment bye-pass and extensive cut and fill structures at or near the shelf margins (Ministry of Mines and Steel Development, 2009). The developments resulted in the formation of the essential elements (source rock, reservoir rock, traps, and seals) of a petroleum system in the basin (Mohammed et al., 2020).

The eastern segment of the basin also referred to as the Eastern Dahomey Basin or Dahomey Embayment, is found in southwestern Nigeria. The stratigraphy of the Eastern Dahomey Basin, outlined in Table 8, has been discussed by various workers, and several classification schemes were proposed (Billman, 1992; Coker et al., 1983; Elueze and Nton, 2004; Jones and Hockey, 1964; Ogbe, 1972a; Omatsola and Adegoke, 1981). Despite the classification schemes, age assignments, and terminologies of the different lithological units (Nton et al., 2009), within the basin remain mostly controversial. Different stratigraphic names have been proposed for the same formation in other localities and have led to confusion (Billman, 1992; Coker, 2002).
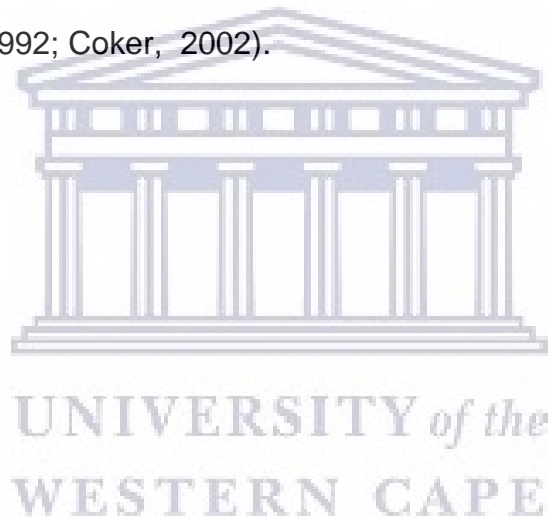
*Table 8: Stratigraphy of the Eastern Dahomey Basin (Modified from Omatsola and Adegoke, 1981).*

| Era | Period | Epoch | Stratigraphy of the Eastern Dahomey Basin | | |
|---|---|---|---|---|---|
| **Cenozoic** | Quaternary | Holocene | Jones and Hockey (1964) | Omatsola and Adegoke (1981) | |
| | | Pleistocene | | | |
| | Tertiary | Oligocene | Coastal Plain Sands | Coastal Plain Sands | |
| | | Eocene | Ilaro Formation | Ilaro Formation | |
| | | | | Ososhun Formation | |
| | | Paleocene | Ewekoro Formation | Akinbo Formation | |
| | | | | Ewekoro Formation | |
| **Mesozoic** | Cretaceous | Late to Early | Abeokuta Formation | Abeokuta Group | Araromi Formation |
| | | | | | Afowo Formation |
| | | | | | Ise Formation |

The stratigraphic units in the Eastern Dahomey Basin, as defined by Omatsola and Adegoke (Omatsola and Adegoke, 1981), consists of the Cretaceous Abeokuta Group and the Tertiary sediments of Ewekoro, Akinbo, Oshosun, Ilaro Formations and the Coastal Plain Sands (Benin Formation).

The Abeokuta Group is further subdivided into Ise, Afowo, and Araromi Formations. The Ise Formation (Fig. 13) is the oldest formation within the Abeokuta Group and rests unconformably on the Crystalline Basement Complex. It comprises of basal conglomerates, medium to coarse-grained sandstones with admixtures of kaolinitic clays. The age is probably Valanginian-Barremian (d'Almeida et al., 2016).



*Figure 13: Field photograph showing outcrop of Ise Formation in the area of study. The researcher using self for scale (Height is 1.85 m). The weathered basement consists of kaolinitic clays that varied in color from grey to brown and reddish.*

The Ise Formation is succeeded by the Afowo Formation. The Afowo Formation is hydrocarbon bearing (Fig. 14). It is composed of fine to medium and coarse-grained sandstones interbedded with clays, shales, claystones, and siltstones.
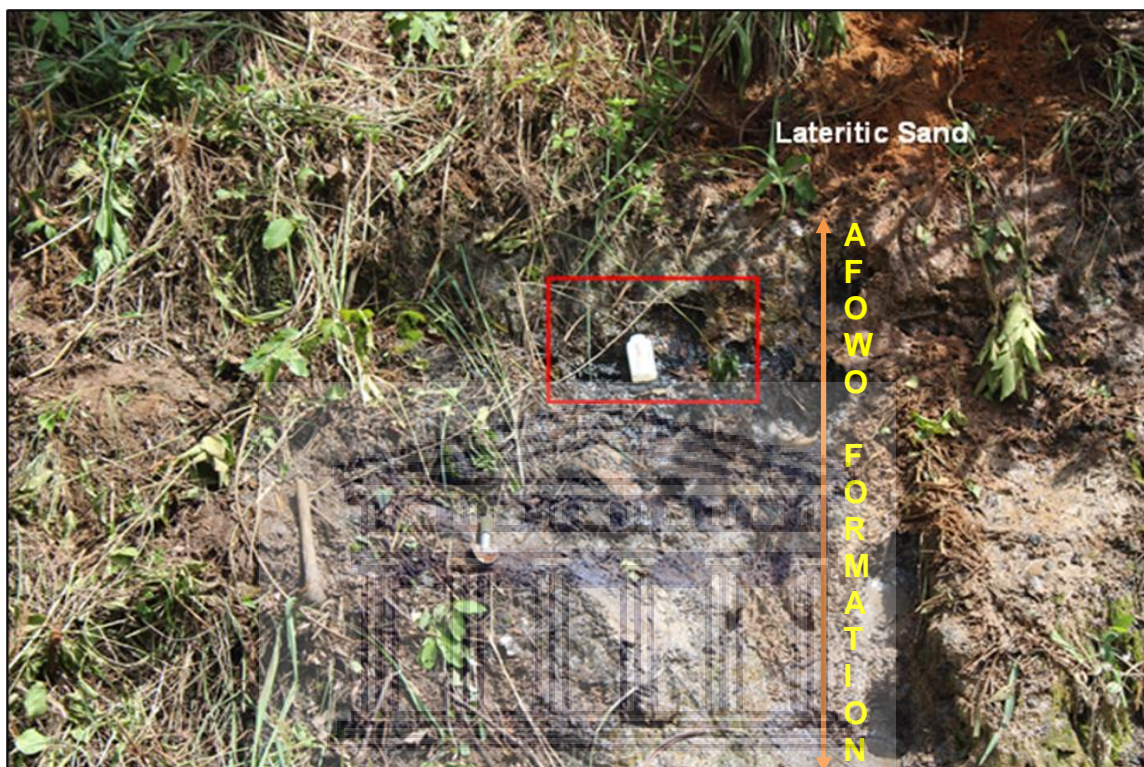


*Figure 14: Field photograph showing outcrop of Afowo and Araromi Formations in the area of study. The outcrop is composed of lateritic sand, oil sand, and claystone; the plastic bottle showed a section of the oil sand. The lateritic sand is assigned to the Araromi Formation. In contrast, the oil sand and claystone are assigned to the Afowo Formation (Mohammed et al., 2020).*

The sandy facies are tar-bearing, while the shales are organic-rich (Enu, 1990). The lower part of the formation is transitional, with mixed brackish to marginal marine facies that alternate with well-sorted, sub-rounded sand, indicating a littoral or estuarine nearshore depositional environment (Elueze and Nton, 2004; Nwajide, 2013). Based on a palynological assemblage, the lower part of the formation was assigned a Turonian age (Billman, 1992), while the upper part ranges into the Maastrichtian.

The formation has also been given a Cenomanian-Coniacian age based on the occurrence of planktonic foraminifera Rotalipora Greenhornensis (d'Almeida et al., 2016).

Overlying the Afowo Formation is the Araromi Formation, the youngest Cretaceous sediment in the Eastern Dahomey Basin. The formation is composed of fine to medium-grained sandstone at the base, overlain by shales, siltstones with interbedded limestone, marl, and lignite (Nton et al., 2009). The Araromi Formation is fossiliferous and contains abundant planktonic foraminifera, ostracods, pollens, and spores. Omatsola and Adegoke (1981) assigned it a Maastrichtian age based on its fossil contents, and it extends into the Paleocene.

The Eastern Dahomey Basin's Tertiary sediments consist of Ewekoro, Akinbo, Oshosun, Ilaro, and Benin (Coastal Plain Sands) Formations.

The Ewekoro Formation overlies the Araromi Formation. It is an extensive limestone body that extends over about 320 km from Ghana in the west to the eastern margin of the basin in southwestern Nigeria (Jones and Hockey, 1964). The limestone body is suggested to be of shallow marine origin due to an abundance of coralline algae, gastropods, pelecypods, fragments of echinoid, and other skeletal debris (Elueze and Nton, 2004). The formation is assigned Palaeocene.

The Ewekoro Formation is succeeded by Akinbo Formation, which ranges from Paleocene to Eocene. It comprises of shale and clayey sequence (Ogbe, 1972b) with kaolinite as the dominant clay mineral (Nton and Elueze, 2005). The basal part of the formation is defined by bands of glauconite with limestone lenses.

Overlying the Akinbo Formation is the Oshosun Formation of Eocene – Oligocene. The Oshosun Formation consists of greenish-grey or beige clay and shale with interbeds of sandstones; the shale is thickly laminated and glauconitic (Nton et al., 2009). The basal beds of the formation range in facies from sandstones to mudstones, claystones, clay-shale, or shale (Okosun, 1998). The formation is rich in phosphate (Jones and Hockey, 1964; Nton, 2001). The occurrences of fishes and sea snakes in the shale indicate that the formation is of marine origin (d'Almeida et al., 2016).

The Ilaro Formation overlies the Oshosun Formation. It comprises of massive, yellowish, poorly consolidated, cross-bedded sandstones (Jones and Hockey, 1964) and ranges from Eocene to Oligocene.

Ilaro Formation is overlain by the Coastal Plain Sands (Jones and Hockey, 1964). The Coastal Plain Sands also referred to as the Benin Formation, is the youngest stratigraphic sequence in the Eastern Dahomey Basin. It consists of poorly sorted sands with clay lenses; the sands are in parts cross-bedded and show transitional to continental characteristics (Nton et al., 2009). The formation span Oligocene to Recent.

# CHAPTER FOUR: MATERIALS AND METHODS

## 4.1: SYNOPSIS OF THE CHAPTER

The chapter introduces the materials that were acquired and the analytical methods that were used. The samples were obtained during the period of fieldwork in 2017 and 2019. The chapter presents an aspect of community engagement that highlights courtesy calls on the communities' chiefs to discuss intents and purpose.

## 4.2: MATERIALS

The materials used for this research consisted of both surface and subsurface samples of oil sands, claystones, shales, oil seeps, and heavy oil from different parts of the basin (Table 9). The samples were obtained from the pristine rainforest of southwestern Nigeria.
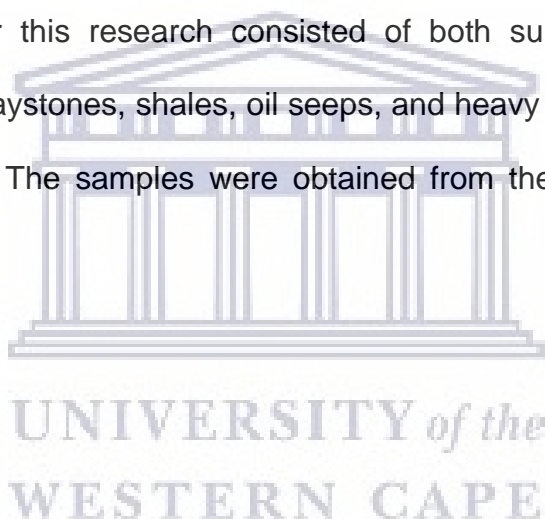
*Table 9: Global Positioning System (GPS) Coordinate Information of the area of study and sample locations*

| Sample ID | Sample Type | Northing | Easting | Elevation (m) | Formation | Remarks |
|---|---|---|---|---|---|---|
| Agbabu-1 | Heavy Oil | 06° 35' 27.0" | 004° 49' 51.7" | 35 | Afowo | Abandoned well |
| Egbe | Oil sand | 06° 38' 14.4" | 004° 48' 14.0" | 30 | Afowo | Outcrop |
| 3- Hanger | Oil sand/Claystone | 06° 42' 19.7" | 004° 12' 00.8" | 27 | Afowo | Outcrop |
| Ijuoke Agotitun | Oil sand/Claystone | 06° 38' 25.7" | 004° 38' 55.5" | 46 | Afowo | Outcrop |
| Ilubinrin-1 | Oil sand | 06° 38' 19.8" | 004° 49' 47.9" | 30 | Afowo | Borehole |
| J4 | Oil sand/Claystone | 06° 40' 755" | 004° 18' 613" | 21 | Afowo | Outcrop |
| J4-BH1 | Claystones | 06° 40' 45.3" | 004° 18' 36.6" | -12 | Afowo | Borehole |
| J4-BH2 | Oil sand/Clayey Sands | 06° 40' 26.6" | 004° 18" 22.7" | 18 | Afowo/Ise | Borehole encountered water |
| Mafowoko | Oil seeps | 06° 40' 24.9" | 004° 12' 02.7" | 20 | Afowo | Seeps in stream water |
| Mile-2-1 | Oil seeps | 06° 36' 55.6" | 004° 49' 49.7" | 21 | Afowo | Seeps in stream water |
| Mile-2-2 | Oil seeps | 06° 36' 55.7" | 004° 49' 46.8" | 15 | Afowo | Seeps in stream water |
| Ode - Aye -1 | Oil sand | 06° 38' 10.2" | 004° 45' 59.7" | 33 | Afowo | Borehole |
| Orisunbare | Oil sand | 06° 41' 00.8" | 004° 21' 56.0" | 28 | Afowo | Outcrop |
| Araromi – Obu | Core | N/A | N/A | N/A | Afowo | Courtesy of Government Agency |
| Erekiti Luwoye (A8) | Core | N/A | N/A | N/A | Afowo | Courtesy of Government Agency |
| Ijagun (A-11) | Core | N/A | N/A | N/A | Afowo | Courtesy of Government Agency |
| Ajabgba (EY-5) | Core | N/A | N/A | N/A | Afowo | Courtesy of Government Agency |
| Igbotu (EY-22) | Core | N/A | N/A | N/A | Afowo | Courtesy of Government Agency |
| Ohosu (EY-19) | Core | N/A | N/A | N/A | Afowo | Courtesy of Government Agency |
| Lewumeji (EY-12) | Core | N/A | N/A | N/A | Afowo | Courtesy of Government Agency |

*Note: Coordinate data for the cores were not available.*

A total number of thirty-nine (39) samples of source rocks consisting of ten outcrop samples of claystones, nineteen sidewall samples of claystones, and ten shale samples from cores were assessed for source rock analysis. The outcrop samples were obtained from locations J4, 3- Hanger and Ijuoke Agotitun, while the sidewall samples were acquired from well J4-BH1. For the core samples, one source rock was assessed for well Ijagun (A-11), while three source rocks at different depths were appraised for well Lewumeji (EY-12).  Two source rocks at different depths were evaluated for well Igbotu (EY-22) while one source rock each was assessed for wells Araromi Obu, Erekiti Luwoye (A8), and Ajagba (EY-5).

The hydrocarbon characterization used three oil seep samples, one sample of heavy crude from an abandoned well, seven oil sand samples from two wells, three oil sand samples from cores, and nine outcrop samples of oil sands. The core samples were provided by an agency of the Federal Government of Nigeria.

The sample acquisition strategy included authorization from the Ministry of Solid Minerals and courtesy visits (Figs. 15 and 16) to the host communities' chiefs, during which the objectives were discussed and consented to. Some of the field photographs at locations of sample acquisition are shown in Figures 17 to 30.

*Figure 15: Field photograph showing Alagbabu of Agbabu (Seated third from left with white cap and dressed in customary regalia) and some of his subjects.*



*Figure 16: Field photograph showing the Chief of Ode-Aye (left, dressed in traditional clothing) and the author (right) during a visit to the site where the Ode-Aye Borehole was drilled. Oil Palm, Kola nut, Coffee trees are grown in the area.*

*Figure 17: Field photograph showing the researcher collecting oil seeps from a stream at Mile-2 in Ondo State, southwestern Nigeria.*



*Figure 18: Field photograph showing field assistant collecting oil seep samples at Mafowoku-Imobi stream in Ogun State, southwestern Nigeria.*

*Figure 19: Field photograph showing spring water in an oil sand outcrop at 3-Hanger, Ogun State. The spring water is a source of water for the community.*



*Figure 20: Field photograph showing bitumen exposure by River Ominla in Ondo State, southwestern Nigeria.*

53

*Figure 21: Field photograph showing field assistant at the Agbabu-1 wellhead. The well, now abandoned, encountered heavy oil at a shallow depth. The bamboo wood on top of the wellhead was used to collect heavy oil samples from the well.*



*Figure 22: Field photograph showing outcrop of oil sand at J4 (Onikitinbi), Ogun State. The roll tape measure (inset) shows a section of the oil sand. The sand is saturated with bitumen, and the bitumen gives the sand its dark color.*

*Figure 23: Field photograph showing an intermediate section of J4-BH1. The steps alongside the borehole wall indicated intervals where sidewall samples were acquired.*



*Figure 24: Field photograph of J4-BH1 borehole, showing the researcher measuring sample depths. The well was sited at the base of the J4 oil sand outcrop. It penetrated claystones, and no oil sand was encountered.*
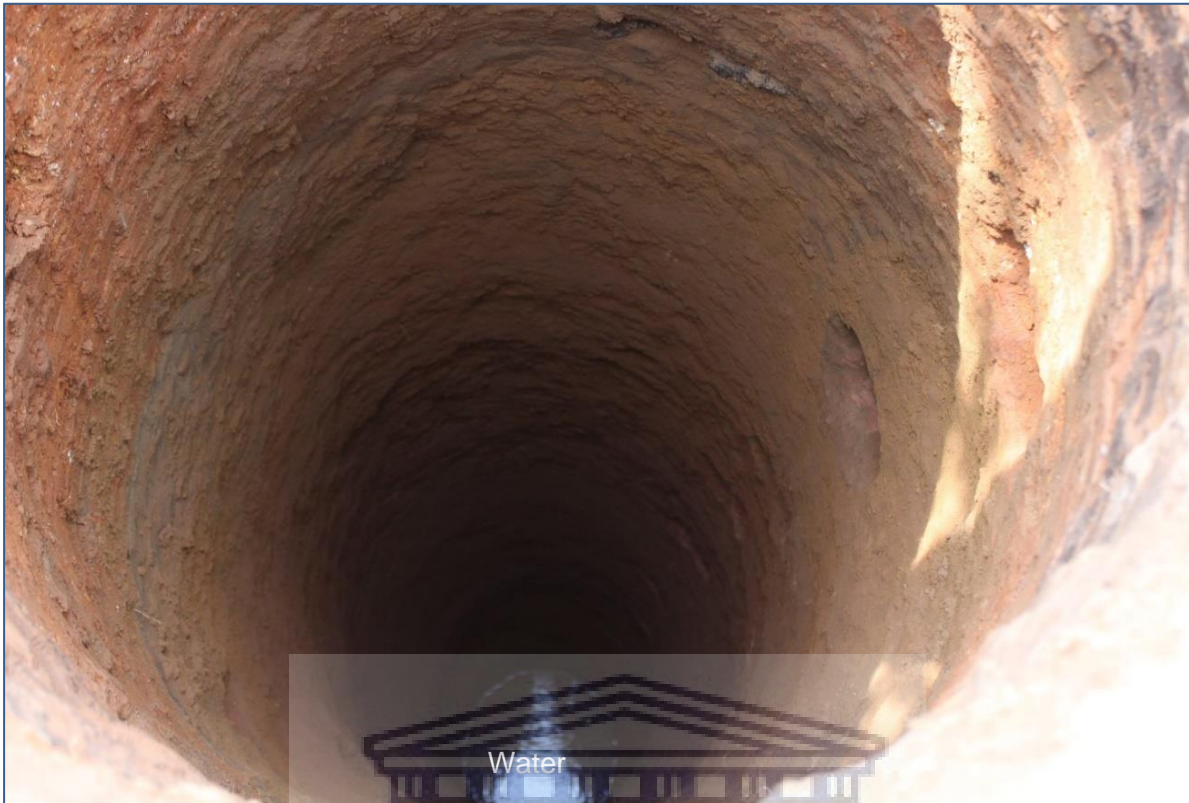
*Figure 25: Field photograph showing J4-BH2 borehole. The borehole encountered water, and it was completed as water well for the community of Onikitinbi. The lithology from the surface to 0.5 m consisted of oil sand.*



*Figure 26: Field photograph showing wellhead after drilling and sample acquisition.*

Oil sand

*Figure 27: Field photograph showing a section of Ilubinrin-1 borehole. The borehole penetrated oil sand at a depth of 1.10m from the surface.*



*Figure 28: Field photograph showing the exposure of oil sand at a road cut.*

Water pond

Oil sand

*Figure 29: Field photograph showing outcrop of oil sand at close proximity to Ode-Aye borehole.*



*Figure 30: Field photograph showing the digging of Ode-Aye-1. The borehole penetrated oil sands.*

## 4.3: METHODS

Several analytical techniques were used to evaluate the samples. The source rocks consisting of shales and claystones were assessed for source richness, maceral composition, and hydrocarbon generating potentials with a multi-parameter method. The multi-parameter approach consisted of Rock-Eval using a Hydrocarbon Analyzer with Kinetics (HAWK) pyrolysis instrument, organic petrography, gas chromatography (GC), loss on ignition (LOI), and thermogravimetric analysis (TGA). Kerogen extraction was carried out on some of the shale and claystone samples and later evaluated using organic petrography.

In contrast to the source rocks, the oil sands, oil seeps, and heavy oil were analyzed by methods consisting of multi-ramp pyrolysis, thermal desorption gas chromatography (TD-GC), column chromatography, gas chromatography, gas chromatography-mass spectrometry (GC-MS), inductively coupled plasma-mass spectrometry (ICP-MS), carbon isotopes, and CHNS Elemental Analyzer. Besides, analyses were also carried out using ASTM (American Society for Testing and Materials) 5291C, D70, D1552, D7169, D5018, D4377, and D8045.

## 4.3.1: ROCK EVALUATION (ROCK-EVAL) PYROLYSIS

Pyrolysis measurements of the source rocks were carried out using the HAWK method (A. Maende, 2016) at Agat Laboratories, Calgary, Canada. The samples were air-dried to remove any atmospheric moisture content and were then individually ground to a powder with an Agate mortar and pestle.

A portion of each of the powdered samples was tested for the presence of carbonates, and no acid digestion occurred, indicating the absence of mineral carbon in the source rock.

The pulverized samples were individually weighed in HAWK (Fig. 31) crucible on a four decimal place balance and placed in the instrument's autosampler tray.



*Figure 31: HAWK* Pyrolysis Instrument*

The crucibles were transferred by the autosampler to the raised HAWK pedestal for placement into the oven. Sample weights of between 10 mg and 20 mg were used, and two cycles of analyses were performed.

The first cycle is pyrolysis. Through programmed temperature heating of up to 650 °C, organic compounds in the analyzed sample were carried by helium from the oven to the flame ionization detector (FID). The FID flame was lit by a mixture of hydrogen and air, resulting in the ionization of the organic compounds; the FID then detected the hydrocarbon constituents. The HAWK oven was cooled down to 300 °C at the end of the first cycle.

The second cycle of analysis involved the oxidation of the remaining sample that had already been pyrolyzed. The samples were subjected to programmed heating to a maximum of 750 °C in the presence of dry air, which was used to transport the

oxidation products to two infra-red (IR) detectors, one of which detects the CO bonds'
bandwidth. In contrast, the second infrared detector detects the $CO_2$ bonds'
bandwidth.

The HAWK machine allows pyrolysis programming to start at temperatures as low as
50 °C or a standby temperature of 100 °C; it ends at a selected maximum that is
usually 650 °C. A maximum temperature of 750 °C is adequate when one is only
interested in measuring generated hydrocarbons together with total organic carbon
(TOC).

For carbonate carbon measurements, the oxidation cycle is set to run up to a
maximum temperature of 850 °C; inorganic carbonate carbon measurements were not
needed for these samples, and the oxidation cycle ended at a temperature of 750 °C.
Pyrolysis instruments such as HAWK evaluate hydrocarbons generated during the
thermal decomposition of kerogen at programmed temperatures. In addition, the
HAWK measures both the total organic carbon content (TOC) and the carbonate
carbon.

Some of the parameters that are determined from pyrolysis instruments such as  the
HAWK  instrument includes the following:

a) Thermally free or producible hydrocarbons that have already been generated
by the thermal breakdown of kerogen. It is designated  S1  and expressed as
milligram hydrocarbons per gram rock.

The S1 is detected from the start of the pyrolysis cycle at  50 °C or 180 °C and
ends at  300 °C.

b) The thermal decomposition of kerogen is known to start at about 300 °C.
The hydrocarbons that are generated between the temperature range of 300
°C to 650 °C are termed S2. The S2, expressed in milligram hydrocarbons per

gram of rock, measures the kerogen's potential to generate hydrocarbons if subjected to increased burial temperatures. It is also used as an indicator of the amount of hydrogen associated with the kerogen.

c) The temperature at which the maximum generation of S2 hydrocarbons occurs during pyrolysis is known as Tmax.  The Tmax is expressed in °C, and it is used to appraise the source rock's maturity. It varies with each class of kerogen.

d) The amounts of carbon dioxide generated and recorded between 300 °C to 400 °C during pyrolysis are known as S3. The S3 is expressed in milligram $CO_2$ per gram of the rock. Besides the measurements of carbon dioxide, the amounts of carbon monoxide during pyrolysis are also recorded.  The S3 is used as an indicator of the quantity of oxygen associated with the kerogen.

e) After the pyrolysis cycle, the pyrolysis instrument is cooled down before the commencement of the oxidation cycle. During the oxidation cycle, measurements are made separately for carbon dioxide that evolved during the early part of the oxidation cycle, designated as S4, and for the latter part of the oxidation cycle, which is defined as S5.

Carbon dioxide measurements in the latter part of the oxidation cycle (S5) occurs within a temperature range of 550 to 850 °C, and it represents $CO_2$ that evolved from the decomposition of carbonates. Measurements of carbon monoxide are also done simultaneously during the oxidation cycle. Both the S4 and S5 are expressed in milligrams $CO_2$ per gram of the rock.

f) Total Organic Carbon (TOC) measurements on the analyzed rock sample are determined from the pyrolysis and oxidation parameters.  The TOC measures the organic richness of the rock, and it is express in weight %.

In addition to the critical parameters of S1, S2, S3, S4, TOC, and Tmax, three other parameters are derived from S1, S2, and total organic carbon. These are Hydrogen Index (HI), Oxygen Index (OI), and Production Index (PI)

The HI is computed from $S2/TOC \times 100$. It indicates the amount of hydrocarbon that can be generated relative to the amount of TOC in the source rock. It is expressed in milligram hydrocarbon per gram TOC.

The Oxygen Index is derived from $S3/TOC \times 100$. It indicates the amount of carbon dioxide that can be produced relative to the amount of TOC in the source rock. The OI is expressed in milligram $CO_2$ per gram TOC.

Production Index (PI) is derived from $S1/(S1+S2)$. The PI represents the quantity of hydrocarbon that has been produced relative to the amount that could be generated.

## 4.3.2: ORGANIC PETROGRAPHY

The organic petrographic analysis, vitrinite, and bitumen reflectance (% VRo and % BRo, respectively) measurements were performed on polished pellets of rock chips and kerogen concentrates. The analysis was carried out at the Geological Survey of Canada, Calgary.

The pellet blocks were constructed by mixing rock chips, and kerogen concentrates, and slow curing resin in plastic molds. The pellets were polished using a multi-step polishing method and Leco polishing machine. The random reflectance measurement was carried out under oil immersion following the ASTM D7708-11 method (Hackley et al., 2011; Hackley et al., 2015). The petrographic analysis was performed using a Zeiss Axioplan microscope equipped with LED light and ultraviolet (UV) light sources

and Diskus-Fossil System for reflectance measurements. Fluorescence microscopy was carried out using ultraviolet G 365 nm excitation with a 420 nm barrier filter.

### 4.3.3: KEROGEN EXTRACTION

A four-stage approach was used to extract kerogen from the source rock (Horvath and Jackson, 1981) at the University of the Western Cape.

a) Sample Preparation

Source rock samples were prepared for kerogen extraction by drying them in an oven at a temperature of 60 °C for thirty minutes. The dried samples were pulverized to a fine powder in a porcelain mortar with a pestle. Approximately 10 grams of the crushed sample was weighed into a thimble.

b) Removal of extractable organic matter

The soluble organic matter was extracted from the powdered rock samples with 120:80 benzene/methanol solution using a Soxhlet extraction apparatus for about forty-eight hours. However, if the color persists in the extraction solution after forty-eight hours, the extraction was continued until the solution turned colorless.

c) Removal of carbonate minerals

The extracted powder was dried in an oven at a temperature of 50 °C and then treated with hydrochloric acid to remove the carbonate minerals. The dried powder was placed in a Pyrex beaker; 0.5N HCL was slowly stirred into the mixture until effervescence (liberation of $CO_2$) ceased. The beaker was then covered with a watch glass and allowed to stand on a steam bath for 4 to 5 hours at a low-temperature setting, about 50 °C. Occasional stirring and sonication were necessary to ensure the complete removal of carbonate. The

mixture was then allowed to stand overnight, the supernatant solution decanted, and fresh acid added. The steam bath/stirring/sonication procedure was repeated.

The supernatant solution was decanted, and the solid residue was then washed with distilled water. The final residue was air-dried.

d) Removal of silicates

The dried residue was transferred to hydrofluoric acid (HF)- resistant beaker, and a 1:4 HCL/HF mixture was added. The suspension was allowed to stand for 8 to 10 hours with occasional stirring. The solid residue was allowed to settle and the supernatant acid solution decanted. A fresh acid mixture was added, and the process repeated until the residual rock material is no longer coarse. The solid residue was then mixed with distilled water; the mixture was centrifuged, and the supernatant solution decanted. The washing process was repeated until the supernatant solution turned neutral to pH paper. The residue was allowed to air dry.

## 4.3.4: LOSS ON IGNITION (LOI)

The loss on ignition test was carried out using a furnace at the University of the Western Cape. Source rock samples were dried in an oven at a temperature of 105°C for 24 hours and then pulverized to a fine powder. The crushed samples were weighed individually in the crucibles on a four decimal place balance and placed in an oven at a temperature of 550°C for twenty-four hours; the crucibles were labeled to correspond to the individual sample. The samples were removed from the oven after twenty-four hours, allowed to cool, and then reweighed.

The difference in weights provided an estimate of the organic matter content of the samples.

## 4.3.5: THERMOGRAVIMETRIC ANALYSIS (TGA)

Thermogravimetric analysis (TGA) was performed on source rock samples with Perkin Elmer STA 6000 at the University of the Western Cape.

The analysis used source rock samples that had been dried in an oven at a temperature of 105°C for 24 hours and then pulverized to a fine powder. The dried and pulverized sample was loaded individually with a spatula into the instrument's sample pan that resides in the furnace; the sample pan is supported by a precision balance that measures the sample's weight. The sample's heating was carried out within a temperature range of 40 °C to 700 °C at a rate of 10 °C/minute in a nitrogen atmosphere with a purge rate of 20 ml/minute.

## 4.3.6: SOLVENT EXTRACTION

About 5 to 20 grams of each powdered rock sample was subjected to Soxhlet extraction for 72 hours using dichloromethane as solvent at the Geological Survey of Canada, Calgary. Activated copper grains were added to the extract at the end of extraction or during solvent removal to remove any elemental sulfur. After removing most of the solvent using a rotary evaporator, the extract contents were filtered to remove copper, copper sulfide, and other solids. The residue was retained and weighed as total extract after removing the remaining solvent using a gentle stream of nitrogen.
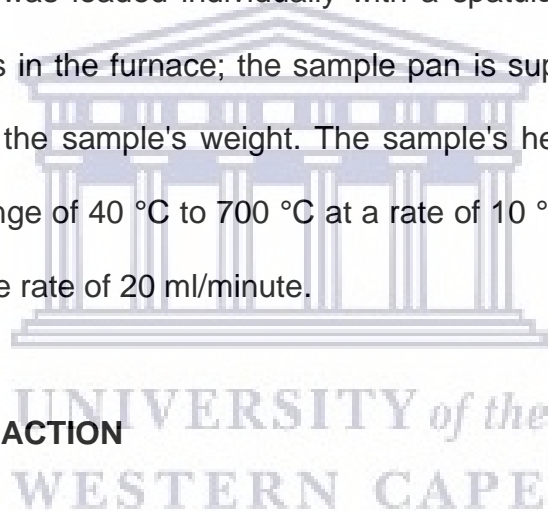
### 4.3.7:  COLUMN CHROMATOGRAPHY FRACTION

Rock extracts and crude oils were de-asphaltened with *n*-pentane at the Geological Survey of Canada, Calgary. They were then separated into aliphatic, aromatic, and polar fractions by column chromatography using a mixture of silica gel and alumina (1:3 by weight) as support.  *n*-Pentane (3.5 mL per gram of support) was used to elute the aliphatic fraction, followed by *n*-pentane/dichloromethane (1:1 by volume and 4 mL per gram of support) to isolate the aromatic fraction.  Methanol (4 mL per gram of support) and chloroform (6 mL per gram of support) were finally used to obtain the polar fraction.

### 4.3.8:  GC AND GC-MS OF $C_{12}^+$ HYDROCARBON FRACTIONS

GC analysis of saturated fractions was completed on a Varian 3700 GC equipped with a flame ionization detector (FID) at the Geological Survey of Canada, Calgary.  A 30m $\times$ 0.25mm $\times$ 0.25$\mu$m DB-1 fused silica capillary column was used with helium as the carrier gas.  The samples were injected using a split injector heated at 320 °C.

The temperature program was 60°C (@6°C/min) $\rightarrow$300°C (30min). The FID temperature was maintained at 320 °C.

GC-MS analysis of the aliphatic fractions was carried out on an Agilent Triple Quad MS system in selected ion monitoring (SIM) mode.  Split injection (1:10) was employed into an HP-5MS 30m $\times$ 0.25mm $\times$ 0.25$\mu$m capillary column with helium as carrier gas at a flow rate of 1.2 mL/min.  The mass spectrometer ion source was operated at 70 eV ionization voltage.

GC-MS analysis of the aromatic fractions was performed on an Agilent 6890 series GC coupled to a 5973 series Mass Selective Detector (MSD) operated in SIM mode. The split injection was employed into a J and W DB-5 30m × 0.32mm × 0.25μm capillary column at 300 °C. Helium was used as carrier gas at a flow rate of 1.2 mL/min.

The GC oven temperature was programmed as follows: 40°C (@4°C/min)→325°C (15min).

Compound identification was based on a comparison of GC retention times and mass spectra with those reported in the literature and historical data in the GSC-Calgary organic geochemistry laboratories.

## 4.3.9: THERMAL DESORPTION GAS CHROMATOGRAPH (TD-GC)

The TD-GC analysis was carried out using an Agilent 7890A GC instrument at Agat Laboratories, Calgary. The samples' hydrocarbon composition was determined by separating the hydrocarbon compound mixtures into their components. A mass of 100 mg of each sample was heated to desorb and capture hydrocarbons.

The hydrocarbons were separated using a capillary column and a long tube with a silica-coated interior. The column separated the components based on their boiling points, resulting in hydrocarbons with the lowest molar mass eluting first, and the highest molar mass eluting last. The separated fractions were detected by the flame ionization detector (FID), which measures ions per unit time to quantify the relative proportion of each hydrocarbon component.

## 4.4.0: HAWK PETROLEUM ASSESSMENT METHOD (HAWK-PAM)™

The HAWK petroleum assessment method (A. Maende, 2016) was carried out using the HAWK pyrolysis instrument at Agat Laboratories, Calgary, and Wildcat Technologies, Humble, Texas.

The assessment utilized five zones using multiple ramp and isotherm routines assigned during a single sample analysis.

A ramp rate of 25°C was used to generate five petroleum peaks – four on oil fractions and one on kerogen. Each isotherm has its own specific Tmax indicative of the maximum evolution temperatures. The HAWK-PAM measurements enable better quantification of the volatile oil than was previously possible on pyrolysis instruments since the analysis is initiated at 50°C. Also, this method allows for the measurement of API.
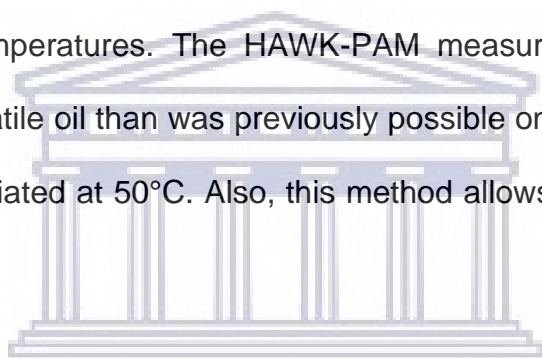
## 4.4.1: CHNS (CARBON, HYDROGEN, NITROGEN, SULFUR) ANALYZER

The total Carbon, Hydrogen, Nitrogen, and Sulfur was assessed using Vario EL Cube Elemental Analyzer at Stellenbosch University.

A known weight of the dried, homogeneous sample was weighed into an Aluminium foil boat, and the sample was introduced into the combustion column at 1050 °C. The Combustion column was filled with Tungsten trioxide ($WO_3$) and then enriched with oxygen.

The C, H, N, and S in the samples were oxidized to form the following gaseous reaction products:

A.    $CO_2$

B.    $H_2O$

C.    $N_2$ and $NOX$

D.    $SO_2$ and $SO_3$

The Argon carrier gas carries the gaseous products through the reduction tube filled with copper wire. The reduction column reduces the NOx to $N_2$ and $SO_3$ to $SO_2$. All the volatile halogen compounds produced during combustion bound to the silver wool in the reduction column. The pure gasses were then carried to the adsorption columns. The $N_2$ does not adsorb and therefore reached the Thermal conductivity detector (TCD) first. The $CO_2$, $H_2O$, and $SO_2$ each get adsorbed onto the adsorption columns at room temperature for effective separation. The adsorption columns are then heated sequentially to desorb the different products and are carried through to the TCD (Thermal conductivity detector).

## 4.4.2: INDUCTIVELY COUPLED PLASS-MASS SPECTROMETRY (ICP-MS)

The trace element analysis was carried out using the Agilent 7900 ICP-MS at Stellenbosch University. Approximately 0.5 g of dried homogeneous sample was weighed directly into the microwave digester Teflon vessel; 6ml of $HNO_3$ and 2 ml of HCl were added. The acidified sample was then digested using the MARS microwave digester. The vessel was cooled, and the sample was diluted ten times to reduce the acid concentration.

The digested samples were introduced into the instrument via autosampler by the peristaltic pump. The sample passes through the nebulizer, which produces a fine aerosol. The large droplets were removed by a spray chamber, and small droplets then pass through to the plasma. In ICP-MS, the plasma torch is positioned

horizontally and generates positively charged ions rather than photons. Once the ions are produced in the plasma, they are directed into the mass spectrometer via the interface region, which is maintained at a vacuum of 1 - 2 torr with a mechanical roughing pump. This interface region consists of two metallic cones (usually made of nickel), called the sampler and a skimmer cone. Each cone features a small (0.6 - 1.2 mm) orifice to allow the ions through to the ion optics, where they are guided into the mass separation device. Once the ions have been successfully extracted from the interface region, they are directed into the main vacuum chamber by a series of electrostatic lenses called ion optics. A turbomolecular pump maintains the operating vacuum in this region at about $10^{-2}$ torr. The optic area electrostatically focuses the ion beam towards the mass separation device and stops photons, particulates, and neutral species from reaching the detector.

The ion beam containing all the analyte and matrix ions exit the ion optics and pass into the heart of the mass spectrometer - the mass separation device, where a second turbomolecular pump maintains an operating vacuum of approximately

$10^{-6}$ torr. The separation device allows analyte ions of a particular mass-to-charge ratio (m/z) to the detector and filters out all the non-analyte, interfering, and matrix ions. In the final process, an ion detector converts the ions into an electrical signal. This signal is expressed as counts using Masshunter software for calculating the results.

### 4.4.3: $^{\delta}$13C ISOTOPIC ANALYSIS

Analysis of $^{\delta}$13C on the whole oil (oil sands and oil seeps) was performed using Continuous Flow-Elemental Analysis-Isotope Ratio Mass Spectrometry (CF-EA-IRMS) technology at the University of Calgary.

A Thermo DeltaVPlus ® mass spectrometer was interfaced with either an Elementar Isotope CUBE® or Costech 4010® elemental analyzer via a ConfloIV® device. All materials were packed in tin cups of varying and appropriate size, which were dropped by autosampler onto a quartz tube combustion reactor. The temperature of the reactor was maintained at ~1000 ℃. Flash-combustion was achieved by injecting a pulse of $O_2$ (gas) precisely at the time of the sample drop.

The eluent gases were then swept by the helium carrier stream through a reduction reactor (~650 ℃), which reduces NOx species in the samples to $N_2$ (gas).

GC separation of $N_2$ and $CO_2$ was achieved before the gas stream was leaked through the Conflo-IV open split into the mass analyzer's ion source. $\delta$13C values were determined by comparing the respective sample peak areas, as [Vs], to reference gas peaks also inlet through the open split.

Stable isotope ratios are expressed as delta ($\delta$). They are measures of a 'per mill' (‰)or parts per thousand difference between the isotope ratio of a sample and a known (International) standard material. Values are reported relative to the 'Vienna Peedee Belemnite' (VPDB) formation for Carbon (Craig, 1957).

### 4.4.4: CRUDE OIL ASSAY

The assessments for Carbon, Hydrogen, Nitrogen, Density, API gravity, weight %, and Sulfur were performed using **ASTM D5291C** (ASTM, 2010)**, ASTM D70** (ASTM, 2009)**, ASTM D1552** (Zhao and Shaw, 2007)**,** respectively**.** Besides, Boiling Point Distribution, Viscosity, Water Contents, and Total Acid Number were determined using **ASTM D7169** (ASTM, 2011a)**, ASTM D5018** (Kayukawa et al., 2017)**, ASTM D4377** (ASTM, 2011b)**, and ASTM D8045** (Rahimi, 2019)**.** The analyses were carried out at CanmetENERGY, Devon.

For the descriptions of the ASTM Standards, see https://www.astm.org/

## GEOCHEMICAL EVALUATION OF   SOURCE ROCK POTENTIAL

### 5.1:    RESULTS AND DISCUSSION

The chapter presents and discusses the results of source rock assessments. It begins with the evaluation of source rock that underlies outcrops of oil sands and is then followed by the appraisal of borehole and core samples.

### 5.2:    ROCK-EVAL RESULTS FROM J4 LOCATION (OGUN BELT)

The pyrolysis measurements of the claystones analyzed from the outcrop of the Afowo Formation located in the Ogun Belt are presented in Table 10 and Figures 32, 33, 34, 35, and 36. The outcrop is located at latitude 06° 40' 755" N, and longitude 04° 18' 613" E at an elevation 21 m above mean sea level (Table 1). It has a thickness of 11.65 m, and the lithology is composed sequentially of 8.42 m of lateritic sand, 0.79 m of oil sand, and 2.44 m of claystone.

The critical questions in source rock screening and evaluation relate to the quantity and quality of the organic matter in the rock, its potential to generate oil or gas, and whether the rock has been adequately heated to produce oil or gas.  Except for the sample acquired at a depth of 8.7m, the pyrolysis results (Table 10) provided critical source rock evaluation parameters.

*Table 10: HAWK summary data showing the pyrolysis results of the Afowo claystones (Mohammed et al., 2019).*

| Sample ID | Sample Depth (m) | Tmax °C | S0 (mg/g) | S1 (mg/g) | S2 (mg/g) | S3 (mg/g) | PC (%) | PI | S2/S3 | S1/TOC | TOC % | HI | OI |
|-----------|------------------|---------|-----------|-----------|-----------|-----------|--------|------|-------|--------|-------|-----|-----|
| AF-1 | 8.7 | - | 0.05 | 0.18 | 0.22 | 1.38 | 0.03 | 0.45 | 0.16 | 0.22 | 0.81 | 26 | 169 |
| AF-2 | 9.0 | 424 | 0.03 | 2.85 | 22.98 | 1.79 | 2.14 | 0.11 | 12.84 | 0.43 | 6.57 | 349 | 27 |
| AF-3 | 9.3 | 420 | 0.10 | 2.58 | 27.15 | 2.96 | 2.47 | 0.09 | 9.17 | 0.19 | 13.40 | 202 | 22 |
| AF-4 | 9.6 | 417 | 0.08 | 10.02 | 56.33 | 3.24 | 5.51 | 0.15 | 17.39 | 0.54 | 18.46 | 305 | 17 |
| AF-5 | 9.9 | 423 | 0.07 | 8.21 | 50.64 | 4.56 | 4.88 | 0.14 | 11.11 | 0.58 | 14.17 | 357 | 32 |
| AF-6 | 11.3 | 419 | 0.02 | 2.69 | 16.71 | 3.28 | 1.61 | 0.14 | 5.09 | 0.45 | 5.95 | 280 | 55 |
| AF-7 | 11.65 | 426 | 0.03 | 3.05 | 31.48 | 8.08 | 2.87 | 0.09 | 3.90 | 0.23 | 13.33 | 236 | 60 |

*Note: The clay sample at a depth of 8.70 m is very lean in its hydrocarbon generating potential since its S2 value is less than*

*0.5 mg HCs/g rock. Subsequently, its Tmax value could not be estimated.*

*Tmax; °C = Temperature at which the maximum rate of generation of hydrocarbons occurs during the thermal break down of kerogen.*

*S0, mg HCs/g rock = Free hydrocarbons that are present in the sample.*

*S1, mg HCs/g rock = Thermally free hydrocarbons that are detected from the start of the pyrolysis up to 300 °C.*

*S2; mg HCs/g rock = Volume of hydrocarbon that was generated during the thermal breakdown of kerogen.*

*S3; mg CO$_2$/g rock = The amount of CO$_2$ that was produced during the pyrolysis of kerogen.*

*PC; wt. % = Pyrolyzable organic carbon*

*PI= Production Index; TOC = Total Organic Carbon (wt. %); HI = Hydrogen Index; OI= Oxygen Index.*

The source rock results at a depth of 8.7 m were compromised by poor data quality due to a small S2 value (0.22 mg HC/g) and excluded from the analysis and interpretation. When the S2 peak is small, inaccurate Tmax values are often selected during the Rock Evaluation analysis (Peters, 1986), which complicates the interpretation (Dembicki, 2009).

The results indicate an abundance of total organic carbon within the range of 5.95 % to 18.46 wt. % and exhibited a degree of variability with depth. A general increase in organic carbon content (Table 10, Fig. 32) from 6.57 wt. % to 18.46 wt. % was observed from the depth of 9.0 m to 9.6 m, while the TOC content for the lower part of the sequence from 9.9 m to 11.65 m showed significant variation and did not increase with depth. A TOC value of 14.17 wt. % was recorded at a depth of 9.9 m, while measurements at the depths of 11.30 m and 11.65 m showed variation in TOC values from 5.95 wt.% to 13.33 wt.%.
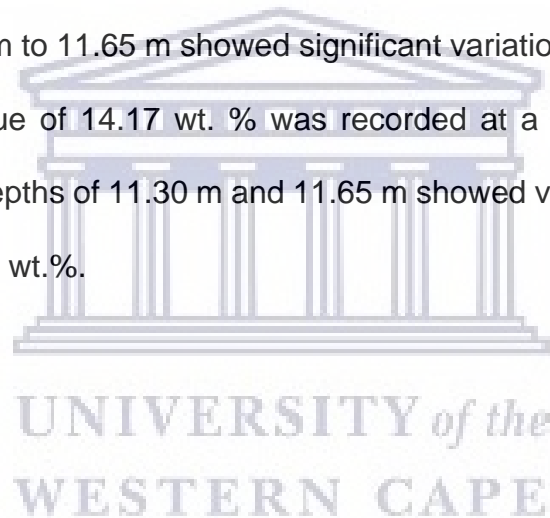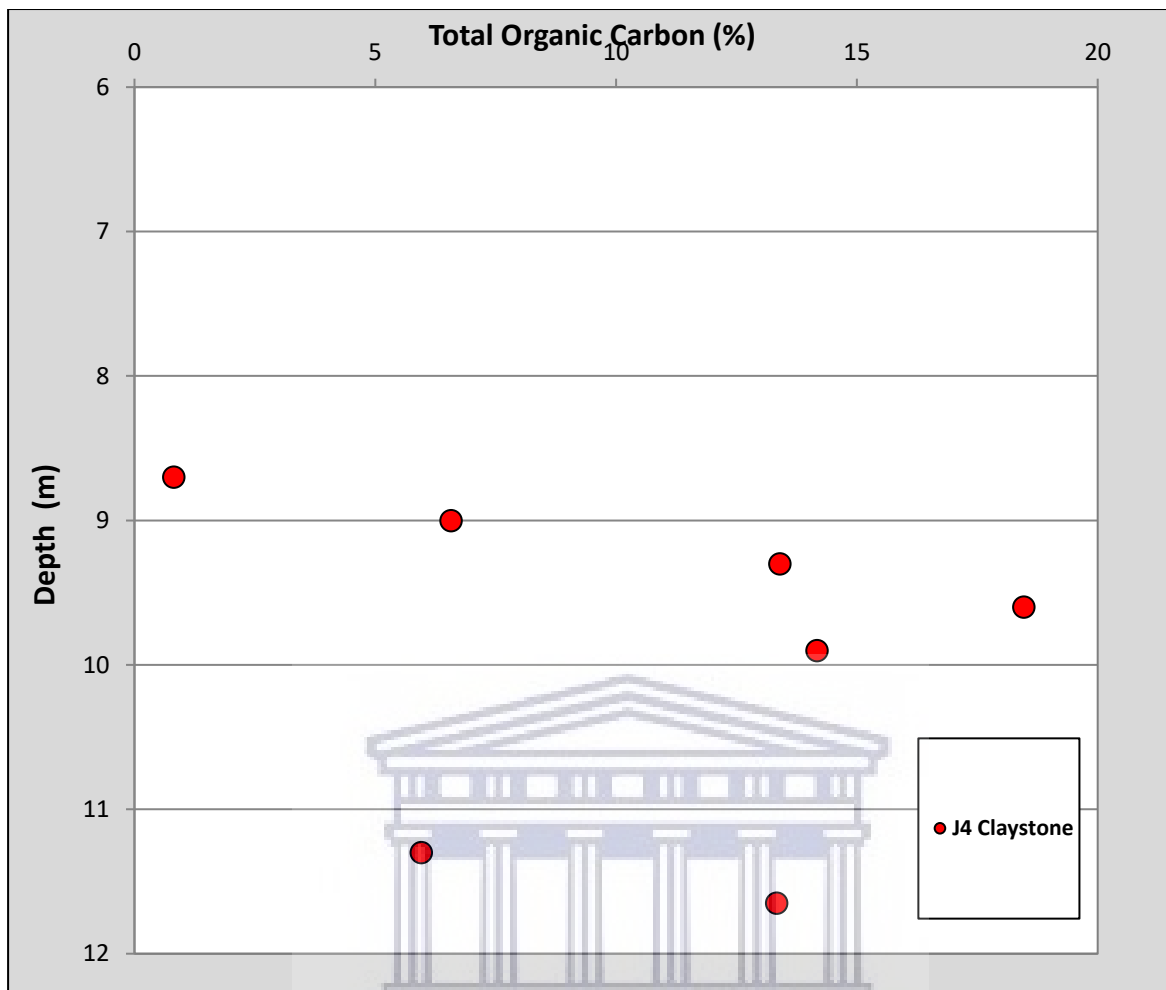
*Figure 32: Profile of total organic carbon (TOC, wt. %) for an outcrop of Afowo claystone underlying the oil sand deposits at the J4 location (Mohammed et al., 2019).*

The hydrocarbon generating potential remaining in the rock's kerogen (S2) ranged from 16.71 mg HC/g rock to 56.33 mg HC/g rock and indicated variable patterns similar to that described for Total Organic Carbon. The variations in Total Organic Carbon and S2 over the depth intervals reflected relative changes in the abundance of organic matter and hydrocarbon generating potentials remaining in the rock's kerogen. The high TOC and S2 of the source rock appear to suggest a low level of thermal maturity; thermal maturation of organic matter mostly parallels a decrease in TOC and S2 due to thermal cracking of the kerogen to generate petroleum (Mohammed et al., 2020).

The total organic carbon (TOC, wt.%) and the hydrocarbon yields from kerogen (S2) were used to evaluate the source richness. The high TOC values (6.57 wt. % to 18.46 wt.%) and S2 values (16.71 mg HC/g rock to 56.33 mg HC/g rock) indicated that the claystones have excellent source richness and excellent hydrocarbon generating potential. Also, thermally free hydrocarbon (S1) ranged from 2.58 mg HC/g rock to 10.02 mg HC/g rock, suggesting that the claystones could be exploited as unconventional hydrocarbon resources, similar to oil shales.

Kerogen typing and petroleum quality are primarily influenced by hydrogen content in the constituent organic matter of the source rock. The cross plot of S2 mg HC/g rock against TOC wt. % (Fig. 33) indicated good quality organic matter in the rock and showed Type II and Type II/III kerogens. The hydrogen index (HI) showed a variation from 202 mg HC/g TOC to 357 mg HC/g TOC (Table 10). Source rocks at the depths of 9.0 m, 9.6 m, 9.9 m displayed HI within the range of 305 mg HC/g TOC to 357 mg HC/g TOC indicating Type II kerogen with the potential to generate oil. In contrast, the HI index for similar source rocks at depths of 9.3 m, 11.3 m, and 11.65 m presented values within the range of 202 mg HC/g TOC to 280 mg HC/g TOC which is typical of Type II – Type III kerogen. The oxygen index (OI), another useful parameter for kerogen typing, ranged from 17 mg $CO_2$/g TOC to 60 mg $CO_2$/g TOC and showed variability with depth. The cross plot of HI versus OI is shown in Figure 34.
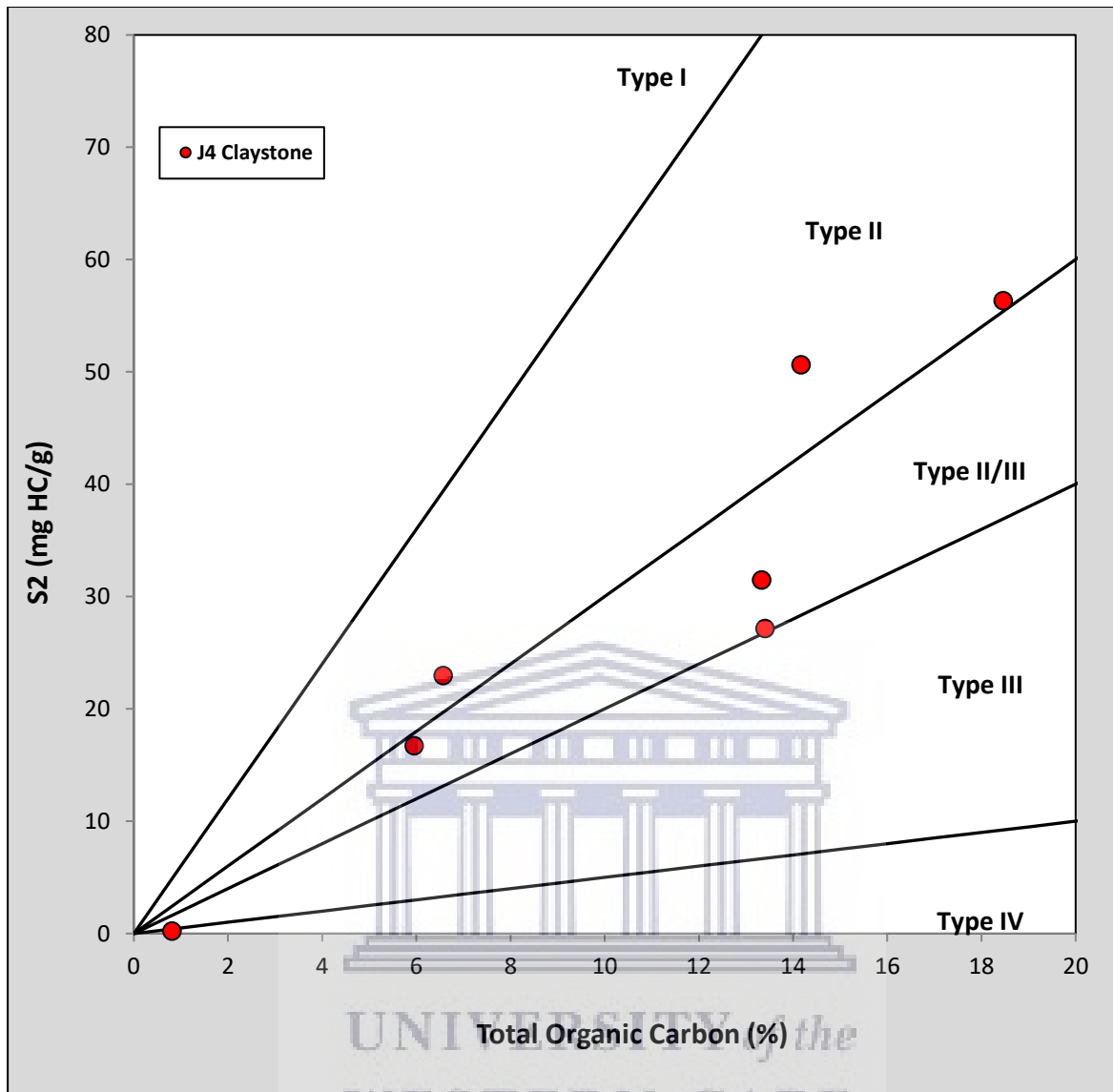
*Figure 33: Cross plot of S2 against TOC showing kerogen type. The result for the claystone at a depth of 8.7 m was compromised and excluded from the analysis and interpretation. The outlier with very low TOC and S2 showed the results for the source rock at a depth of 8.7 m (Mohammed et al., 2019).*
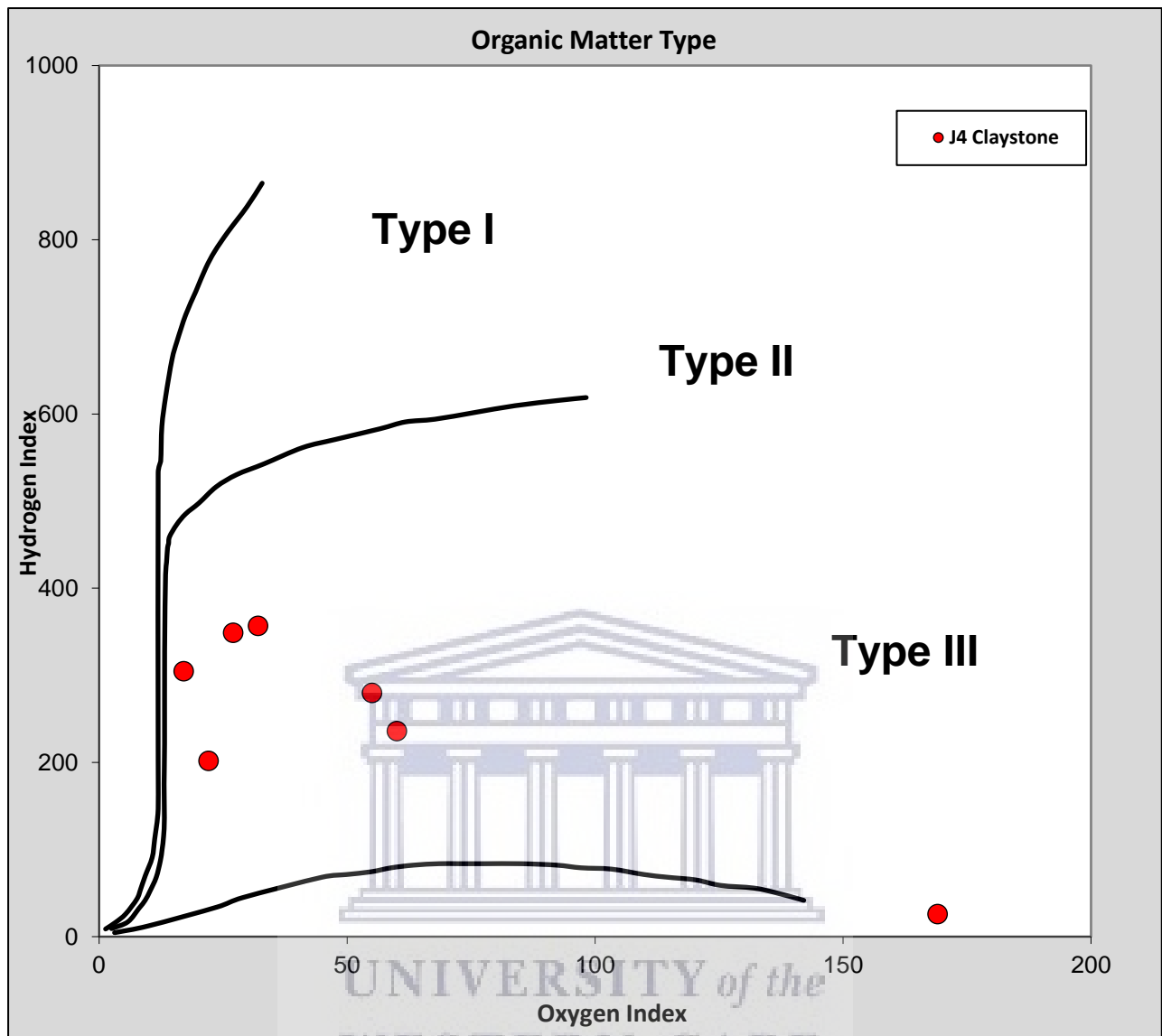
*Figure 34: Display of Hydrogen Index versus Oxygen Index showing kerogen types. The outlier with very low HI and high OI showed the source rock's result at a depth of 8.7 m (Mohammed et al., 2019).*

Hydrocarbon generation due to the thermal breakdown of organic matter in the source rock during its burial history is a part of the overall process of thermal metamorphism of organic matter (Tissot and Welte, 1984). The hydrocarbon types produced by petroleum source rocks throughout its evolutionary pathway are influenced by the quantity/quality of organic matter and organic maturation temperature. In Rock-Eval, Tmax is the principal parameter for determining the thermal maturity of kerogen. The Tmax values for the source rock ranged from 417 °C to 426 °C, indicating thermal

immaturity. The degree of the organic matter's thermal evolution agrees with the observations made from the interpretations of high S2 and TOC contents for the source rock. The highest Tmax value recorded for the source rock sample was 426 $^o$C at a depth of 11.65 m, whereas the source rock sample acquired at a depth of 9.6 m presented the lowest Tmax value of 417 $^o$C (Table 10, Fig. 35). While a Tmax value of 424 $^o$C was recorded for the source rock at a depth of 9.0 m, the source rock at the depths of 9.3 m, 9.6 m, 9.9 m, and 11.3 m presented lower Tmax values of 420 $^o$C, 417 $^o$C, 423 $^o$C, and 419 $^o$C respectively. It has been recognized that Tmax generally increases with increasing depth (Espitalie et al., 1977). Still, variations in Tmax measurements with increasing depths can be caused by mineral matrix effects and retention of heavy resins and asphaltene compounds from the bitumen (Espitalie et al., 1980), resulting in Tmax reversals.
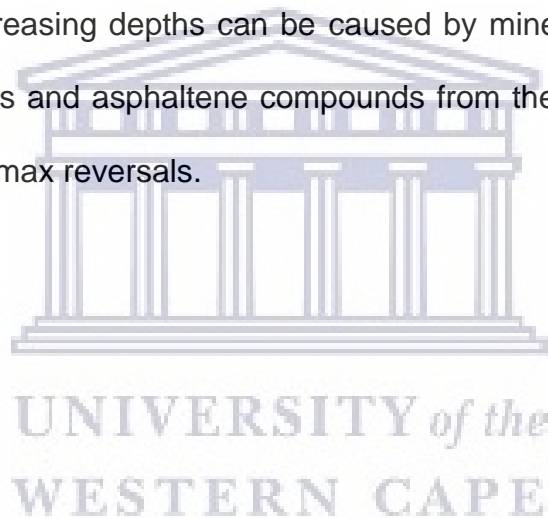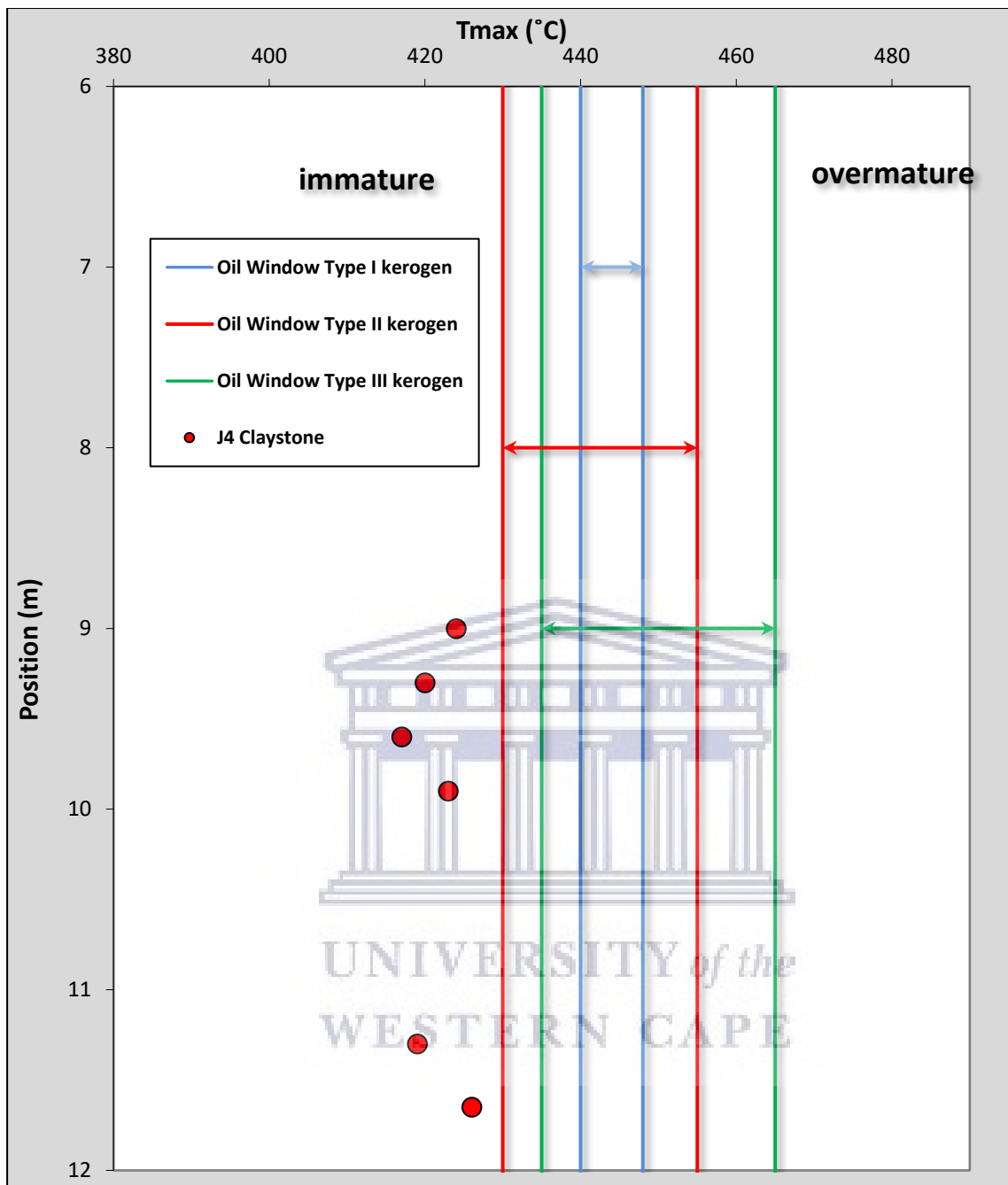
*Figure 35: Profile of Tmax for the source rock. The Tmax showed maturation temperatures below 435 °C, suggesting thermal immaturity (Mohammed et al., 2019).*

The cross plots of S2 versus TOC and HI against OI (Figs. 33 and 34) illustrated the source rock's kerogen types. The cross plots showed Type II and Type II/III kerogens and suggested marine and terrestrial sedimentation. These kerogen types are prone to generate both oil and gas at higher maturation temperatures.

Besides the cross plots of S2 versus TOC and HI against OI, the cross plot of HI

against Tmax (Fig. 36) indicated a dominance of oil and gas prone Type II/III kerogen. The cross plot of HI against Tmax (Fig. 36) combines an indicator of kerogen type, HI, with a maturity indicator, Tmax (Espitalié, 1986), and some geochemists prefer it ( Dembicki, 2017).
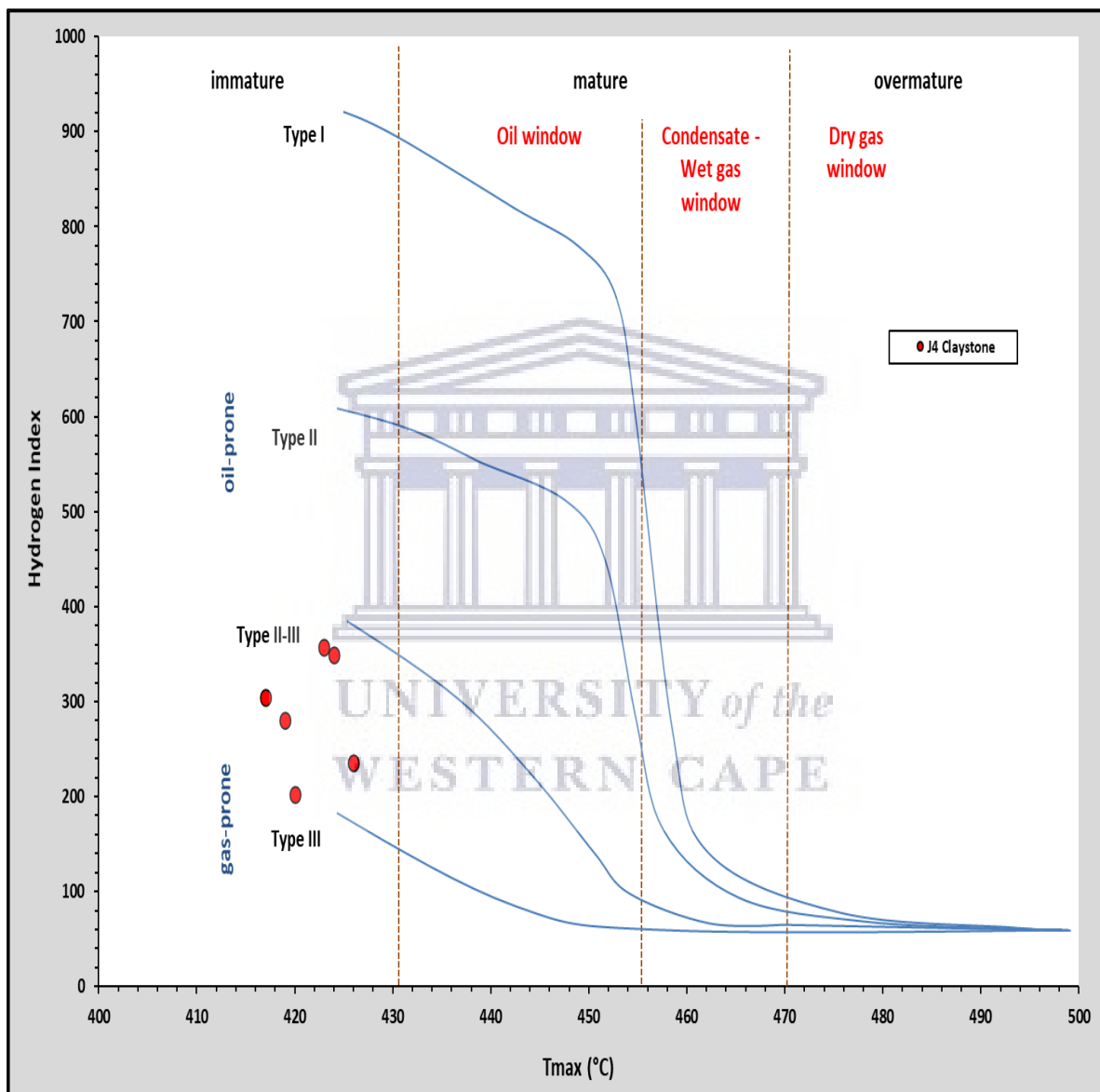


*Figure 36: Cross plot of HI against Tmax showing Type II-III kerogen (Mohammed et al., 2019).*

The rock evaluation results of the claystones (Table 10, Figs. 32, 33, 34, 35, and 36) suggest thermal immaturity, Type II, Type II to Type III kerogen, and the potential to generate both oil and gas at higher Tmax. The high TOC, S2, and S1 values suggest

that the claystones can be burned directly to produce a combustible fuel (Cook and Sherwood, 1991). The results further illustrated that the claystones could not have been the source of the hydrocarbons in the overlying sand. The hydrocarbons in the overlying sand (oil sand) may have been generated by different source rocks within the basin, where they attained a greater burial depth and temperature.

## 5.3: RESULTS OF LOSS ON IGNITION AND THERMOGRAVIMETRIC ANALYSIS

Rock-Evaluation (Rock-Eval) has been a petroleum industry-standard analysis for source rocks. However, a multi-parameter approach is recommended since single data types may be in error or affected by contamination( Dembicki, 2017). The multi-parameter method requires that more than one analytical method be used to appraise source rocks to establish a high degree of confidence in the results( Mohammed et al., 2020). Thermogravimetric analysis (TGA) and loss on ignition (LOI) could provide valuable information to characterize clay minerals (Jozanikohan et al., 2015) and to determine total organic carbon (Al-Selwi and Joshi, 2015). The additional data from loss on ignition and thermogravimetric analysis complement other measurements for robust source rock evaluation (Mohammed et al., 2020). The source rock (Table 10) was also evaluated by loss on ignition and thermogravimetric analysis to assess complementariness and validate findings.

Results of loss on ignition and thermogravimetric analysis for the five source rocks analyzed in this study are presented in Table 11 and Figures 37, 38, 39, 40, 41, and 42.

.

*Table 11: Loss on Ignition (LOI) summary data showing organic matter contents for the Afowo claystone (Mohammed et al., 2020).*

| Sample ID | Sample Depth (m) | Crucible Weight (g) | Pre LOI Crucible +Sample Weight (g) | Pre LOI Sample Weight (g) | Post LOI Crucible + sample Weight (g) | Post LOI Sample Weight (g) | Total Organic Matter Content (TOM, %) |
|---|---|---|---|---|---|---|---|
| AF-1 | 8.7 | 26.963 | 37.133 | 10.170 | 36.176 | 9.213 | 9.410 |
| AF-2 | 9.0 | 26.387 | 37.662 | 11.275 | 35.373 | 8.986 | 20.300 |
| AF-3 | 9.3 | 27.790 | 37.788 | 9.998 | 34.490 | 6.700 | 32.990 |
| AF-4 | 9.6 | 28.112 | 38.920 | 10.808 | 34.732 | 6.620 | 38.750 |
| AF-5 | 9.9 | 24.760 | 36.032 | 11.272 | 32.267 | 7.507 | 33.400 |

$$Total\ Organic\ Matter\ (TOM) = \frac{Pre\ ignition\ sample\ weight - Post\ ignition\ sample\ weight}{Pre\ ignition\ sample\ weight} \times 100$$
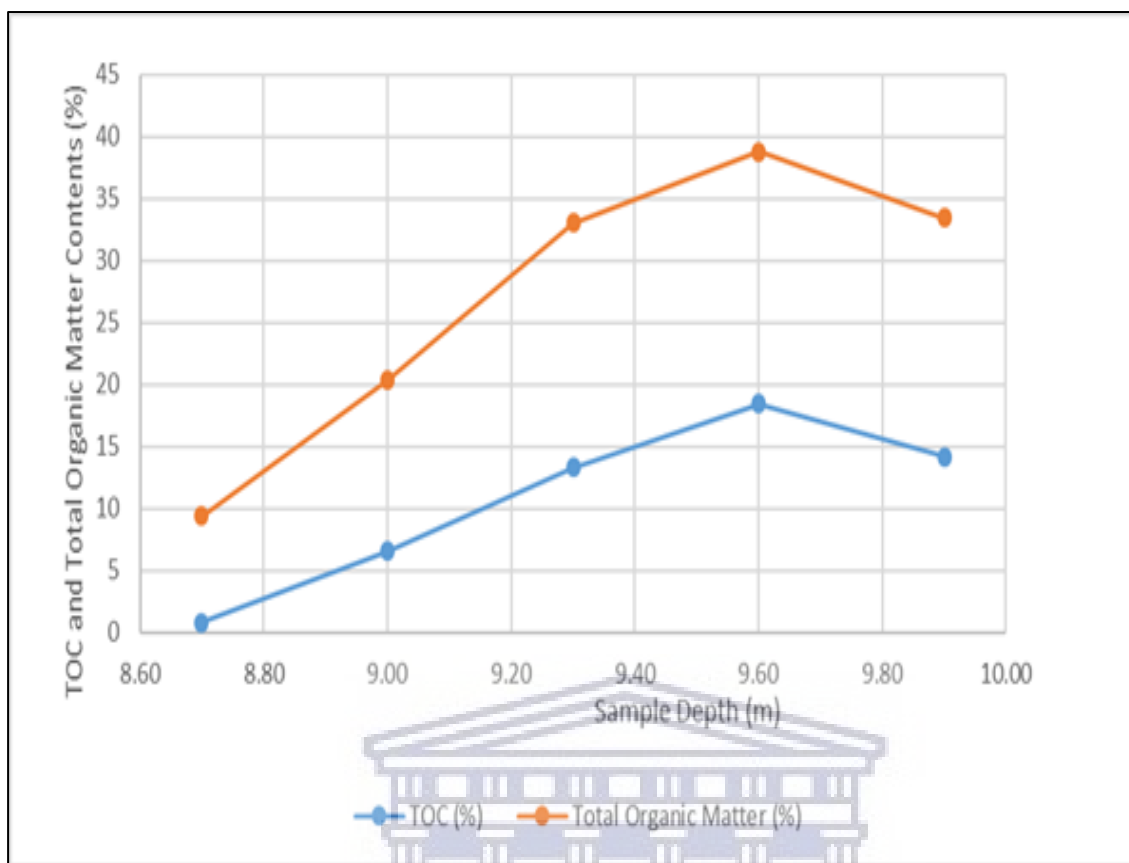
*Figure 37: Display showing a comparison of TOC and TOM (weight, %). The TOC and TOM variations are in sympathy with one another; source rocks with high TOM contents showed high TOC values (Mohammed et al., 2020).*

The loss on ignition results in Table 11 and Figure 37 indicated an abundance of organic matter. The total organic matter (TOM) content ranged from 9.410 wt. % to 38.750 wt.t %, and it showed a degree of variability with depth. The TOM comprises all the elements that are components of organic matter, such as carbon, hydrogen, nitrogen, and oxygen. It is used as a proxy for organic carbon. A general increase in TOM (Table 11, Fig. 37) from 9.410 wt. % to 38.750 wt. % was recorded throughout interval 8.7 m to 9.6 m.  The TOM content for the sample at a depth of 9.9 m showed a lower value (33.400 wt. %) when compared to the preceding TOM (38.750 wt. %) at 9.3 m, indicating variation in organic matter richness (Mohammed et al., 2020).

The results obtained from Thermogravimetric Analyses (TGA) are displayed in figures 38, 39, 40, 41, and 42.
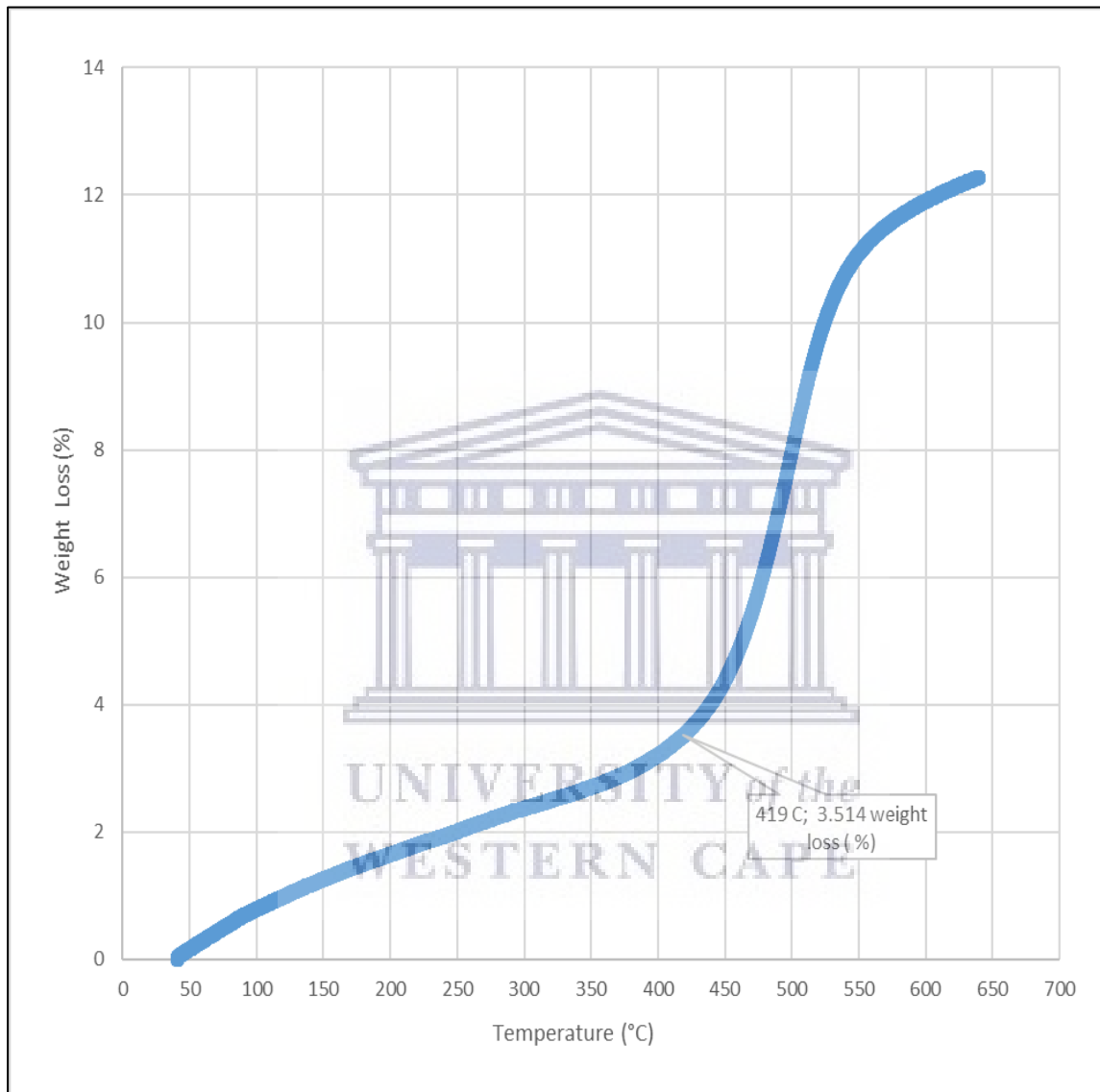


*Figure 38: Display of thermogravimetric analysis for the source rock at a depth of 8.7 m. The inflection corresponding to the temperature of 419 °C and weight loss of 3.514 % is estimated to be the onset temperature at which the maximum generation of hydrocarbons occurred from the thermal breakdown of kerogen (Mohammed et al., 2020).*
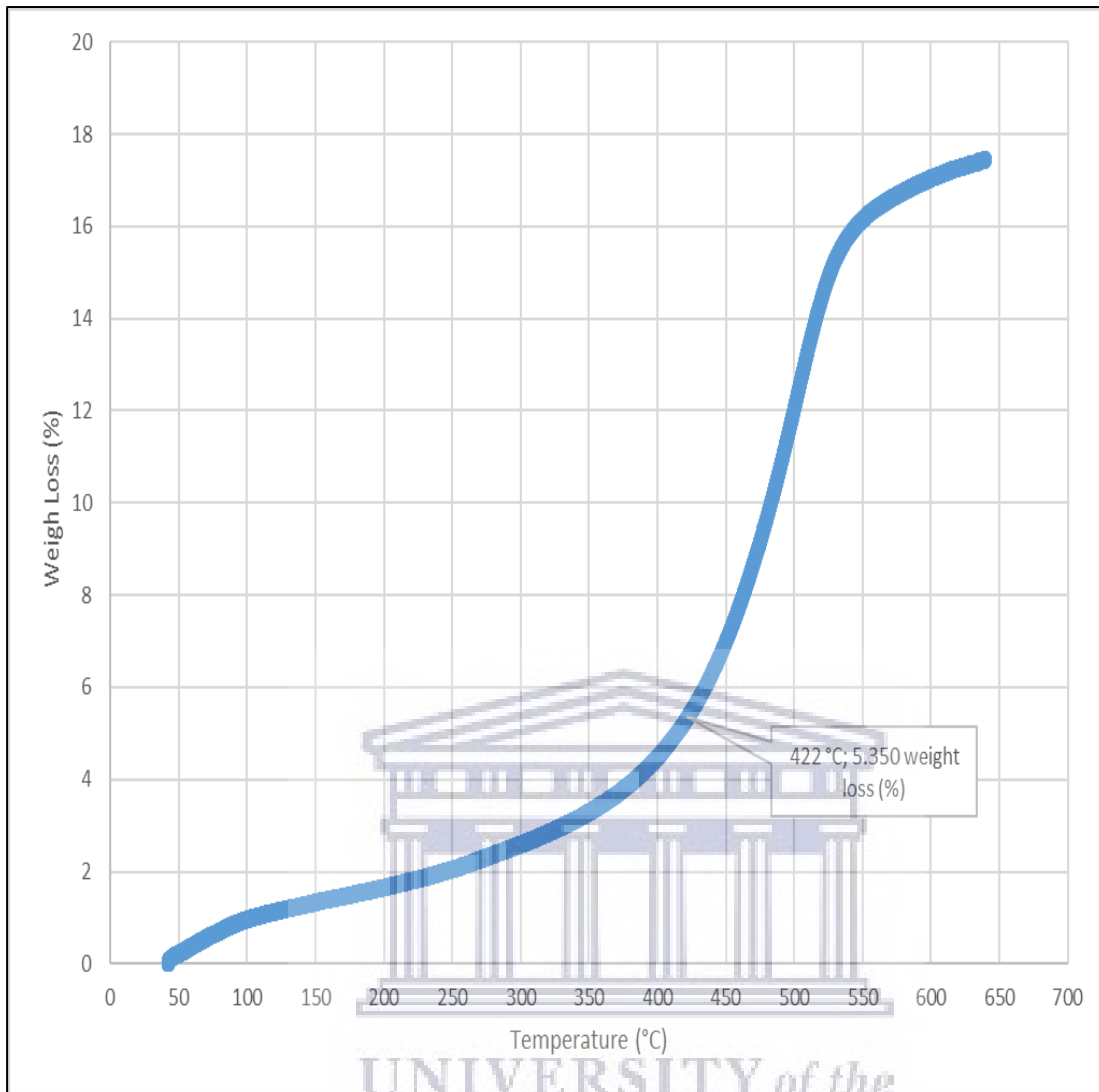
*Figure 39: Display showing thermogravimetric analysis (TGA) for the source rock at a depth of 9.0 m. The inflection point corresponding to the temperature of 422 °C and weight loss of 5.350 % is estimated to be the onset temperature at which the maximum generation of hydrocarbons occurred from the pyrolysis of kerogen (Mohammed et al., 2020).*
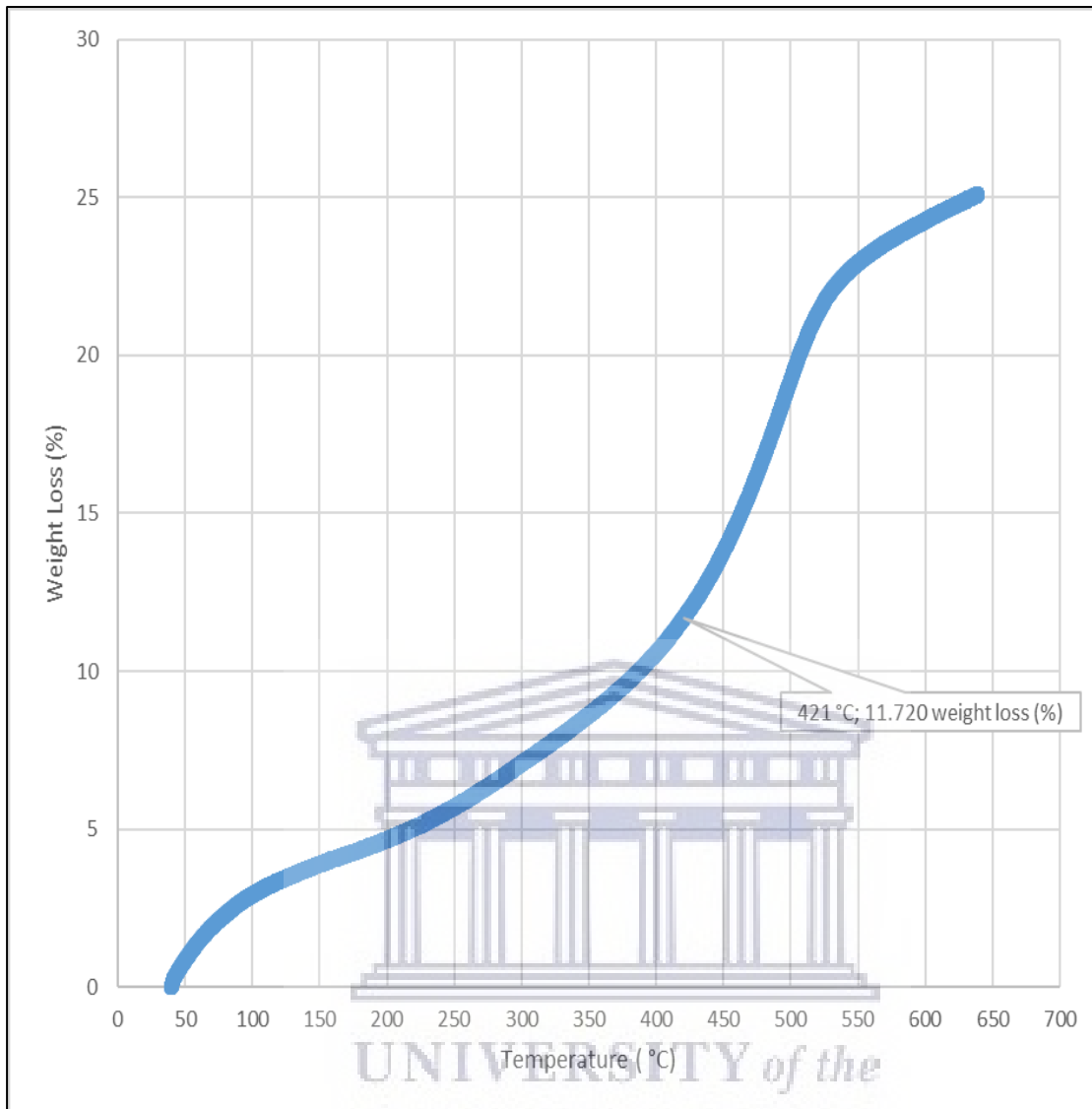
*Figure 40: Display showing TGA for the source at a depth of  9.3 m. The inflection point corresponding to a temperature of 421 ℃ and weight loss of 11.720 (%) is estimated to be the onset temperature at which the maximum generation of hydrocarbon occurred from the thermal break down of kerogen in the rock (Mohammed et al., 2020).*
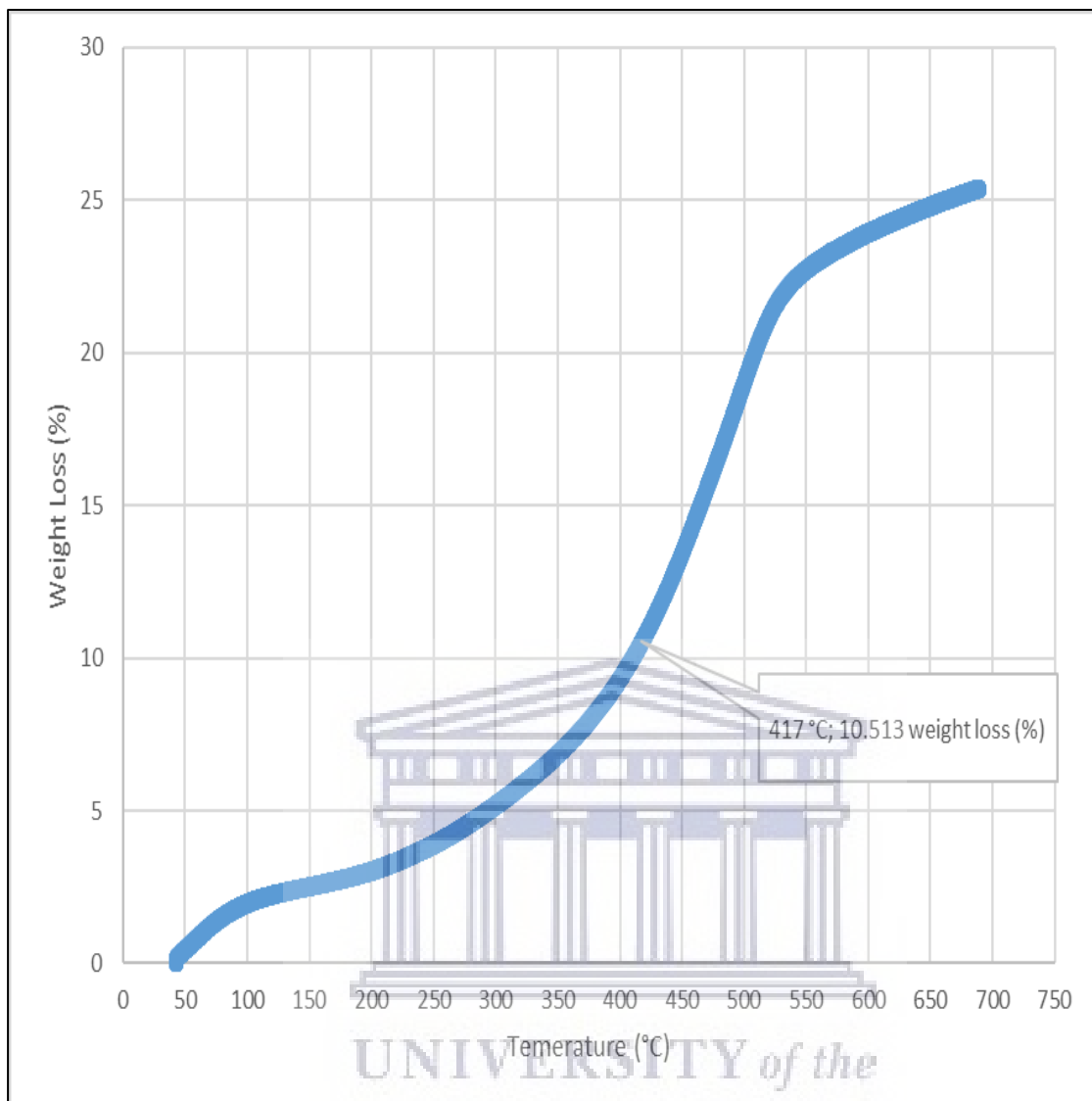
*Figure 41: Display showing thermogravimetric analysis for the source rock at a depth of 9.6 m. The inflection point corresponding to a temperature of 417 °C and weight loss of 10.513 % is estimated to be the onset temperature at which the maximum generation of hydrocarbons occurred from the thermal break down of kerogen in the rock (Mohammed et al., 2020).*
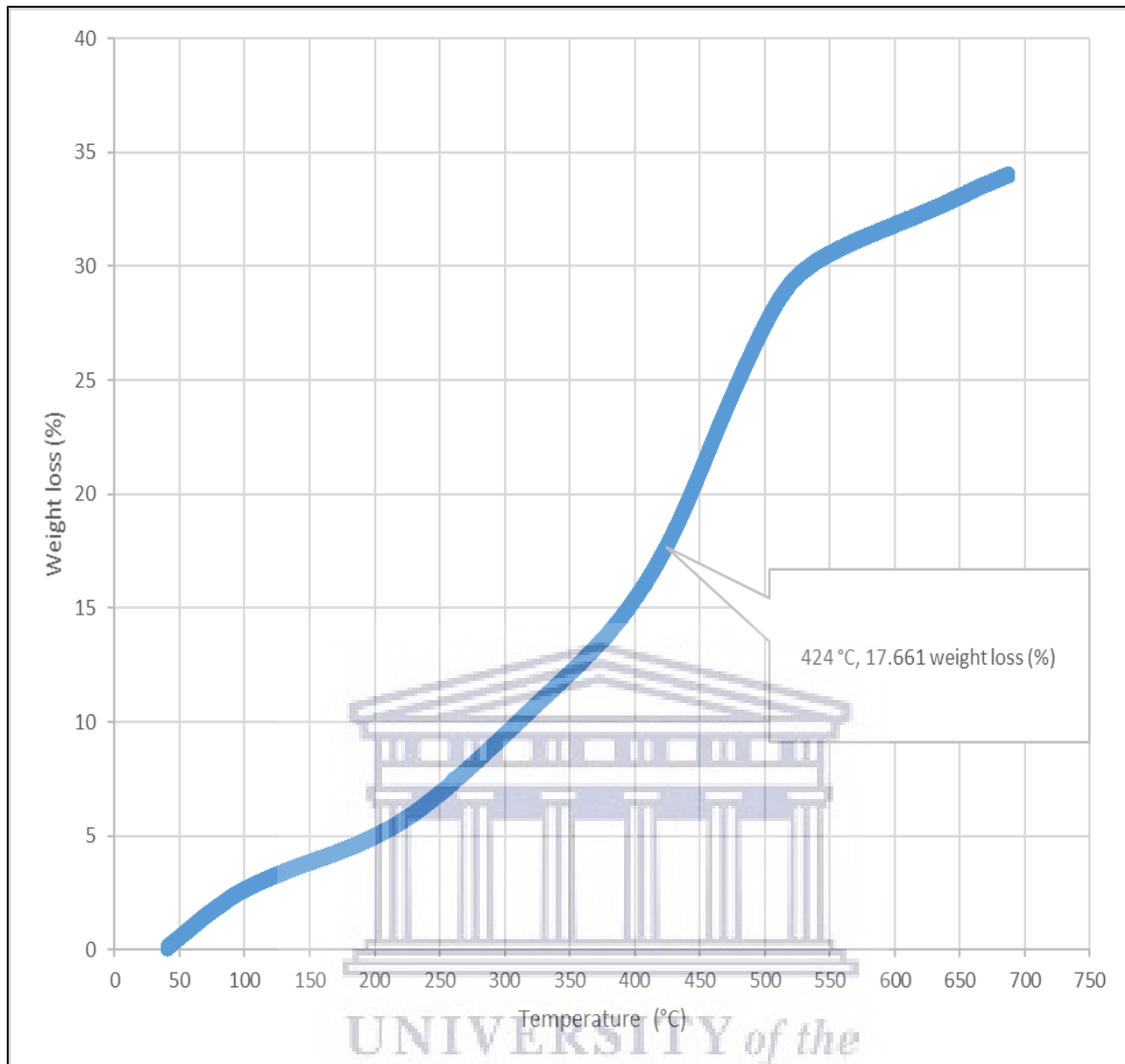
*Figure 42: Display showing thermogravimetric analysis for source rock at a depth of 9.9 m. The inflection point corresponding to the temperature of 424 °C and weight loss of 17.661 (%) is estimated to be the onset temperature at which the maximum generation of hydrocarbons occurred from the thermal break down of kerogen in the rock (Mohammed et al. 2020).*

The results indicate organic maturation temperature (Tmax) within the range of 417°C to 424 °C. The weight loss/gain upon heating the samples in TGA appears to reflect its composition; it ranged from 3.514 % to 17.661% at the temperatures interpreted as Tmax. The TGA curves (Figs. 38, 39, 40, 41, and 42) showed different curvatures reflecting mineralogy, composition, and decomposition (Mohammed et al., 2020).

The analytical results from loss on Ignition (LOI) and thermogravimetry presented in Table 11 and Figures 37, 38, 39, 40, 41, and 42 support the geochemical data from rock-eval pyrolysis (Table 10). The total organic matter (Table 11) is distinct from total organic carbon; it comprises of other elements such as hydrogen, nitrogen, oxygen, and organic carbon that are components of organic matter. The TOM results suggest a rich source rock. The trends of total organic matter contents (TOM, wt. %) and total organic carbon (TOC, wt. %) from loss on ignition and Rock-Eval pyrolysis suggest a positive correlation (Fig. 37). Source rocks with high TOM contents have corresponding high TOC. The Tmax values from TGA (Figs. 38, 39, 40, 41, and 42) showed a range of 417 °C to 424 °C, which is similar to Tmax estimated from Rock-Eval (Fig. 43).



| | AF-8.7m | AF-9.0m | AF-9.3m | AF-9.6m | AF-9.9m |
|---|---|---|---|---|---|
| Tmax from Pyrolysis | | 424 | 420 | 417 | 423 |
| Tmax from TGA | 419 | 422 | 421 | 417 | 424 |
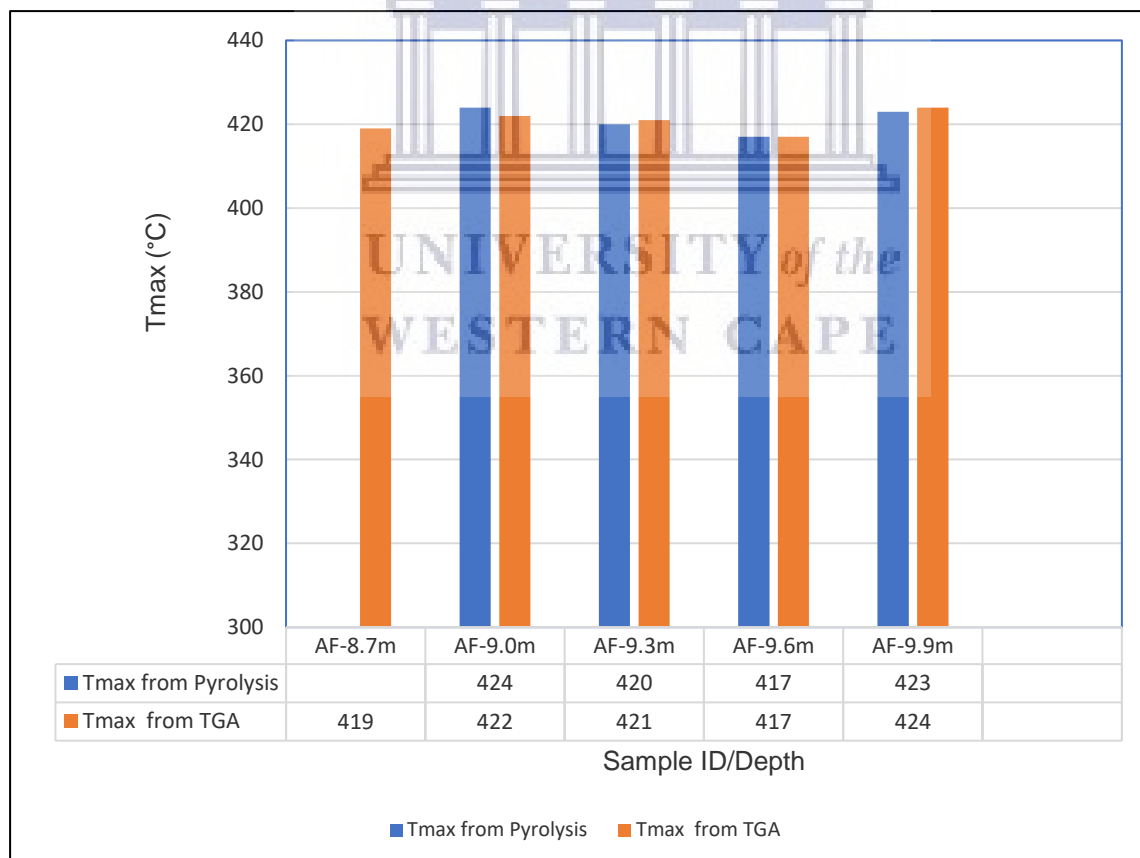
*Figure 43: Display showing a comparison of Tmax from Rock-Eval and TGA. The results indicated compatible Tmax from the different measurements. While it was not possible to obtain Tmax from Rock-Eval pyrolysis for the source rock at a depth of 8.7 m, reliable Tmax was estimated for the same sample with the aid of thermogravimetry.*

It was possible to assess Tmax for the sample at 8.7 m from thermogravimetric analysis; the constraint of lean S2 made it challenging to determine its Tmax using Rock-Eval (Mohammed et al., 2020). The results from both loss on ignition and thermogravimetric study showed that the source rock is rich in organic matter contents and is thermally immature, confirming that a different source rock generated the hydrocarbons in the overlying sands.

## 5.4: ROCK-EVAL RESULTS FROM 3-HANGER AND IJUOKE AGOTITUN

Rock-Eval measurements for the source rocks obtained from 3 Hanger (Ogun State) and Ijuoke Agotitun (Ondo State) are presented in Table 12 and Figures 44, 45, 46, and 47. The source rocks underlies the oil sands.

The total organic carbon contents (Table 12) for the source rocks ranged from 6.49 wt. % to 8.91 wt. %, indicating excellent source richness. The TOC contents for the source rock obtained from 3 Hanger in the Ogun Belt ranged from 6.49 wt. % to 8.91 wt. % and showed a decrease with depth. In contrast, the source rock underlying the oil sand at Ijuoke Agotitun (Table 12) presented a TOC value of 7.19 wt. %.

*Table 12: HAWK summary displaying Rock-Eval results for source rocks from 3-Hanger and Ijuoke Agotitun.*

| Sample ID | Depth (m) | Tmax °C | S0 (mg/g) | S1 (mg/g) | S2 (mg/g) | S3 (mg/g) | PC (%) | PI | S2/S3 | S1/TOC | TOC % | HI | OI |
|-----------|-----------|---------|-----------|-----------|-----------|-----------|--------|------|-------|--------|-------|-----|-----|
| 3H-1 | 1.5 | 414 | 0.00 | 0.57 | 9.05 | 8.13 | 0.82 | 0.06 | 1.11 | 0.06 | 8.91 | 101 | 91 |
| 3H-2 | 3.0 | 410 | 0.00 | 0.31 | 5.65 | 1.53 | 0.51 | 0.05 | 3.69 | 0.05 | 6.49 | 87 | 23 |
| IA-1 | 1.4 | 415 | 0.00 | 1.01 | 7.81 | 2.90 | 0.75 | 0.11 | 2.69 | 0.14 | 7.19 | 108 | 40 |

*Note :*

*3H = 3- Hanger*

*IA=   Ijuoke Agotitun*
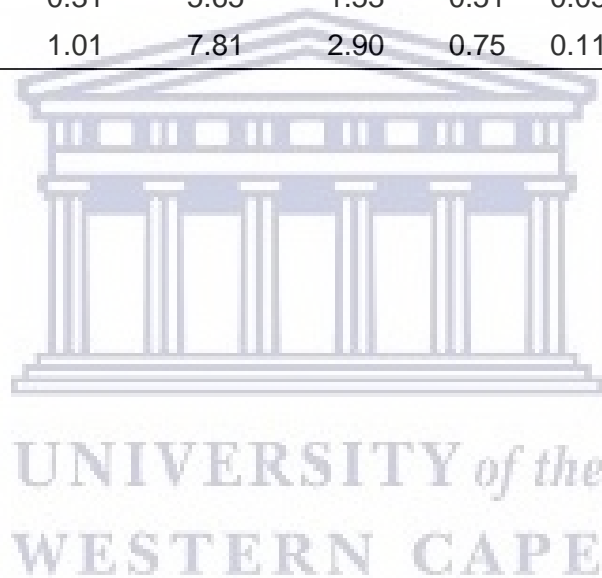
The hydrocarbon generating potential remaining in the rock's kerogen (S2) ranged from 5.65 mg HC/g rock to 9.05 mg HC/g rock, indicating that they have good potential to generate hydrocarbons. The variations in S2 are in sympathy with changes in the TOC contents; source rocks with high TOC contents displayed consistently high S2 values. The cross plots of hydrocarbon yield from kerogen versus Total organic Carbon (Fig. 44), Hydrogen Index against Oxygen Index (Fig. 45), Hydrogen Index against Tmax (Fig. 46) all suggested Type III kerogen, indicating terrestrial sedimentation.
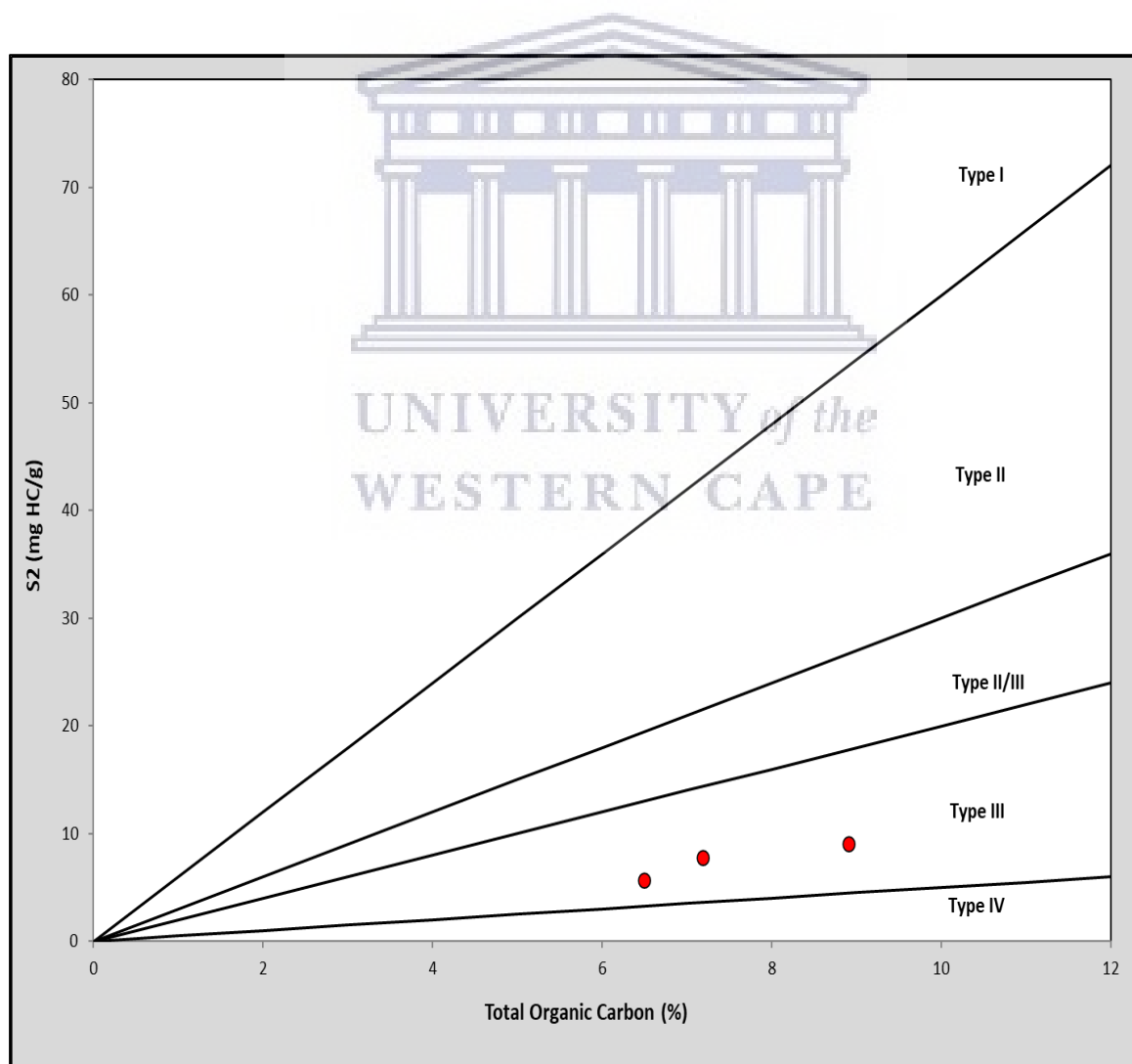


*Figure 44: Cross plot of S2 against TOC indicating Type III kerogen*
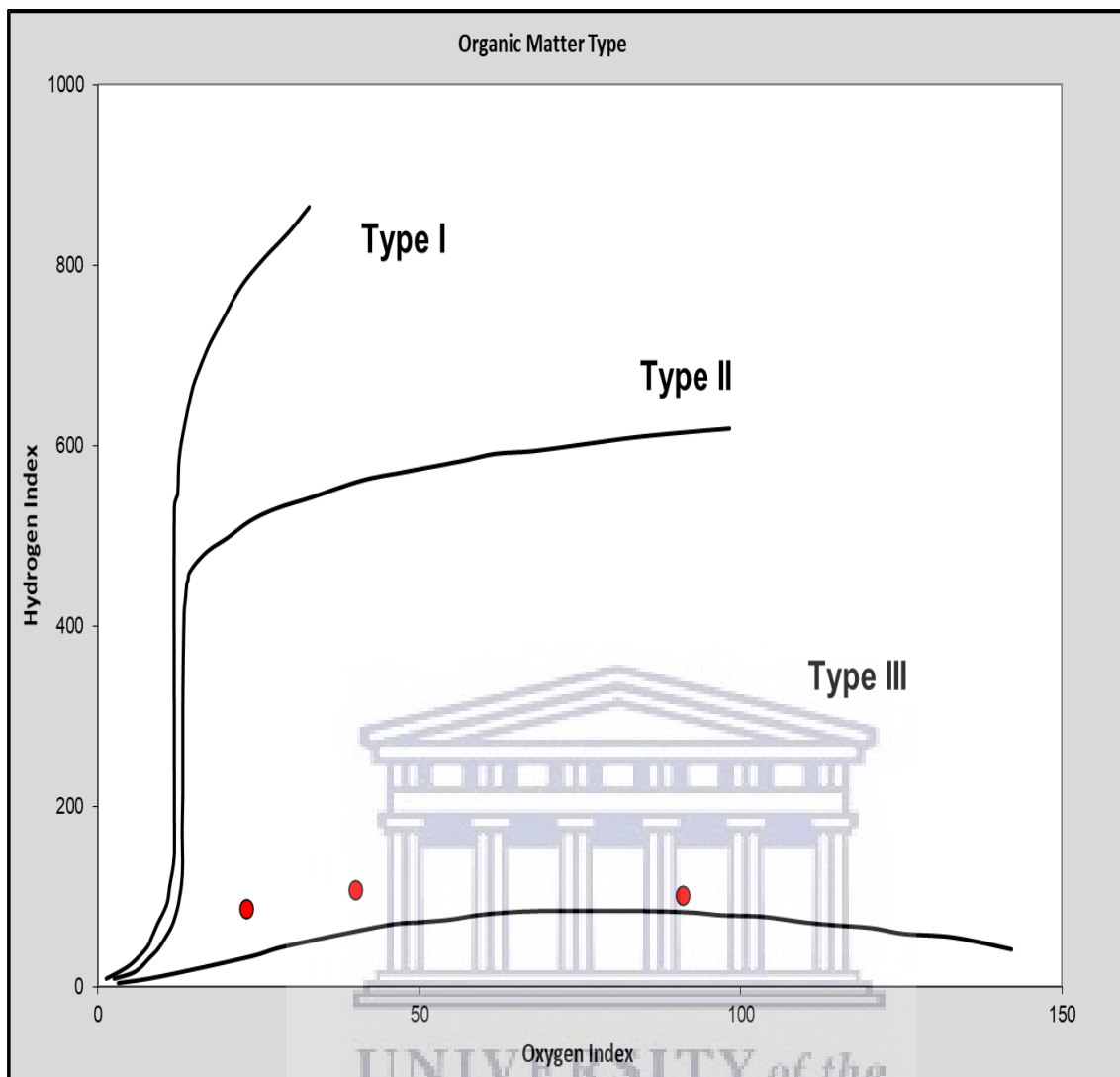
*Figure 45: Cross plot of Hydrogen Index versus Oxygen Index showing Type III kerogen.*
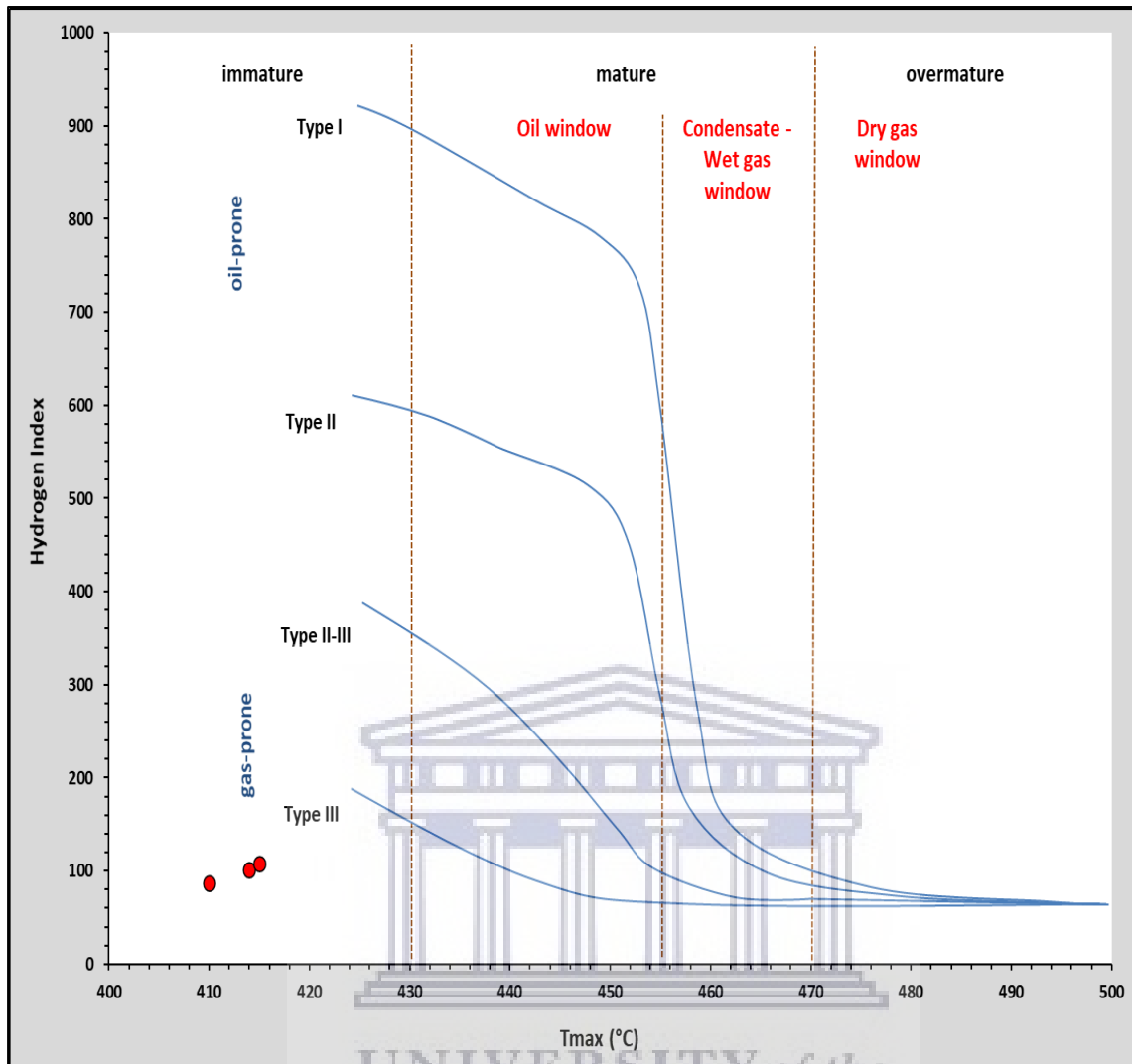
*Figure 46: Display of Hydrogen Index against Tmax indicating Type III kerogen and thermal immaturity.*

The Tmax (Table 12, Fig. 47) ranged from 410 °C to 415 °C, indicating that the kerogen has not attained the requisite temperature to generate hydrocarbons. The kerogen type suggested that the rocks have the potential to produce gas at a higher maturation temperature. The results also indicated that different source rocks generated the hydrocarbons in the overlying sands at greater burial depths and temperatures.
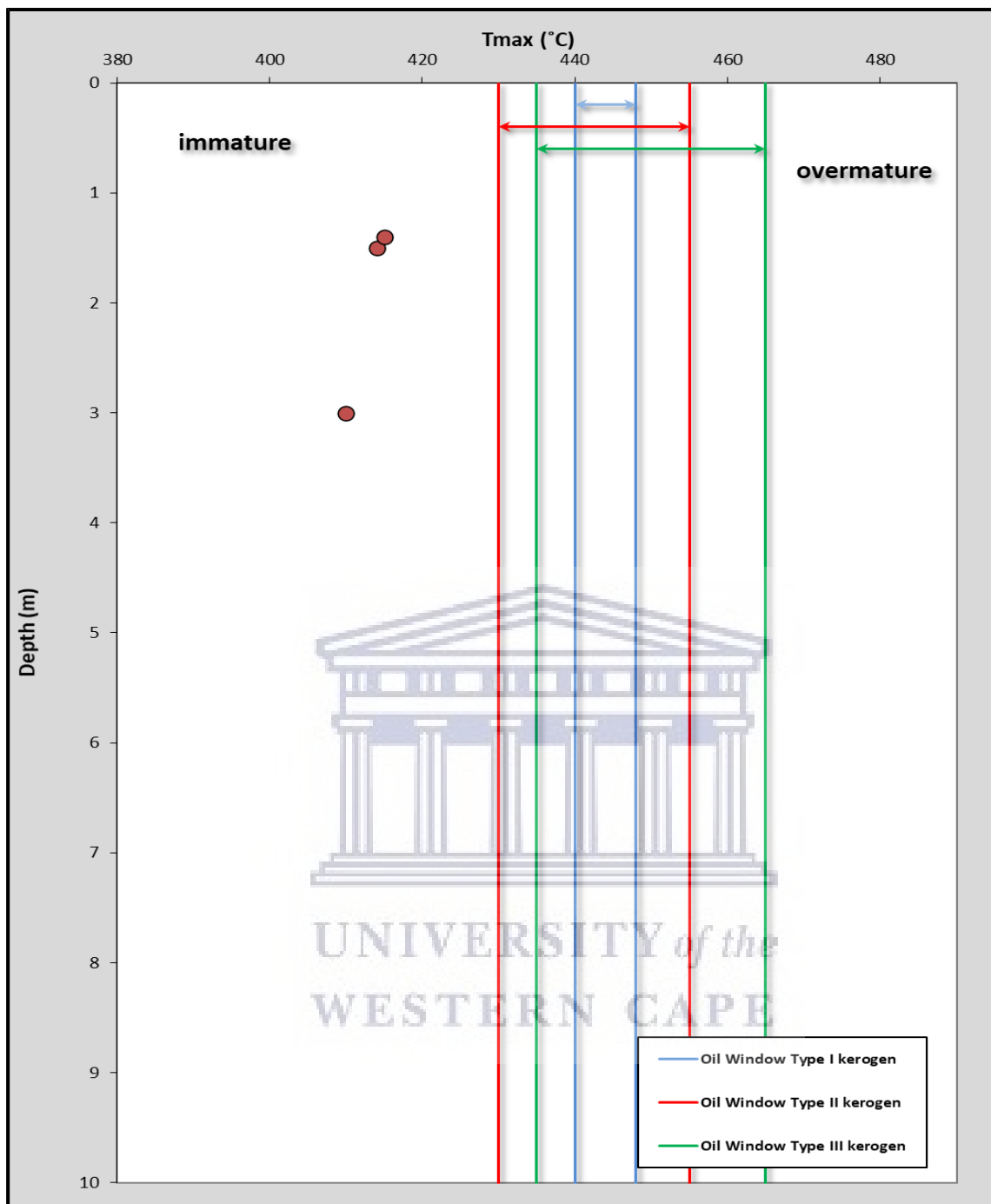
*Figure 47:  Display showing the profile of Tmax. The pattern indicated immature Type III kerogen.*

## 5.5: ROCK-EVAL RESULTS FROM WELL SAMPLES

Source rocks acquired from the sidewall of the J4-BH1 borehole were appraised for their hydrocarbon generating potential. Also, the Rock-Eval analysis was carried out on the cores of shales that were provided by an agency of the government.

## 5.6: J4-BH1 SOURCE ROCK EVALUATION

The Rock-Eval results for the claystones acquired from the J4-BHI borehole are presented in Table 13 and Figures 48, 49, 50, 51, and 52. The borehole (Fig. 23) was sited at the base of the J4 oil sand outcrop (Table 9) within the poorly understood Ogun belt.
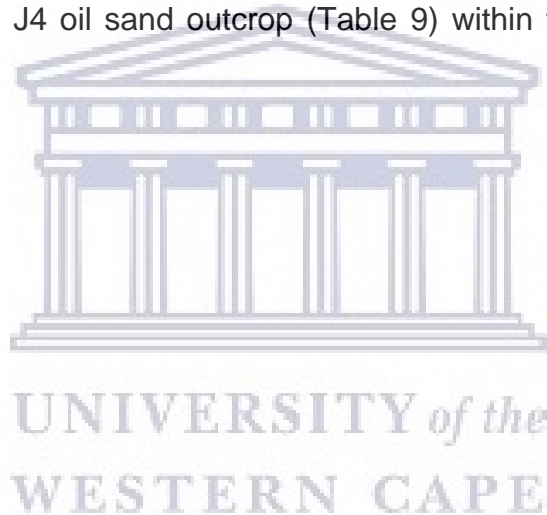
*Table 13: HAWK Summary showing the results of Rock Evaluation Pyrolysis for J4-BH1 Source Rocks.*

| Sample ID | Depth (m) | Tmax °C | S0 (mg/g) | S1 (mg/g) | S2 (mg/g) | S3 (mg/g) | PC (%) | PI | S2/S3 | S1/TOC | TOC % | HI | OI |
|---|---|---|---|---|---|---|---|---|---|---|---|---|---|
| J4-1 | 0.75 | 420 | 0.00 | 0.42 | 11.41 | 3.31 | 1.01 | 0.04 | 3.45 | 0.05 | 8.60 | 132 | 38 |
| J4-2 | 1.0 | 413 | 0.00 | 0.36 | 6.51 | 3.33 | 0.58 | 0.05 | 1.95 | 0.05 | 7.73 | 84 | 43 |
| J4-3 | 1.5 | 416 | 0.00 | 0.31 | 7.52 | 2.90 | 0.67 | 0.04 | 2.59 | 0.04 | 7.33 | 102 | 39 |
| J4-4 | 2.0 | 420 | 0.00 | 0.26 | 6.95 | 1.87 | 0.61 | 0.04 | 3.72 | 0.05 | 5.37 | 129 | 34 |
| J4-5 | 2.5 | 422 | 0.00 | 0.40 | 10.58 | 8.47 | 0.93 | 0.04 | 1.25 | 0.03 | 14.10 | 75 | 60 |
| J4-6 | 3.0 | 413 | 0.00 | 0.12 | 1.13 | 0.78 | 0.11 | 0.10 | 1.45 | 0.13 | 0.96 | 117 | 81 |
| J4-7 | 3.5 | 418 | 0.00 | 0.09 | 1.32 | 1.17 | 0.12 | 0.06 | 1.13 | 0.06 | 1.58 | 83 | 73 |
| J4-8 | 4.0 | 426 | 0.00 | 0.15 | 2.95 | 1.10 | 0.26 | 0.05 | 2.68 | 0.07 | 2.14 | 138 | 51 |
| J4-9 | 4.5 | 418 | 0.00 | 0.09 | 1.64 | 1.68 | 0.15 | 0.05 | 0.98 | 0.03 | 2.90 | 56 | 57 |
| J4-10 | 5.1 | 424 | 0.00 | 0.13 | 3.71 | 2.14 | 0.33 | 0.03 | 1.73 | 0.03 | 4.60 | 80 | 46 |
| J4-11 | 5.5 | 426 | 0.01 | 1.47 | 55.00 | 4.80 | 4.80 | 0.03 | 11.46 | 0.07 | 21.10 | 260 | 22 |
| J4-12 | 6.0 | 418 | 0.00 | 0.69 | 19.84 | 7.50 | 1.75 | 0.03 | 2.65 | 0.05 | 15.07 | 131 | 49 |
| J4-13 | 6.5 | 410 | 0.00 | 0.23 | 3.01 | 2.12 | 0.28 | 0.07 | 1.42 | 0.05 | 4.66 | 64 | 45 |
| J4-14 | 7.0 | 413 | 0.00 | 0.11 | 2.46 | 1.72 | 0.22 | 0.04 | 1.43 | 0.04 | 3.06 | 80 | 56 |
| J4-15 | 7.5 | 406 | 0.00 | 0.18 | 0.60 | 0.75 | 0.07 | 0.23 | 0.80 | 0.21 | 0.84 | 71 | 88 |
| J4-N | 7.7 | 405 | 0.01 | 0.04 | 0.24 | 0.68 | 0.02 | 0.14 | 0.35 | 0.05 | 0.85 | 28 | 80 |
| J4-S | 7.7 | 412 | 0.00 | 0.33 | 1.26 | 0.87 | 0.14 | 0.21 | 1.45 | 0.21 | 1.54 | 82 | 56 |
| J4-E | 7.7 | 407 | 0.01 | 0.17 | 0.61 | 2.62 | 0.07 | 0.22 | 0.23 | 0.15 | 1.16 | 52 | 226 |
| J4-W | 7.7 | 408 | 0.01 | 0.70 | 2.20 | 0.92 | 0.25 | 0.24 | 2.39 | 0.51 | 1.38 | 159 | 66 |
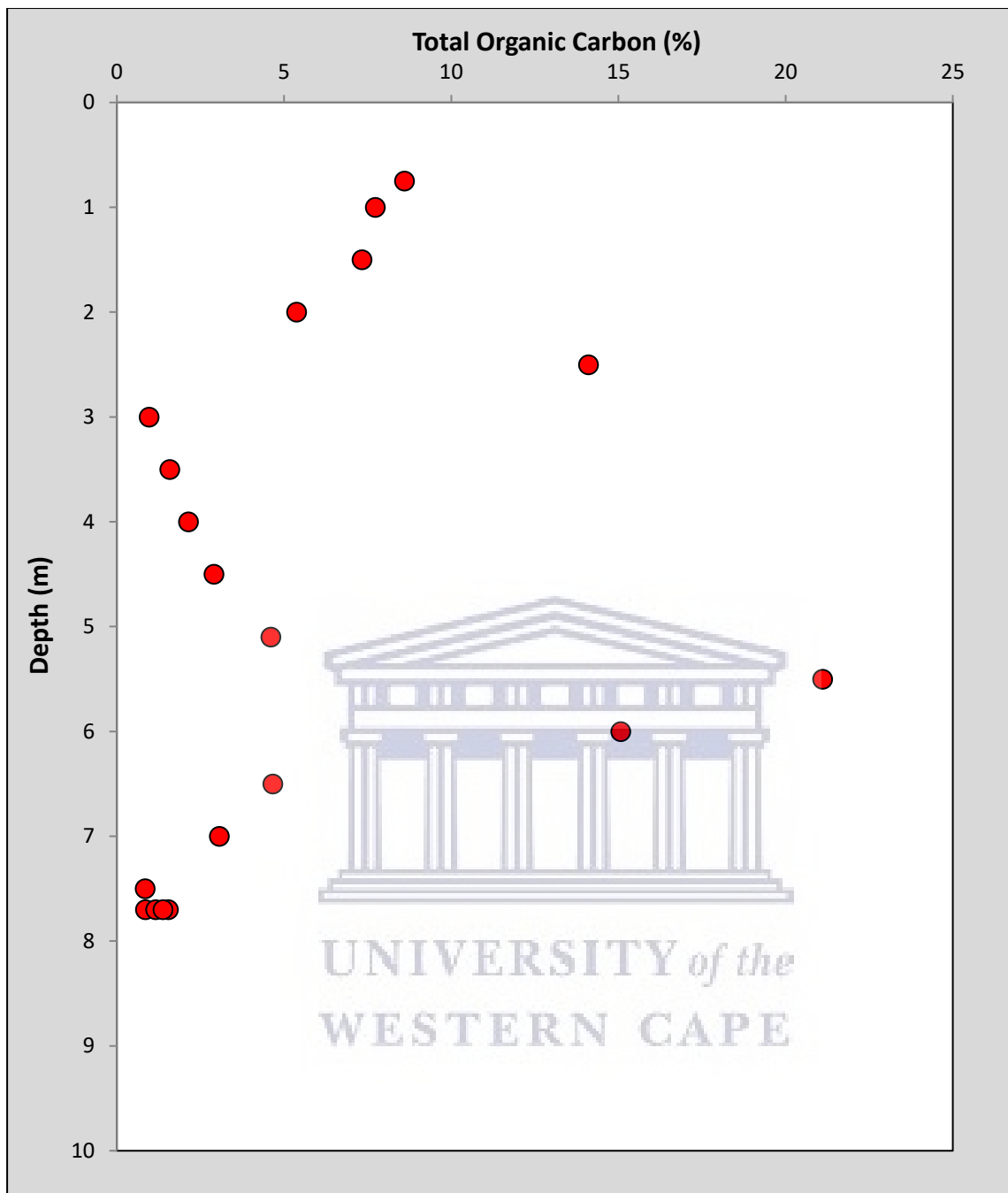
*Figure 48: Total Organic Carbon profile showing variations with depth.*
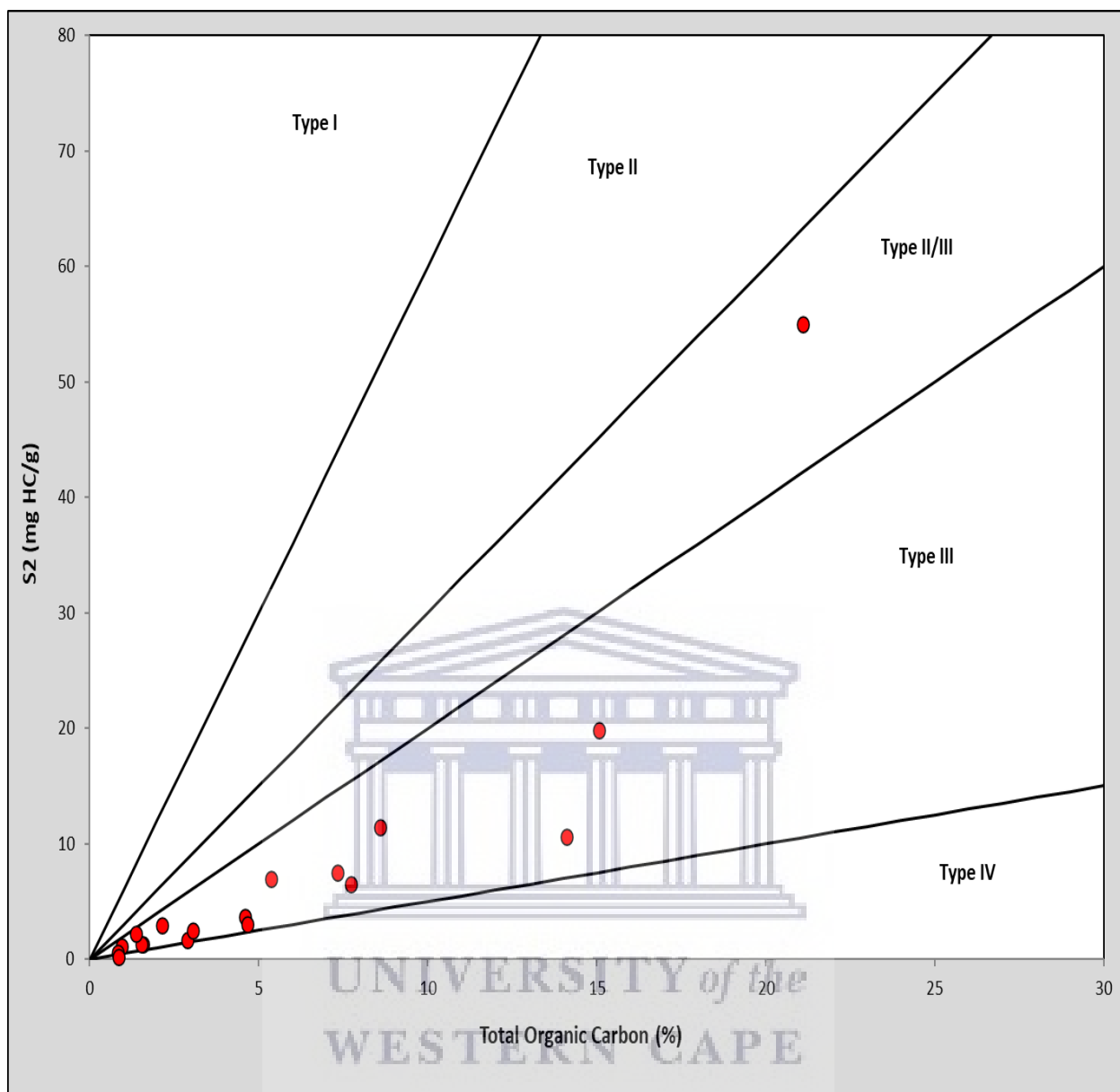
*Figure 49: Cross plot of S2 versus TOC showing kerogen types.*

http://etd.uwc.ac.za/
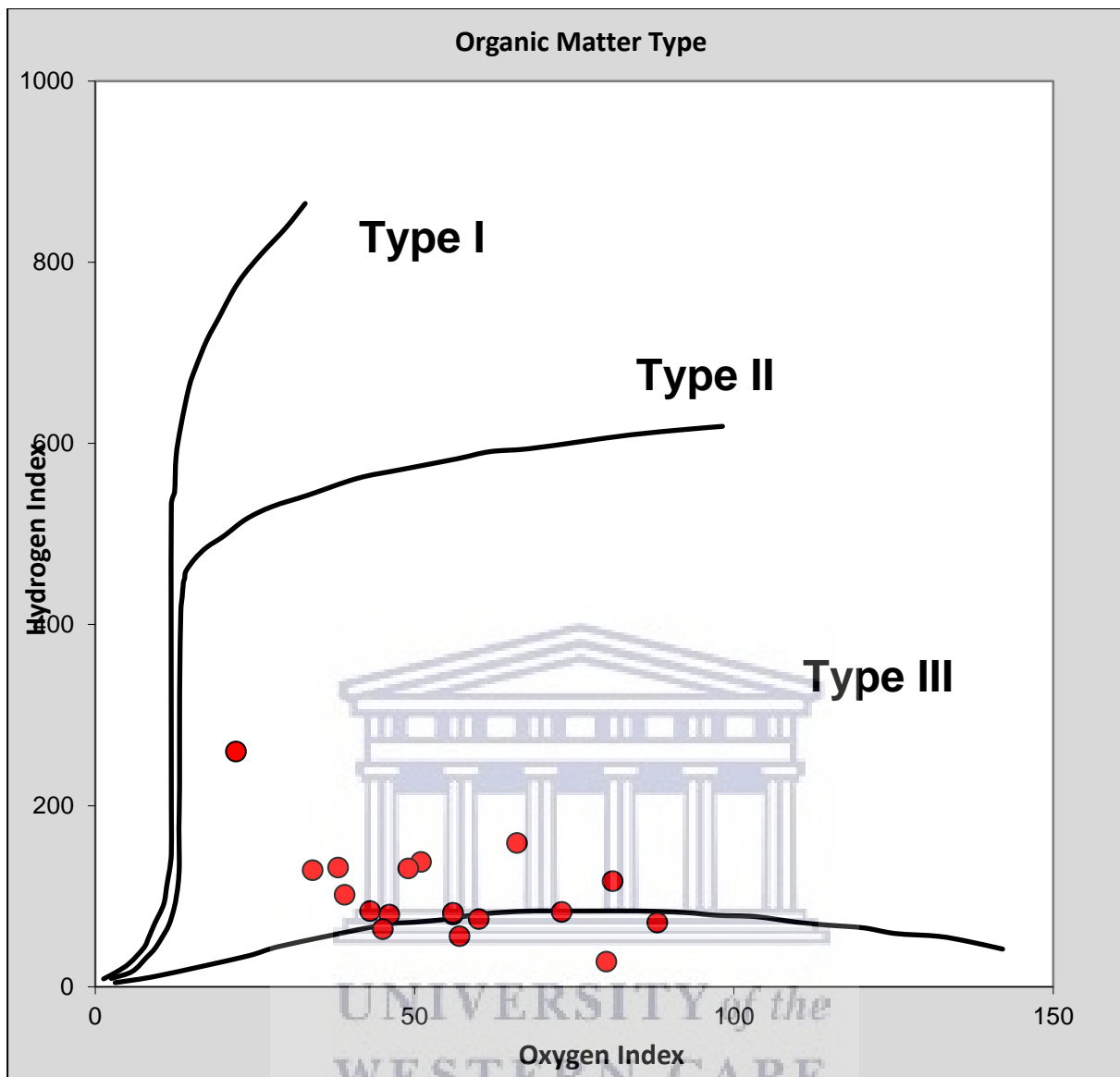
*Figure 50: Cross plot of Hydrogen Index against Oxygen Index showing kerogen types.*
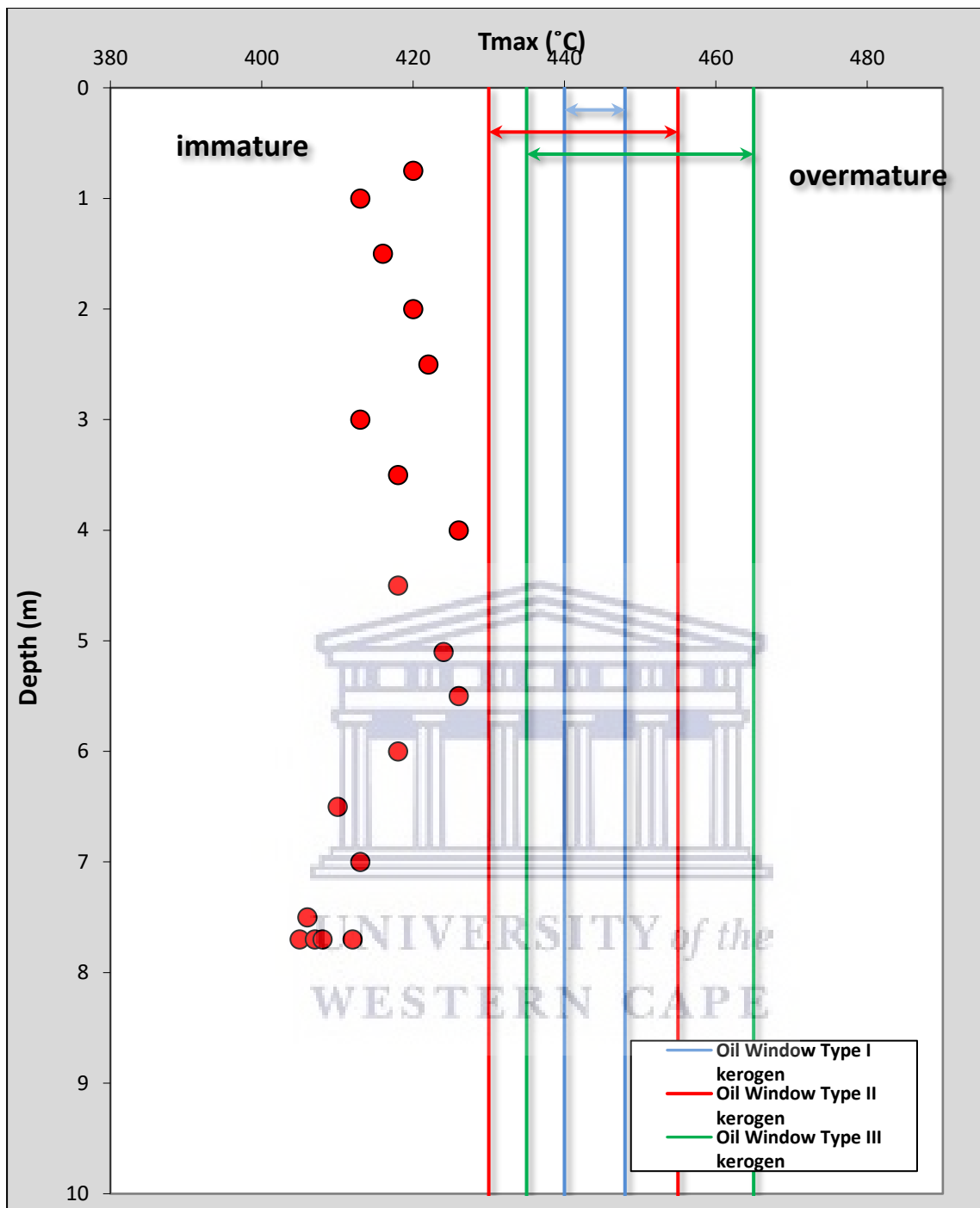
*Figure 51: Display of the Tmax profile, indicating that the kerogen had not attained thermal maturity.*
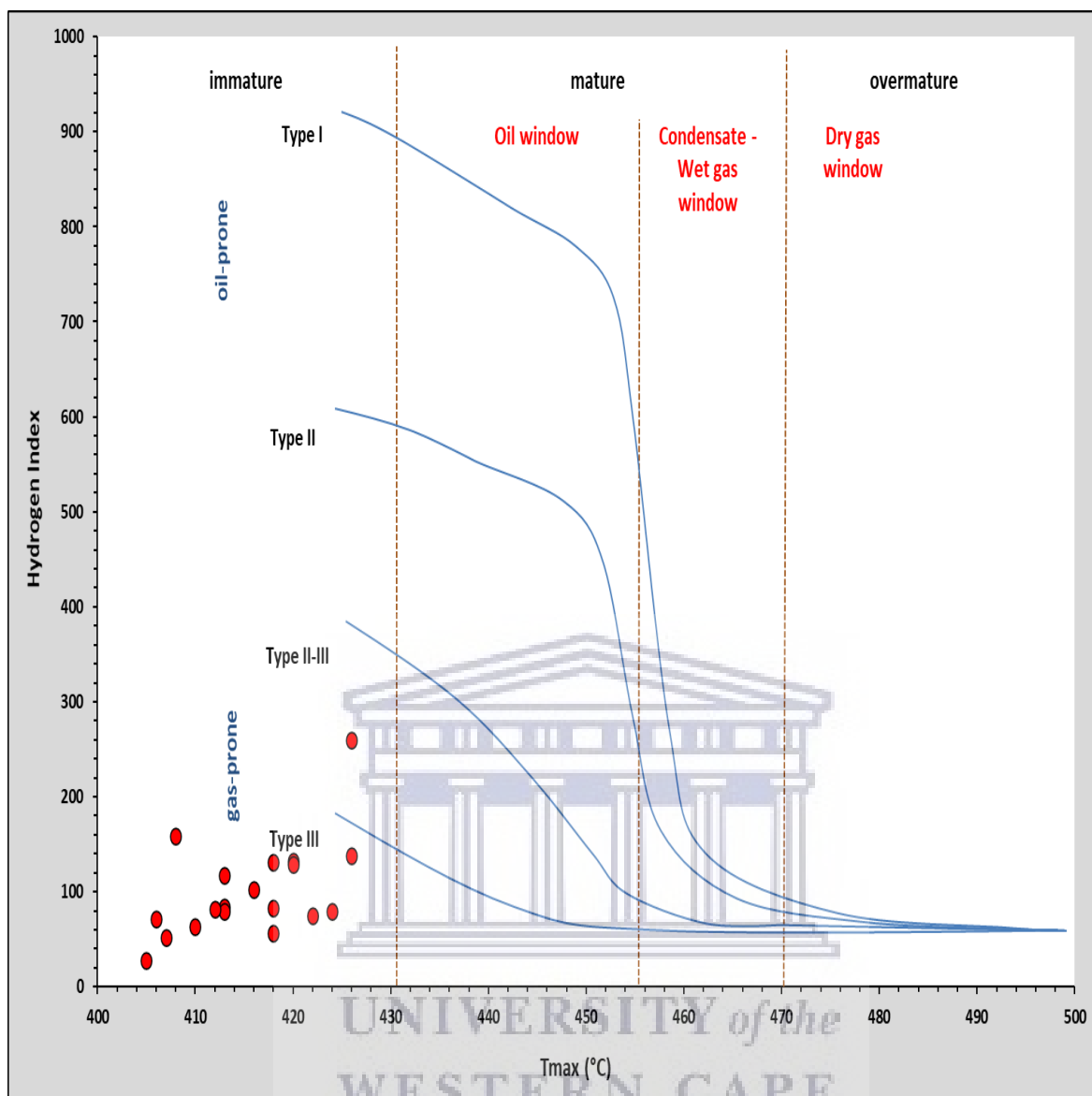
*Figure 52: Cross plot of Hydrogen Index versus Tmax showing an abundance of Type III kerogen.*

The total organic carbon (TOC, wt. %) for the claystones is not constant throughout the logged intervals. Instead, it exhibits an intricate degree of variability with depth. The TOC contents varied from 0.84 wt. % to 21.10 wt. % (Table 13, Fig. 48) reflecting variations in lithofacies and organic matter richness. The lithofacies encountered in the borehole from top to bottom may be broadly classified as a succession of dark-colored claystone from the depth of 0.75 m to 2.5 m, preceded by greyish claystone from the depth of 2.5 m to 3.5 m, followed by dark-colored claystone from 3.5 m to 7.0

m and greyish claystone over intervals 7.0 m to the borehole's total depth of 7.7 m. The dark-colored lithofacies showed higher TOC values than their greyish counterparts.

Total organic carbon values for intervals 0.75 m to 2.5 m, where the dark-colored lithofacies was penetrated, ranged from 7.33 wt. % to 14.10 wt. % while intervals 2.5 m to 3.5 m comprising of greyish claystone lithofacies displayed TOC values within the range of 0.96 wt. % to 1.58 wt. %.  A general increase in TOC contents from 2.14 wt. % to 21.10 wt. % was recorded for the dark-colored lithofacies from the depth of 4.0 m to 5.5 m, while the TOC content for the lower part of the sequence from 6.0 m to 7.0 m showed significant variation and did not increase with depth. A TOC value of 15.07 wt. % was obtained at a depth of 6.0 m while measurements at the depths of 6.5 m and 7.0 m displayed TOC values of 4.66 wt. % and 3.06 wt.% respectively. Greyish claystone facies encountered over intervals 7.5 m to the well's total depth (TD) at 7.7 m showed a variation in TOC from 0.84 wt. % to 1.54 wt. %. The four source rocks acquired at a depth of 7.7 m from four cardinal positions (North, South, West, and East) presented a variation in TOC from 0.85 wt. % to 1.54 wt. % and thus illustrates the heterogeneous nature of the Afowo formation. Semiquantitative source richness interpretation using total organic carbon (Peters, 1986) of the source rocks penetrated by the borehole indicates a fair to excellent hydrocarbon source richness.

The hydrocarbon generating potential remaining in the rock's kerogen (S2) ranged from 0.24 mg HC/g rock to 55.00 mg HC/g rock and illustrated patterns reflecting variations in organic richness and hydrocarbon generating potential.

The total organic carbon (TOC, wt.%) and the hydrocarbon yields from kerogen (S2) were used collectively to appraise source richness and hydrocarbon generating

potential. The range of TOC (0.84 wt. % to 21.10 wt. %) and S2 (0.24 mg HC/g rock to 55.00 mg HC/g rock) values indicated fair to excellent source richness and hydrocarbon generating potential that spanned a broad spectrum from mediocre to first-rate.

Free hydrocarbons (S0) were within the range of 0.00 mg HCs/g rock to 0.01 mg HCs/g rock, while hydrocarbons that have already been generated by the rock's kerogen (S1) ranged from 0.04 mg HC/g rock to 1.47 mg HCs/g rock. The production index (PI), which represents the amount of hydrocarbon already generated relative to the total amount that could be produced (Dembicki, 2017), varied from 0.03 to 0.24, suggesting that the kerogen has not been heated enough to generate hydrocarbons.

The hydrogen index (HI) ranged from 28 to 260. In contrast, the oxygen index (OI) varied from 22 to 226 (Table 13). Both HI and OI index indicated a preponderance of Type III kerogen (Fig. 50).

Organic maturation temperature (Fig. 51) varied from 405 °C to 426 °C and exhibited some degrees of variability with depth. Tmax over intervals 0.75 m to 1.5 m showed a reversal from 420 °C to 416 °C and decreased with depth while Tmax measurements from depths between 2.0 m to 2.5 m increased with depth from 420 °C to 422 °C. The sections below 2.5 m presented a series of Tmax increments and reversals with depth, possibly due to mineral matrix effects and retention of heavy resins and asphaltene compounds from the bitumen (Espitalié, 1986). Source rock samples at a depth of 7.7 m were acquired at four cardinal positions (N, S, W, and E), and the results indicated Tmax and TOC anisotropy.

The TOC and Tmax showed variations depending on the direction of measurements. Total organic carbon for these source rocks (Table 13) ranged from 0.85 wt.% to 1.54

wt. %, while Tmax varied from 405 °C to 412 °C. The variations in measurements indicate the heterogeneous and anisotropic nature of the Afowo Formation.

The cross plots of S2 against TOC (Fig. 49), HI versus OI (Fig. 50), and HI against Tmax (Fig. 52) were used to determine kerogen type and the hydrocarbon types that the kerogen could generate at maturity. The results indicate an abundance of Type III kerogen with potential for gas generation at maturity. The findings also show that other source rocks at deeper burial depths and higher Tmax generated the hydrocarbons in the overlying sand.

## 5.7:    ROCK-EVAL RESULTS FROM CORES OF SHALE SOURCE ROCK

Rock-Eval results for cored shale source rocks from seven wells are presented in Table 14, Figures 53, 54, 55, 56, and 57.  The wells penetrated intervals of oil sands, and the shales that were evaluated were acquired below the oil sand intervals.
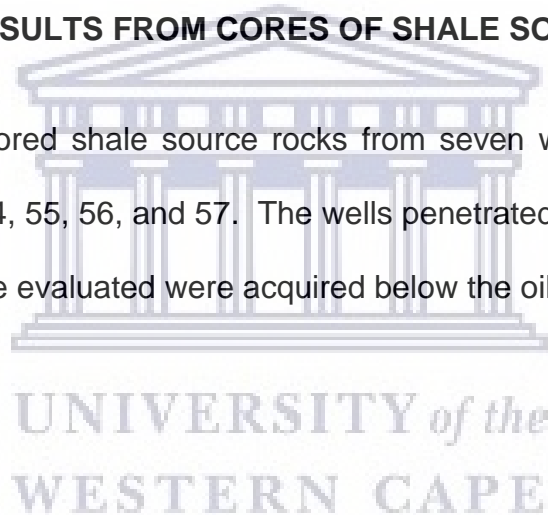
*Table 14: Hawk summary showing Rock-Eval Results for Cored Source Rocks*

| Well ID | Depth (m) | Tmax °C | S0 (mg/g) | S1 (mg/g) | S2 (mg/g) | S3 (mg/g) | PC (%) | PI | S2/S3 | S1/TOC | TOC % | HI | OI |
|---|---|---|---|---|---|---|---|---|---|---|---|---|---|
| A-11 | 28.6 | 416 | 0.00 | 0.09 | 1.35 | 3.47 | 0.12 | 0.06 | 0.39 | 0.03 | 2.94 | 45 | 117 |
| EY-12 | 109.5 | 422 | 0.00 | 0.03 | 0.40 | 1.28 | 0.04 | 0.07 | 0.31 | 0.03 | 1.19 | 33 | 107 |
| EY-12 | 58.5 | - | 0.00 | 0.03 | 0.08 | 2.00 | 0.01 | 0.27 | 0.04 | 0.06 | 0.52 | 15 | 387 |
| EY-12 | 91.5 | - | 0.00 | 0.03 | 0.13 | 2.05 | 0.01 | 0.19 | 0.06 | 0.04 | 0.78 | 16 | 263 |
| EY-22 | 82.5 | 377 | 0.00 | 0.69 | 3.11 | 6.34 | 0.32 | 0.18 | 0.49 | 0.13 | 5.18 | 60 | 122 |
| EY-22 | 94.5 | 391 | 0.00 | 0.95 | 9.26 | 31.90 | 0.87 | 0.09 | 0.29 | 0.04 | 21.36 | 43 | 149 |
| EY-19 | 64.5 | 422 | 0.00 | 0.03 | 0.45 | 4.80 | 0.04 | 0.06 | 0.09 | 0.01 | 3.90 | 11 | 123 |
| Araromi Obu | 56.5 | - | 0.00 | 0.01 | 0.03 | 1.26 | 0.00 | 0.25 | 0.02 | 0.02 | 0.51 | 5 | 245 |
| A8 | 80.5 | 426 | 0.00 | 0.02 | 1.00 | 1.53 | 0.09 | 0.02 | 0.65 | 0.01 | 1.44 | 69 | 105 |
| EY-5 | 112.5 | 416 | 0.00 | 0.10 | 0.78 | 2.02 | 0.07 | 0.11 | 0.39 | 0.06 | 1.74 | 44 | 116 |

*Note:*

*A-11= Ijagun; EY-12 = Lewumeji; EY-22= Igbotu*

*EY-19= Ohosu; A8= Erekiti Luwoye; EY-5= Ajagba*
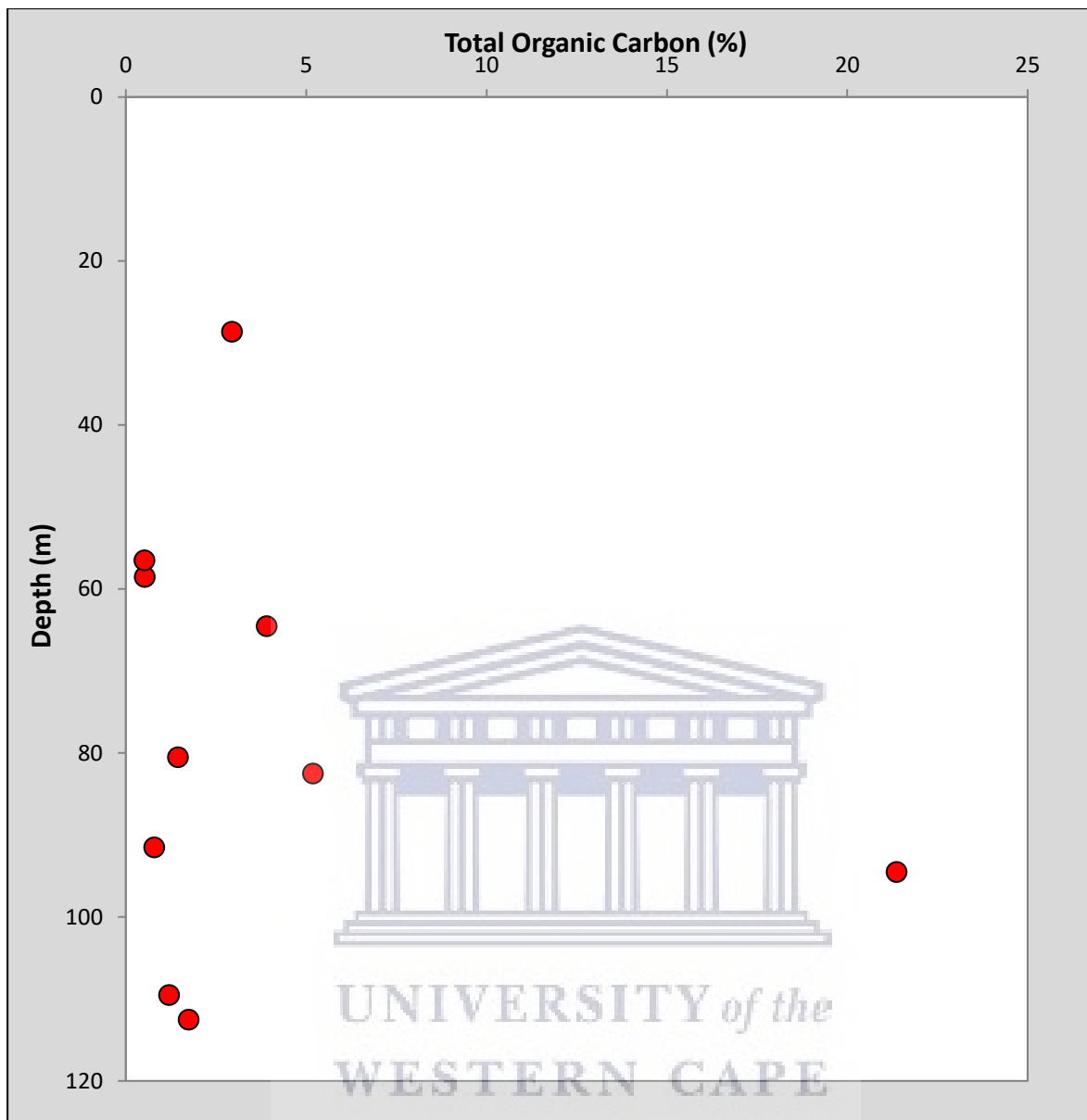
*Figure 53: Profile of Total Organic Carbon*
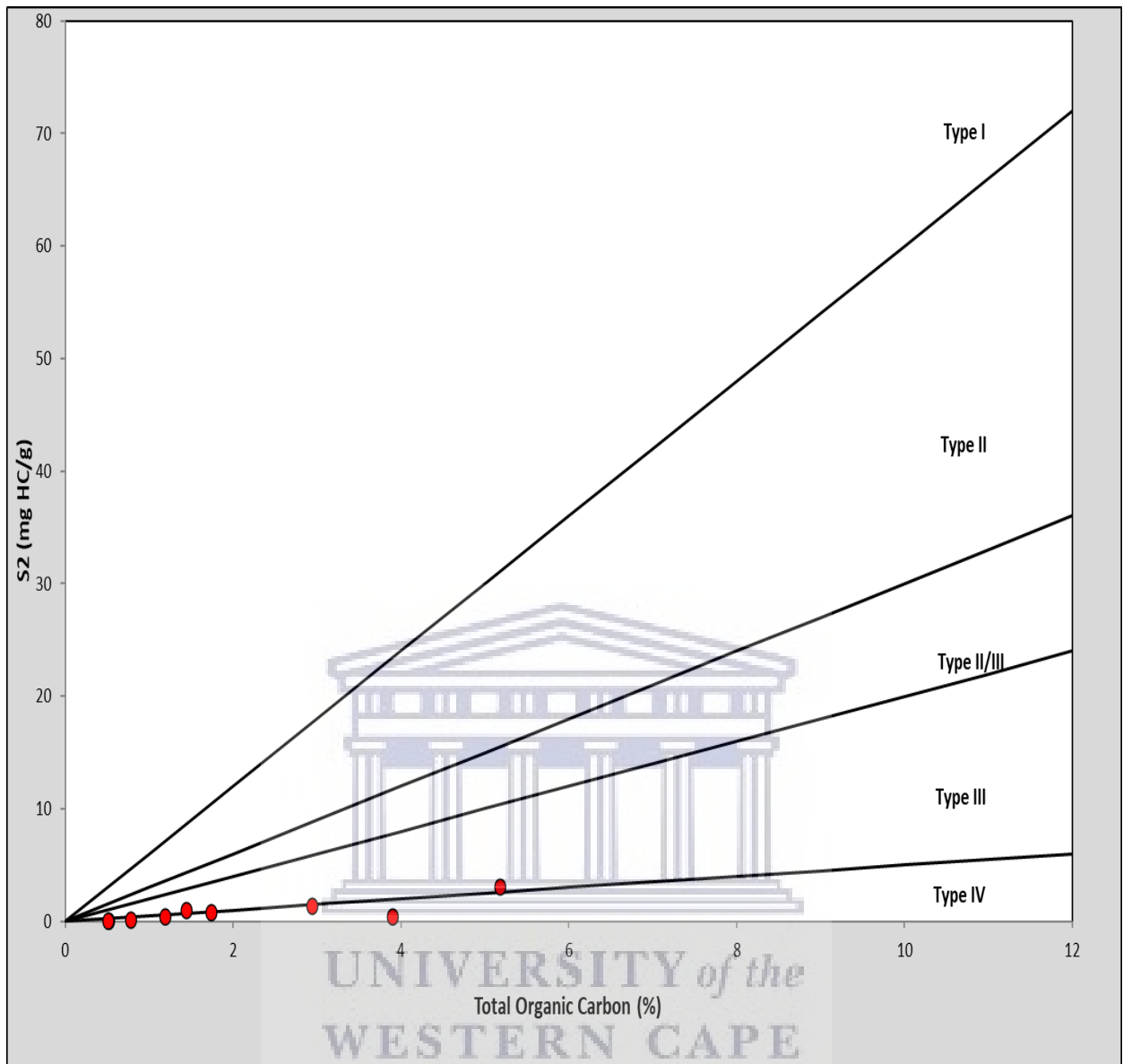
*Figure 54: Cross plot of S2 versus TOC showing kerogen types.*
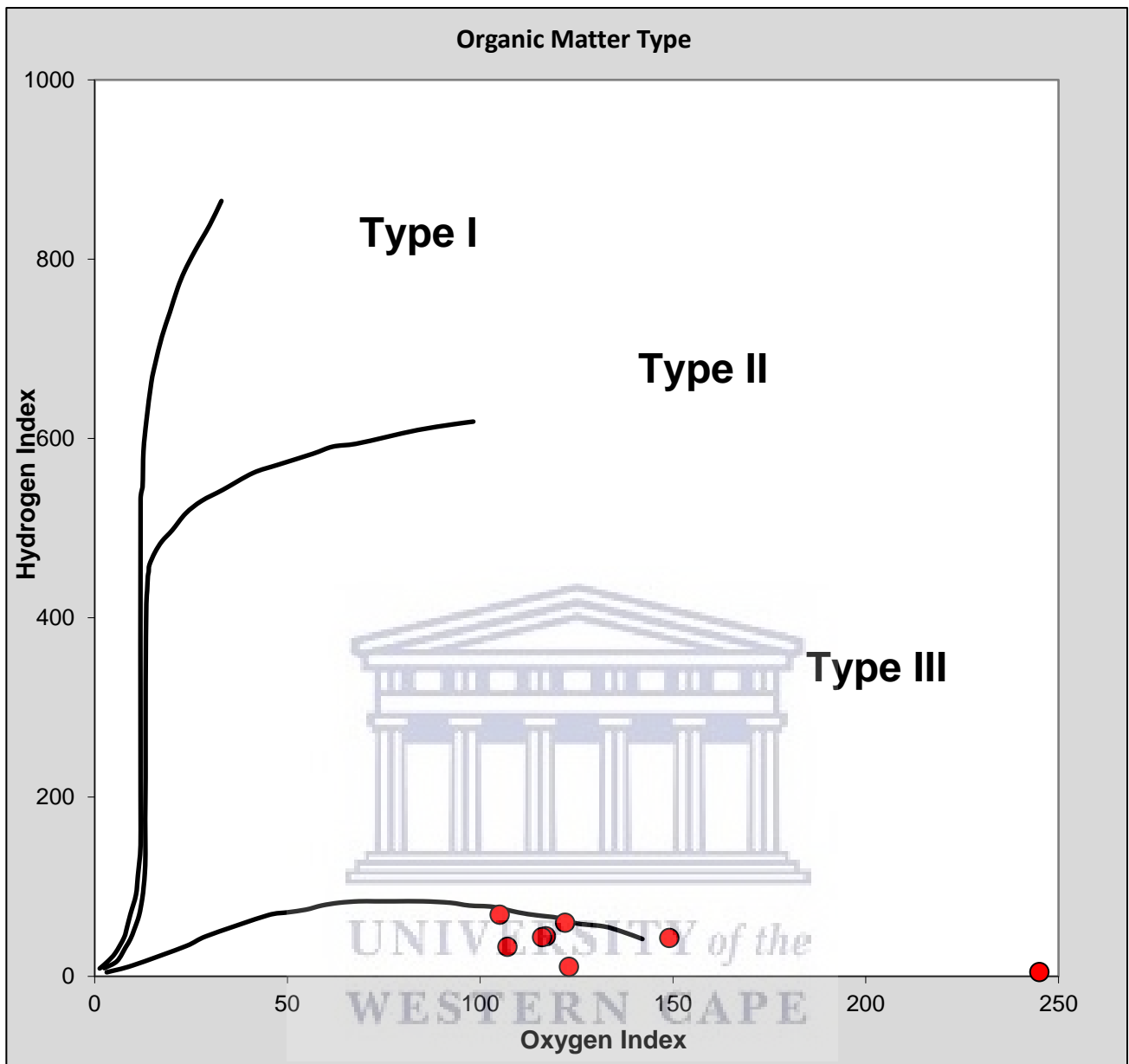
*Figure 55: Cross plot of Hydrogen Index versus Oxygen Index showing Type IV kerogen with zero potential to generate hydrocarbons.*
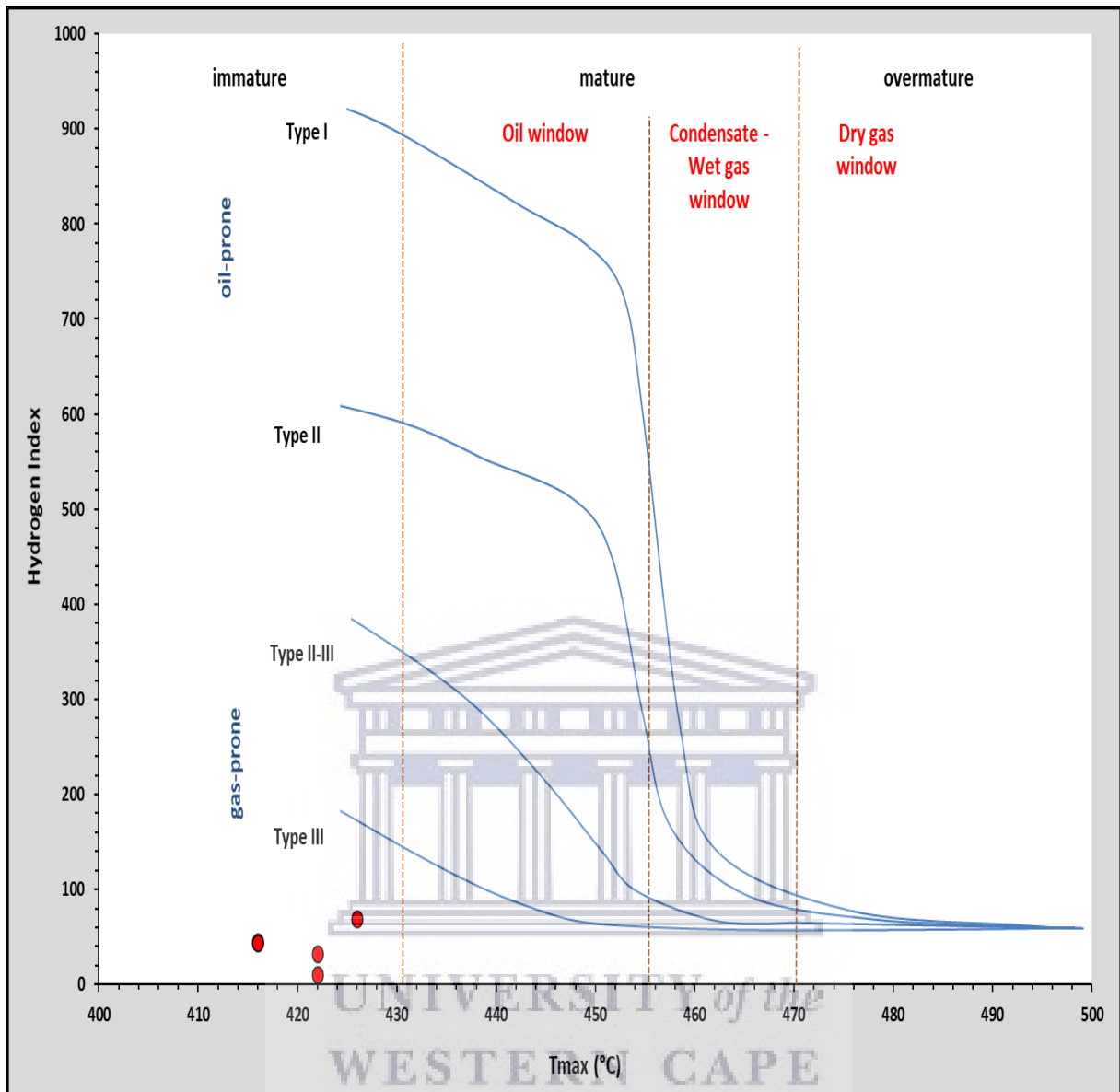
*Figure 56: Cross plot of Hydrogen index and Tmax, indicating thermal immaturity.*
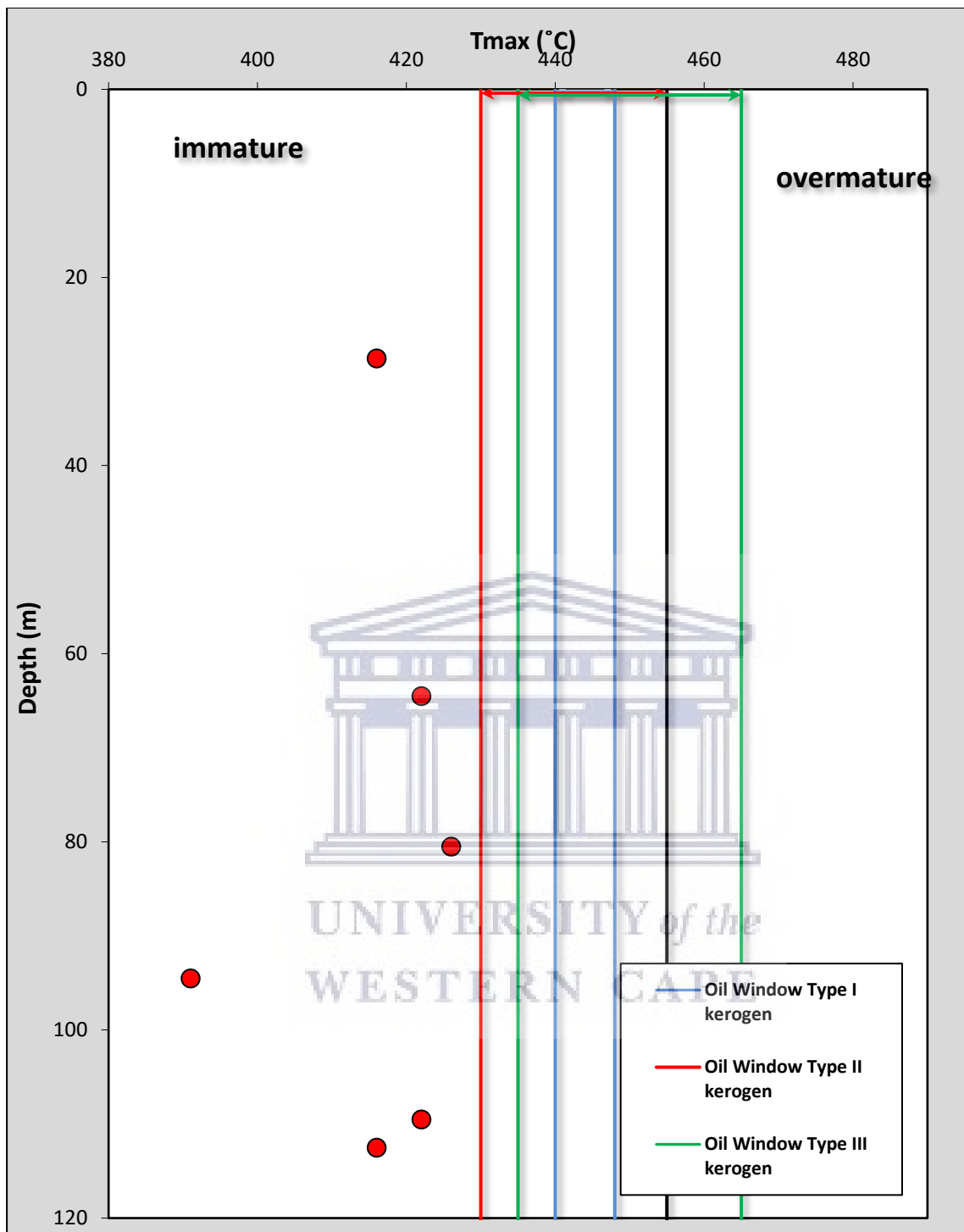
*Figure 57: Profile of Tmax showing that the rocks are thermally immature.*

Total organic carbon (Table 14, Fig. 53) from these wells ranged from 0.51 wt. % to 21.36 wt. %. The highest TOC of 21.36 wt. % was recorded in well EY-22 while the lowest TOC of 0.51 wt. % was logged for Araromi Obu. The range of TOC values suggested fair to excellent source richness.

The hydrocarbon generating potential remaining in the rock's kerogen (S2) ranged from 0.03 mg HC/g rock to 9.26 mg HC/g rock. It demonstrated patterns reflecting variations in organic richness and hydrocarbon generating potential of the source rocks. The total organic carbon (TOC, wt.%) and the hydrocarbon yields from kerogen (S2) were used to assess source richness and hydrocarbon generating potential. The TOC range (0.51 wt. % to 21.36) and S2 values (0.03 mg HC/g rock to 9.26 mg HC/g rock) indicated fair to excellent source richness with hydrocarbon generating potential ranging from deficient to good. Free hydrocarbons (S0) for all the samples were 0.00 mg HC/g rock, while thermally free hydrocarbons (S1) varied from 0.01 mg HC/g rock to 0.95 mg HC/g rock. The production index (PI) fluctuates from 0.02 to 0.27, suggesting that the kerogen has not been heated enough to generate hydrocarbons. Hydrogen index (HI) ranged from 5 mg HC/g TOC to 60 mg HC/g TOC, while the oxygen index (OI) index varied from 105 mg $CO_2$/g TOC to 387 mg $CO_2$/g TOC (Table 14). The low HI index and correspondingly high OI index suggested an abundance of Type IV kerogen.

The cross plots of S2 against TOC (Fig. 54), and HI versus OI (Fig. 55), were used to determine kerogen type and the hydrocarbon types that the kerogen could generate at maturity. The data (Table 14, Figs. 54 and 55) indicates an abundance of Type IV kerogen with zero hydrocarbon generation potential. Besides, the cross plot of HI against Tmax (Fig. 56) suggested that the source rocks are thermally immature.

Organic maturation temperature (Tmax, Fig. 57) ranged from 377 °C to 426 °C, indicating that the constituent kerogen in the source rock did not attain the requisite temperature to produce hydrocarbons. It was impossible to obtain Tmax for some of the source rocks due to lean S2 values ( Dembicki, 2009; Peters, 1986). The evaluation results indicate that the source rocks are thermally immature, suggesting that the hydrocarbons in the sands penetrated by the boreholes were generated by different petroleum source rocks.

## 5.8: SOURCE ROCK EXTRACT AND GAS CHROMATOGRAPHIC ANALYSIS FOR MATURITY ASSESSMENT

Extractable organic matter (EOM), also known as bitumen, is the amount of organic matter in mg/g that can be extracted from fine-grained sediment rocks using organic solvents. Unlike crude oil, bitumen is indigenous to the rock in which it is found (Peters et al., 2005).

Two source rocks from the J4-BH1 borehole with high total organic carbon contents of 21.10 wt. % and 15.07 wt. % (Table 13) were extracted, de-asphaltened, and fractionated into saturates, aromatics, and polar fractions.  The saturate fraction contained saturated hydrocarbon compounds, while the aromatic and resin fractions consisted of aromatic compounds and Nitrogen, Sulphur, and Oxygen (NSO) bearing compounds, respectively. Results from the fractionation of the extractable organic matter for the source rocks (Table 15, Fig. 58) showed high proportions of polar compounds relative to the saturated and aromatic hydrocarbon fractions.

*Table 15: Results of Source Rock Extract and Fractionation*

| WELL ID | Sample Depth (m) | Extract weight (mg) | ASPHALT (mg) | Hydrocrabons (mg) | aromatics (mg) | Resin (mg) | Saturate (mg) | Sat/Aro ratio | HC % | Polars % | Sats % | Aros % |
|---|---|---|---|---|---|---|---|---|---|---|---|---|
| J4 - BHI | 5.5 | 71.1 | 1.98 | 19.07 | 10 | 18.1 | 9.07 | 0.91 | 26.82 | 28.24 | 12.76 | 14.06 |
| J4 - BHI | 6 | 81.71 | 2.7 | 24.37 | 11.27 | 19.92 | 13.1 | 1.16 | 29.82 | 27.68 | 16.03 | 13.79 |

*Note:*

*HC; consists of Saturate and Aromatic fractions*

*Polars; consist of Resin,  Nitrogen, Sulphur, and Oxygen bearing compounds.*

*Sats; Saturates*

*Aros; Aromatics*
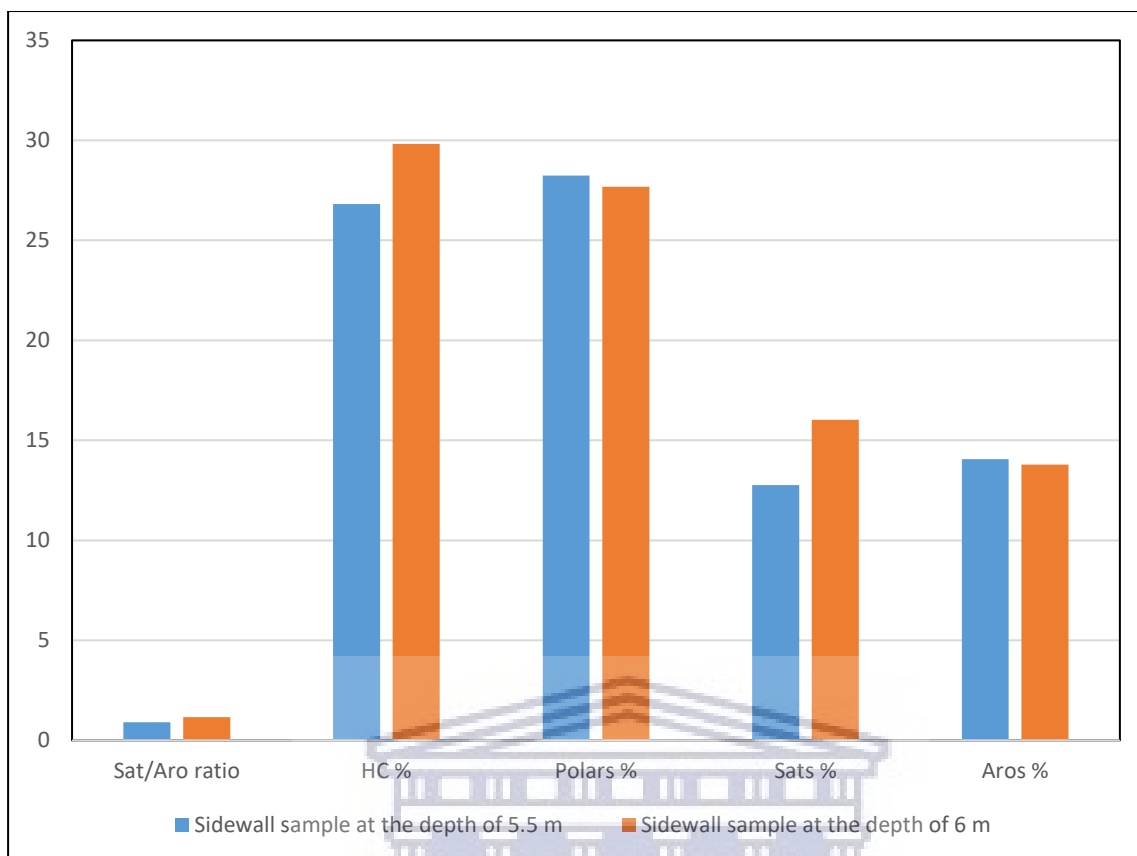
*Figure 58: Fractionation results of extractable organic matter (EOM) showing polar, saturate, and aromatic portions.*

For the source rock at a depth of 5.5 m, the saturated and aromatic fractions were 12.76 % and 14.06 %, respectively, while the polar portion amounted to 28.24 %. In contrast, the source rock at a depth of 6 m yielded saturates of 16.03 %, aromatics of 13.79 %, and a polar fraction of 27.68 %. The higher proportion of the polar compounds relative to saturated and aromatic fractions for these source rocks may be potentially related to a low level of thermal maturity. The result also reflects the molecular composition of the constituent kerogen (Tissot and Welte, 1984).

The saturated fractions were assessed by Gas Chromatographic (GC) analysis, and the results provide clues to inferring the maturity of the organic matter in the rock. Compositional changes reflecting a lower level of maturity for the samples showed a bimodal distribution of n-alkanes (Figs. 59 and 60) and odd carbon number predominance in the C25 to C33 range of n-paraffins. The dominance of heavy molecular weight n-alkanes in the chromatograms suggested thermal immaturity as they have not been cracked to lighter products. The bimodal fingerprints from gas chromatography, Carbon Preference Index (CPI) computed from the areas of n-paraffin peaks were used to indicate the level of maturity. It has been demonstrated that most immature source rocks have a CPI greater than 1.0, while mature source rocks have a CPI of about 1.0 (Bray and Evans, 1965; Scalan and Smith, 1970). The CPI for the source rocks (Table 16) ranged from 3.03 to 3.51, suggesting a low level of thermal maturity.
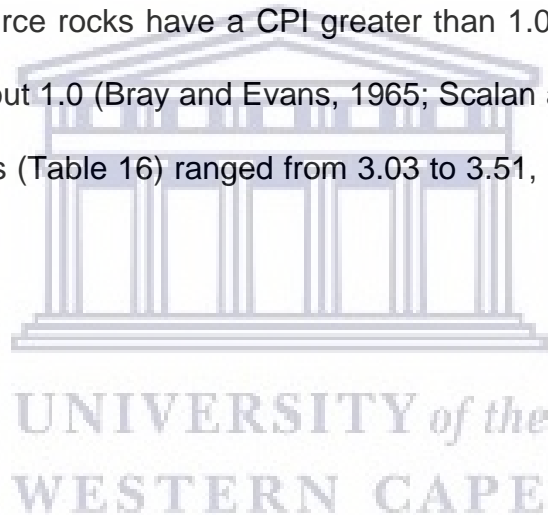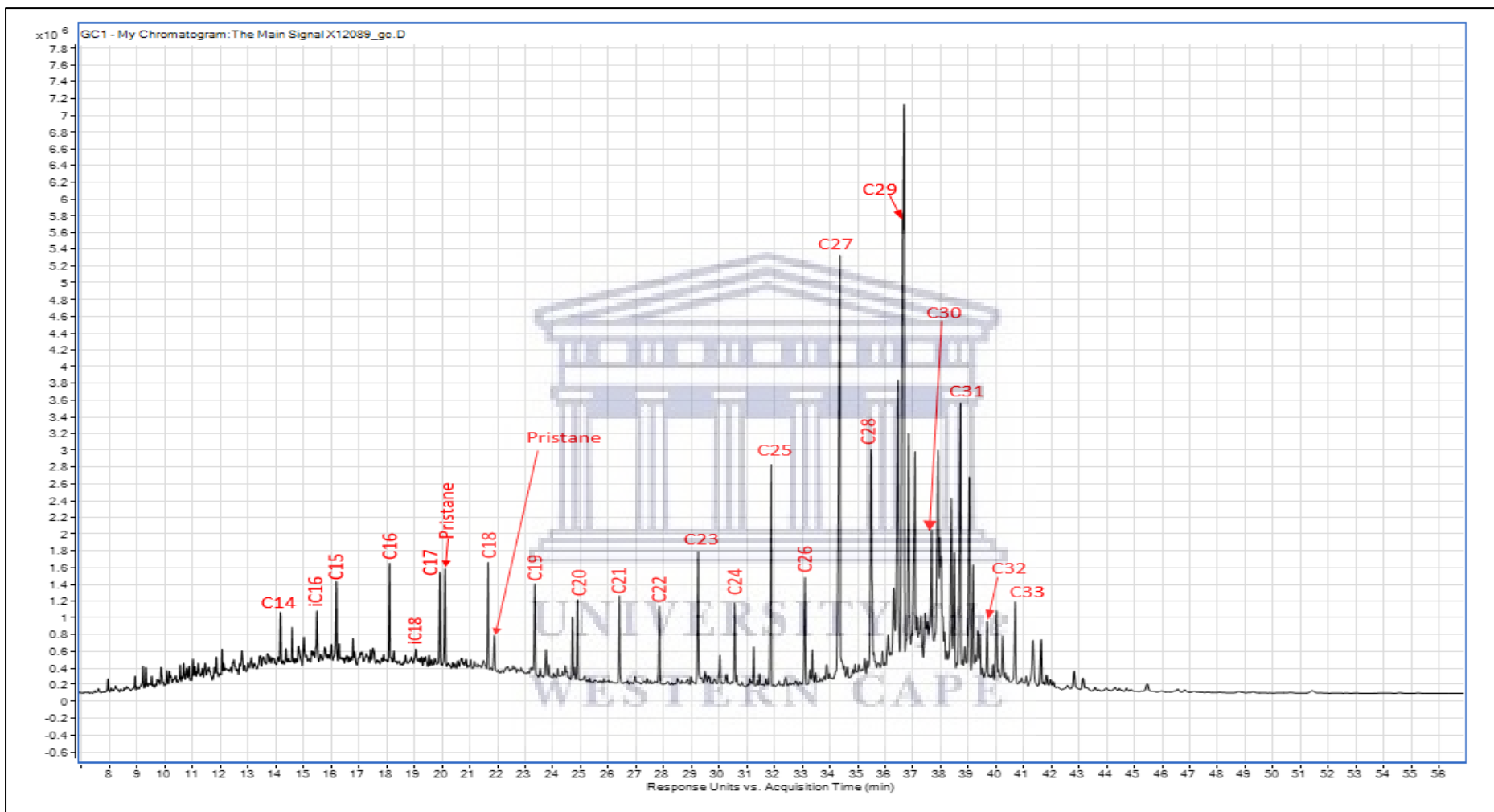
*Figure 59: Gas Chromatogram of Saturate Fraction of source rock at a depth of 5.5 m showing a bimodal distribution of n-alkane.*
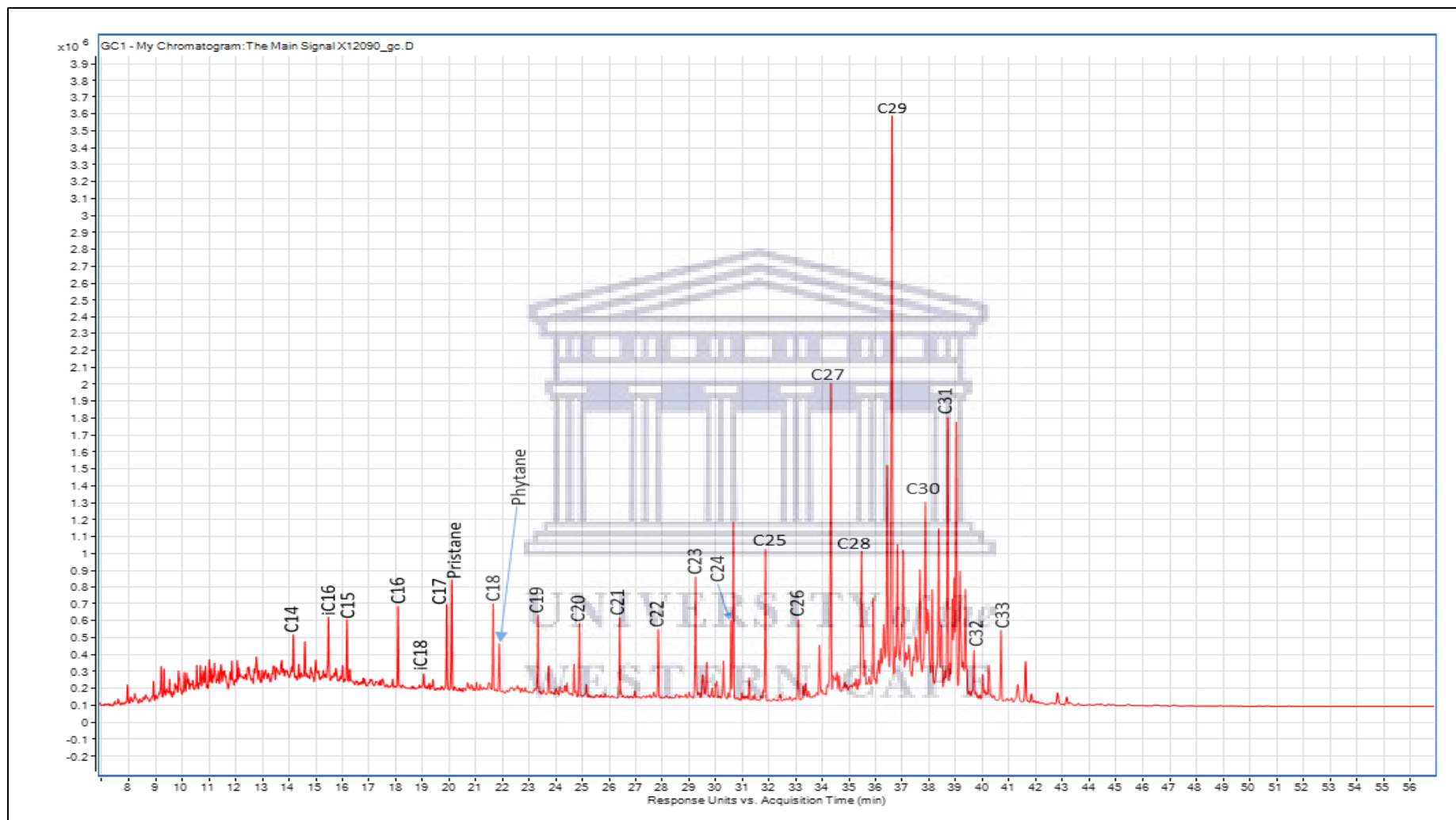
*Figure 60: Gas Chromatogram of Saturate Fraction of source rock at a depth of 6.0 m showing a bimodal distribution of n-alkane.*

*Table 16: GC results showing CPI, and Pristane/Phytane, Pristane/n-C17, and Phytane/n-C18 ratios.*

| Well Name | Sample Type | Sample Depth (m) | CPI | Pristane Phytane | Pristane n-C17 | Phytane n-C18 |
|-----------|-------------|------------------|-----|------------------|----------------|---------------|
| J4-BH1 | Source Rock | 5.5 | 3.03 | 2.44 | 1.16 | 0.42 |
| J4-BH1 | Source Rock | 6.0 | 3.51 | 2.10 | 1.41 | 0.66 |

*Note:*

*n-C17; C17 Normal Paraffins*

*n-C17; C18 Normal Paraffins*

The pristane/phytane ratio is a widely used geochemical parameter to determine the relative oxygen content (oxicity) in a depositional environment. While other likely sources of pristane and phytane have been reported (Chappe et al., 1982; Goossens et al., 1984; Rowland, 1990), the phytyl side chain of chlorophyll in phototrophic organisms and bacteriochlorophyll a and b in purple Sulphur bacteria (Brooks et al., 1969; Powell and McKirdy, 1973) make up the most abundant source of pristane and phytane in sediments.

Reducing or anoxic conditions in sediments promote the phytyl side chain's cleavage to yield phytol, which undergoes reduction to dihydrophytol and then phytane (Peters et al., 2005). In oxic conditions, the dominant product of phytol conversion is pristane. Thus, the pristane/phytane (Pr/Ph) ratio provides information on the oxicity of the source rock depositional environment. Didyk et al. (1978) postulated that a Pr/Ph ratio of less than 1 in crude oil indicates anoxic source rock deposition, while a Pr/Ph > 1 suggests that the source rock was deposited in the oxic environment. While it is highly recommended to use multiple sources of data to validate the oxicity of the depositional environment rather than any finite conclusion based on Pr/Ph alone (Ten Haven et al., 1987), the parameter is still widely applied. It seems to work well if the data is

adequately analyzed (Fabianńska et al., 2003). In general, high Pr/Ph (>3.0) indicates terrigenous organic matter input under oxic conditions, while low values (<0.8) show anoxic, commonly hypersaline or carbonate environments (Peters et al., 2005).

The source rocks' Pr/Ph ratio ranged between 2.44 and 2.10 and indicated a suboxic depositional environment. The gas chromatograms showed features typical of immature terrestrial material deposited in the suboxic environment (bimodal n-alkane distribution, high CPI value, high Pristane/nC17 ratio, and pristane/phytane ratio of 2.10 to 2.44).

## 5.9 ORGANIC PETRROGRAPHY

The total amount of hydrocarbons that can be generated and the relative proportion of oil and gas depends on the composition of the parent kerogen in petroleum source rocks (Staplin, 1969; Tissot et al., 1974). The evaluation and characterization of petroleum source rock have relied extensively on geochemical analysis with particular emphasis on Rock Evaluation (Rock-Eval) Pyrolysis. As laudable as it may be, geochemical analysis and interpretation of source rock potential are constrained by drawbacks such as the following:

a)  It is based on bulk rock samples

b)  Inability to identify the organic components

c)  Indirect analysis by the interpretation of geochemical parameters

d)  Inability to identify and quantify mixed kerogen

e)  Interpretation errors in the evaluation of hydrocarbon potential may result from a kerogen mix.

These drawbacks can be addressed by optical microscopy as isolated kerogen is studied directly under the microscope.

Optical microscopy enables direct identification of the different types of macerals in the kerogen, identifies different types of kerogen, and provides information on the composition, preservation, and maturation of kerogen. Therefore, the optical analysis is a  more complete form of analysis to evaluate and characterize petroleum source rocks than geochemistry.

Organic petrography has been a common form of analysis in the study of coal and its ranking (Stach et al., 1982; Taylor et al., 1991; Teichmüller, 1974;  Teichmüller, 1987). Coal contains abundant vitrinite maceral, which originates from humic gels that are believed to be derived from the lignin cellulose cell walls of higher plants (Teichmüller, 1989). Vitrinite maceral is also found in source rock kerogen, and the optical properties of vitrinite can be used to assess thermal maturity (Bostick, 1979).

Vitrinite reflectance is considered the most robust petrographic parameter for the determination of thermal maturity in hydrocarbon exploration (Corcoran and  Doré, 2005; Dembicki, 2009; Hackley et al., 2015; Taylor et al., 1998). The increase in the reflectance of vitrinite with an increase in time and temperature parallels the degree of coal maturation, and it was used as a means to rank coal ( Teichmüller, 1982). The systematic increase in vitrinite reflectance is related to sediments' hydrocarbon generation history (Dembicki, 2017). The microscopy of kerogen provides an independent assessment of the quantity, quality, and thermal maturity of organic matter (Peters et al., 2005).

Maceral observations and reflectance measurements were carried out on polished pellets of rock chips, and kerogen concentrates. The rock chips made use of two source rocks at the depths of 5.5 m and 6.0 m from the J4-BH1 borehole. Kerogen concentrates were the products of kerogen extraction from Igbotu (EY-22) source rock at a depth of 93 m, two source rocks at the depths of 3 m, and 4.5m from the J4-BH1

borehole and one source rock at a depth of 3 m from the 3-Hanger outcrop.

Petrographic analysis of the two polished rock chip pellets indicated the absence of a true vitrinite maceral. Therefore, the reflectance of solid bitumen was measured and used to determine the thermal maturity of the rock in conjunction with Hawk/TOC Tmax results. Solid bitumen is the secondary product of the thermal decomposition of reactive kerogen during late diagenesis and early catagenesis (Hunt, 1979; Jacob, 1989). Several equations have been proposed for estimating equivalent vitrinite reflectance from the measured bitumen reflectance (Bertrand, 1993; Jacob, 1989; Landis and Castaño, 1995). For this study, the Jacob equation

$$\%VR_o \text{ equivalent} = 0.618(\%BR_o) + 0.4$$

where

$\% VR_o$ = Vitrinite Reflectance and $\% BR_o$ is Reflectance of Solid Bitumen

was used to determine the $\%VR_o$ equivalent from the measured bitumen reflectance. Classification of the main groups of dispersed organic matter was reported according to the International Committee for Coal and Organic Petrology (ICCP) vitrinite and liptinite classification (ICCP, 1998; ICCP, 2017).  Vitrinite reflectance equivalent (**%**$R_o$) for the organic-rich source rock at a depth of 5.5 m was estimated to be 0.34 **%**$R_o$ (Fig. 61, Plate a), and the maceral consisted mostly of liptinite (Figs. 61 and 62, Plates B to H) of terrestrial plant origin. The liptinite maceral mainly consisted of greenish-yellow to bright yellow fluorescing pollen, sporinite, suberinite, cutinite, and resinite with a high relative amount of reworked inertinite and vitrinite maceral.

In contrast, **%**$R_o$ for the source rock at a depth of 6.0 m was 0.38 **%**$R_o$, and the maceral similarly consisted of liptinite of terrestrial origin. The liptinite maceral (Figs. 63 and

64) is composed mostly of greenish-yellow to bright yellow fluorescing pollen, sporinite, suberinite, resinite, and rare botryococcus algae with trace amounts of reworked inertinite and vitrinite macerals. The resinite showed various stages of oxidation (Fig. 64, Plate E). Maceral composition and vitrinite reflectance for these rocks indicated the presence of Type II organic matter with a low level of thermal maturity. These petroleum source rocks are prone to generate oil at a higher degree of thermal maturity.
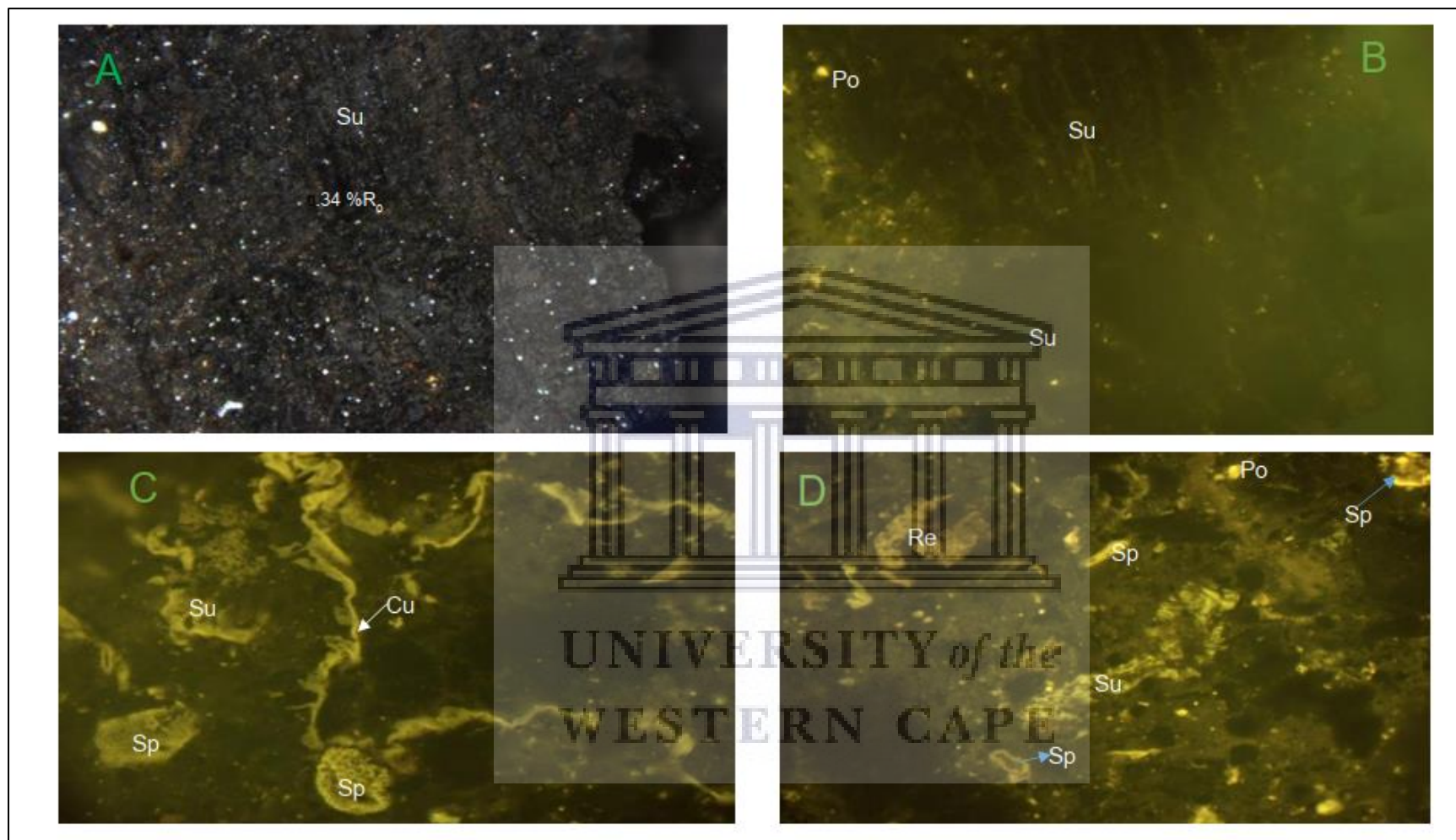
*Figure 61: Photomicrographs of organic-rich source rock at a depth of 5.5 m from J4-BH1 borehole showing the reflectance of solid bitumen (Plate A). The macerals consisted of liptinite (Plates B, C, and D) of terrestrial origin. The liptinite macerals include suberinite (Su), Cutinite (Cu), Sporinite (Sp), Resinite (Re), and Pollen (Po).*
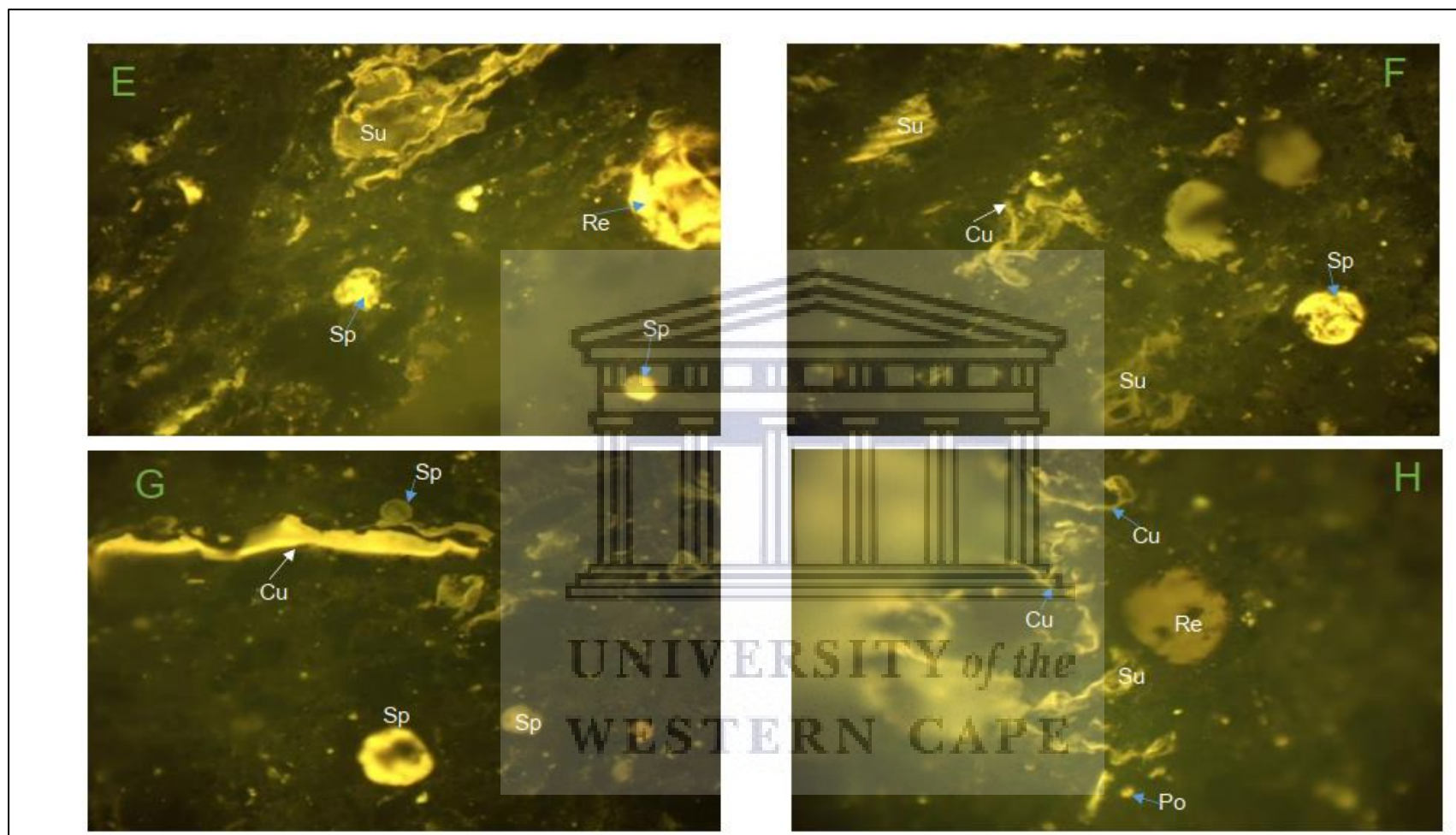
*Figure 62: Photomicrographs of organic-rich source rock at a depth of 5.5 m from J4-BH1 borehole, indicating the dominance of liptinite macerals. The liptinite macerals (Plates E, F, G, and H) include Suberinite (Su), Cutinite (Cu), Sporinite (Sp), Pollen (Po), and resinite (Re).*
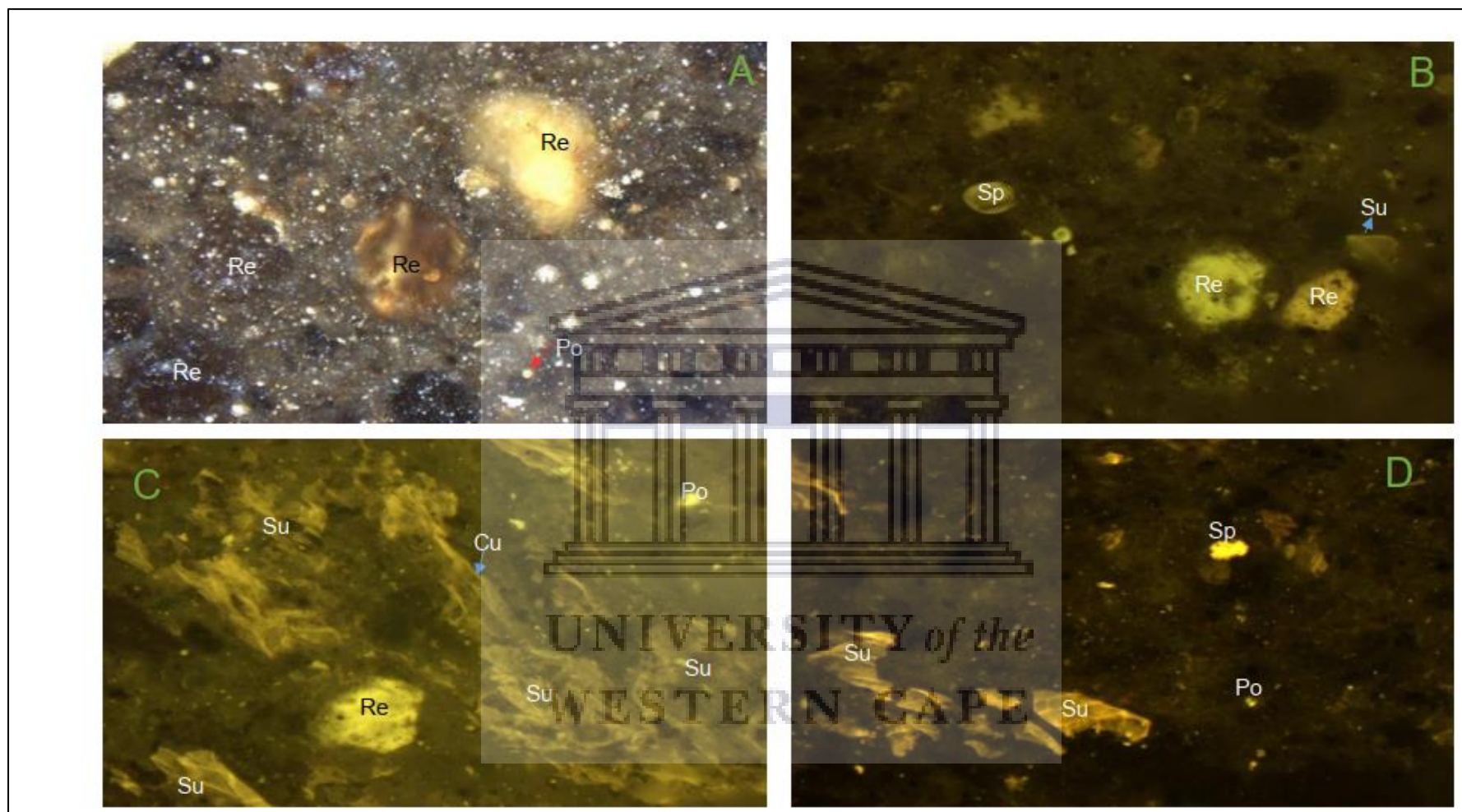
Figure 63: Photomicrographs of organic-rich claystone at a depth of 6.0 m from J4-BH1 borehole. The claystone consists mostly of liptinite macerals (plates a, b, c, and d) of terrestrial plant origin. The liptinite macerals include suberinite (Su), Cutinite (Cu), Sporinite (Sp), and Resinite (Re), and Pollen (Po).
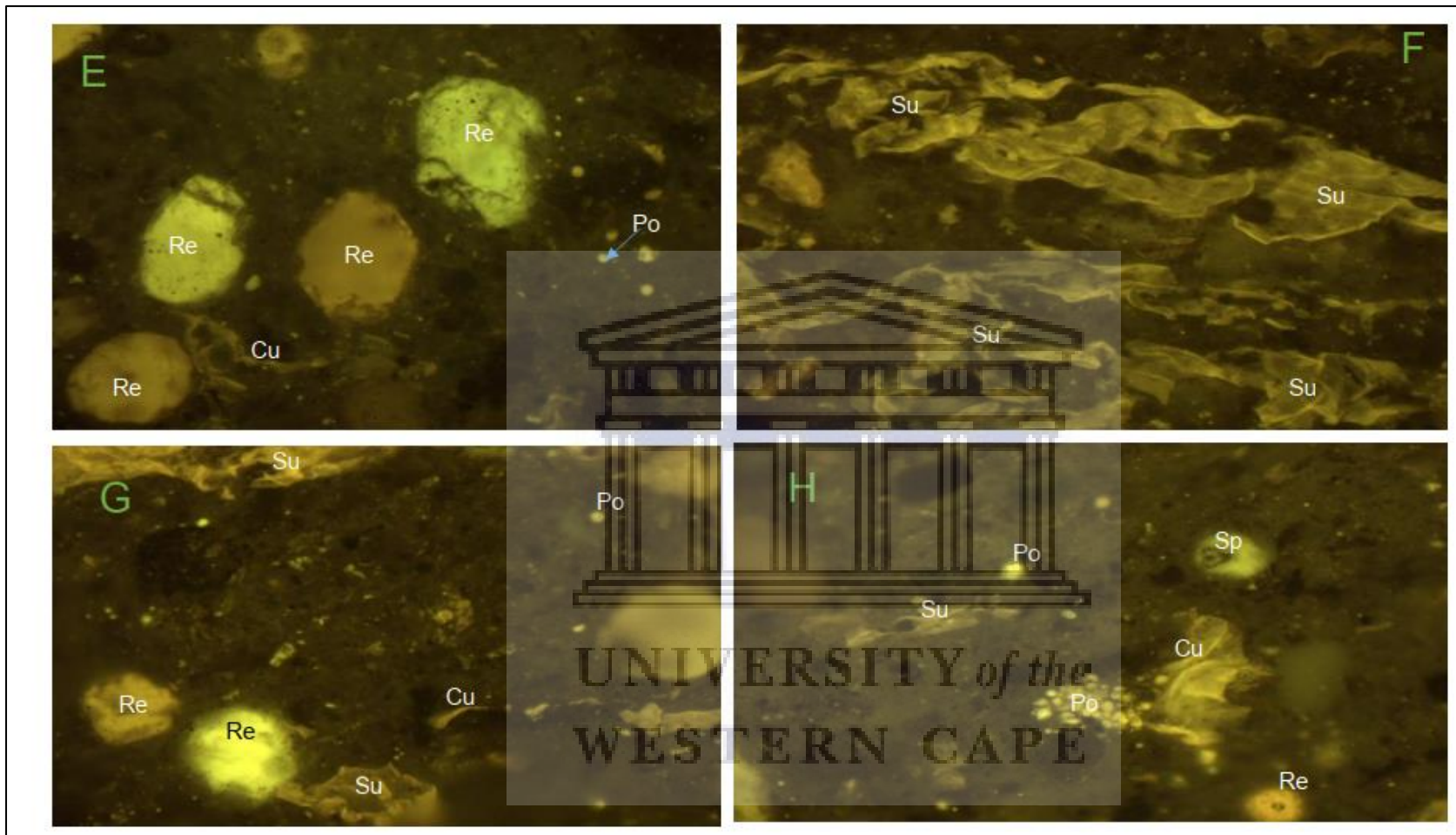
Figure 64: Photomicrographs of organic-rich source rock at a depth of 6.0 m from J4-BH1 borehole. The macerals include liptinite (plates E, F, G, and H) of terrestrial plant origin. The liptinite macerals consists of suberinite (Su), Cutinite (Cu), Sporinite (Sp), Pollen (Po), and resinite (Re). The resinite showed various stages of oxidation (Plate E).

Contrasting the rock chip samples that showed an absence of true vitrinite, optical analysis of the kerogen concentrates indicated an abundance of vitrinite maceral resulting in the measurements of their reflectance. Random reflectance measurements were carried out under oil immersion following the ASTM D7708-11 method and Hackley et al. ( 2015). The vitrinite maceral consisted of telovitrinite, gelinite, and corpogelinite. More than 30 counts of measurements were made on each of the kerogen concentrates to obtain statistically reliable results (Barker and Pawlewicz, 1993). The results of the reflectance measurements and their histograms are displayed in Figures 65, 66, 67, 68, 69, 70, 71, and 72. The histograms of the reflectance measurements indicate data set of a single in situ population that is devoid of reworked groups of vitrinite. The vitrinite reflectance for the samples ranged from 0.47 %$R_o$ to 0.56 %$R_o$.
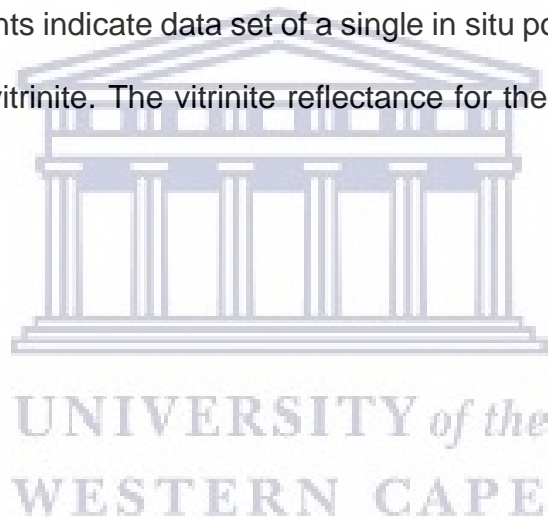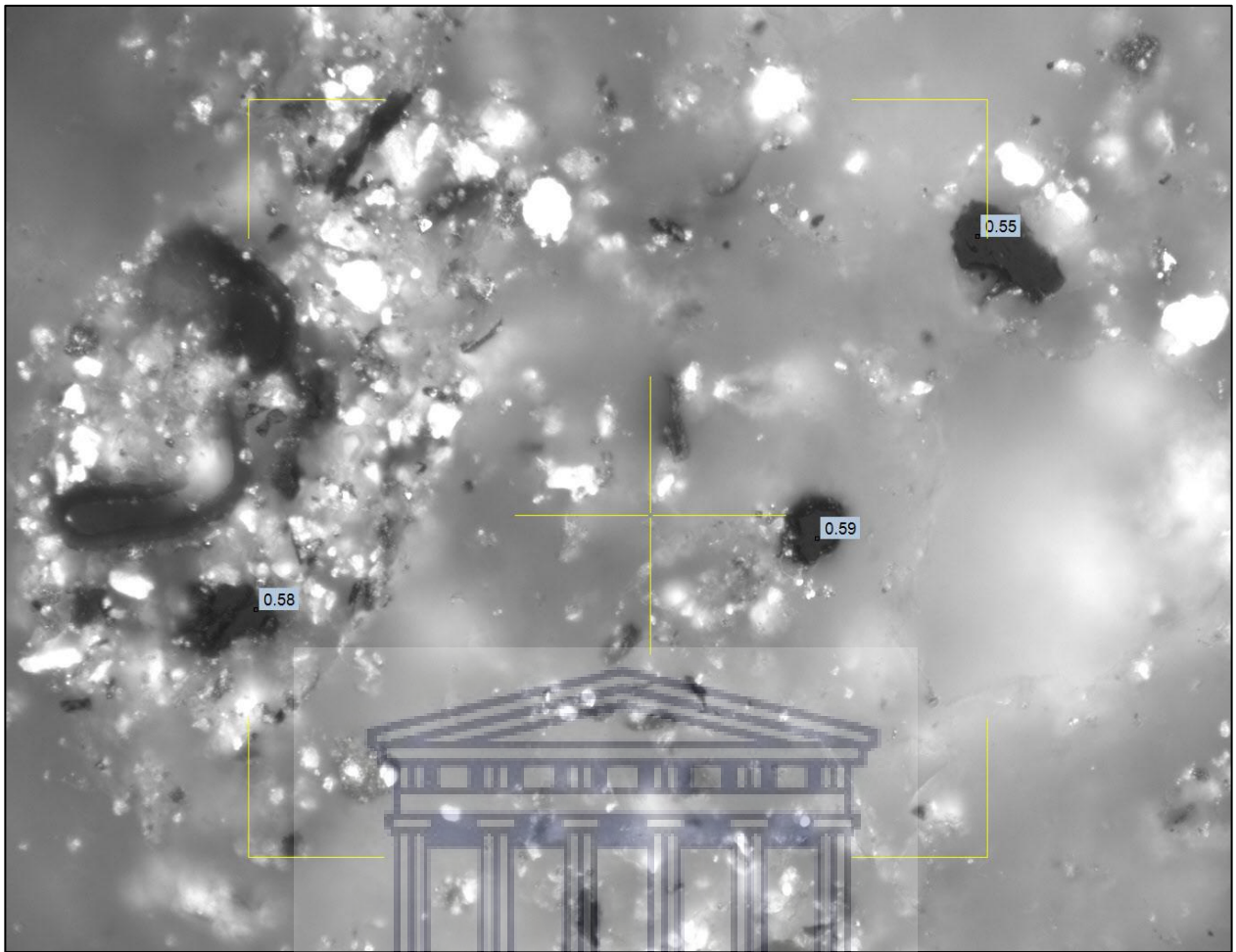
*Figure 65: Photomicrograph of kerogen concentrate displaying vitrinite maceral and reflectance values. The kerogen concentrate was extracted from the source rock at a depth of 3.0 m from J4-BH1 borehole.*

The histogram displays vitrinite reflectance measurements:

- Y-axis: 40%, 30%, 20%, 10%
- X-axis: 0, 0.1, 0.2, 0.3, 0.4, 0.5, 0.6, 0.7, 0.8, 0.9, 1.0%

Measure count = 54
Reflectance Rr = 0.564 %
s = 0.051 %

| | | | |
|---|---|---|---|
| 0.45 - 0.50 % R | 17 % | 0.60 - 0.65 % R | 22 % |
| 0.50 - 0.55 % R | 20 % | 0.65 - 0.70 % R | 4 % |
| 0.55 - 0.60 % R | 37 % | | |
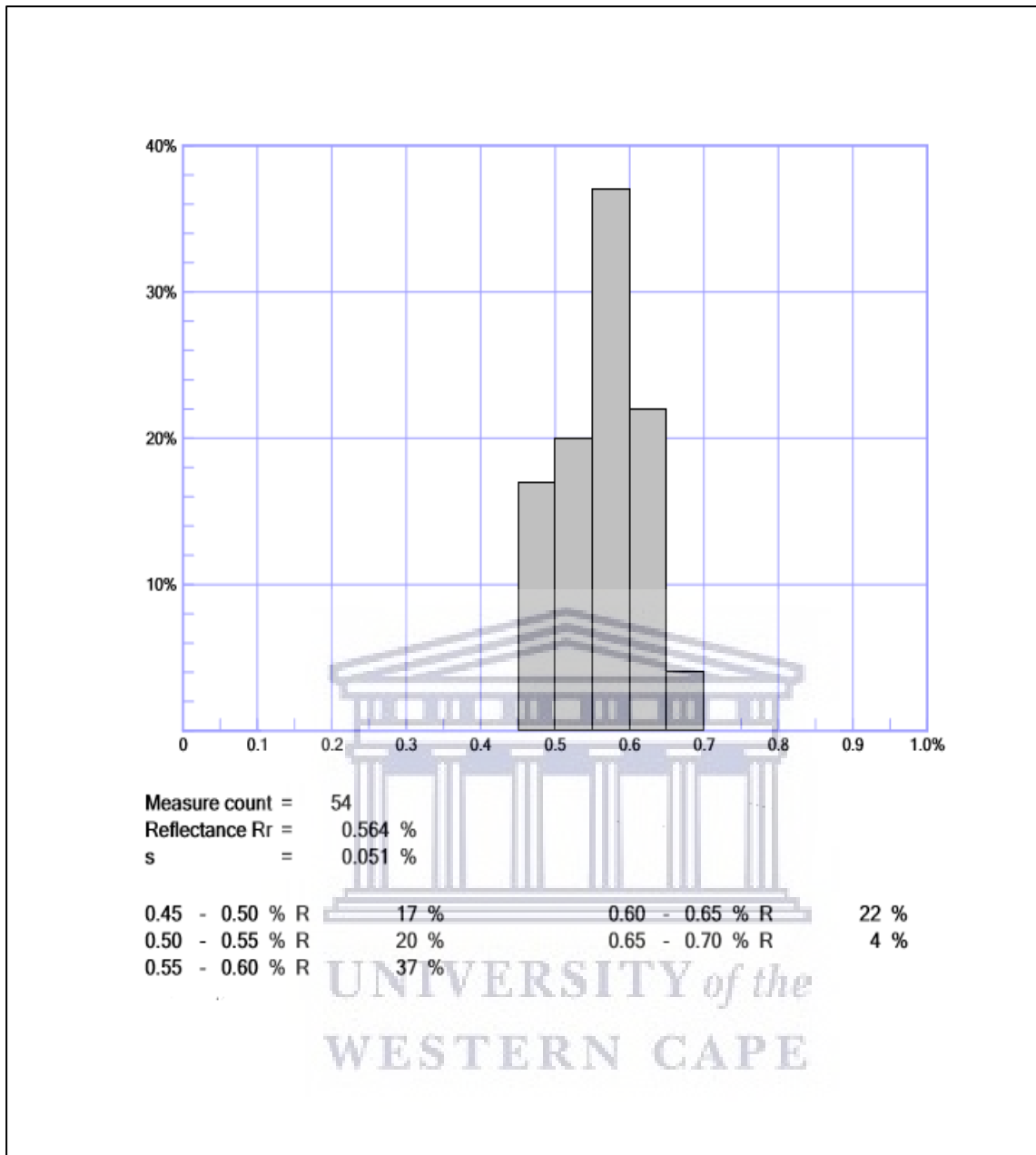
*Figure 66: Histograms of vitrinite reflectance measurement for kerogen concentrate. The kerogen was extracted from the source rock at a depth of 3.0 m in J4-BH1 borehole.*

*Figure 67: Photomicrograph of kerogen concentrate displaying vitrinite maceral and its reflectance values. The source rock was acquired at a depth of 4.5 m from J4-BH1 borehole.*
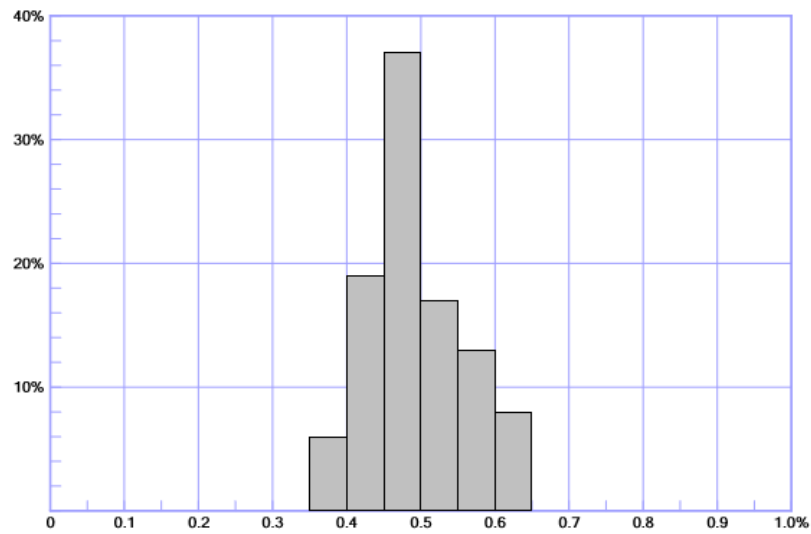
Measure count   =     52
Reflectance Rr  =    0.493  %
s               =    0.063  %

| 0.35 - 0.40 % R | 6 % | 0.50 - 0.55 % R | 17 % |
| 0.40 - 0.45 % R | 19 % | 0.55 - 0.60 % R | 13 % |
| 0.45 - 0.50 % R | 37 % | 0.60 - 0.65 % R | 8 % |
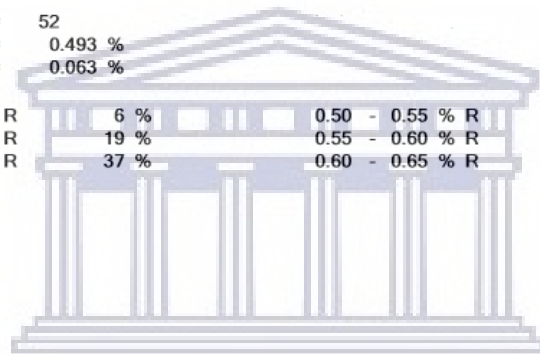
*Figure 68: Histograms of vitrinite reflectance measurements for kerogen concentrates. The kerogen was extracted from the source rock at a depth of 4.5 m from J4-BH1 borehole.*
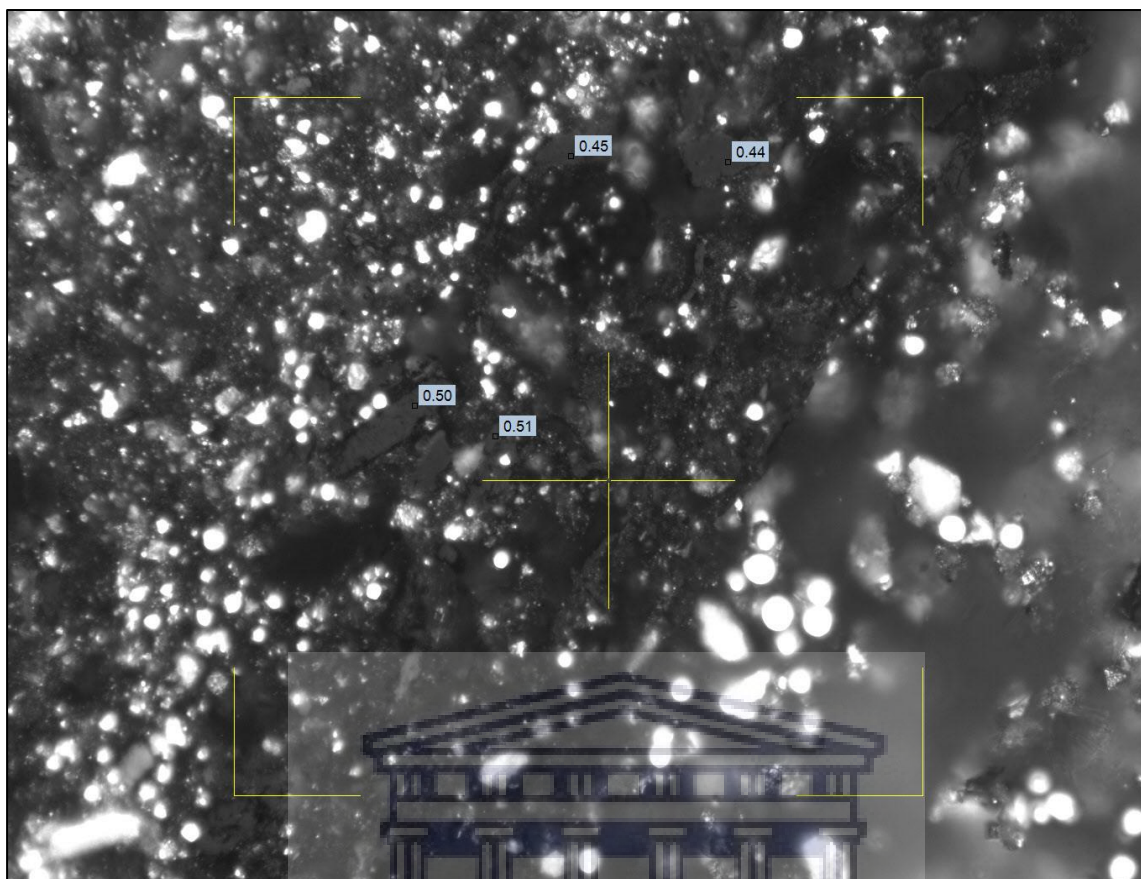
*Figure 69: Photomicrograph of kerogen concentrate from 3-Hanger outcrop showing vitrinite maceral and its reflectance values. The source rock was acquired at a depth of 3 m.*
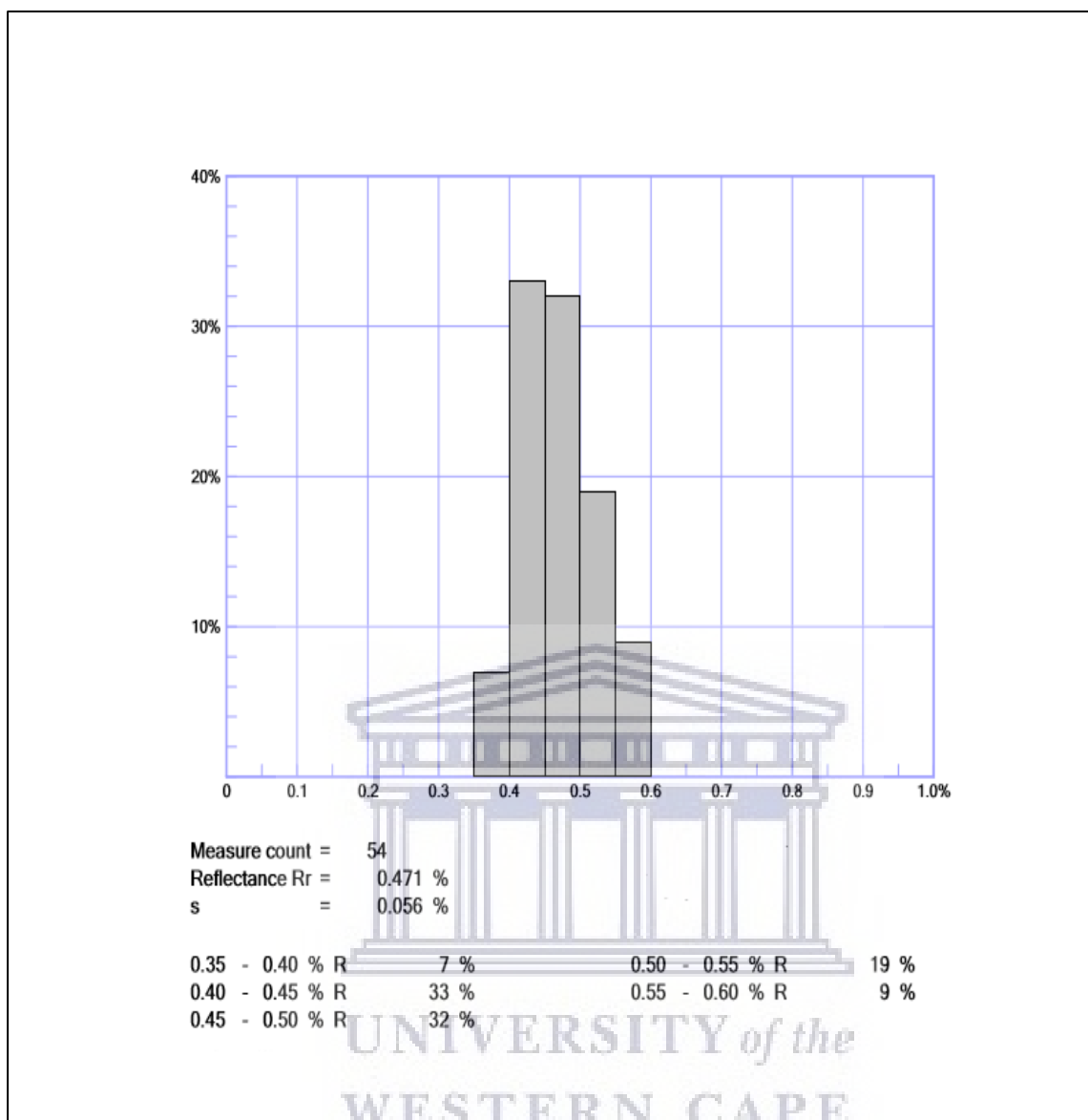
*Figure 70: Display showing histograms of vitrinite reflectance measurements for 3-Hanger kerogen concentrate. The source rock was acquired at a depth of 3 m.*
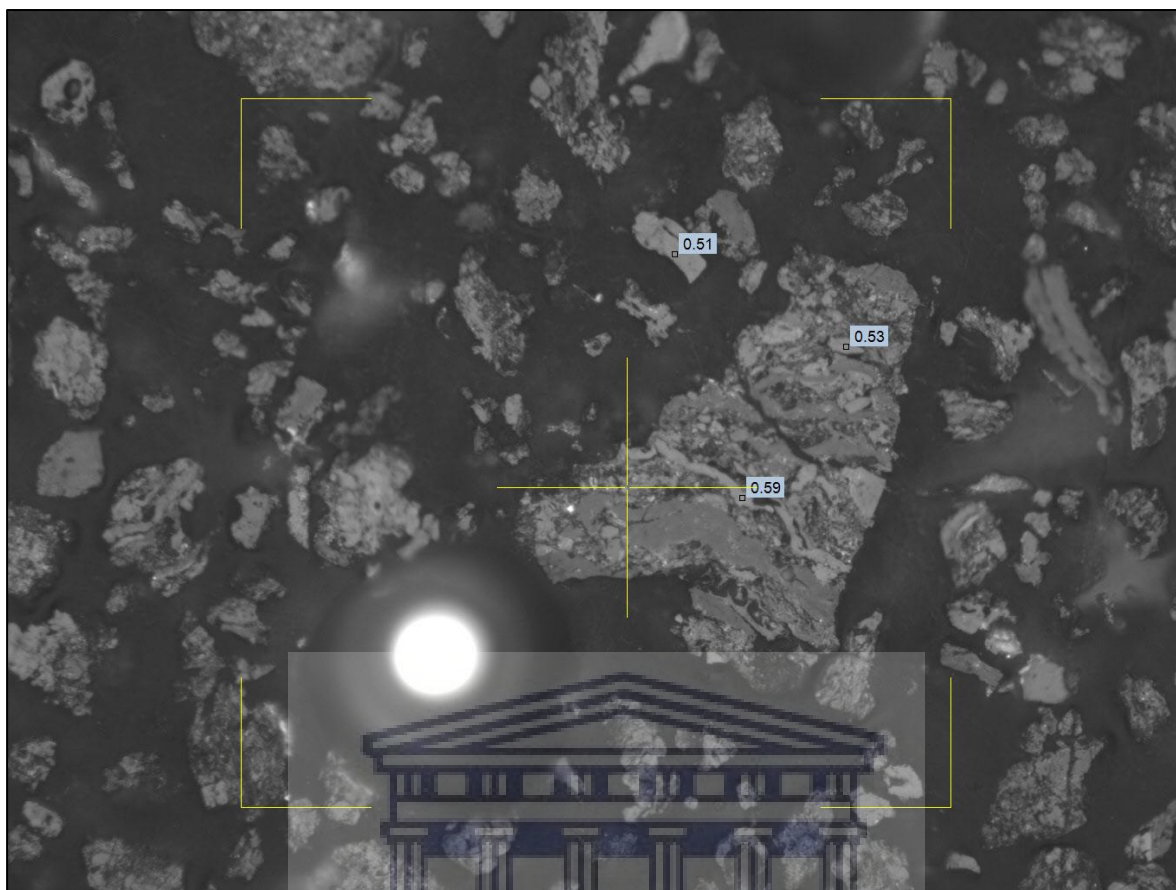
*Figure 71: Photomicrograph of kerogen concentrate, showing vitrinite maceral and its reflectance values. The kerogen was extracted from Igbotu (EY-22) source rock; sample depth was 93 m.*
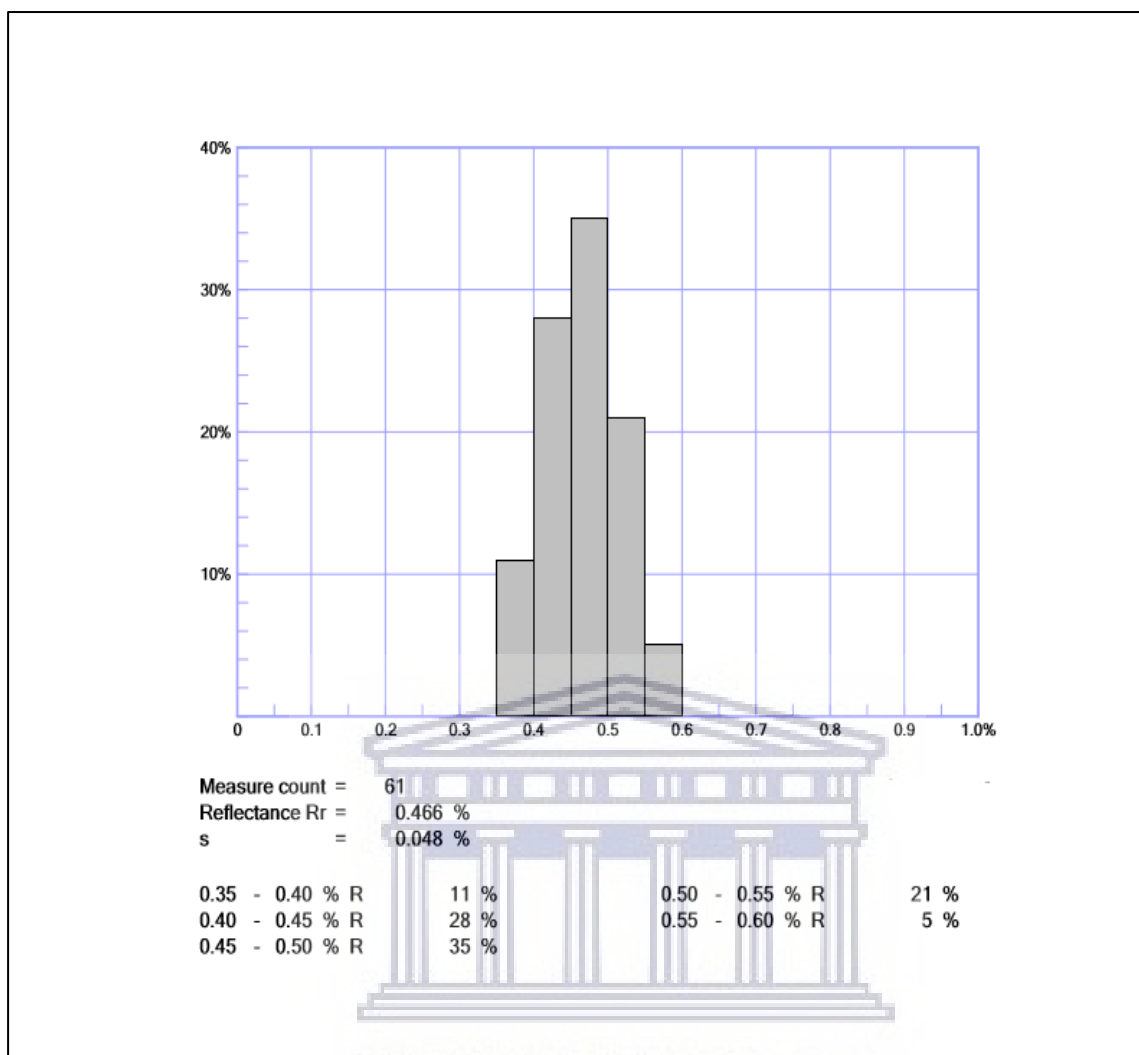
*Figure 72: Display showing histograms of vitrinite reflectance measurements for Igbotu (EY-22) source rock. The source rock was acquired at a depth of 93 m.*

Petrographic analysis of the kerogen concentrates revealed the presence of coaly particles and greenish-yellow to yellow fluorescing liptinite macerals consisting of sporinite, pollen, cutinite, suberinite, and resinite (Figs. 73, 74, 75, and 76). Some of the kerogen concentrates contained a high percentage of framboidal and euhedral pyrite (Fig. 74, Plate D).
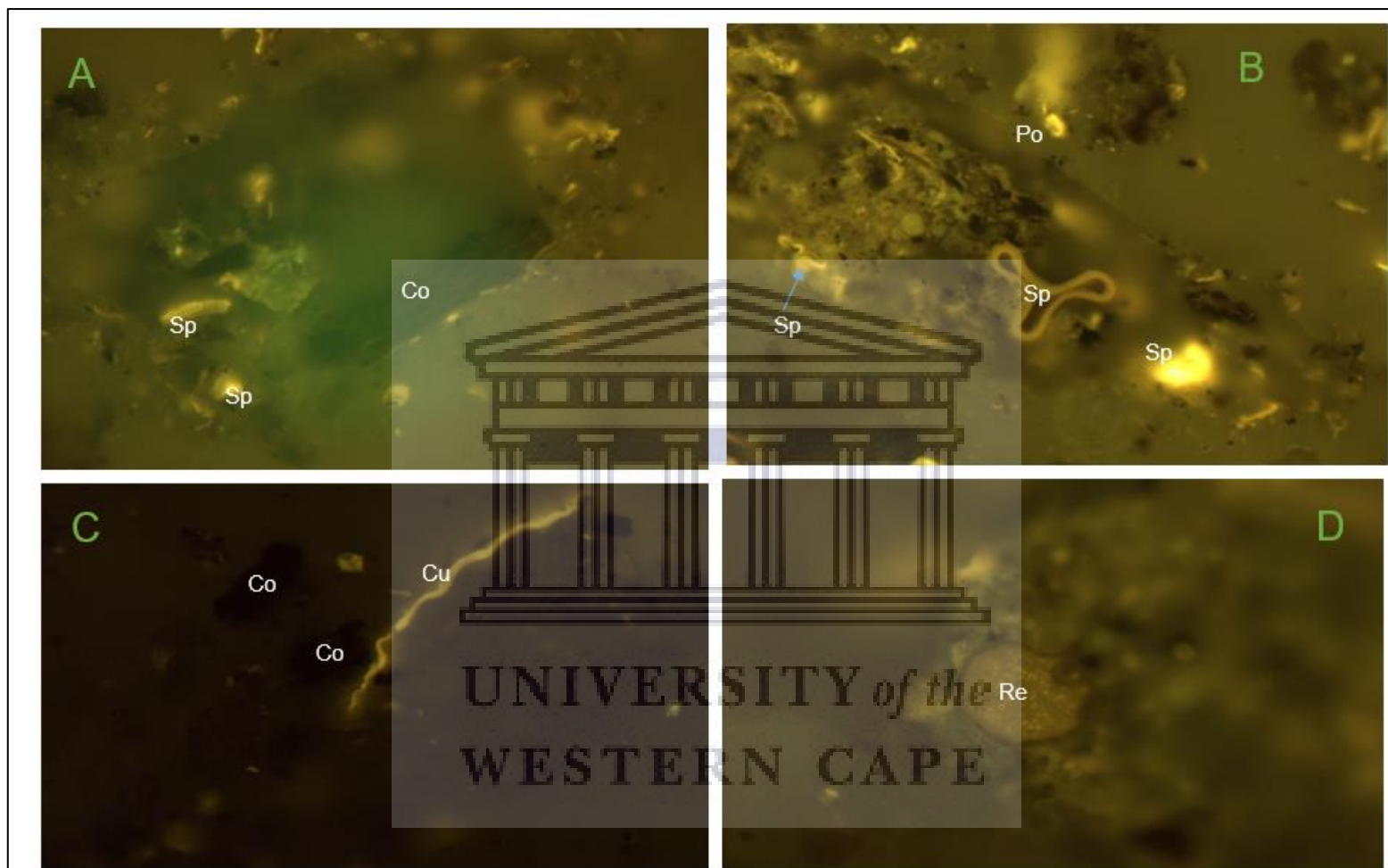
*Figure 73: Photomicrographs of kerogen concentrate from the source rock at a depth of 3 m (J4-BH1 borehole). The kerogen contains coaly particles (Co) with some Liptinite macerals (Plates A, B, C, and D). The liptinite macerals includes Sporinite (Sp), Resinite (Re), and Cutinite (Cu).*
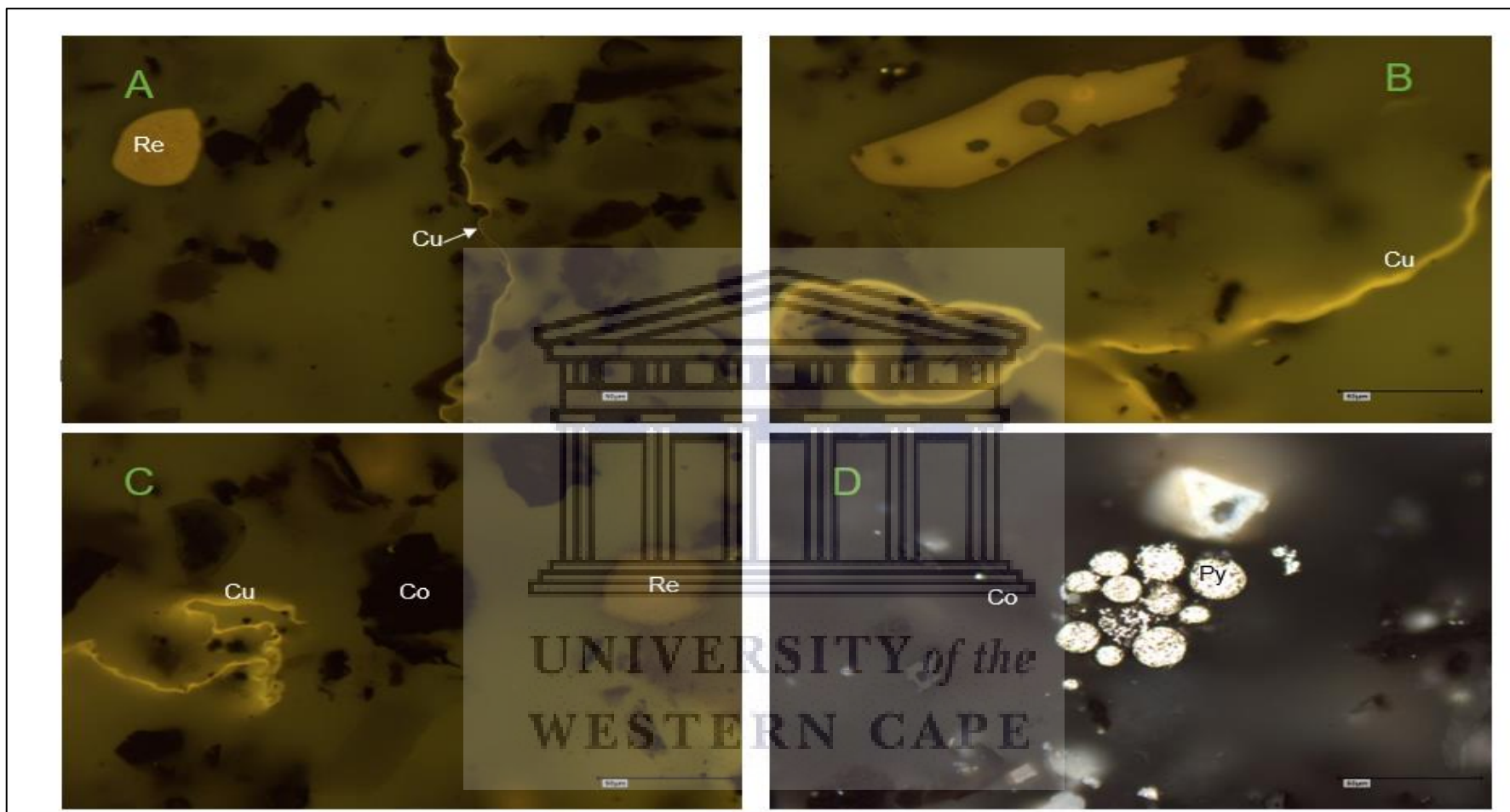
*Figure 74: Photomicrographs of kerogen concentrate from the source rock at a depth of 4.5 m (J4-BH1 borehole). The kerogen contained coaly particles (Co) with liptinite macerals (Plates A, B, and C) and Framboidal Pyrite (Plate D, Py). The liptinite macerals includes Resinite (Re), and Cutinite (Cu).*
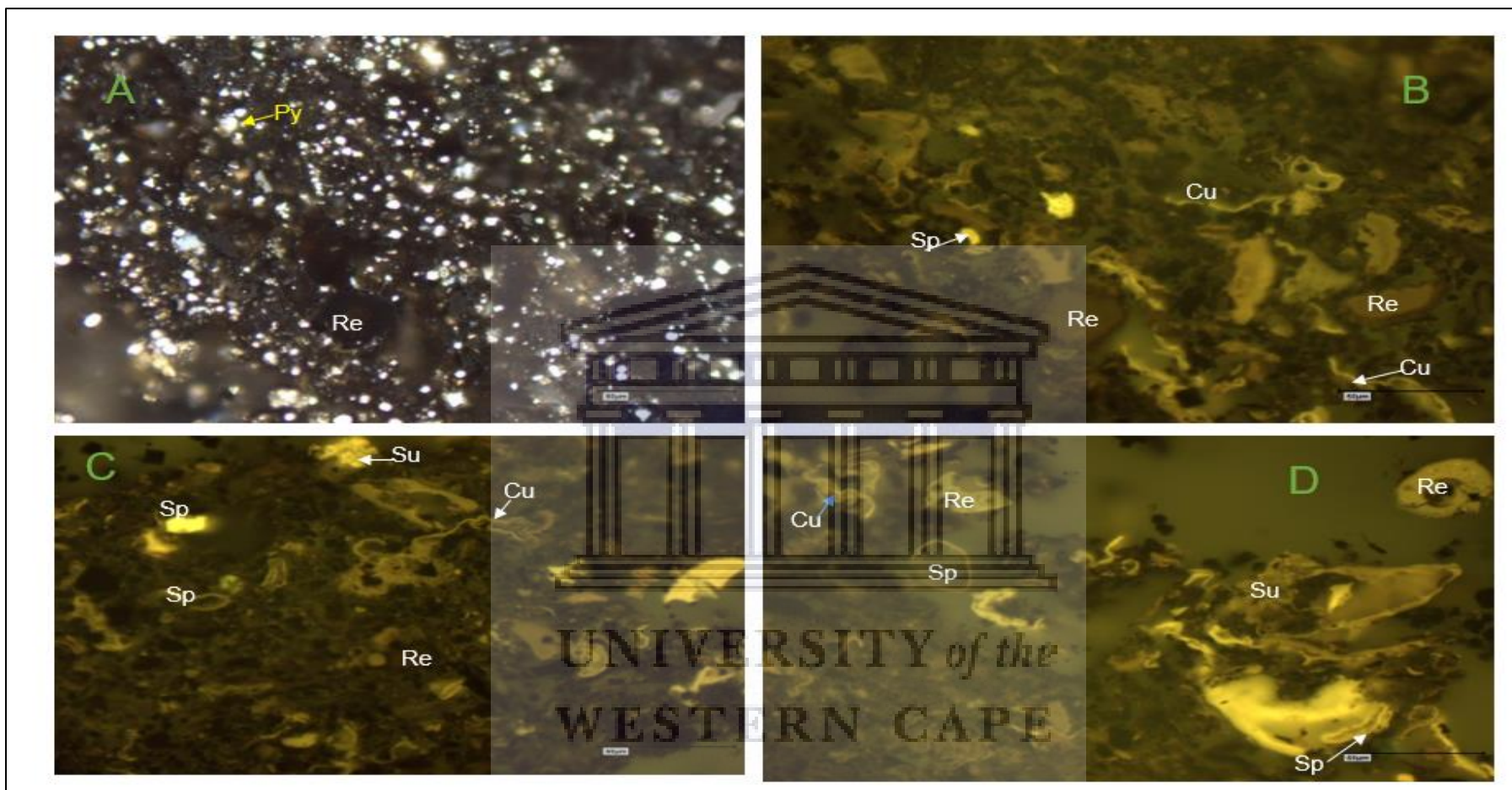
Figure 75: Photomicrographs of kerogen concentrate from the source rock at a depth of 3 m (3-Hanger outcrop). The kerogen is composed of liptinite macerals (plates a, b, c, and d) of terrestrial plant origin. The liptinite macerals includes Cutinite (Cu), Suberinite (Su), Sporinite (Sp), and resinite (Re). Euhedral pyrite mineral (Plate A, Py) is present in the kerogen.
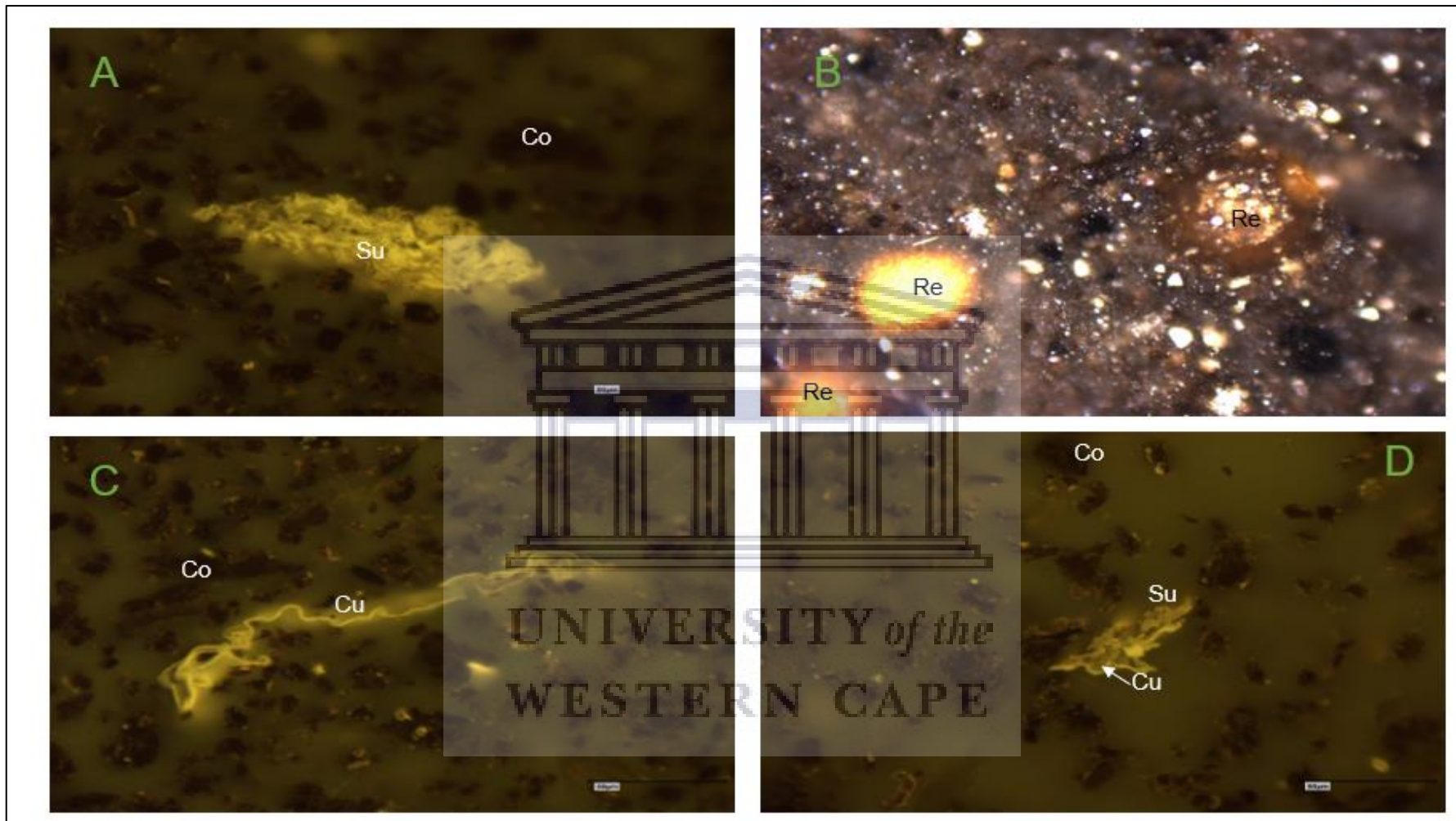
*Figure 76:Photomicrographs of kerogen concentrate from the source rock at a depth of 93 m (Igbotu, EY-22). The kerogen consists of liptinite macerals (plates a, b, c, and d) of terrestrial plant origin with some coaly particles (Co). The liptinite macerals includes Cutinite (Cu), Suberinite (Su),* and resinite (Re).

The petrographic analysis indicates a dominance of oil-prone Type II organic matter, consisting of greenish-yellow to yellow and bright yellow fluorescing liptinite macerals. The liptinite macerals are composed of sporinite, pollen, resinite, cutinite, and suberinite, with vitrinite reflectance showing a range of 0.34 %$R_o$ to 0.56 %$R_o$, suggesting that the organic matter is thermally immature.

# CHAPTER SIX

## HYDROCARBON CHARACTERIZATION

### 6.1: RESULTS AND DISCUSSION

The chapter presents and discusses the results that were obtained and used to characterize the oil sands and heavy oils from the Eastern Dahomey Basin. The deposits have been categorized based on their mode of occurrence and geochemistry. Several geochemical techniques were used to make the characterization.

### 6.2: MODE OF OCCURRENCE

The hydrocarbon resources of the Eastern Dahomey Basin occur as oil sand, heavy oil, and oil seeps. The oil sand, also referred to as tar sand or bituminous sand are found as outcrops in areas of dense vegetation where they are exposed by road cuttings and along river banks and at breaks of slopes. Some boreholes that were drilled in the basin intersected intervals of oil sands where they are overlain and underlain by organic-rich shales. The oil seeps are found emanating from the outcrop of oil sands on sunny days, and in some localities, they are found in streams. Heavy oils were encountered in some wells that were drilled in the basin, and in contrast to the oil sands, the heavy oil could flow from the sandstone reservoirs to the wellbore. These occurrences demonstrate that a working petroleum system exists in the basin.

## 6.3: HYDROCARBON COMPOSITION AND API GRAVITY FROM PETROLEUM ASSESSMENT METHOD

Inexpensive and straightforward geochemical analyses can provide timely information on hydrocarbon reservoirs (Jarvie et al., 2001) for informed decisions. Rock-Eval pyrolysis has been used majorly as a geochemical tool to characterize petroleum source rocks (Barker, 1974; Espitalie et al., 1977). Recent advances in pyrolysis instruments have made it possible to use the tool for reservoir studies (Maende et al., 2017) to characterize petroleum in both conventional and unconventional plays.

The hydrocarbon composition and API gravity of oil sands and heavy oil were evaluated with the aid of HAWK – PAM (Hydrocarbon Analyzer with Kinetics – Petroleum Assessment Method). The petroleum assessment method separates the volatile hydrocarbon components into four distinct yields (Oil-1, Oil- 2, Oil- 3, and Oil-4) to provide compositional information. Besides the composition information that it provides, the assessment also used the four yields to predict the API gravity. The four petroleum peaks correspond to the Saturates, Aromatics, Resins, and Asphaltenes categories (Maende et al. 2017). Petroleum fractions consisting of Oil-1, Oil-2, and Oil-3 are composed of saturates and aromatics with carbon numbers in the range of C4 to C19. The carbon (C) number for Oil-1 ranged from C4 to C5, while that of Oil -2, and Oil- 3 are from C6-C10, and C11-C19 respectively. Oil -4 is composed of polar compounds with a carbon number of C20-C36.

The results from the HAWK-PAM method are shown in Table 17.

*Table 17: Results of HAWK-PAM showing crude oil composition and API gravity*

| Sample ID | Sample Type | Depth (m) | Weight (mg) | Oil-1 (mg HC/g rock) | Tmax Oil-1 (°C) | Oil-2 (mg HC/g rock) | Tmax Oil-2 (°C) | Oil-3 (mg HC/g rock) | Tmax Oil-3 (°C) | Oil-4 (mg HC/g rock) | Tmax Oil-4 (°C) | Total Fractions (mg HC/g rock) | API Gravity Prediction |
|---|---|---|---|---|---|---|---|---|---|---|---|---|---|
| MF-1 | Oil Seeps | N/A | 5.50 | 0.08 | 13 | 0.37 | 61 | 13.58 | 142 | 105.25 | 263 | 119.28 | 14.31 |
| IJ-1 | Oil sand/Outcrop | 1.15 | 8.70 | 0.02 | 8 | 0.12 | 64 | 1.68 | 145.00 | 13.37 | 271 | 15.20 | 5.12 |
| IL-1 | Oil sand/well | 3.10 | 6.00 | 0.02 | 9 | 0.46 | 66 | 8.01 | 145.00 | 28.77 | 255 | 37.26 | 12.25 |
| OH-1 | Oil sand/Well | 18.00 | 8.10 | 0.02 | 9 | 0.19 | 65 | 3.75 | 145.00 | 26.88 | 290 | 30.85 | 12.56 |
| OD-1 | Oil sand/Well | 4.10 | 9.90 | 0.02 | 10 | 0.17 | 66 | 3.73 | 146.00 | 24.99 | 264 | 28.91 | 8.66 |
| EG | Oil sand/Outcrop | N/A | 7.80 | 0.02 | 10 | 0.22 | 65 | 3.68 | 145 | 28.12 | 293 | 32.04 | 9.5 |
| OR | Oil sand /Outcrop | N/A | 7.30 | 0.03 | 10 | 0.19 | 66 | 5.63 | 146 | 50.06 | 286 | 55.91 | 9.46 |
| J4-1 | Oil sand/Outcrop | N/A | 10.10 | 0.02 | 10 | 0.23 | 67 | 4.84 | 145 | 31.02 | 256 | 36.12 | 10.02 |
| J4-1 | Oil Sand/Outcrop | 7.80 | 12.80 | 0.00 | 8 | 0.17 | 55 | 4.89 | 131.00 | 22.58 | 232 | 27.64 | 11.58 |
| J4-2 | Oil Sand/Outcrop | 8.10 | 15.70 | 0.00 | 3 | 0.28 | 54 | 8.72 | 131.00 | 39.21 | 247 | 48.21 | 13.56 |
| J4-3 | Oil Sand/Outcrop | 8.40 | 22.80 | 0.01 | 11 | 0.17 | 54 | 5.28 | 131.00 | 21.76 | 233 | 27.22 | 11.00 |

*Note on Abbreviations*

*MF-1 = Mafowoku ; IJ-1=  Ijuoke Agotitun ; IL= Ilubinrin ; OH = Ohosu (EY-28) ; OD-1 = Ode- Aye BH1; EG= Egbe; OR = Orisunbare; J4 = Onikitibi*

The results (Table 17) showed a dominance of oil - 4 fractions followed by Oil- 3. The amounts of Oil -1 and Oil-2 are all less than 0.5 mg HC/g rock, indicating the absence of light end molecular components. The quantities of Oil- 3 varied from 1.68 mg HC/g rock to 13.58 mg HC/g rock. In contrast, the amounts of Oil-4 ranged from 13.37 mg HC/g rock to 105.25 mg HC/g rock.

When hydrocarbons are generated from the thermal break down of kerogen, the original crude oil is generally light with an API gravity of 30° to 40°. Crude oil becomes heavy after the removal of the low-end molecular components resulting in the accumulation of the heavy end molecular components with low API gravity. Once oil has accumulated in the reservoir, its quality can be drastically changed (Levinson, 1974). The degradation of the crude oil is attained through several processes (Bailey et al., 1973), and it can be so severe as to alter the characters of the crude oil from its initial quality. Microbial degradation, also known as biodegradation, is a significant factor that alters the composition and characteristics of crude oil after their migration and entrapment in reservoirs. Some of the effects of biodegradation are related to loss of light end molecular components, increase in heavy molecular components, decrease in API gravity, rise in metal and sulfur content, and removal of some geochemical fossils (biomarkers). The transition in oil quality from unaltered oil to biodegraded oil is reflected by the decrease in normal alkanes (n-alkanes), and a relative increase in phytane and pristane, until only the latter isoprenoids are left or finally eliminated in heavily biodegraded oils (Deroo et al., 1974).

The range of values for Oil-1 and Oil- 2 and the dominance of Oil-4 indicate the absence of low molecular end components consistent with biodegraded oils. The sum of all the petroleum fractions ranged from 15.20 mg HC/g rock to 119.28 mg HC/g rock (Table 17) with the heavy oil presenting the highest value of 119.28 mg HC/g rock.

In contrast to the oil seeps, the sum of the petroleum fractions for the oil sand ranged from 15.20 mg HC/g rock to 55.91 mg HC/g rock, indicating that the heavy oil has more hydrocarbon components. The predicted API gravity for the oil sands ranged from 5.12 °API to 13.56 °API, while that of the heavy oil stood at 14.31 °API. The range of API gravities and dominance of the heavy end molecular components in the fractions suggests that the crude oils are biodegraded.

## 6.4: CRUDE OIL ASSAY

Total Acid Number (TAN), Viscosity, Boiling point distribution, Weight Percent Sulphur, and API gravity measurements are components of the analyses that are referred to as Crude Oil Assay. Crude Oil Assay provides a means to assess the market value of the oil as well as determining its refining and transportation characteristics (Dembicki, 2017). Crude oils contain organic acids that are collectively called naphthenic acids after the first group of such compounds characterized in petroleum (Peters et al., 2005). Biodegradation increases the acid contents of crude oil, leading to an increase in refining cost and the installations of expensive corrosion-resistant materials. The results of the oil assay are presented in Table 18 and Figures 77 to 78. The analyses made use of heavy oils from Agbabu well, and heavy oil of Mile-2 oil seeps.

*Table 18: Results of Crude Oil Assay*

| Sample Number/Name | Test | Method | Param | Reported Result | Results Units |
|---|---|---|---|---|---|
| 190204-01/ Agbabu Heavy Oil | | | | | |
| | CHN | | | | |
| | | ASTM D5291C | Carbon | 78.94 | Wt % |
| | | | Hydrogen | 11.17 | Wt % |
| | | | Nitrogen | 0.63 | Wt % |
| | Density-Pyc | | | | |
| | | ASTM D70 | Density-15.6 C | 1.001 | g/ml |
| | | | API | 9.8 | |
| | S_D1552 | | | | |
| | | ASTM D1552 | Sulfur | 0.54 | Wt % |

Boiling Point Distribution

| Sample Number | Sample Name | Test | Method | Param | | Reported Result | Results Units |
|---|---|---|---|---|---|---|---|
| 190204-01 | Agbabu Heavy Oil | | | | | | |
| | | Simdis HT | | | | | |
| | | | ASTM D7169 | Mass% | BP | | |
| | | | | 0.5 | 217.2 | | °C |
| | | | | 1 | 231.6 | | |
| | | | | 2 | 250.6 | | |
| | | | | 3 | 264.8 | | |
| | | | | 4 | 278 | | |
| | | | | 5 | 289.8 | | |
| | | | | 6 | 299.8 | | |
| | | | | 7 | 309 | | °C |

| Mass % | BP | |
|---|---|---|
| 8 | 317.8 | °C |
| 9 | 326.6 | |
| 10 | 335 | |
| 11 | 343.4 | |
| 12 | 351.6 | |
| 13 | 359.2 | |
| 14 | 366.8 | |
| 15 | 374.4 | |
| 16 | 381.8 | |
| 17 | 389.2 | |
| 18 | 396.2 | |
| 19 | 403 | |
| 20 | 409.2 | |
| 21 | 414.8 | |
| 22 | 420.2 | |
| 23 | 425 | |
| 24 | 429.4 | |
| 25 | 434 | |
| 26 | 438.4 | |
| 27 | 443.6 | |
| 28 | 449 | |
| 29 | 455 | |
| 30 | 461.4 | |
| 31 | 468 | |
| 32 | 474.6 | |
| 33 | 481 | |
| 34 | 487.4 | |
| 35 | 493.8 | °C |

| Mass % | BP |
| --- | --- |
| 36 | 499.8 |
| 37 | 505.6 |
| 38 | 511.4 | °C |
| 39 | 517 |
| 40 | 522.6 |
| 41 | 528 |
| 42 | 533.6 |
| 43 | 539.6 |
| 44 | 545.8 |
| 45 | 552 |
| 46 | 558.4 |
| 47 | 564.8 |
| 48 | 571.2 |
| 49 | 577.8 |
| 50 | 584.4 |
| 51 | 590.8 |
| 52 | 597.2 |
| 53 | 603.4 |
| 54 | 610 |
| 55 | 616.4 |
| 56 | 623 |
| 57 | 629.6 |
| 58 | 636.4 |
| 59 | 643.2 |
| 60 | 650.2 |
| 61 | 657.4 |
| 62 | 664.6 |
| 63 | 671.8 |
| 64 | 679.2 |

| Mass % | BP | |
|---|---|---|
| 65 | 686.8 | °C |
| 66 | 694.2 | |
| 67 | 702 | |
| 68 | 709.8 | |
| 69 | 717.8 | |
| 70 | 726.2 | |
| 71 | 735.2 | |
| 72 | 745.2 | |
| 73 | 750 | |
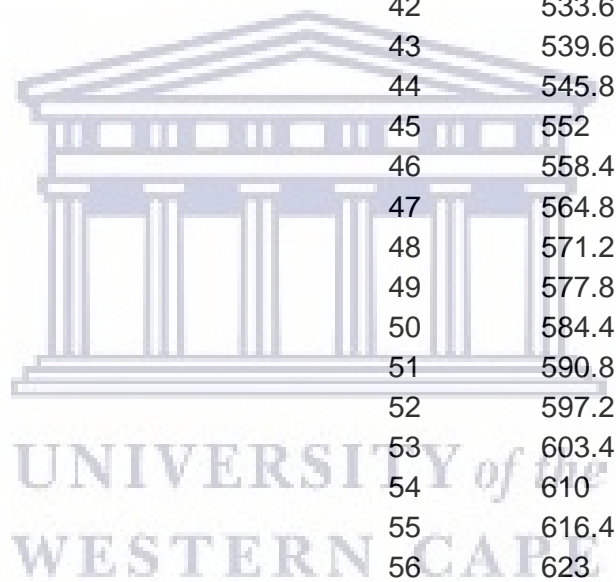
Viscosity, Water Content, and Total Acid Number

| Sample Number | Sample Name | VISC_DYN_D5018 | Method | Parameter | Reported Results | Results Units |
|---|---|---|---|---|---|---|
| | 190204-01/ Agbabu Heavy Oil | | ASTM D5018 | T1 | 50 | °C |
| | | | | Viscosity-T1 | 73560 | |
| | | | | T2 | 60 | |
| | | | | Viscosity-T2 | 35640 | |
| | | | | T3 | 80 | |
| | | | | Viscosity-T3 | 4344 | |
| | | Water_KF_D4377 | ASTM D4377 | Water Content | 5.7 | Wt % |
| 190204-02 | Mile 2-1 | | | | | |
| | | TAN | ASTM D8045 | Total Acid Number | 5.5 | mg KOH/g |
| | | Water_KF_D4377 | ASTM D4377 | Water Content | 16.45 | Wt % |
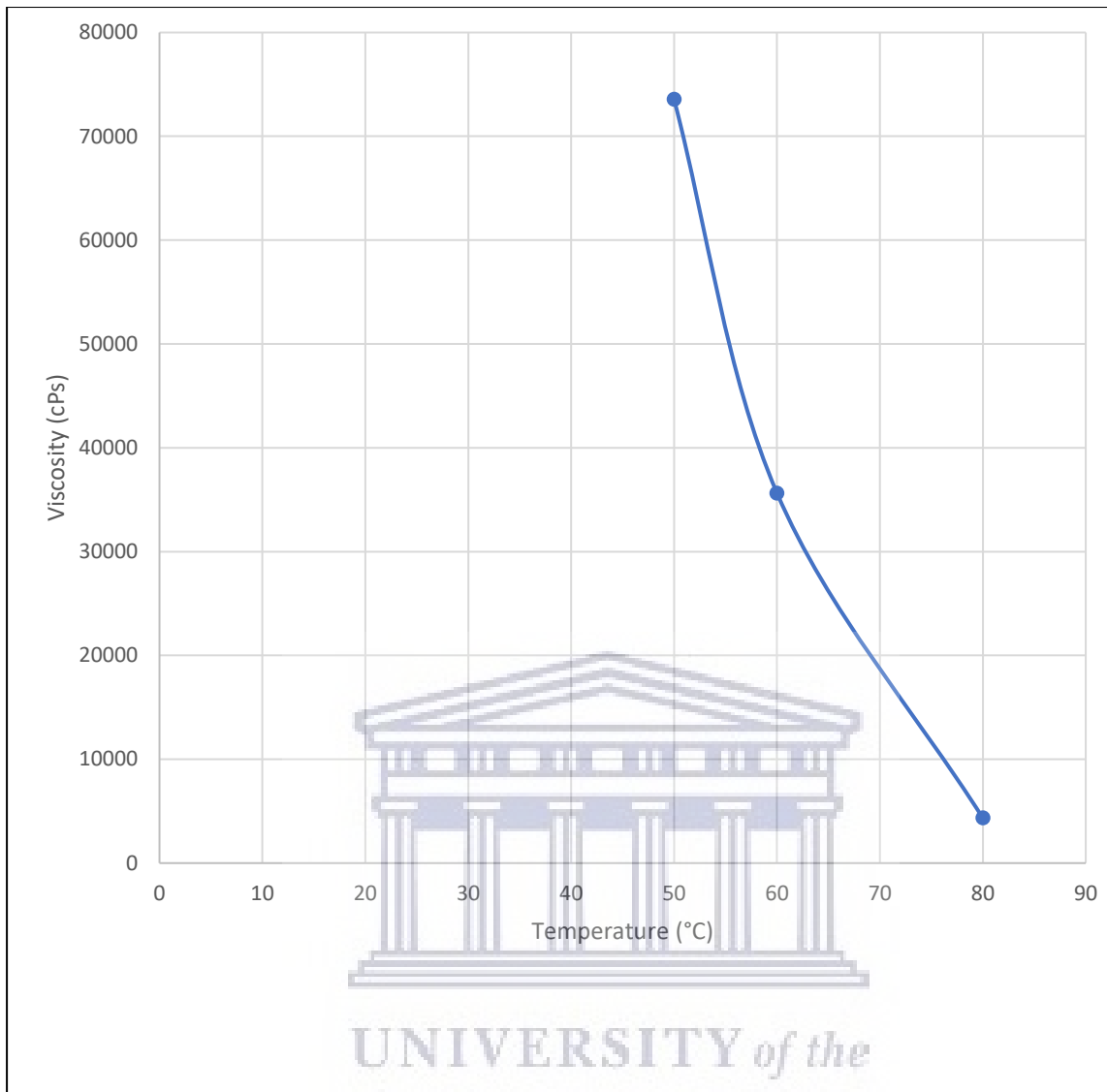
*Figure 77: Cross plot of viscosity versus temperature for Agbabu heavy oil.*
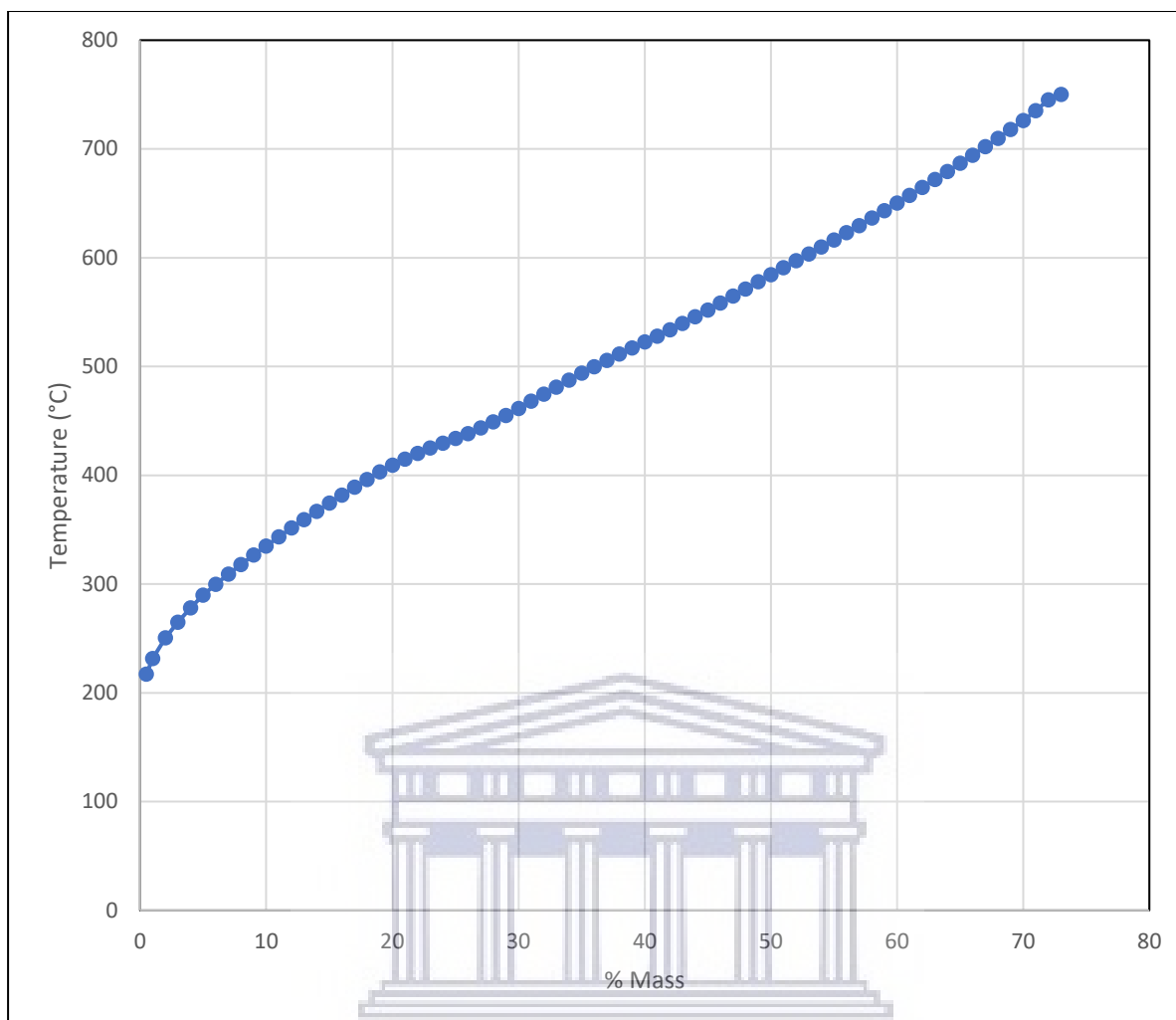
*Figure 78: Boiling point distribution curve showing the absence of light end distillates.*

The CHNS analysis showed that the oil is composed of 78.94 wt. % carbon, 11.17 wt. % hydrogen, 0.63 wt. % nitrogen, and 0.54 wt. % sulfur. The weight percent sulfur is a composite of both free sulfur (elemental sulfur that is dissolved in the oil) and bound sulfur (sulfur in the organic compounds that make up some of the crude oil). Weight percent sulfur increases with decreasing API gravity, and it may be related to biodegradation and the kerogen type that generated the petroleum. The weight percent sulfur of 0.54 wt. % possibly indicates that the oil is biodegraded, and based on the sulfur content, the oil is classified as sour crude (when the sulfur content is >0.5%, Dembicki, 2017).

155

The composition of crude oil, temperature, dissolved gas, and pressure all affect resistance to flow, and as temperature increases, the viscosity decreases. Viscosities were measured at temperatures of 50 °C, 60 °C and 80 °C (Fig. 77) with values of 73560 cPs, 35640 cPs, and 4344 cPs, respectively. The viscosity values are inversely proportional to temperature, and the measurements obtained can be used to predict the viscosity of the oil at different temperatures. The measured API gravity of 9.8° and viscosity showed that the oil is highly viscous, and biodegraded.

Crude oil distillation is the most crucial separation process in the petroleum industry (Austrich et al., 2015). Petroleum is a complex mixture of different compounds which boils over a range of temperature as opposed to a single boiling point for a pure compound. The boiling point distribution curve (Fig. 78) illustrated that petroleum compounds could be distilled from the oil over a temperature range of 217.2 °C to 750 °C and thus, indicates the dominance of middle and heavy distillates and the absence of light end molecular components.

Naturally occurring acids occurs in hydrocarbons, and their acidity causes corrosion of transportation and refining systems. The total acid number (TAN) is a measure of the quantity of the acidic substance in the oil. Total acid number for crude oil can range from less than 0.1 mg KOH/g to 8 mg KOH/g, and TAN values greater than 0.5 mg KOH/g indicates high acid oils (Peters et al., 2005). The total acid number for the crude oil (Table 18) was 5.5 mg KOH/g, indicating high acidic contents.

The water content showed values of 5.7 wt. % and 16.45 wt. % and reflected sample acquisition environments; Mile 2-1 heavy oil was collected from a stream and showed higher water content. In contrast, the heavy crude from Agbabu was obtained from a well and showed a much lower water content.

The results of the crude oil assay suggest heavy, sour crude with a high potential for medium and heavy distillates. This type of oil requires blending and installation of corrosion-resistant materials in their extraction, transportation, and refining.

## 6.5: CHNS ANALYSIS

Petroleum is composed mainly of compounds of carbon and hydrogen with some elements of nitrogen, sulfur, and oxygen. Crude oil consists of saturated hydrocarbons (paraffins, and naphthenes), aromatic hydrocarbons, resins, and asphaltenes. The resins and asphaltenes are made up of high molecular weight polycyclic fractions of crude oils comprising nitrogen, sulfur, and oxygen atoms (Tissot and Welte, 1984). Sulfur is the third most abundant element in petroleum, following carbon and hydrogen. It is present in the medium as well as in heavy fractions of crude oil, and unlike nitrogen, it is not explicitly related to the weightiest portions. Changes in the composition of crude oils are reflected in these elements, and the CHNS content provides a reasonable indication of its quality. The degradation of crude oils increases weight percent sulfur and nitrogen in addition to the loss of light end molecular components. The CHNS results are shown in Table 19 and Figure 79, and 80.

*Table 19: Results of CHNS analysis showing elemental composition*

| Sample ID | Sample Type | Sample Depth (m) | Elemental Composition (wt. %) | | | | C/H | N/S |
|---|---|---|---|---|---|---|---|---|
| | | | C | H | N | S | | |
| ML-21 | Oil seep | N/A | 66.25 | 10.51 | 0.44 | 1.83 | 6.30 | 0.24 |
| MF-1 | Oil seep | N/A | 51.18 | 7.96 | 0.57 | 0.64 | 6.43 | 0.89 |
| ML-22 | Oil seep | N/A | 73.18 | 11.86 | 0.45 | 1.54 | 6.17 | 0.29 |
| OD-1 | Oil sand/well | 2 | 6.92 | 0.65 | 0.08 | 1.16 | 10.73 | 0.07 |
| OD-2 | Oil sand/well | 3.5 | 5.27 | 0.55 | 0.04 | 0.48 | 9.51 | 0.08 |
| OD-3 | Oil sand/well | 4.1 | 9.86 | 1.01 | 0.05 | 0.45 | 9.81 | 0.11 |
| IL-1 | Oil sand/well | 2 | 12.97 | 1.36 | 0.05 | 0.29 | 9.54 | 0.17 |
| IL-2 | Oil sand/well | 2.5 | 10.92 | 1.12 | 0.05 | 0.53 | 9.73 | 0.09 |
| IL-3 | Oil sand/well | 3.1 | 13.22 | 1.42 | 0.10 | 0.26 | 9.30 | 0.38 |
| J4-1 | Oil sand/Outcrop | 8.4 | 8.06 | 0.97 | 0.06 | 0.88 | 8.31 | 0.07 |
| EG-1 | Oil sand/Outcrop | N/A | 11.06 | 1.20 | 0.09 | 0.78 | 9.25 | 0.12 |
| OR-1 | Oil sand/Outcrop | N/A | 12.3 | 1.41 | 0.07 | 0.18 | 8.70 | 0.39 |
| | | | | | | | | |
| Average | | | | | 0.17 | 0.75 | | |

*Note on abbreviations*

*ML= Mile 2; MF= Mafowoku ;  OD-1 = Ode- Aye BH1; IL= Ilubinrin BH1; J4 = Onikitibi ; EG= Egbe ; OR = Orisunbare*

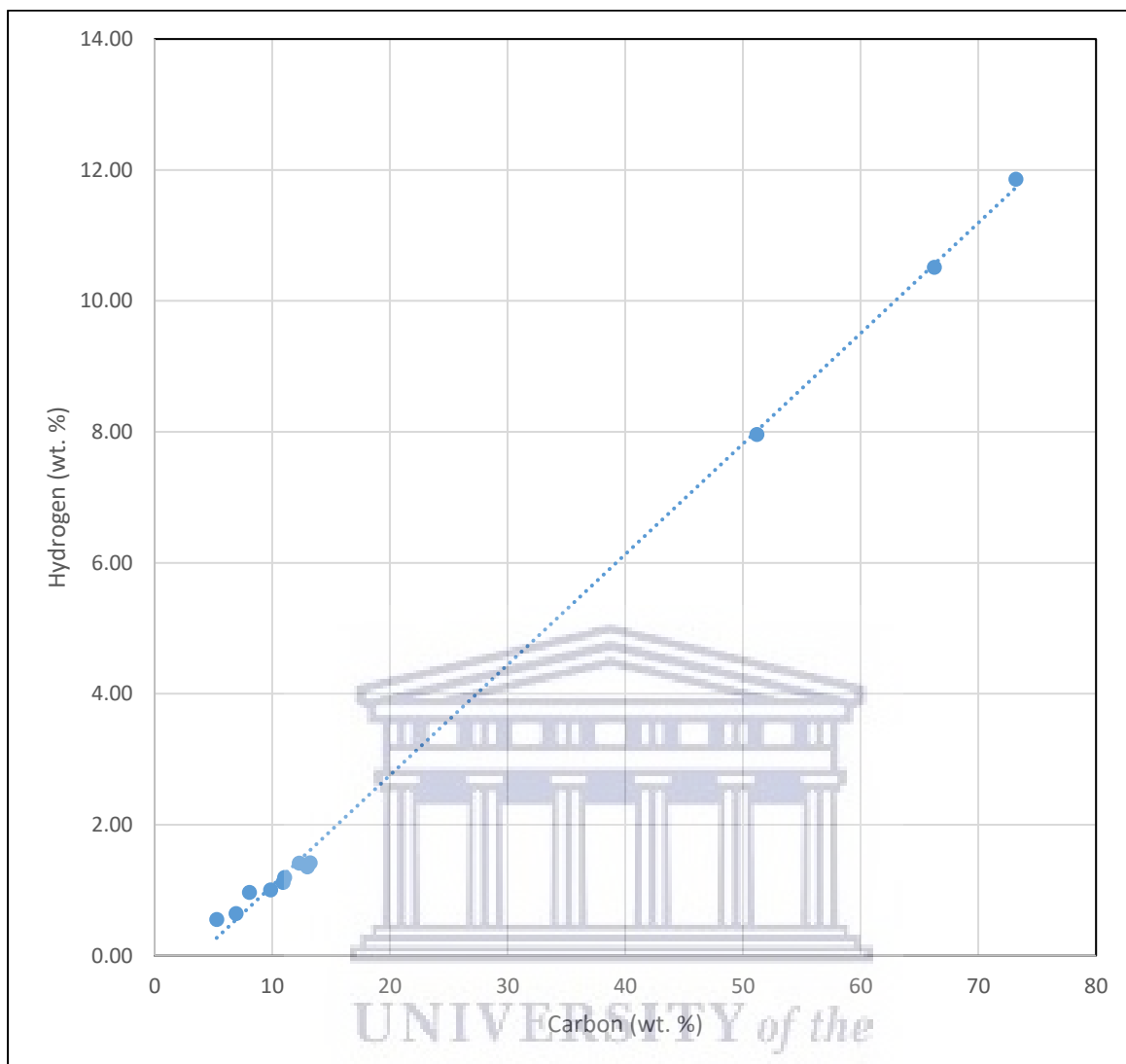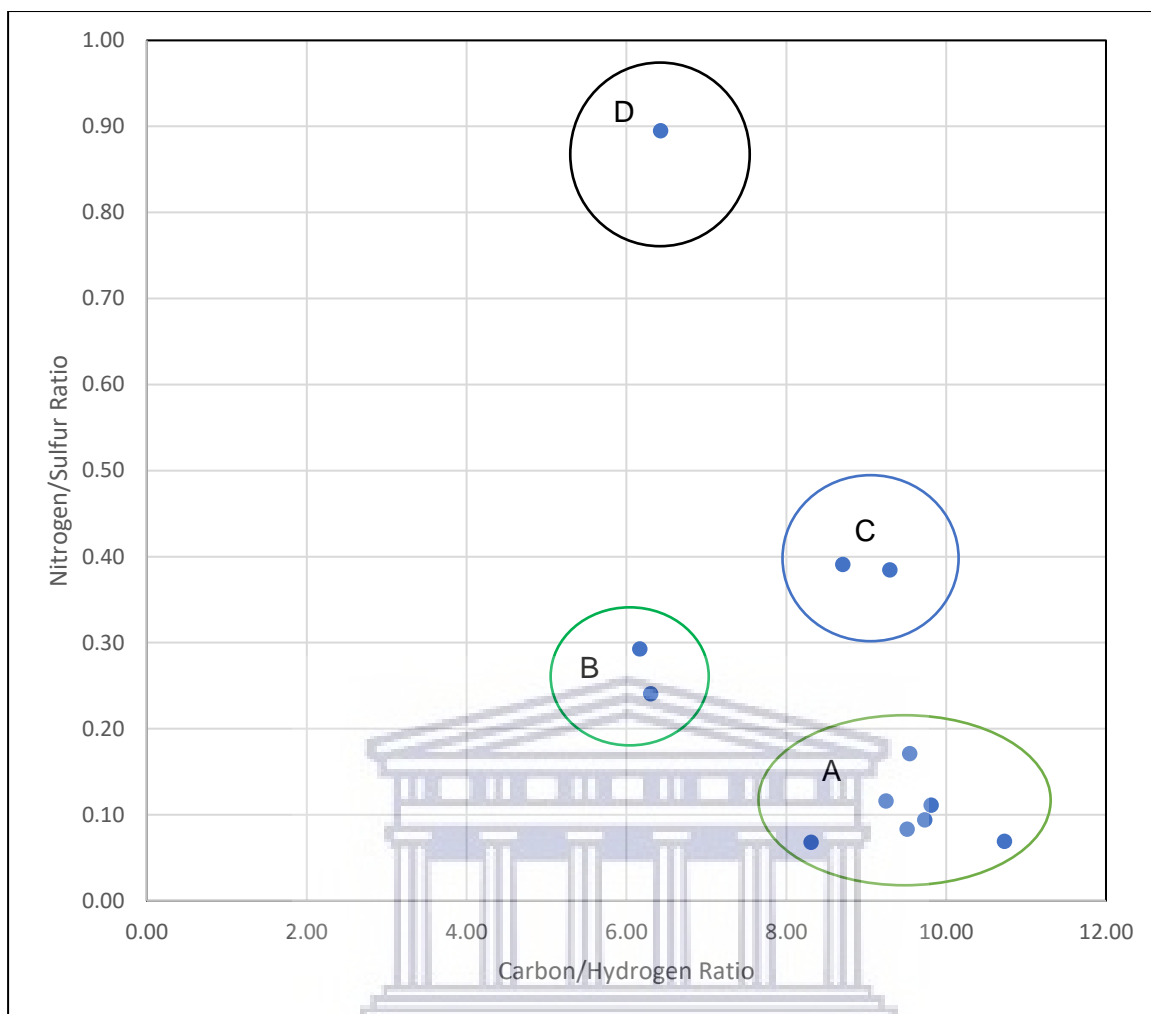*Figure 79: Cross plot of Hydrogen versus Carbon (wt. %).*

*Figure 80: Cross plot of Nitrogen/Sulfur and Carbon/Hydrogen ratios.*

The weight % carbon and hydrogen ranged from 5.27 to 73.18 and 0.55 to 11.86, respectively, while the weight % for nitrogen varied from 0.04 wt. % to 0.57 wt. %. The sulfur contents of the oils ranged from 0.18 wt % to 1.83 wt %. The heavy oils from the seeps presented the highest amounts of carbon (73.18 wt. %) and hydrogen (11.86 wt. %). The carbon content for the oil sands ranged from 5.27 wt. % to 13.22 wt. % while hydrogen varied from 0.55 wt. % to 1.42 wt. %, potentially indicating that efficient extraction processes are required to recover hydrocarbons from the oil sands. The low carbon and hydrogen contents of the sands suggests that large scale mining of the oil sands may be required for economic recovery.

Sulfur contents for the heavy oils varied from 0.64 wt. % to 1.83 wt. % while its nitrogen content ranged from 0.44 wt. % to 0.57 %. In contrast, the oil sands displayed sulfur contents varying from 0.26 % to 1.16 wt. % while its nitrogen contents ranged from 0.04 wt.% to 0.09 wt.%. The variations in the sulfur and nitrogen content possibly indicates the degrees of hydrocarbon degradation, and redox conditions of the depositional environments of the source rock. The sulfur and nitrogen content averaged 0.75 wt. % and 0.17 wt. %, respectively, suggesting the presence of heavy end molecular components that dominates biodegraded oils.

The cross plot of hydrogen and carbon (Fig. 78) showed a positive linear relationship indicating that as the hydrogen content increases, there is a corresponding increase in weight percent carbon. The display of nitrogen/sulfur ratio and carbon/hydrogen ratio (Fig. 79) indicates four clusters of hydrocarbons; these clusters may be related to mixed sources and the extent of biodegradation. For cluster A (OD-1, OD-2, OD-3, IL-1, IL-2, EG-1, and J4-1), carbon/hydrogen ranged from 8.31 to 10.73, while nitrogen/sulfur varied within 0.07 to 0.17.

The ratios of carbon/hydrogen and nitrogen/sulfur for cluster B (ML-21 and ML-22) ranged from 6.30 to 6.17 and 0.24 to 0.29, respectively. Cluster C (OR-1 and IL-3) had a carbon/hydrogen ratio of 8.70 to 9.30, while its nitrogen/sulfur ratio ranged from 0.38 to 0.39. Cluster D (MF-1) showed a carbon/hydrogen ratio of 6.43 and nitrogen/sulfur ratio of 0.89. In general, the weight percent of sulfur and nitrogen are higher in the heavy oils than in the oil sands evaluated in this study.

## 6.6: TRACE METAL GEOCHEMISTRY: IMPLICATIONS FOR THE ORIGIN OF CRUDE OILS IN THE EASTERN DAHOMEY BASIN

The presence of various transition metals in crude oil and solid bitumen has been recognized for over 50 years (Treibs, 1934). Of all the trace metals that can be found in petroleum, vanadium and nickel have been well studied. They are used as a source parameter in oil to oil and oil to source rock correlation (Lewan, 1984). Vanadium and nickel constitute the significant elements in crude oil (Boduszynski, 1987) but are not part of the original tetrapyrrole pigments in living organisms (Peters et al., 2005). The association of vanadium and nickel with organic matter in organometallic complexes with porphyrin-type structure is well established. Non-porphyrin tetrapyrrole complexes can also be present (Filby, 1975; Lewan and Maynard, 1982; López and Mónaco, 2017). Vanadium and nickel in crude oil is firmly bound to Metallo-organic complexes that have high molecular weights (MW > 400); (Filby, 1975). They have high thermal stability (Constantinides et al., 1959) and are resistant to microbial degradation, water washing, and weathering (Brunnock and Duckworth, 1968; Davis and Gibbs, 1975). The high thermal stability of metallo-organic complexes of vanadium and nickel suggests that their enrichment in the organic matter of a source rock may be reflected in part in its migrated crude oil (Lewan, 1980).

Vanadium and nickel are present in crude oils in variable quantities from less than one ppm (parts per million) in some Paleozoic crudes from Algeria and the United States, to up to 1200 ppm vanadium and 150 ppm nickel in Boscan crude from Venezuela (Tissot and Welte, 1984). These metals are selectively preserved in tetrapyrrole complexes, and their relative dominance over one another depends on the level of oxygen in the depositional environment. Vanadium is higher relative to nickel in organic matter deposited under anoxic conditions, and the proportions of vanadyl and nickel porphyrins are used as a source parameter in oil to oil and oil to source correlation (Lewan, 1984).

Recent advances in analytical techniques, including inductively coupled plasma emission spectrometry, have led to a resurgence of interest in metal occurrence in petroleum and the application of transition metal information to natural resource exploration (Curiale, 1984). The concentration of metals in petroleum is a common feature of biodegraded oils, and they can impact the refining processes. Besides, the ash of certain oils and solid bitumens have been proposed as an exploitable metal-containing source, particularly in the case of heavy oils (Erickson et al., 1954; Skinner, 1952).

Oil sands and heavy oils from different parts of the Eastern Dahomey Basin were appraised for their metal content with Inductively Coupled Plasma – Mass Spectrometry (ICP-MS).

Tables 20, and 21, shows the concentration of vanadium (V), nickel (Ni), manganese (Mn), cobalt (Co), copper (Cu), zinc (Zn), lead (Pb), molybdenum (Mo), cadmium (Cd), tin (Sn), mercury (Hg), together with V/Ni and V(V+Ni) ratios in the oil sands, heavy oil and oil seeps. The concentration of these metals is displayed in Figures 81, 82, 83, 84, 85, and 86.

*Table 20: ICP-MS results showing the concentration of Cr, Mn, Fe, Co, Ni, Cu, Zn, Pb, V, and ratios of V/Ni and V(V+Ni) in oil sands,*

*and heavy oil*

| Sample ID | Sample Type | Sample Depth (m) | Cr ppm | Mn ppm | Fe ppm | Co ppm | Ni ppm | Cu ppm | Zn ppm | Pb ppm | V ppm | V/Ni ppm | V/ (V+Ni) | Co/Ni |
|---|---|---|---|---|---|---|---|---|---|---|---|---|---|---|
| ML-21 | Oil seeps | N/A | 6.74 | 28.23 | 9780.70 | 2.35 | 30.36 | 1.71 | 23.53 | 2.23 | 20.86 | 0.69 | 0.41 | 0.08 |
| MF-1 | Oil seeps | N/A | 33.20 | 36.98 | 6192.82 | 2.89 | 23.80 | 6.44 | 35.21 | 8.30 | 32.81 | 1.38 | 0.58 | 0.12 |
| AG-1 | Heavy oil | 7.133 | 0.63 | 0.73 | 135.91 | 0.90 | 30.19 | 0.03 | 2.57 | 0.14 | 13.28 | 0.44 | 0.31 | 0.03 |
| ML-22 | Oil seeps | N/A | 6.39 | 20.76 | 6429.07 | 2.65 | 33.34 | 2.40 | 15.81 | 2.15 | 28.64 | 0.86 | 0.46 | 0.08 |
| OD-1 | Oil sand | 1 | 26.60 | 21.98 | 2960.61 | 1.20 | 6.87 | 4.70 | 8.27 | 9.90 | 13.35 | 1.94 | 0.66 | 0.17 |
| OD-2 | Oil sand | 2 | 13.51 | 8.86 | 7741.61 | 3.90 | 10.79 | 3.42 | 12.76 | 5.02 | 19.37 | 1.80 | 0.64 | 0.36 |
| OD-3 | Oil sand | 3.5 | 6.27 | 6.36 | 2085.54 | 1.34 | 6.01 | 1.04 | 28.48 | 2.52 | 8.07 | 1.34 | 0.57 | 0.22 |
| OD-4 | Oil sand | 4.1 | 9.54 | 11.69 | 3344.44 | 1.76 | 8.65 | 1.77 | 12.91 | 3.63 | 13.42 | 1.55 | 0.61 | 0.20 |
| IL-1 | Oil sand | 2 | 13.89 | 9.82 | 4866.93 | 2.21 | 10.67 | 1.47 | 9.14 | 3.22 | 19.99 | 1.87 | 0.65 | 0.21 |
| IL-2 | Oil sand | 2.5 | 7.42 | 9.31 | 4131.97 | 1.45 | 8.71 | 0.73 | 7.36 | 1.83 | 13.83 | 1.59 | 0.61 | 0.17 |
| IL-3 | Oil sand | 3.1 | 2.92 | 3.67 | 1254.67 | 0.68 | 6.79 | 0.20 | 3.05 | 0.78 | 8.53 | 1.26 | 0.56 | 0.10 |
| J4-1 | Oil sand | 0 | 29.57 | 24.15 | 7732.13 | 2.30 | 10.03 | 3.59 | 9.75 | 7.56 | 23.64 | 2.36 | 0.70 | 0.23 |
| J4-2 | Oi sand | 8.4 | 32.62 | 42.58 | 15921.18 | 9.54 | 19.31 | 6.23 | 25.91 | 9.40 | 36.49 | 1.89 | 0.65 | 0.49 |
| EG-1 | Oil sand | N/A | 19.02 | 9.04 | 6645.90 | 1.60 | 9.46 | 2.70 | 7.62 | 3.54 | 14.21 | 1.50 | 0.60 | 0.17 |
| OR-1 | Oil sand | N/A | 9.77 | 8.02 | 995.24 | 1.11 | 8.76 | 0.75 | 5.39 | 3.29 | 12.13 | 1.38 | 0.58 | 0.13 |
| Sum | | | 218.08 | 242.18 | 80218.71 | 35.86 | 223.76 | 37.18 | 207.77 | 63.50 | 278.61 | 21.845 | 8.597 | 2.761 |

*Note on Abbreviations*

*ML= Mile 2; MF= Mafowoku ;  AG= Agbabu; OD-1 = Ode- Aye BH1; IL= Ilubinrin BH1; J4 = Onikitibi ; EG= Egbe ; OR = Orisunbare*

*Table 21: ICP-MS results displaying the concentration of Mo, Cd, Sn, and Hg in oil sands, and heavy oils.*

| Sample ID | Sample Type | Sample Depth (m) | Mo ppm | cd ppm | Sn ppm | Hg ppm |
|-----------|-------------|------------------|--------|--------|--------|--------|
| ML-21 | Oil seeps | N/A | 0.61 | 0.01 | 0.04 | 0.00 |
| MF-1 | Oil seeps | N/A | 0.41 | 0.13 | 0.27 | 0.03 |
| AG-1 | Heavy oil | 7.133 | 0.22 | 0.00 | 0.22 | 0.01 |
| ML-22 | Oil seeps | N/A | 0.83 | 0.02 | 0.05 | 0.00 |
| OD-1 | Oil sand | 1 | 0.35 | 0.01 | 0.19 | 0.03 |
| OD-2 | Oil sand | 2 | 3.46 | 0.17 | 0.26 | 0.02 |
| OD-3 | Oil sand | 3.5 | 0.77 | 0.02 | 0.09 | 0.01 |
| OD-4 | Oil sand | 4.1 | 1.07 | 0.02 | 0.17 | 0.01 |
| IL-1 | Oil sand | 2 | 1.39 | 0.07 | 0.16 | 0.01 |
| IL-2 | Oil sand | 2.5 | 1.72 | 0.03 | 0.10 | 0.01 |
| IL-3 | Oil sand | 3.1 | 0.53 | 0.01 | 0.03 | 0.00 |
| J4-1 | Oil sand | 0 | 0.29 | 0.01 | 0.33 | 0.02 |
| J4-2 | Oil sand | 8.4 | 0.11 | 0.03 | 0.41 | 0.09 |
| EG-1 | Oil sand | N/A | 1.04 | 0.04 | 0.21 | 0.01 |
| OR-1 | Oil sand | N/A | 0.34 | 0.00 | 0.07 | 0.01 |
| Sum | | | 13.128 | 0.576 | 2.581 | 0.252 |
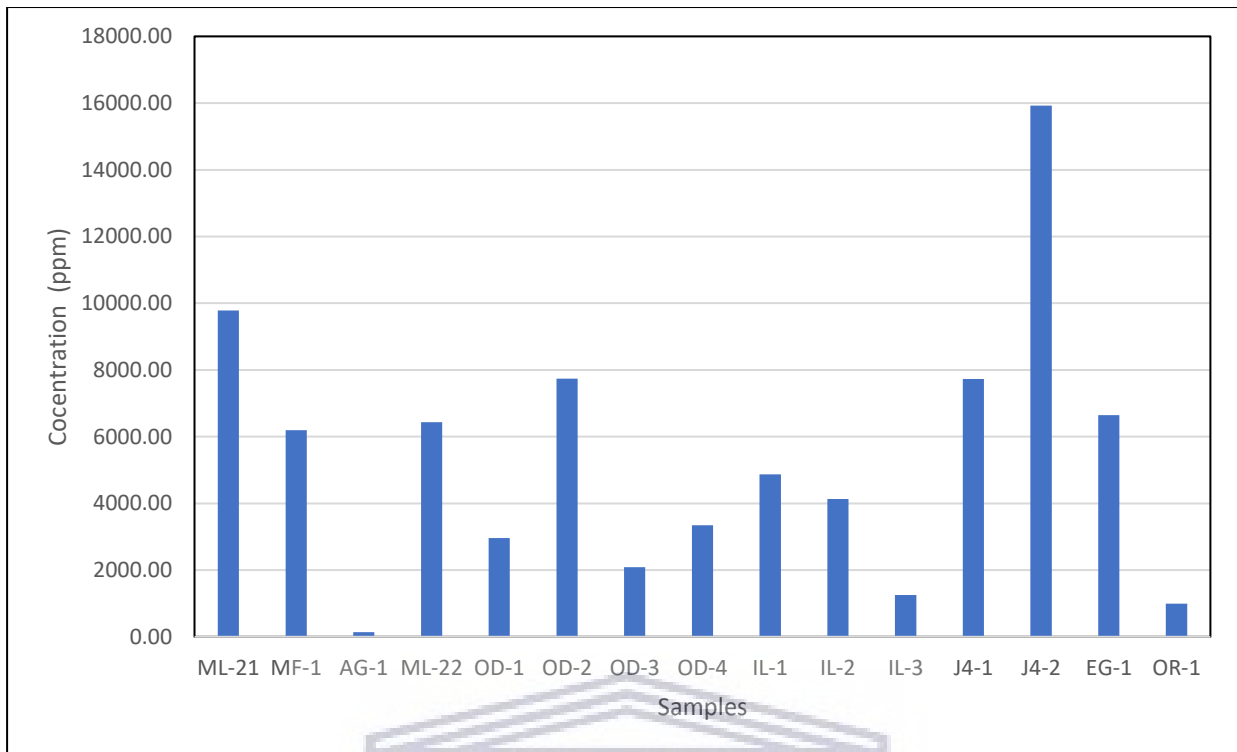
*Figure 81: Display showing concentration (ppm) of Fe in oil sands and heavy oil.*
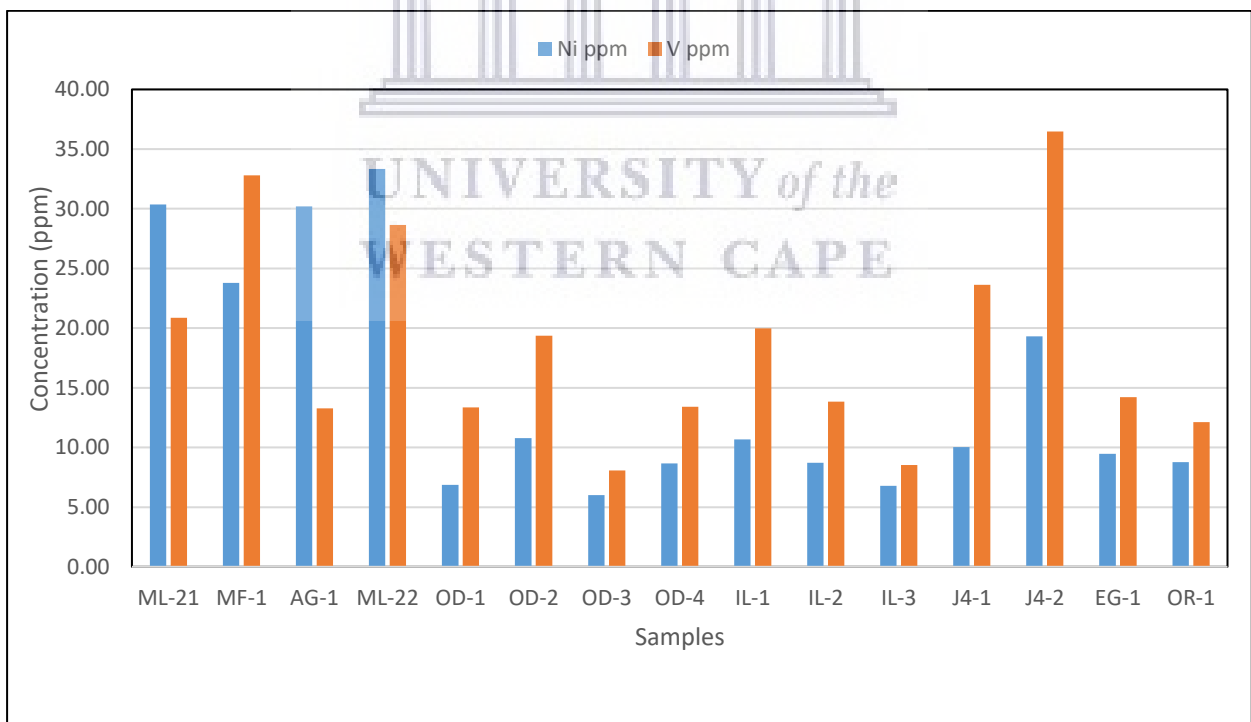


*Figure 82: Display showing concentration (ppm) of V and Ni in oil sands and heavy oil.*
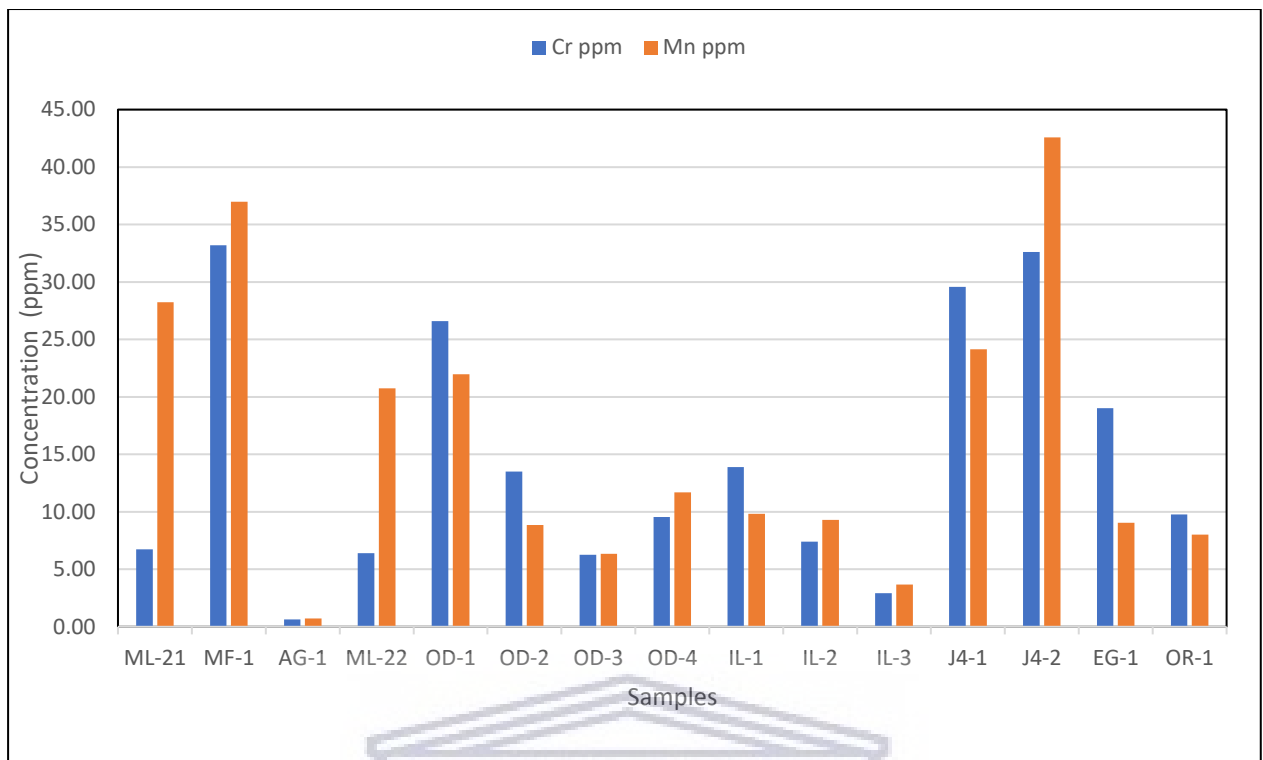
*Figure 83: Display of concentration (ppm) of Cr and Mn in oil sands and heavy oil.*
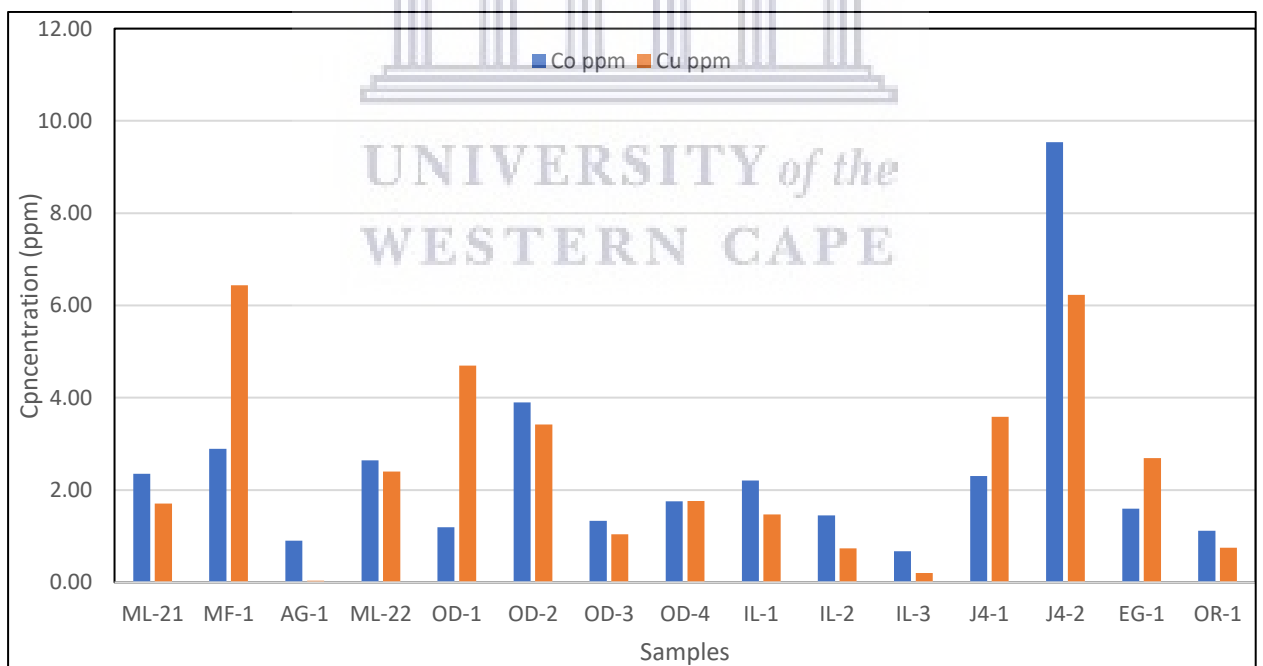


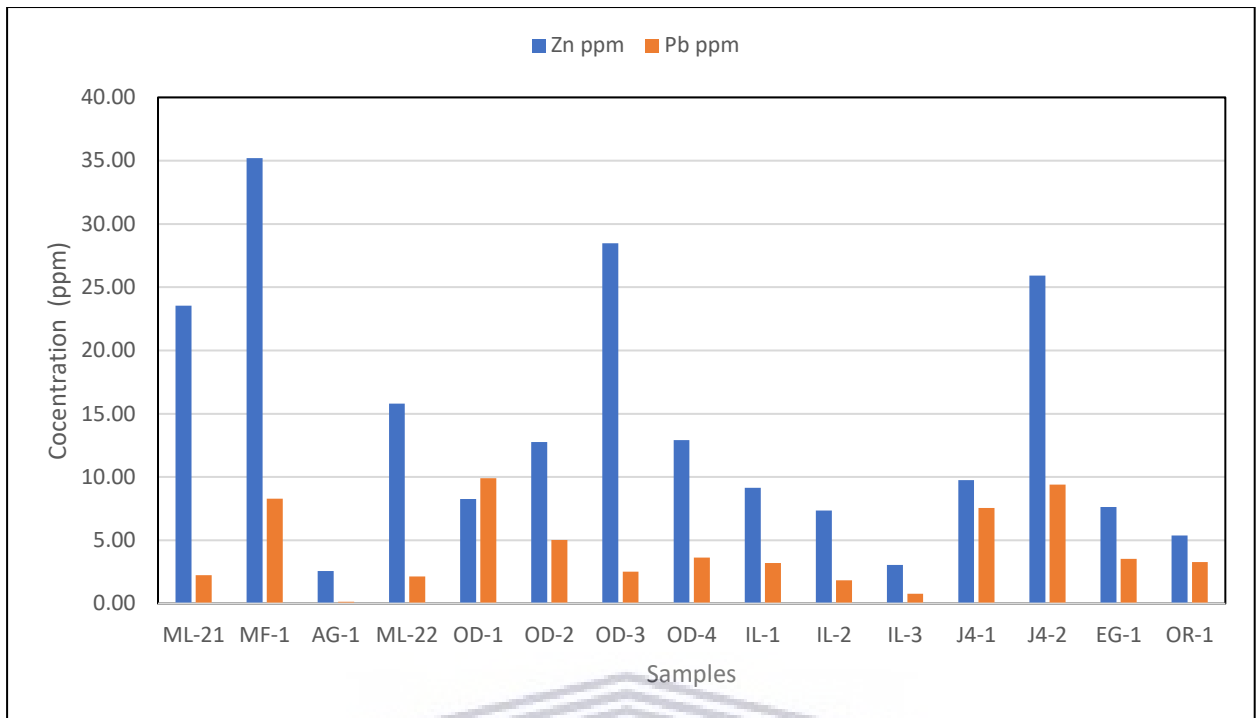*Figure 84: Display of concentration (ppm) of Co and Cu.*

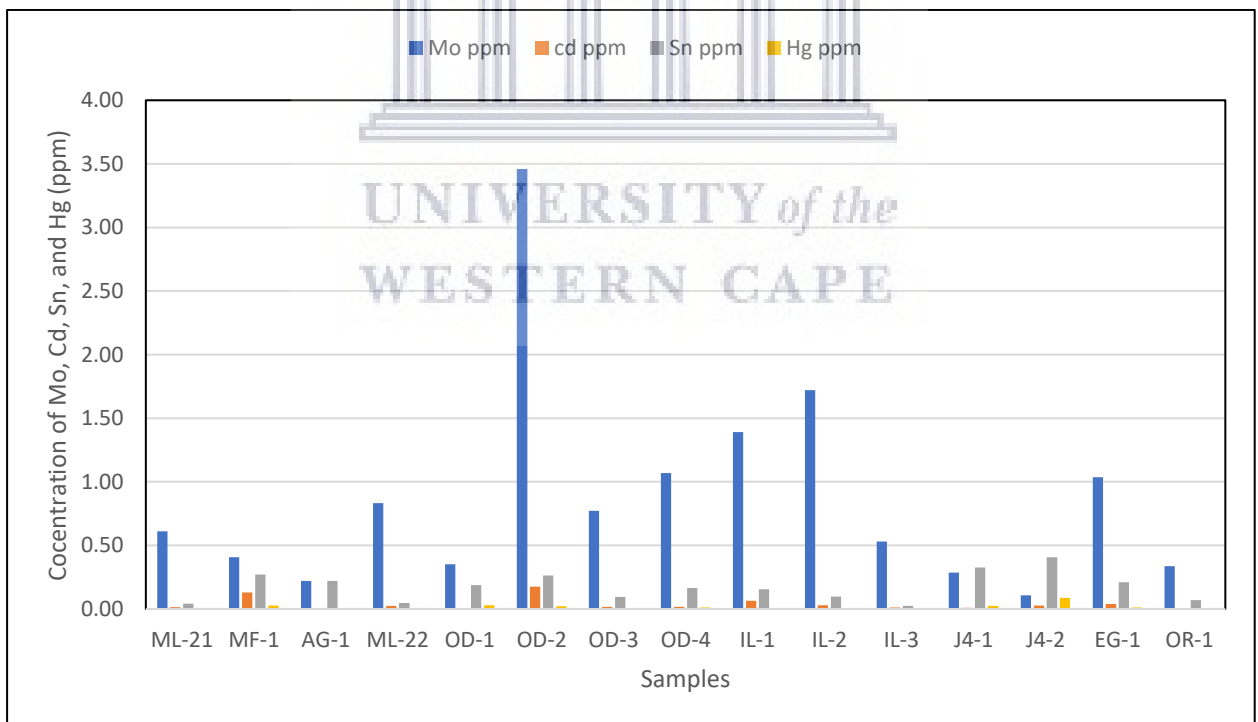*Figure 85: Display of concentration (ppm) of Zn and Pb.*



*Figure 86: Display of concentration of Mo, Cd, Sn, and Hg*

Of all the metals examined (Tables 20 and 21), Fe is the most abundant, and its total concentration in the oil sand and heavy oil is 80218.71 ppm. It is followed by V (278.61 ppm), Mn (242.18 ppm), Ni (223.76 ppm), Cr (218.08 ppm), Zn (207.77 ppm), Pb (63.50 ppm), Cu (37.18 ppm), and Co (35.86 ppm). The concentration of Fe ranged from 135.91 ppm to 15921.18 ppm. Chromium concentration varied from 0.63 ppm to 33.20 ppm, while Mn ranged from 0.73 to 42.58 ppm. Cobalt concentration fluctuated between 0.68 ppm to 9.54 ppm, and Cu ranged between 0.03 ppm to 6.44 ppm. The concentration of Zn and Pb varied from 2.57 ppm to 35.21 ppm and 0.14 ppm to 9.90 ppm, respectively. Vanadium concentration ranged from 8.07 ppm to 36.49 ppm while the concentration of Ni varied from 6.01 ppm to 33.34 ppm. Molybdenum, Cd, Sn, and Hg are present in a concentration of less than 4.00 ppm (Table 21). The enrichment of these heavy metals in the crude oils reflects biodegradation, and the deposits can potentially be exploitable mineral containing source (Erickson et al., 1954; Skinner, 1952). The high concentration of Fe relative to other metals in the samples may reflect the clastic nature of both the reservoir rock (sandstone) and argillaceous source rock (shale). In contrast to argillaceous sediments, carbonates are relatively free of Fe (Pettijohn, 1975).

The concentration of V and Ni, together with V/Ni, V/(V+Ni), and Co/Ni ratios is shown in Table 20. The preservation of tetrapyrroles is favored in sediments under anaerobic conditions (Brongersma et al.; 1951; Drozdova and Gorskiy, 1972; Gorham and Sanger, 1967) and their accompanying organic matter (Didyk et al., 1978; Koyama and Tomino, 1967; Zobell, 1946). These conditions are typical of reducing environments with oxidation potential (Eh) values, usually less than zero (Krumbein and Garrels, 1952). Vanadium is preferentially enriched over Ni in reducing conditions, and the proportions of V/Ni and V/(V+Ni) are useful indicators of paleo-redox

conditions during source rock deposition (Lewan, 1984; López and Mónaco, 2017; Moldowan et al., 1986).

Three heavy oils (ML-21, AG-1, and ML-22) have a low V concentration relative to Ni. In contrast, the oil sands and the MF-1 heavy oil showed a dominance of V over Ni (Fig. 82). The three heavy oils with V/Ni ratio (<1) and V/(V+Ni) less than 0.5 may have been derived from terrestrial organic matter that was deposited in suboxic conditions. The oil sands and MF-1 heavy oil have V/Ni (>1) and V/(V+Ni) greater than 0.5; these were possibly derived from marine and mixed organic matter that was deposited under anoxic conditions.

Besides the V/Ni ratio, the geochemical ratio of Co/Ni has been used to assess organic matter input in source rocks (Akinlua et al., 2007; Udo et al., 1992). The Co/Ni ratio (Table 20) for the oil sands and heavy oils ranged from 0.03 to 0.49, suggesting source rocks with inputs of terrestrial and marine organic matter. While the three heavy oils (ML-21, AG-1, and ML-22) have a Co/Ni ratio of less than 0.1, the oil sands and MF-1 heavy oil have Co/Ni ratio greater than 0.1. Crude oils in ML-21, AG-1, and ML-22 are inferred to have been derived from a source rock with terrestrial organic matter input. In contrast, the crude oils in the oil sands and MF-1 with Co/Ni ratio greater than 0.1 may have been generated from a source rock with marine and mixed organic matter input.

The cross plot of Co/Ni and V/Ni ratios (Fig.87) suggests various organic matter input in the source rock under suboxic and anoxic conditions.
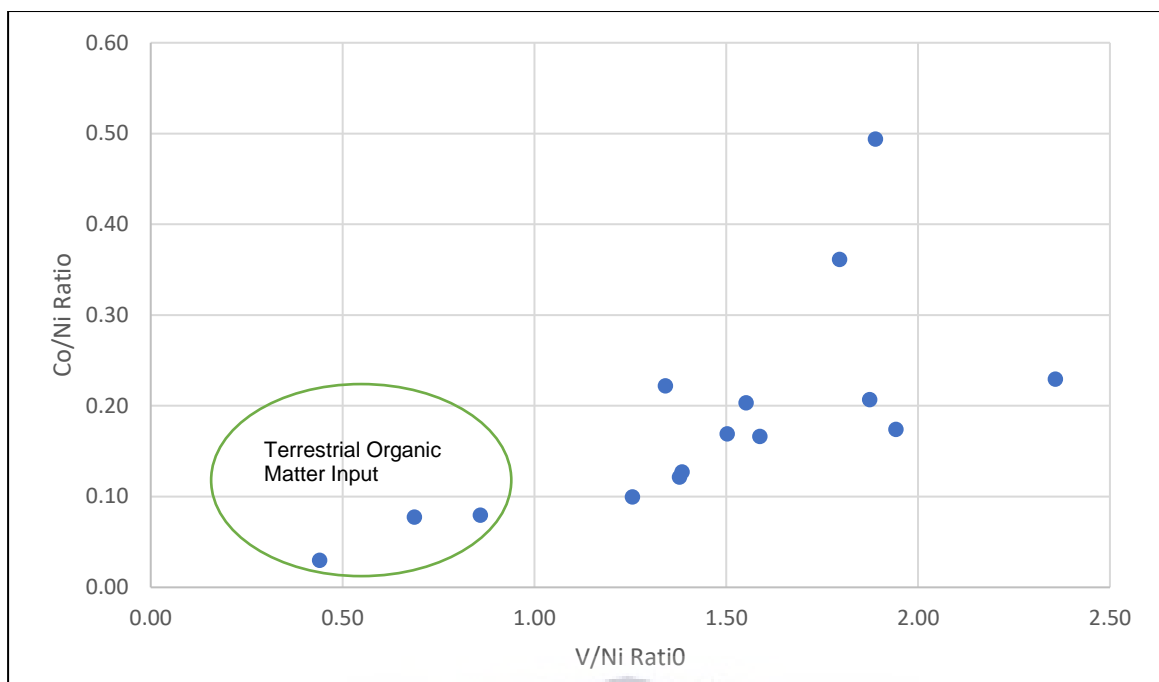
*Figure 87: Cross plot of Co/Ni and V/Ni showing*

Crude oil in ML-21, AG-1, and ML-22 with Co/Ni (<0.1) and V/Ni (<1) is interpreted to have been generated by a source rock with terrestrial organic matter input under suboxic conditions. In contrast, crude oils in the sands and MF-1 with Co/Ni ratio (>0.1) and V/Ni ratio (>1) are inferred to have originated from a source rock with mixed to marine organic matter input under anoxic conditions.

## 6.7: STABLE CARBON ISOTOPE MEASUREMENTS ON WHOLE OILS

Carbon is the most dominant element in petroleum. It consists of two stable isotopes (Cabon-12 and Carbon-13), which differ by the Mass of only one neutron in the nucleus.

Natural variations in the stable isotopes of carbon are caused by equilibrium exchange and kinetic fractionation processes (Hoefs, 1973) in the different carbon cycles. Carbon isotopes, therefore, provide information on the generation, maturation, and genetic correlation of hydrocarbons and their precursors, which can be used in oil and

gas exploration (Stahl, 1977). Processes that occur after the pyrolysis of kerogen to generate oil commonly have small effects on $\delta^{13}C$ values of oils. As a result, $\delta^{13}C$ contents of oils are used for oil – oil and oil – source rock correlations and, in conjunction with other geochemical properties, can indicate the likely age and depositional environment of source rocks (Chung et al., 1992).

Carbon isotope ratios can be measured on whole oils or source rock extract in addition to their fractions from liquid chromatography to characterize crude oils and to determine the genetic relationships among oils and bitumens (Fuex, 1977; Schoell, 1984; Sofer, 1984; Stahl, 1977).

The results of the carbon isotope measurements on the whole oils (not fractions) are shown in table 22 and Figure 88.
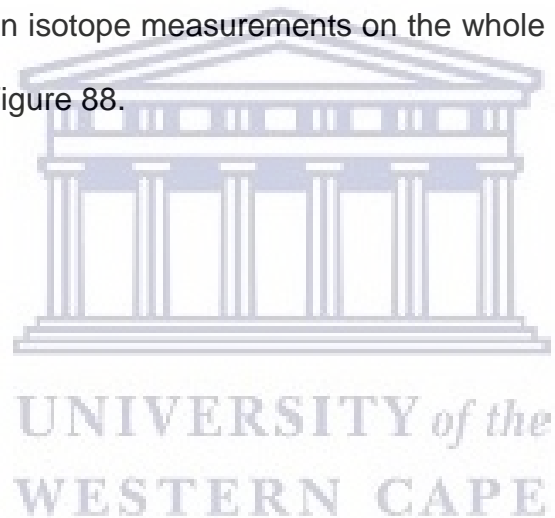
*Table 22:  Results of the Carbon Isotope ratio on whole oil.*

| Sample ID | Sample Number | Sample Type | Sample Depth (m) | $\delta^{13}C$ |
|---|---|---|---|---|
| MF-1 | 1 | Oil seep | N/A | **-26.6** |
| ML-21 | 2 | Oil seep | N/A | **-26.5** |
| ML-22 | 3 | Oil seep | N/A | **-26.1** |
| J4-1 | 4 | Oil sand/Outcrop | N/A | **-25.4** |
| OR-1 | 5 | Oil Sand/Outccrop | N/A | **-25.6** |
| EY-28 | 6 | Oil sand/Core | 15-18 | **-27.7** |
| EG-1 | 7 | Oil sand/Outcrop | N/A | **-26.0** |
| IJ-1 | 8 | Oil sand/Outcrop | 1.15 | **-26.0** |
| OD-1 | 9 | Oil sand/Borehole | 4.1 | **-26.0** |
| IL-1 | 10 | Oil sand/Borehole | 3.1 | **-26.1** |
| 3H-1 | 11 | Oil sand/Outcrop | N/A | **-25.6** |
| AR-1 | 12 | Oil sand/Core | 102.80 - 109 m | **-25.6** |
| EY-22 | 13 | Oil sand/Core | 81-84 | **-26.6** |

*Note on Abbreviations*

*MF= Mafowoku ; ML= Mile 2;; J4 = Onikitibi; OR = Orisunbare; EY-28 = Ohosu borehole, EG= Egbe; IJ = Ijuoke Agotitun; OD-1 = Ode- Aye borehole; IL= Ilubinrin borehole; 3H-1 = 3-Hanger; AR-1 = Araromi Obu borehole; EY-22 = Igbotu borehole*
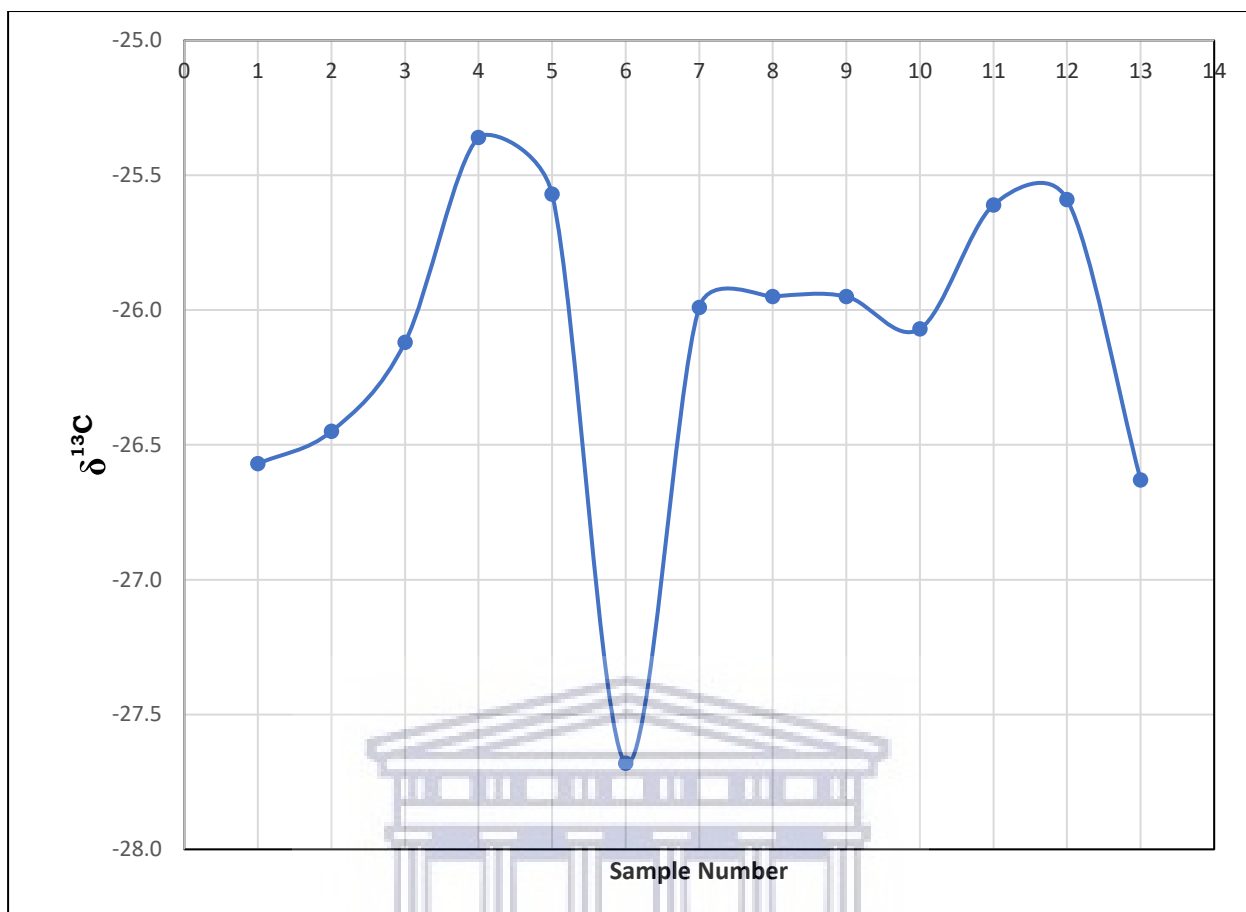
*Figure 88: Display showing carbon isotope ratios on the whole oil.*

The carbon isotope ratios ($\delta^{13}C$) for the whole oil ranged from -27.7 ‰ to -25.4 ‰. For the oil seeps, $\delta^{13}C$ varied from -26.6 ‰ to -26.1 ‰ while the oil sands showed values within the range of -27.7 ‰ to -25.4 ‰. The similarity and dissimilarity in the measured $\delta^{13}C$ ratios potentially indicate that the oils were generated by source rocks of various organic matter inputs. Based on the carbon isotope data presented in Table 22 and Fig. 88, three distinct profiles that may reflect multiple source inputs can be recognized. The first profile is isotopically light with $\delta^{13}C$ of - 27.7 ‰, followed by a profile with $\delta^{13}C$ within the range of -26.6 ‰ to -26.0 ‰. The $\delta^{13}C$ for the third profile fluctuates from -25.6 ‰ to – 25.4 ‰. The more or less identical $\delta^{13}C$ ratios in each of the profiles provide evidence that the oils within a profile may have a common source

rock. A positive correlation is recognized if the $\delta^{13}C$ differs by less than 1 ‰ while similarity is indicated by less than 2 ‰ variations in the data (Sofer, 1984).

Petroleum that are derived from source rocks composing of terrigenous organic matter are isotopically more negative (depleted in $^{13}C$) while petroleum of marine origin are isotopically heavy (Silverman and Epstein, 1958). The variations in $\delta^{13}C$ exhibited by the dataset potentially indicate that the oils were generated from petroleum source rocks composing of terrestrial, and marine organic matter. The crude oil in the sample with $\delta^{13}C$ of -27.7 ‰ is inferred to have been generated from a petroleum source rock composing of terrestrial organic matter. The range of $\delta^{13}C$ ratios (-26.6 ‰ to -26.0 ‰, and -25.6 ‰ to – 25.4 ‰) shown by the oils in profiles two and three, may indicate that they were generated in mixed/marine environments.

## 6.8 THERMAL DESORPTION – GAS CHROMATOGRAPHY (TD-GC)

The results of the TD-GC measurements are presented in Table 23 and Figures 89 to 99. The hydrocarbon components were classified as Light Condensates (nC6 through nC12), Heavy Condensates (nC13 through nC40), Naphthenes (Cyclopentane, Methylcycopentane, Cyclohexane, and Methylcyclohexane), and Aromatics (Benzenes, Toluene, Ethylbenzene, Xylenes).

*Table 23: Hydrocarbon analyses summary table showing the composition of oil sands and heavy oil.*

| Sample ID | Sample Type | Sample Depth (m) | Paraffins | | % Naphthenes | % Aromatics |
|---|---|---|---|---|---|---|
| | | | % Light Condensate | % Heavy Condensate | | |
| J4-1 | Oil sand/outcrop | 7.80 | 0.10 | 95.86 | 0.00 | 0.00 |
| J4-2 | Oil sand/outcrop | 8.10 | 0.24 | 94.22 | 0.00 | 0.00 |
| J4-3 | Oil sand/outcrop | 8.40 | 0.44 | 93.00 | 0.01 | 0.26 |
| OR-1 | Oil sand/outcrop | N/A | 0.24 | 94.92 | 0.00 | 0.00 |
| MF-1 | Heavy oil | N/A | 8.90 | 84.81 | 0.05 | 0.34 |
| AG-1 | Heavy Oil/Borehole | 7.133 | 0.58 | 94.67 | 0.04 | 0.04 |
| ML-21 | Heavy oil | N/A | 0.23 | 97.60 | 0.00 | 0.04 |
| ML-22 | Heavy oil | N/A | 0.65 | 96.94 | 0.00 | 0.04 |
| OD-1 | Oil Sand/Borehole | 1.00 | 0.53 | 55.02 | 35.16 | 5.36 |
| OD-2 | Oil Sand/Borehole | 1.50 | 1.41 | 97.25 | 0.27 | 0.00 |
| OD-3 | Oil Sand/Borehole | 2.00 | 1.62 | 96.20 | 0.12 | 0.22 |
| OD-4 | Oil Sand/Borehole | 2.50 | 2.03 | 95.32 | 0.11 | 0.08 |
| OD-5 | Oil Sand/Borehole | 3.00 | 1.57 | 95.15 | 0.80 | 0.49 |
| OD-6 | Oil Sand/Borehole | 3.50 | 0.40 | 96.31 | 0.00 | 0.00 |
| OD-7 | Oil Sand/Borehole | 4.10 | 0.58 | 96.59 | 0.00 | 0.00 |
| IL-1 | Oil Sand/Borehole | 2.00 | 0.40 | 98.32 | 0.00 | 0.00 |
| IL-2 | Oil Sand/Borehole | 3.10 | 0.59 | 97.54 | 0.40 | 0.07 |
| EG-1 | Oil Sand/Outcrop | N/A | 1.20 | 97.41 | 0.00 | 0.00 |
| J4-BH2 | Oil Sand/Borehole | 0.00 | 0.32 | 97.74 | 0.30 | 0.82 |

*Note on abbreviations*

*J4 = Onikitibi; OR= Orisunbare; MF= Mafowoku ; AG= Agbabu well;  ML= Mile 2; OD = Ode Aye Borehole ; IL= Ilubinrin Borehole , EG= Egbe,*

*J4-BH2= Onikitibi Borehole -2*

J4 Oil Sand
Red – Oil sand at 7.8m
Blue – Oil sand at  8.1 m
Green – Oil sand at  8.4 m
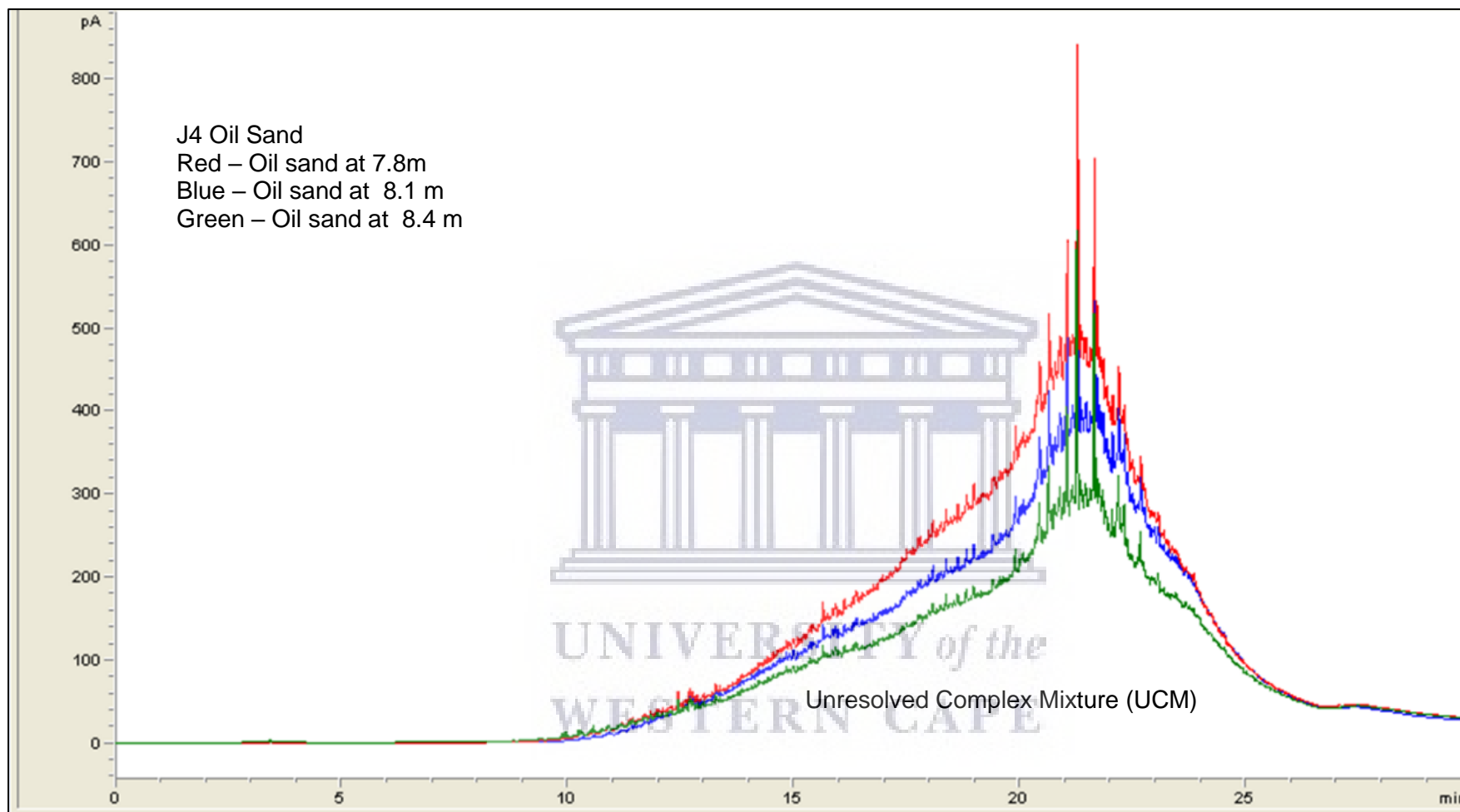
Unresolved Complex Mixture (UCM)

*Figure 89: Gas Chromatograms of J4 oil sands at varying depth showing a dominance of heavy molecular components. Response intensity is shown on the Y-axis in pico Ampere, and Retention time is shown on the X-axis in Minutes.*
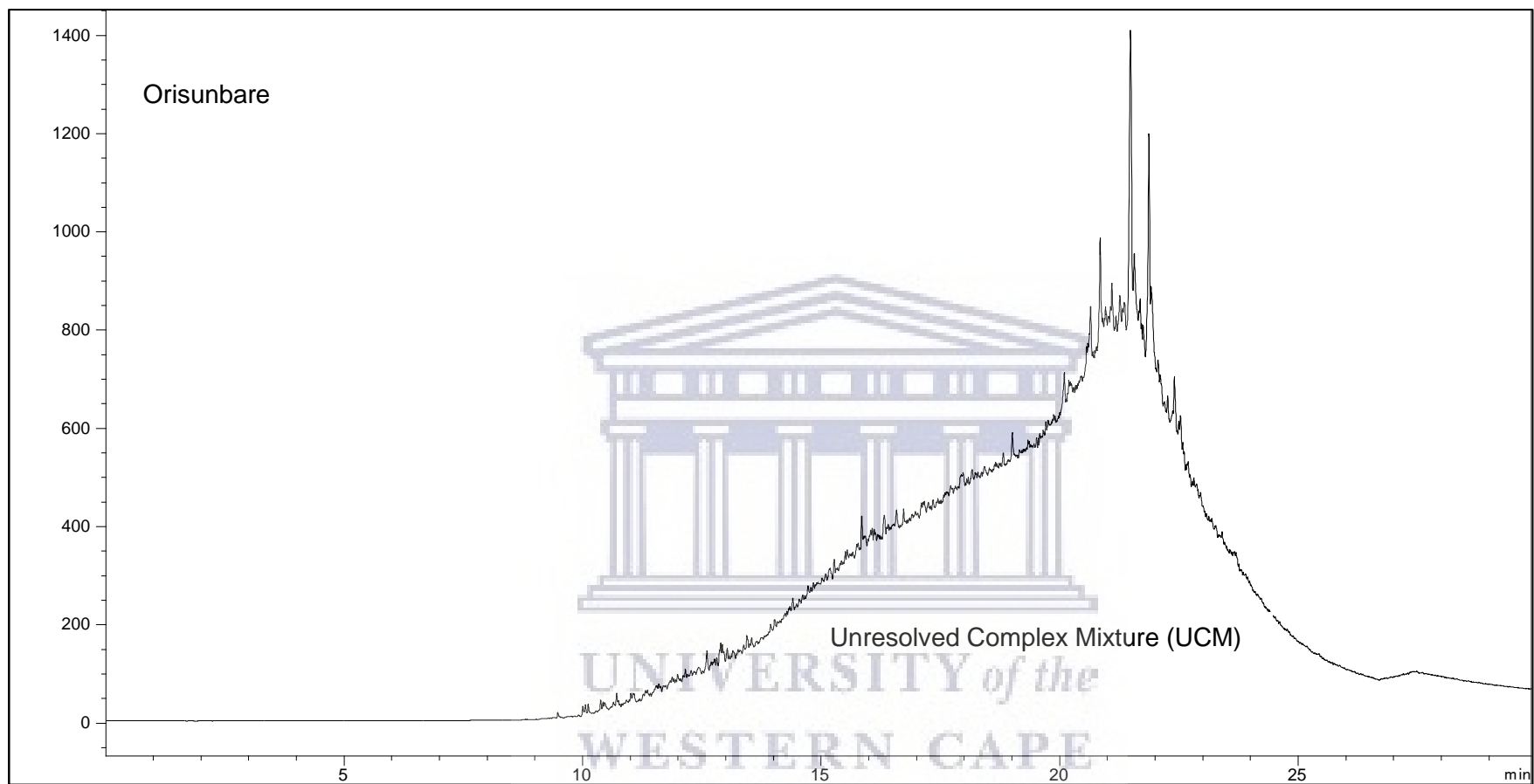
*Figure 90: Gas Chromatogram of Orisunbare oil sand. Response intensity is shown on the Y-axis in pico Ampere, and Retention time is shown on the X-axis in Minutes.*
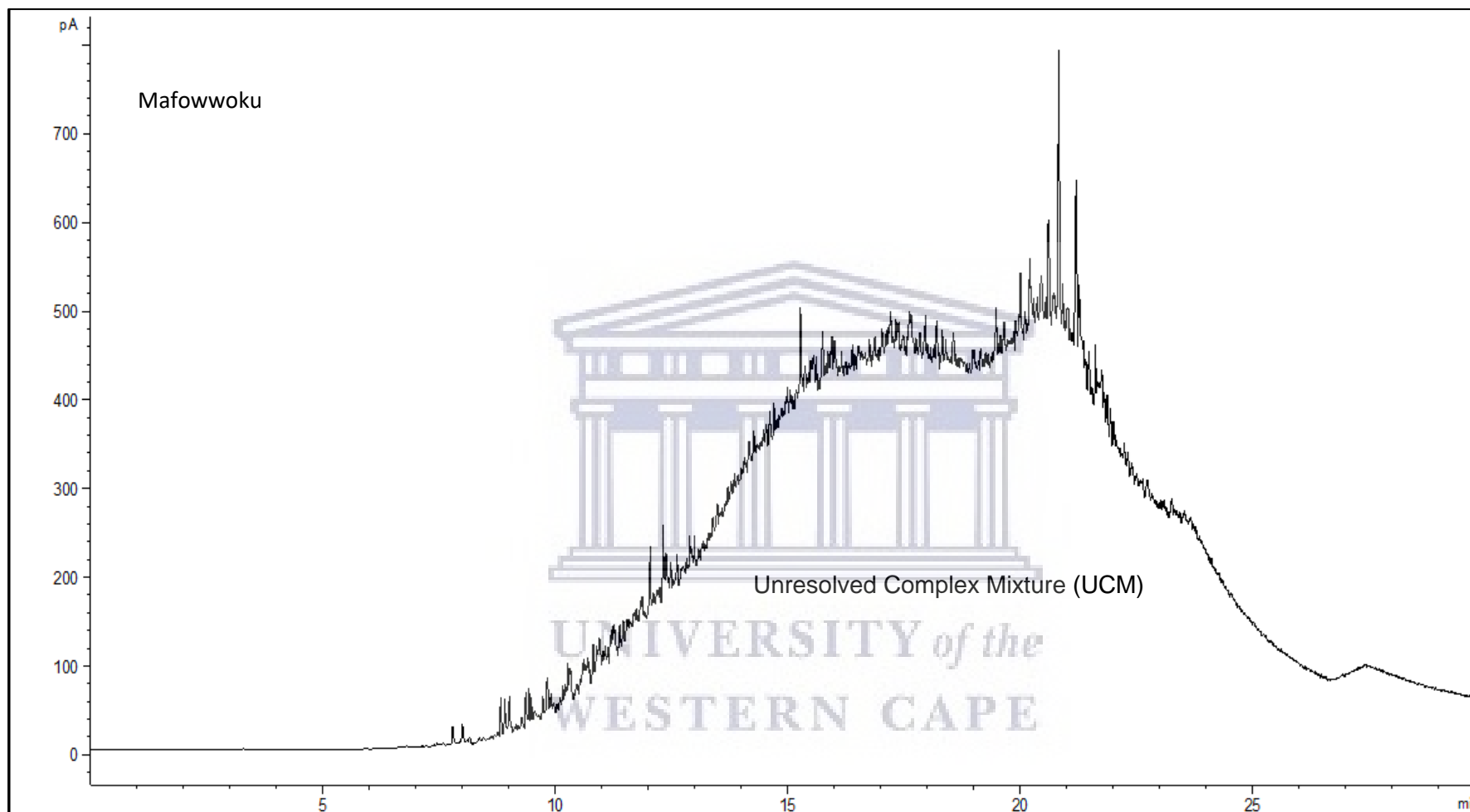
*Figure 91: Gas chromatogram of Mafowoku heavy oil. Response intensity is shown on the Y-axis in pico Ampere, and Retention time is shown on the X-axis in Minutes.*
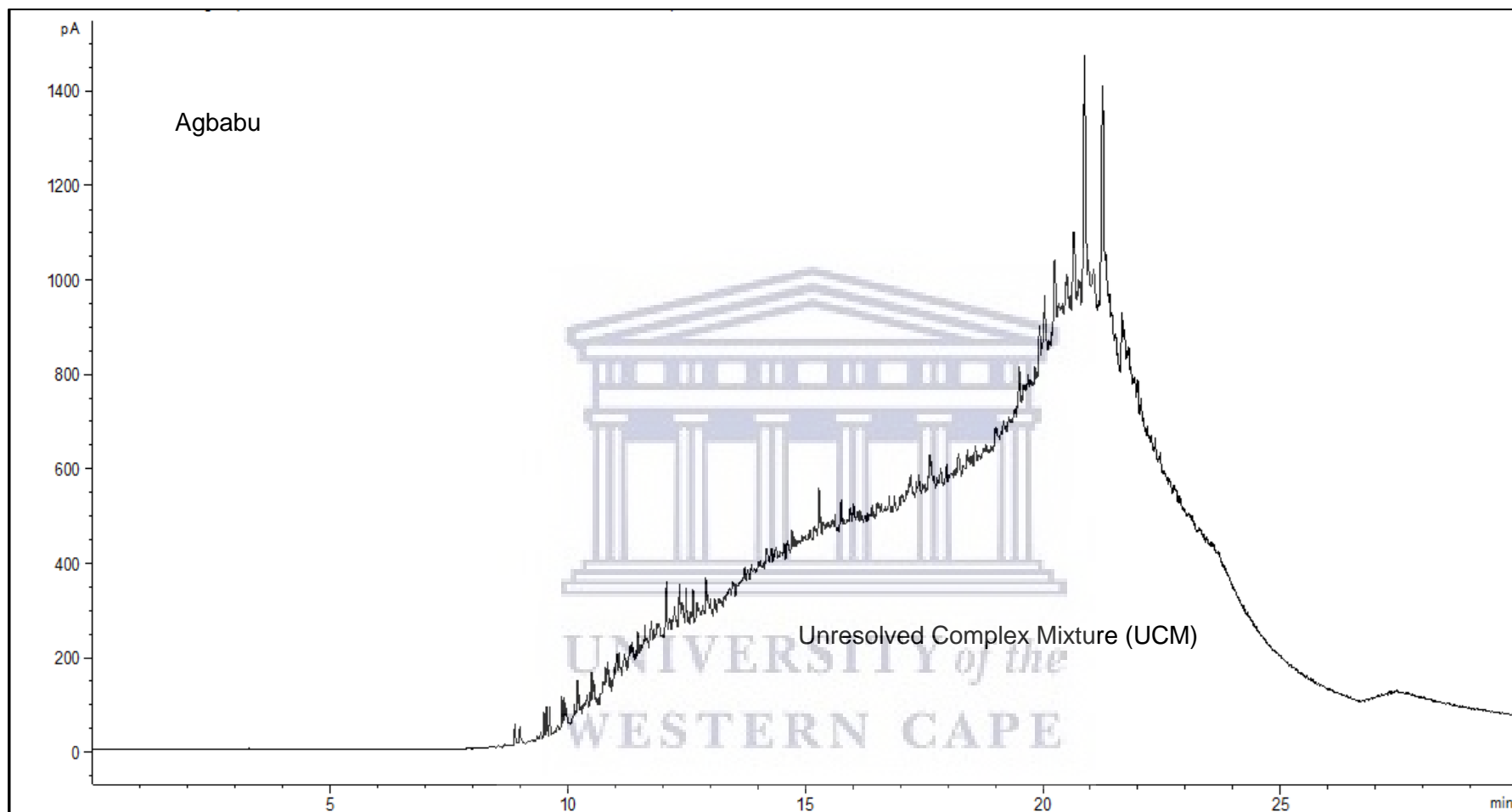
*Figure 92: Gas Chromatogram of Agbabu heavy oil. Response intensity is shown on the Y-axis in pico Ampere, and Retention time is shown on the X-axis in Minutes.*
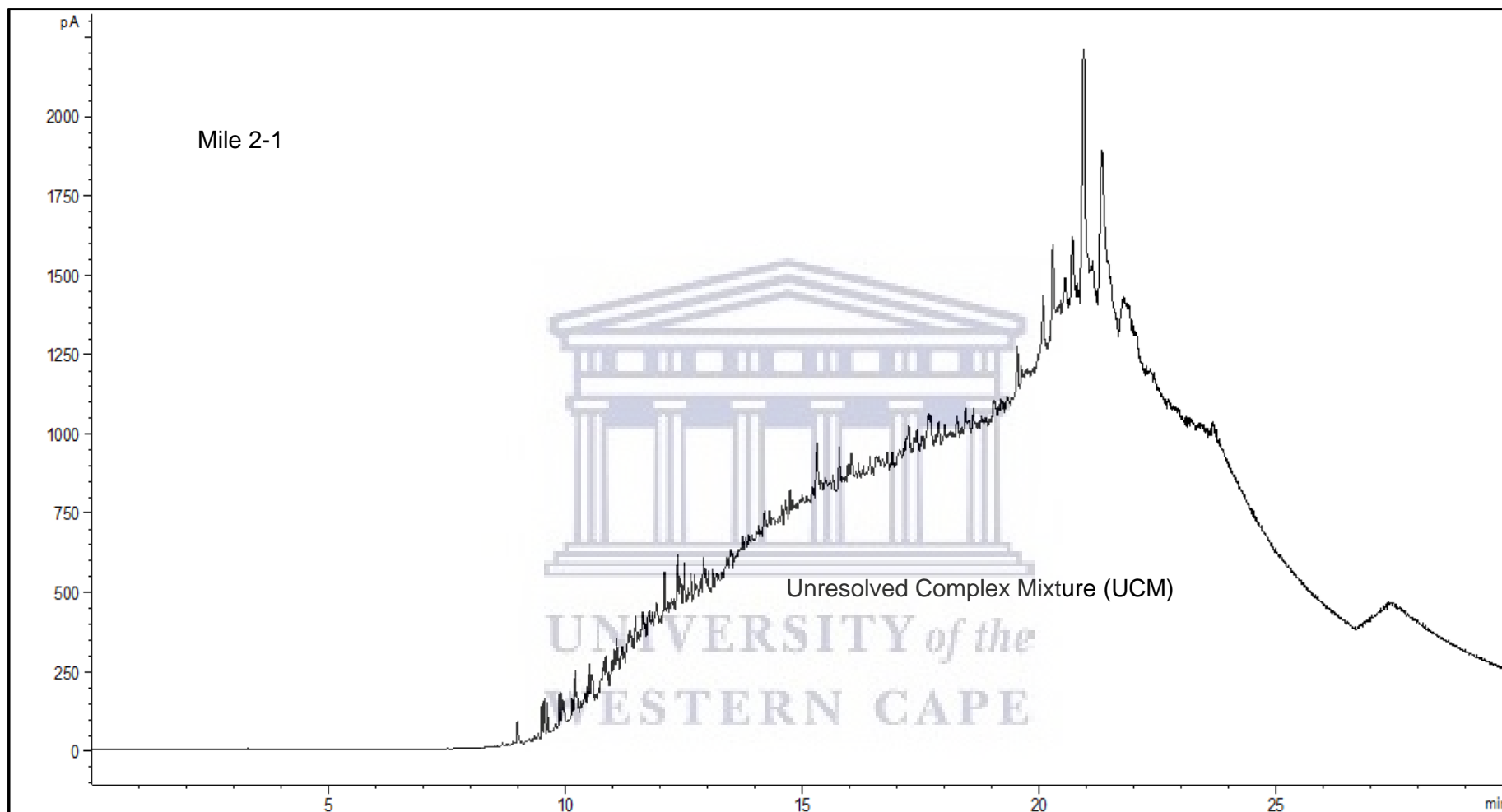
*Figure 93: Gas Chromatogram of Mile 2-1 heavy oil. Response intensity is shown on the Y-axis in pico Ampere, and Retention Time is shown on the X-axis in Minutes.*
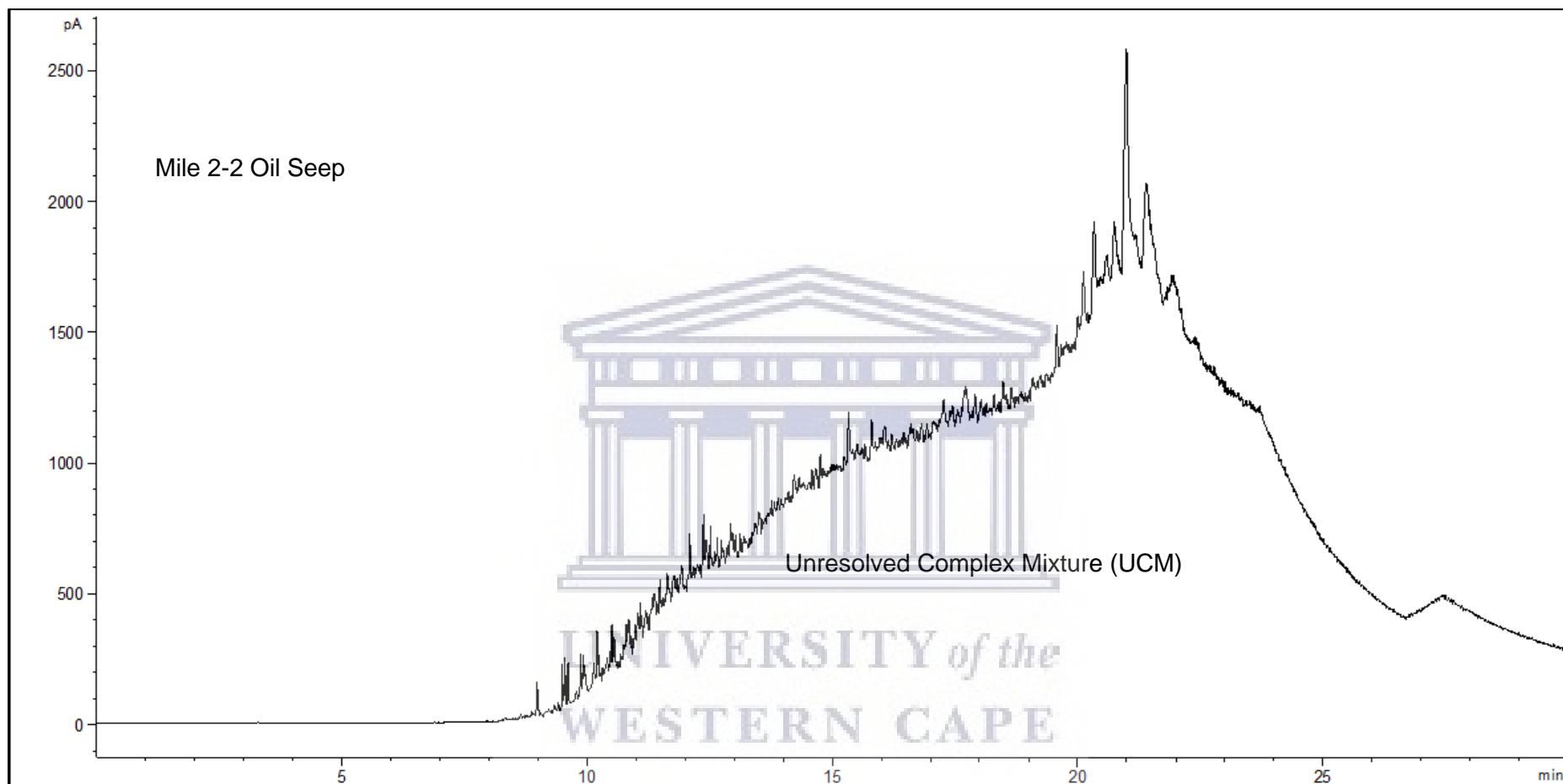
*Figure 94: Gas Chromatogram of Mile 2-1 heavy oil. Response intensity is shown on the Y-axis in pico Ampere, and Retention time is shown on the X-axis in Minutes.*
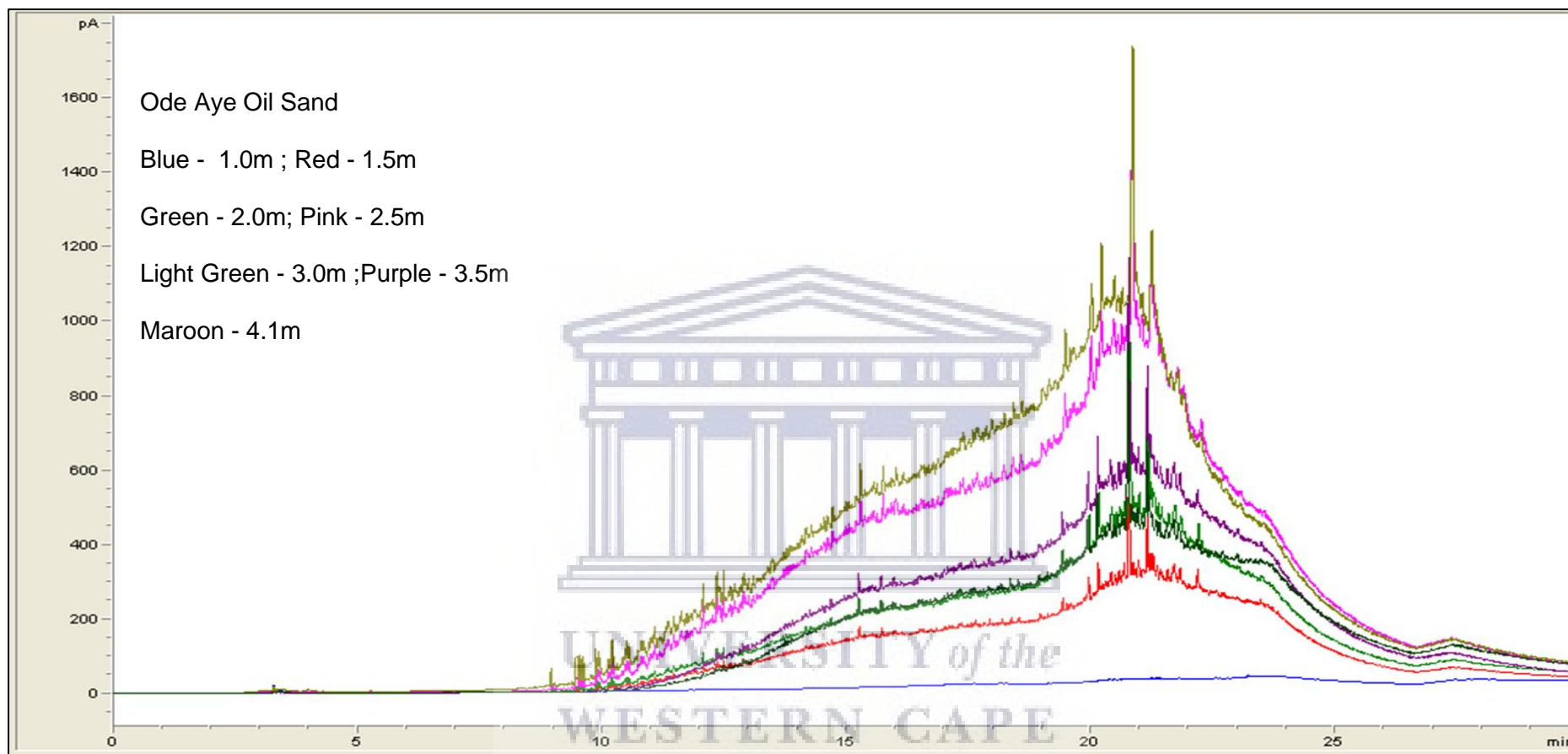
*Figure 95: Gas Chromatograms of Ode – Aye Oil Sand at varying depths. Response intensity is shown on the Y-axis in pico Ampere, and Retention time is shown on the X-axis in Minutes.*

*Figure 96: Gas Chromatogram Ilubinrin Oil Sand at a depth of 2.0 m. Response intensity is shown on the Y-axis in pico Ampere and Retention time is shown on the X-axis in Minutes.*

Ilubinrin Oil Sand at depth of3.1 m.
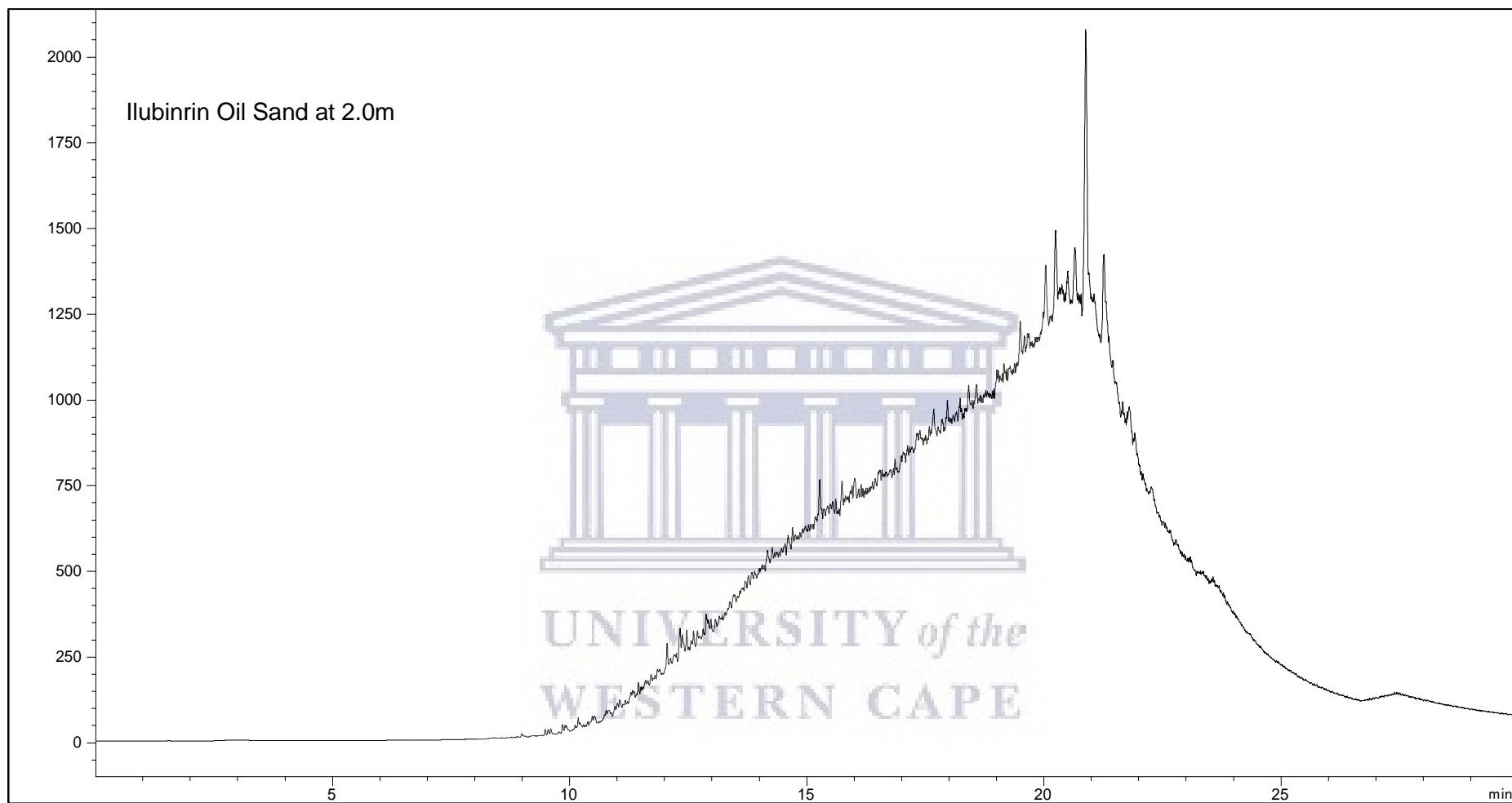
*Figure 97: Gas Chromatogram of Ilubinrin Oil Sand at a depth of 3.1 m. Response intensity is shown on the Y-axis in pico Ampere, and Retention time is shown on the X-axis in Minutes.*

*Figure 98: Gas Chromatogram of Egbe oil sand. Response intensity is shown on the Y-axis in pico Ampere, and Retention time is shown on the X-axis in Minutes.*

*Figure 99: Gas Chromatogram of J4-BH2 oil sand. Response intensity is shown on the Y-axis in pico Ampere, and Retention time is shown on the X-axis in Minutes.*

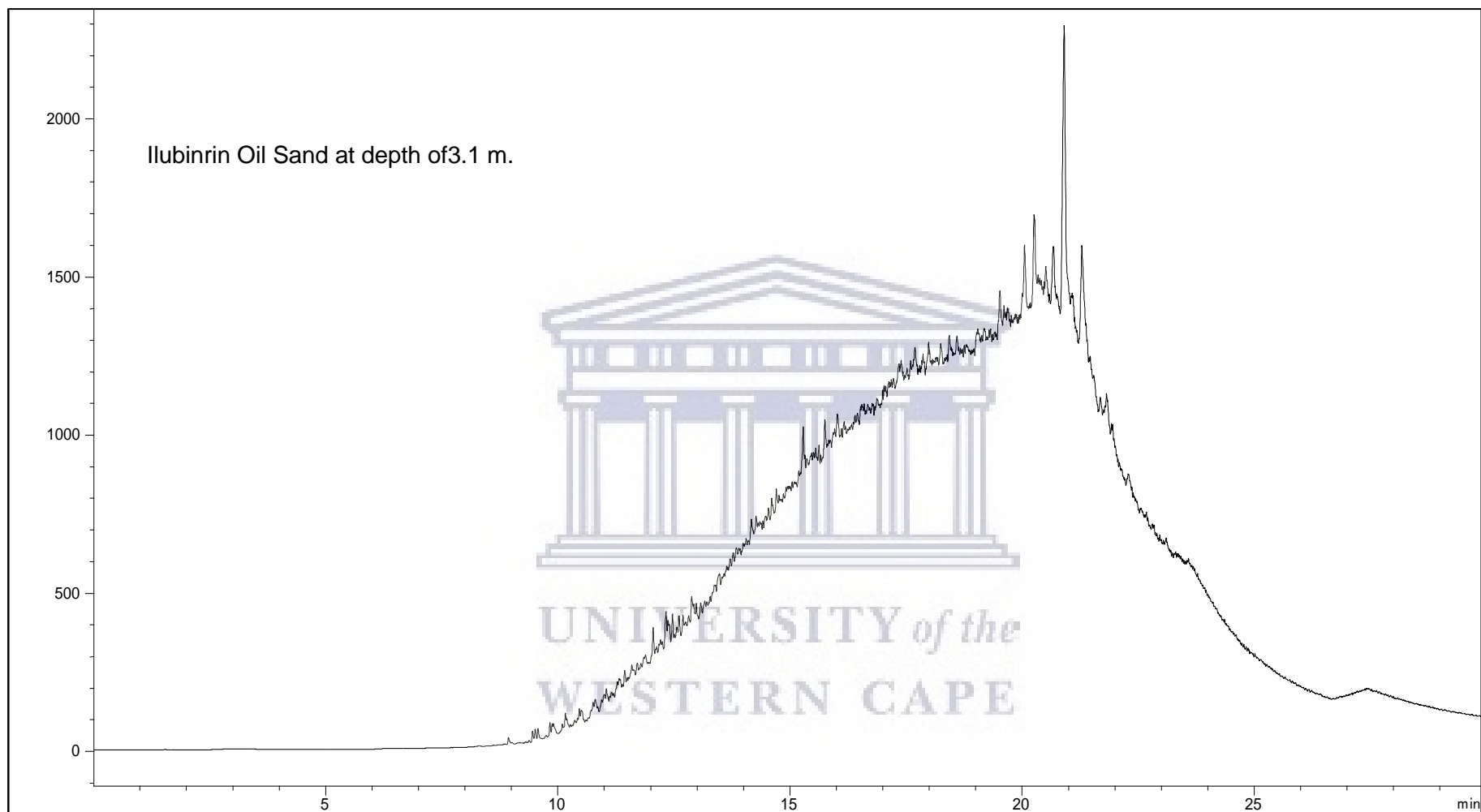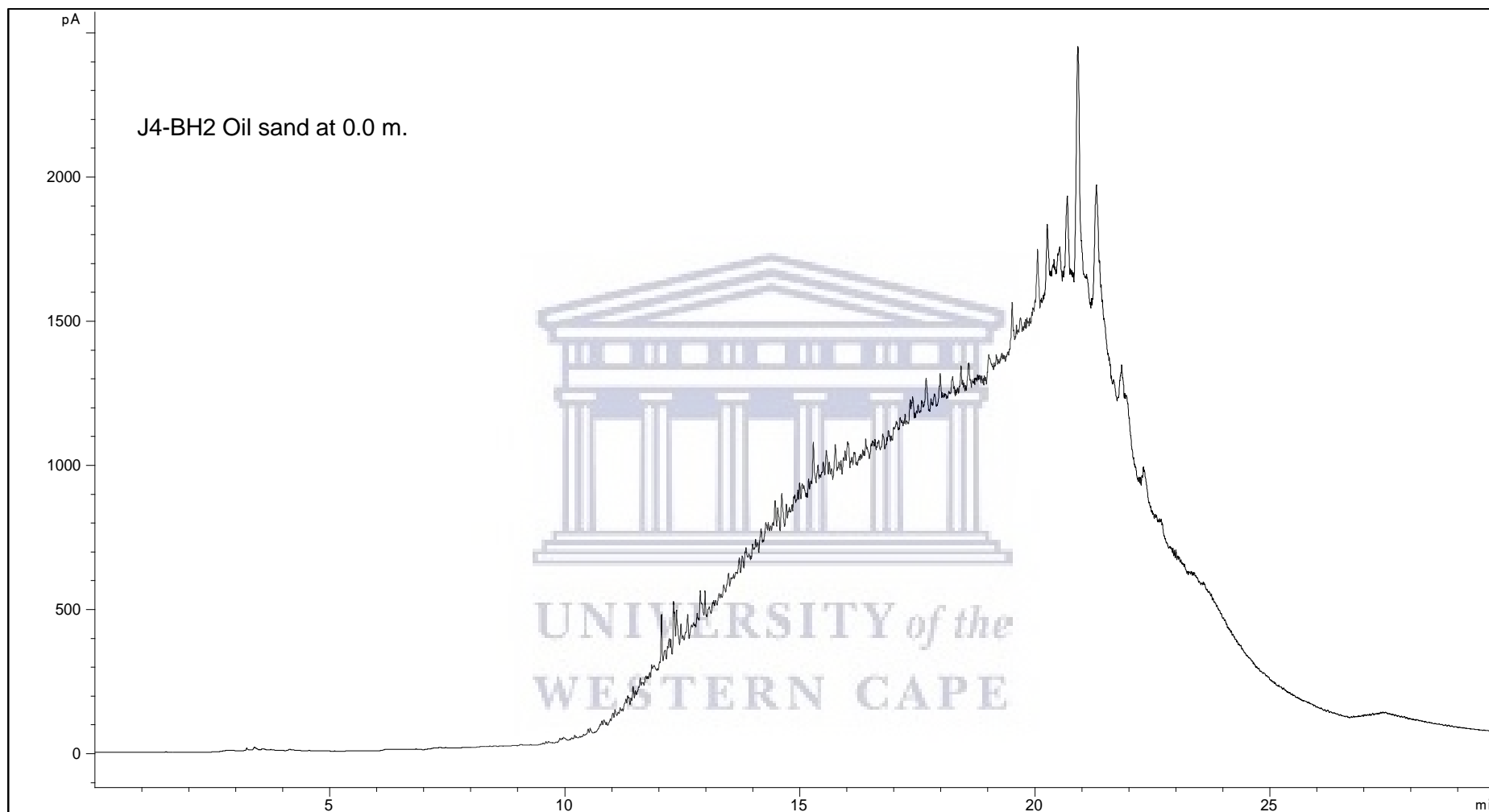Except for sample OD-1 (Fig.95), the TD-GC results of the oil sands and heavy oil produced critical evaluation parameters. The results for OD-1 were compromised by poor chromatogram, possibly resulting from a low concentration of hydrocarbons, and were excluded from the analysis and interpretation. The light condensate varied from 0.1 % to 8.90 %, whereas the naphthenes and aromatics ranged from 0.00 % to 0.82 %.  In contrast, the results illustrate the dominance of a heavy condensate (84.81 % to 98.32 %) with the absence of hydrocarbon chains, C6 – C12, consistent with biodegraded oil.

The progressive change in crude oil quality from unaltered to the biodegraded oil is the decrease in n-alkanes, and attendant relative increase in phytane and pristane, until only the latter isoprenoids are left or removed in the completely biodegraded oil (Connan, 1984; Deroo et al., 1974; Moldowan et al., 1992; Palmer, 1983; Seifert and Moldowan, 1979; Seifert et al., 1984). These changes are evident in the TD-GC results shown in Figures 89 – 99. The chromatograms (Figs. 89 to 99) showed humps of the unresolved complex mixture (UCM) below the peaks, and the response intensity showed no detectable hydrocarbon below 10 minutes retention time. The isoprenoids, pristane, and phytane were completed removed, and the hydrocarbon composition analysis showed the dominance of heavy condensates. The chromatograms for the oil sands and heavy oil are similar and indicated that they are biodegraded. Besides, the dominance of heavy condensate, the absence of light condensate, pristane, and phytane provides good evidence of the severity of the biodegradation. The wide-ranging features of profoundly altered oils presented by these results may have been accelerated by their shallow depths of occurrence, low temperature, and salinity, and water washing (Bailey et al., 1973; Larter et al., 2006; Peters et al., 2005b).

## 6.9: GAS CHROMATOGRAPHY (GC), GAS CHROMATOGRAPHY-MASS SPECTROMETRY (GC-MS).

Gas Chromatography and Gas Chromatography-Mass Spectrometry provides molecular parameter data that is based on the presence or else the relative abundance of specific molecules in an oil or source rock extract. The information derived from molecular parameter data such as GC, and GC-MS are useful in the assessment of biodegradation, and in correlating oil to oil and oil to source rock. Besides, specific molecular parameters, can be used to identify source rock and its thermal maturity, estimate the ages of oil, and categorize depositional environments (Peters et al., 2005). The results of the extracts and column fractionation (Saturate, Aromatics, Resins-Asphaltenes) are presented in Table 24 and Figure 100.
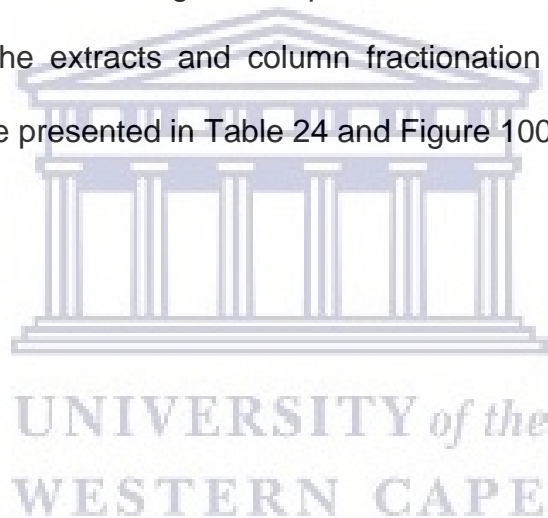
*Table 24: Results of column fractionation showing saturate, aromatic, and polar fractions.*

| Well Name | Sample Type | Sample Depth | Extract weight (mg) | ASPHALT (mg) | Hydrocrabons (mg) | aromatics (mg) | Resin (mg) | Saturate (mg) | Sat/Aro ratio | HC % | Polars % | Sats % | Aros % |
|---|---|---|---|---|---|---|---|---|---|---|---|---|---|
| AG-1 | Heavy Oil | 7.13 | 145.77 | 35.33 | 90.93 | 48.36 | 12.62 | 42.57 | 0.88 | 62.38 | 32.89 | 29.2 | 33.18 |
| OD-1 | Oil sand | 0 | 74.82 | 42.44 | 14.04 | 7.62 | 13.35 | 6.42 | 0.84 | 18.77 | 74.57 | 8.58 | 10.18 |
| OD-1 | Oil sand | 1 | 155.3 | 96.63 | 19.7 | 10.33 | 16.61 | 9.37 | 0.91 | 12.69 | 72.92 | 6.03 | 6.65 |
| OD-1 | Oil sand | 4.1 | 488.29 | 149.12 | 273.38 | 141.39 | 40.68 | 131.99 | 0.93 | 55.99 | 38.87 | 27.03 | 28.96 |

*Note on abbreviations*

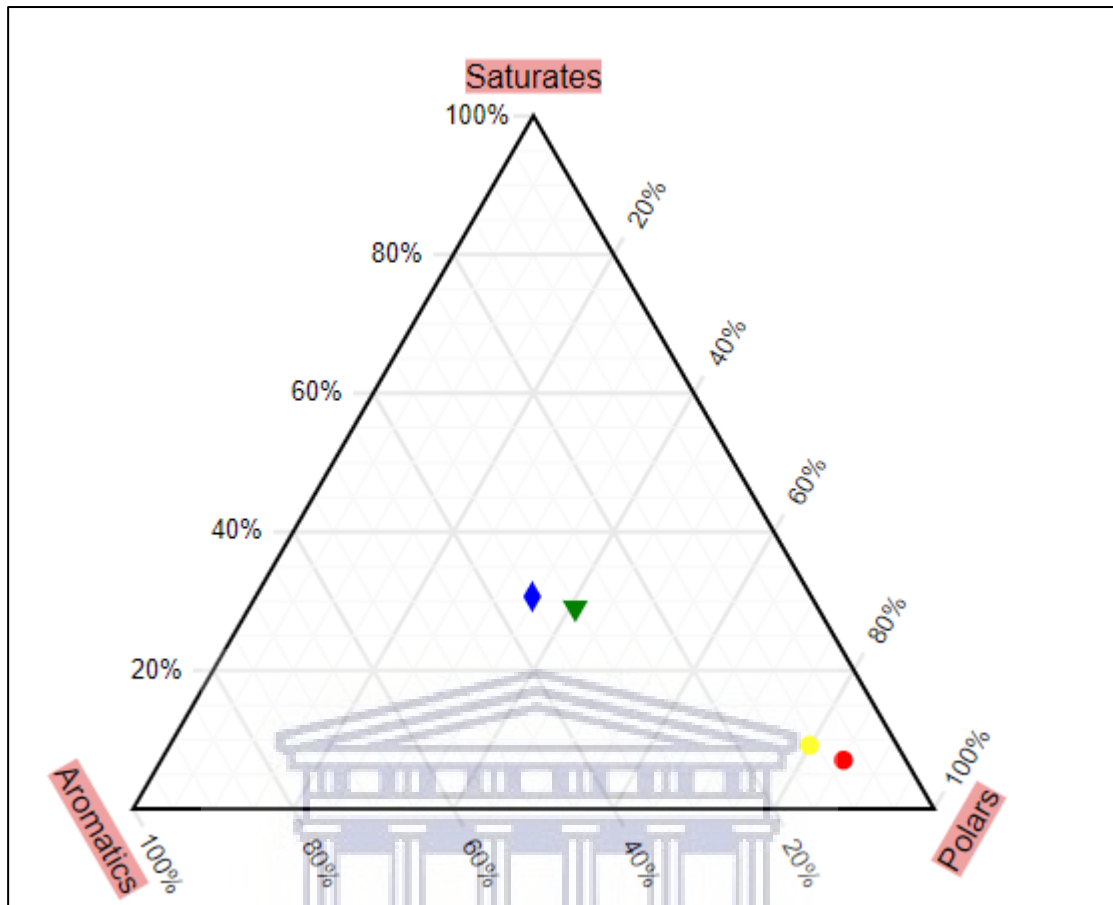*AG = Agbabu heavy oil*

*OD = Ode-Aye borehole*
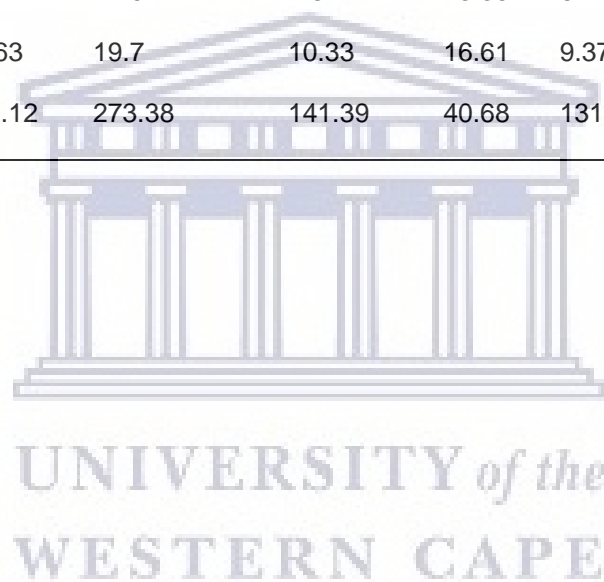
*Figure 100: Ternary diagram showing saturate, aromatic, and polar fractions.*

Legend:

 Blue Diamond; Agbabu *Heavy oil*

Green Triangle-down; Ode-Aye Oil sand at a depth of 4.1 m

Yellow circle; Ode-Aye BH1 Oil sand at 0.0m

Red circle; Ode-Aye BH1 Oil sand at 1.0m

The S-A-R-A results shown in Table 24 and Figure 100 displayed a dominance of polar compounds. The polar compounds varied from 32.89 % to 74.57 %, while the saturates and aromatics ranged from 6.03 % to 29.2% and 6.65 % to 33.18 %, respectively. In undegraded crude oils, the percentage of saturates is highest relative to the aromatics and polar compounds. In contrast, degraded oils contain a higher proportion of polar compounds and low amounts of saturates. The higher percentages of polar and aromatics compounds relative to the saturates (Table 24) indicates that the oil sands and heavy oil are substantially biodegraded.

Gas chromatograms of the saturate fractions (Figs. 101 to 104) showed a loss of the light molecular components and the complete absence of phytane and pristane. Besides, their chromatograms presented humps of unresolved complex mixture (Farrington and Quinn, 2015) below the peaks. The unresolved complex mixture (UCM) consists of bioresistant compounds such as highly branched and cyclic saturated, aromatic, napthoaromatic, and polar compounds that are not amenable to gas chromatography (Peters et al., 2005). The loss of the light molecular components, the humps in the chromatograms, and the complete absence of phytane and pristane, all suggested severe biodegradation.
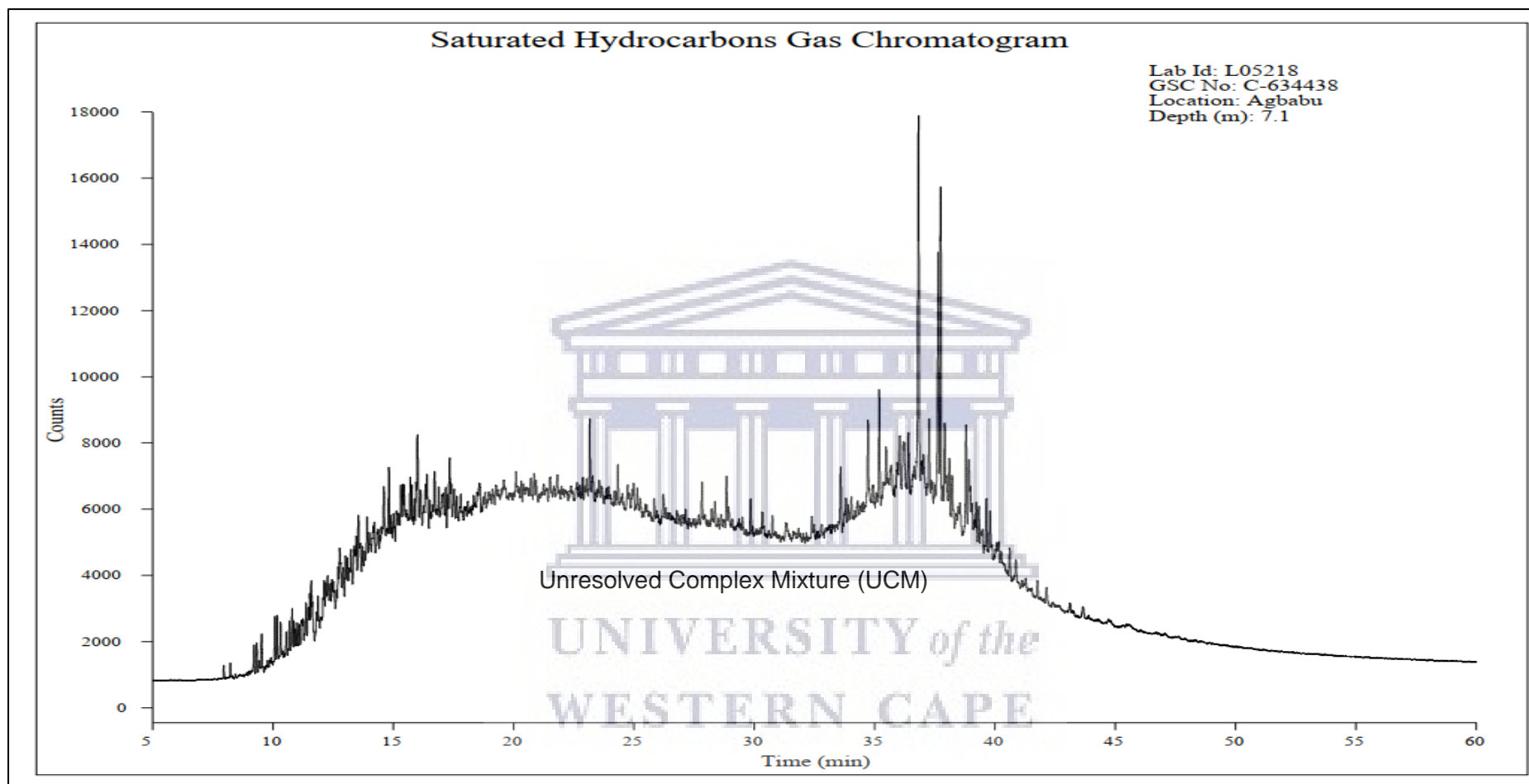
*Figure 101: Gas chromatogram of the saturate fraction of Agbabu heavy oil showing hump of the unresolved complex mixture.*

*Figure 102: Gas chromatogram of the saturate fraction of Ode-Aye oil sand at a depth of 0.0 m showing hump of unresolved complex mixture (UCM).*
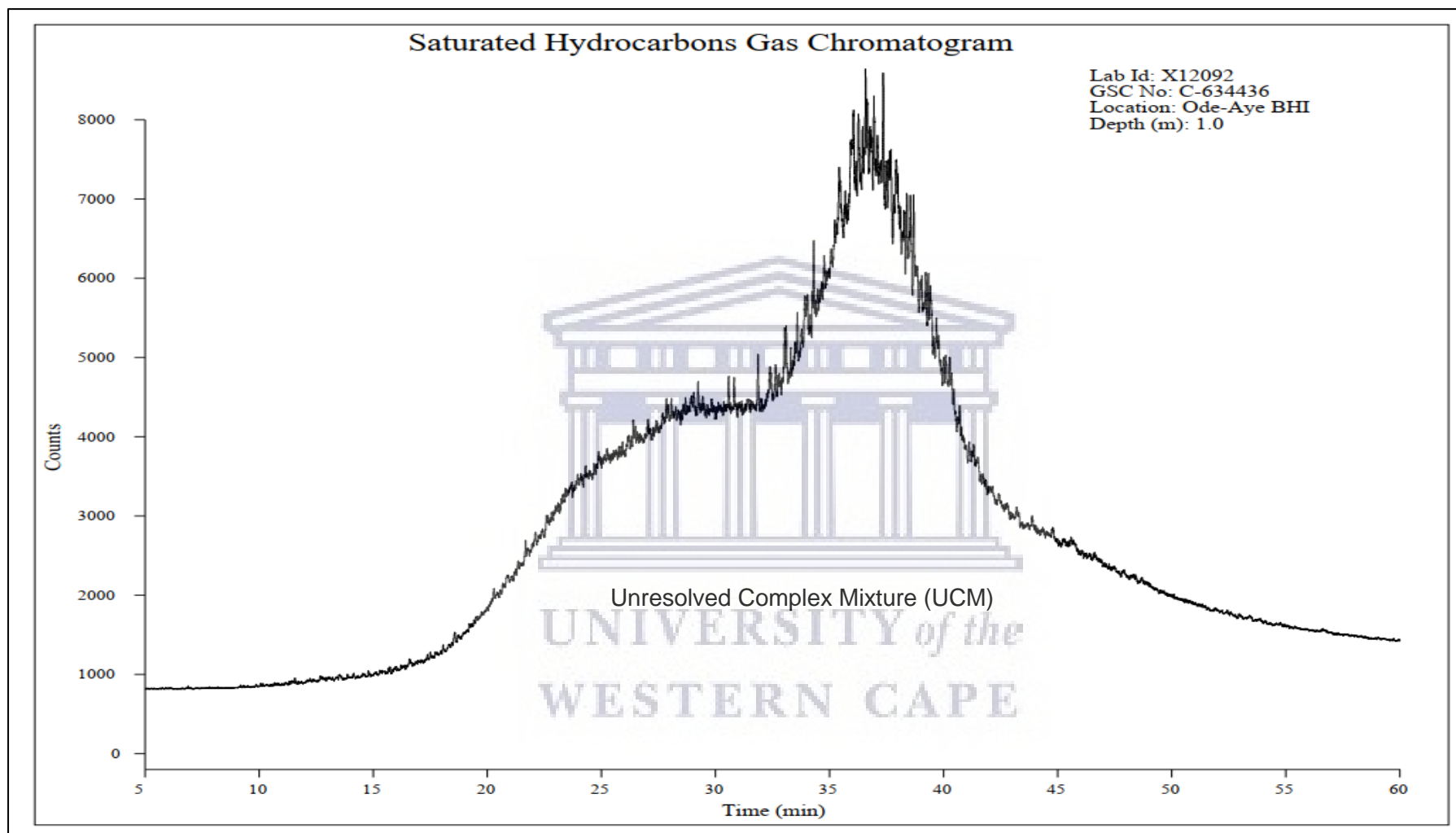
*Figure 103: Gas chromatogram of the saturate fraction of Ode-Aye oil sand at a depth of 1.0 m showing hump of unresolved complex mixture (UCM).*

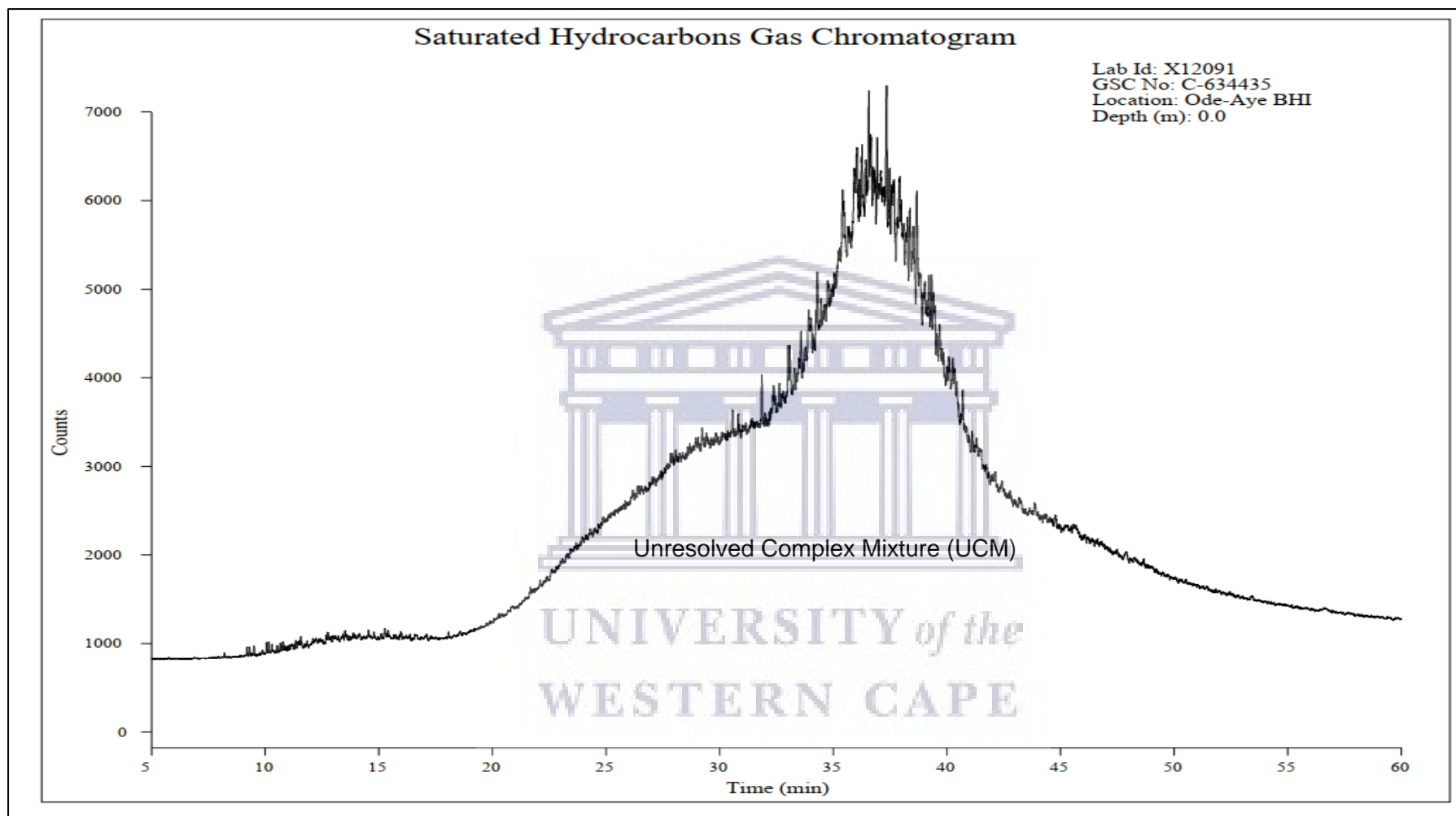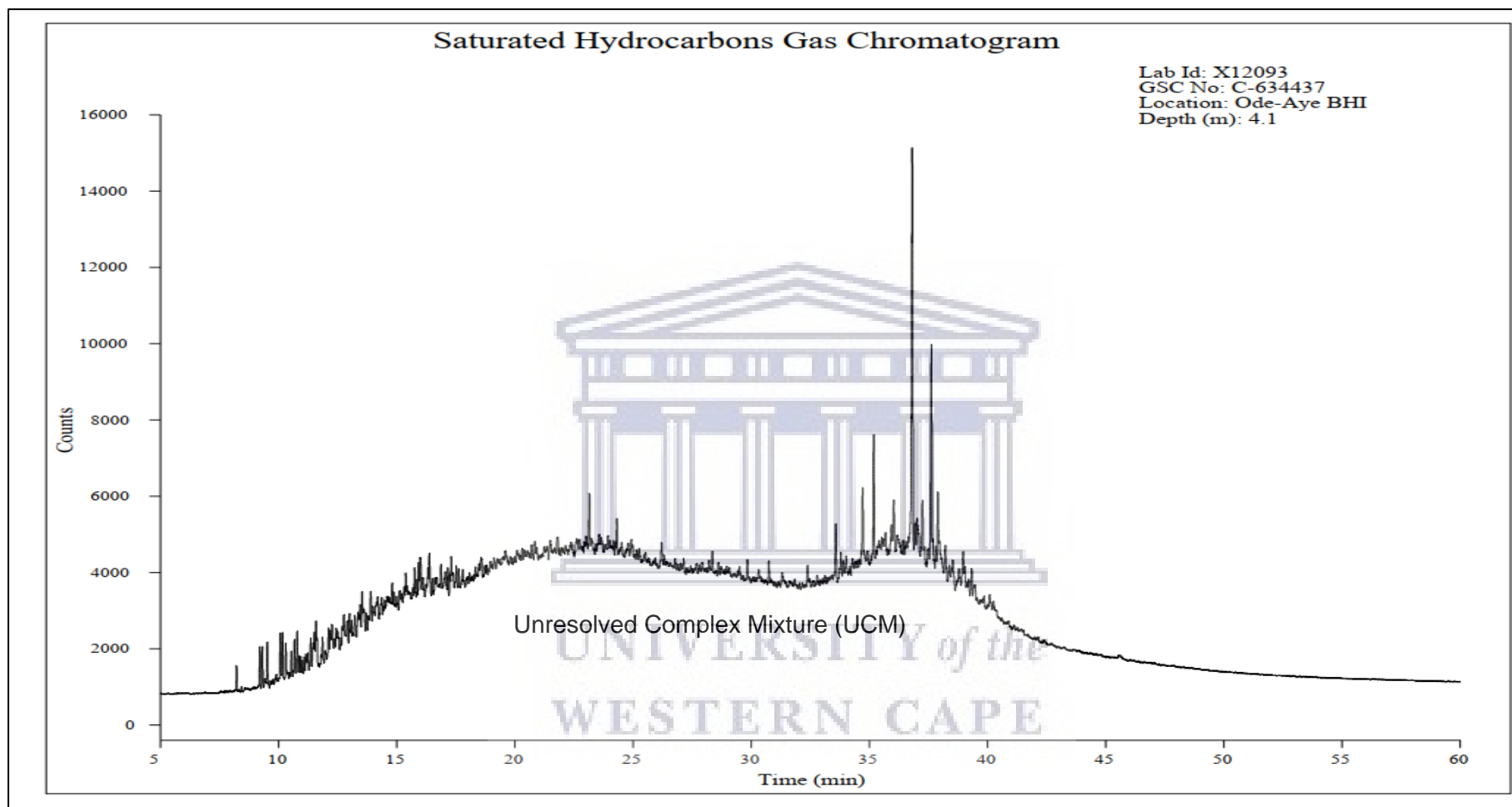*Figure 104: Gas chromatogram of the saturate fraction of Ode-Aye oil sand at a depth of 4.1 m showing hump of unresolved complex mixture (UCM).*

The total ion chromatograms from GC-MS of the saturate and aromatic fractions are shown in Figures 105 to 108 and Figures 109 to 112.  The displays (Figs. 109 – 112) of the aromatic portion showed humps of unresolved complex mixture, typical of severely biodegraded oils.
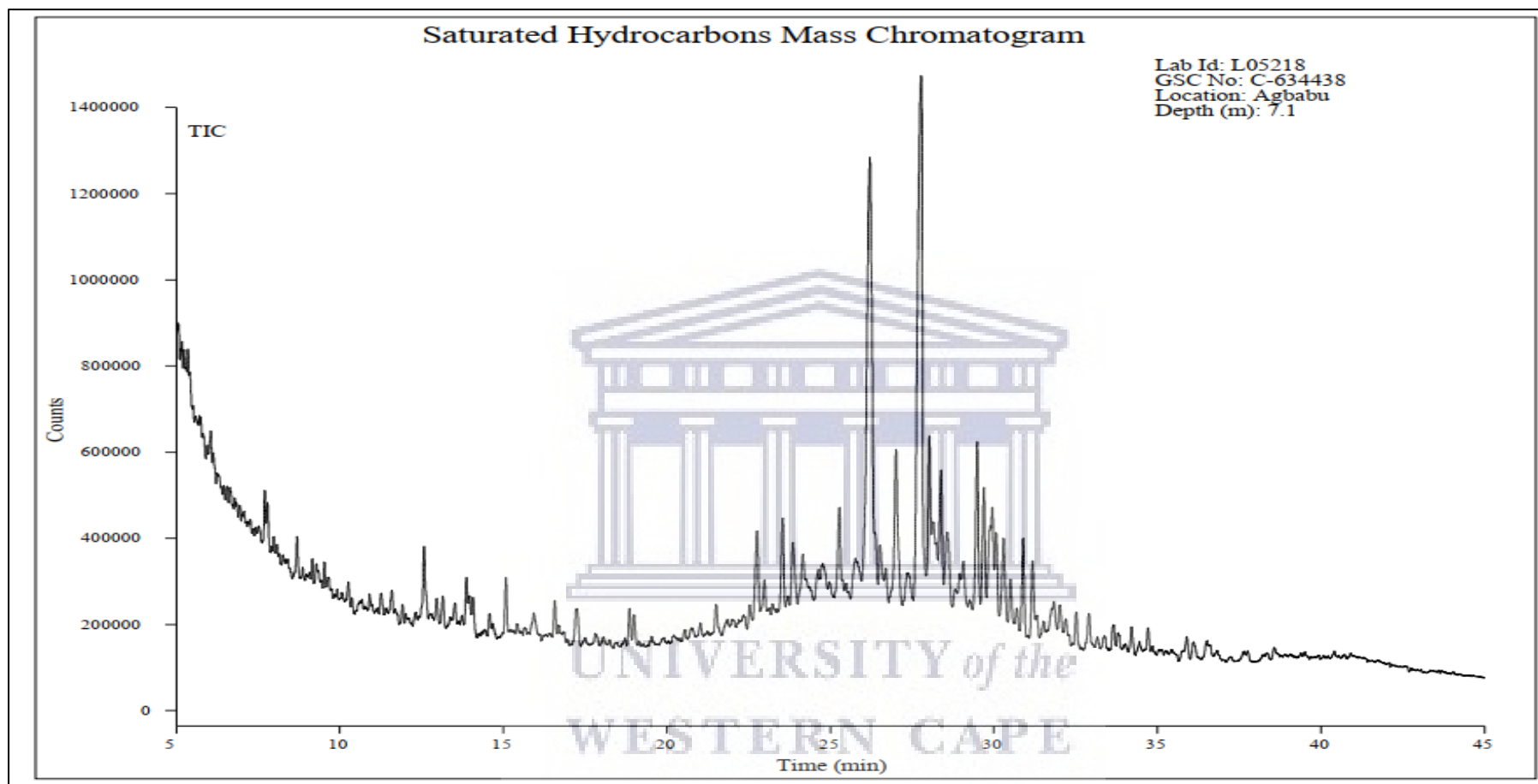
*Figure 105: Display of total ion chromatogram of the saturate fraction of Agbabu heavy oil.*

*Figure 106: Display of total ion chromatogram of the saturate fraction of Ode-Aye oil sand at a depth of 0.0 m.*

*Figure 107: Display of total ion chromatogram of the saturate fraction of Ode-Aye oil sand at a depth of 1.0 m.*

*Figure 108: Display of total ion chromatogram of the saturate fraction of Ode-Aye oil sand at a depth of 4.1 m.*
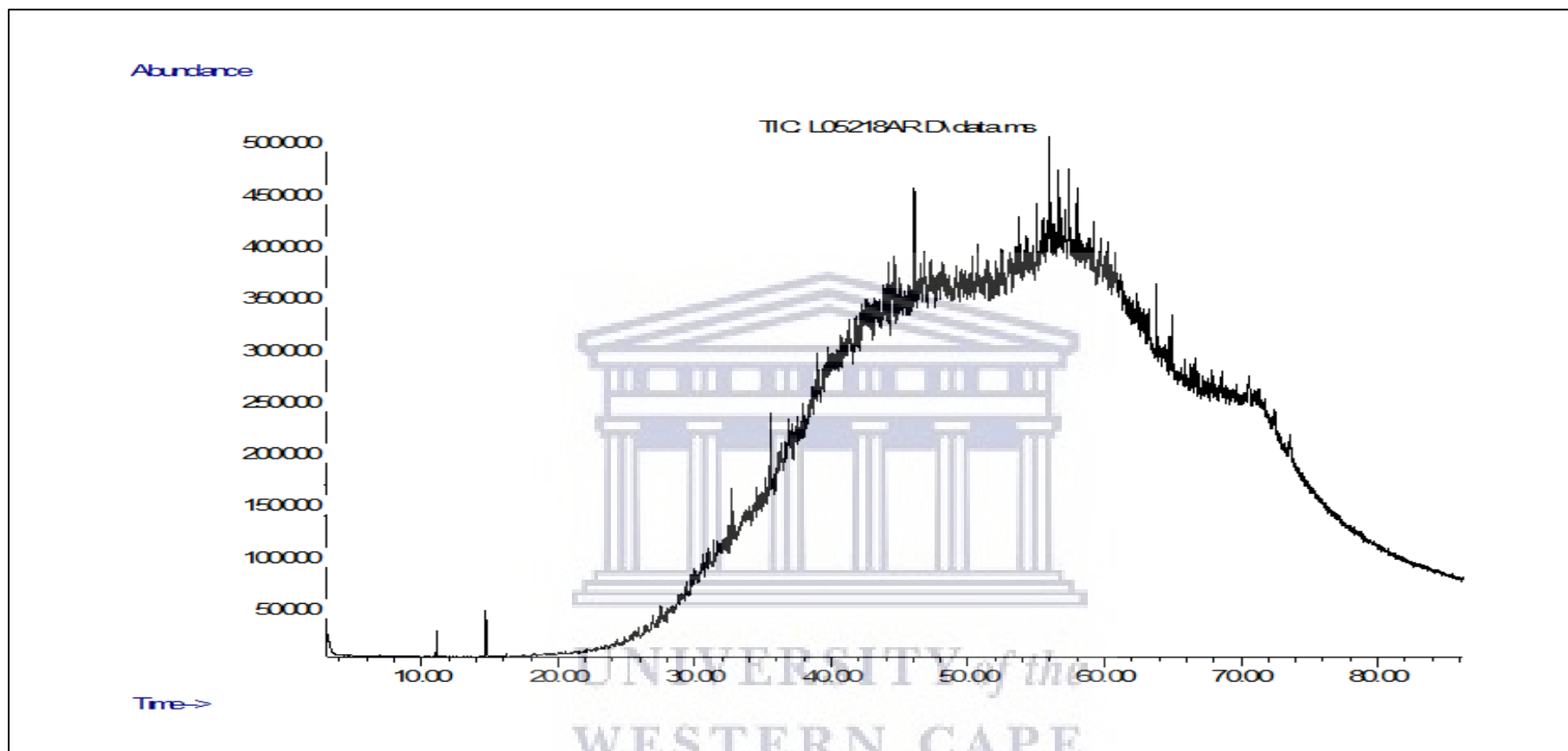
*Figure 109: Display of Total ion chromatogram of the aromatic fraction of Agbabu heavy oil.*
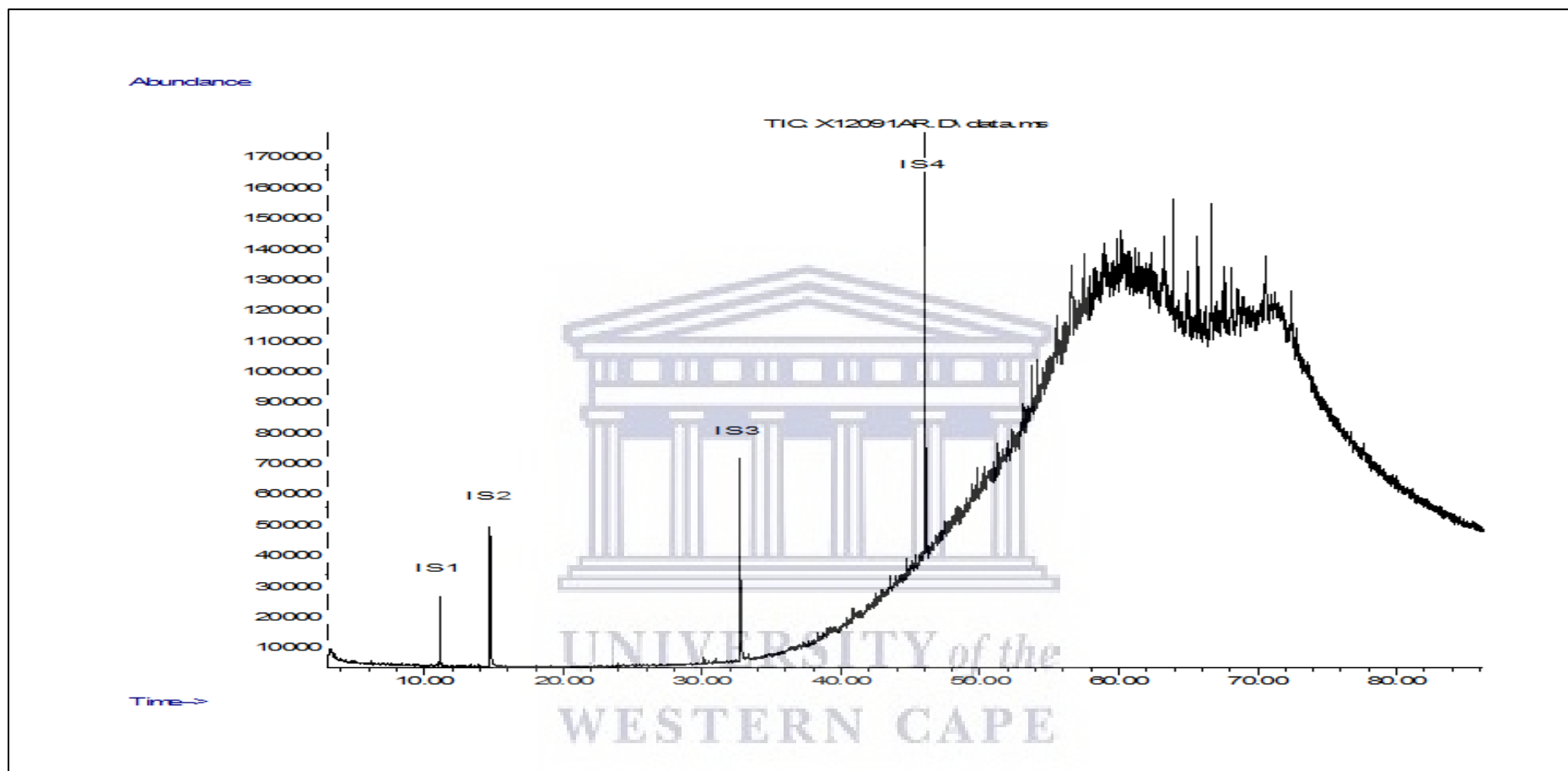
*Figure 110: Display of total ion chromatogram of the aromatic fraction of Ode-Aye oil sand at a depth of 0.0 m.*

*Note: IS1, IS2, IS3, and IS4 are the internal standards used for compound identification.*
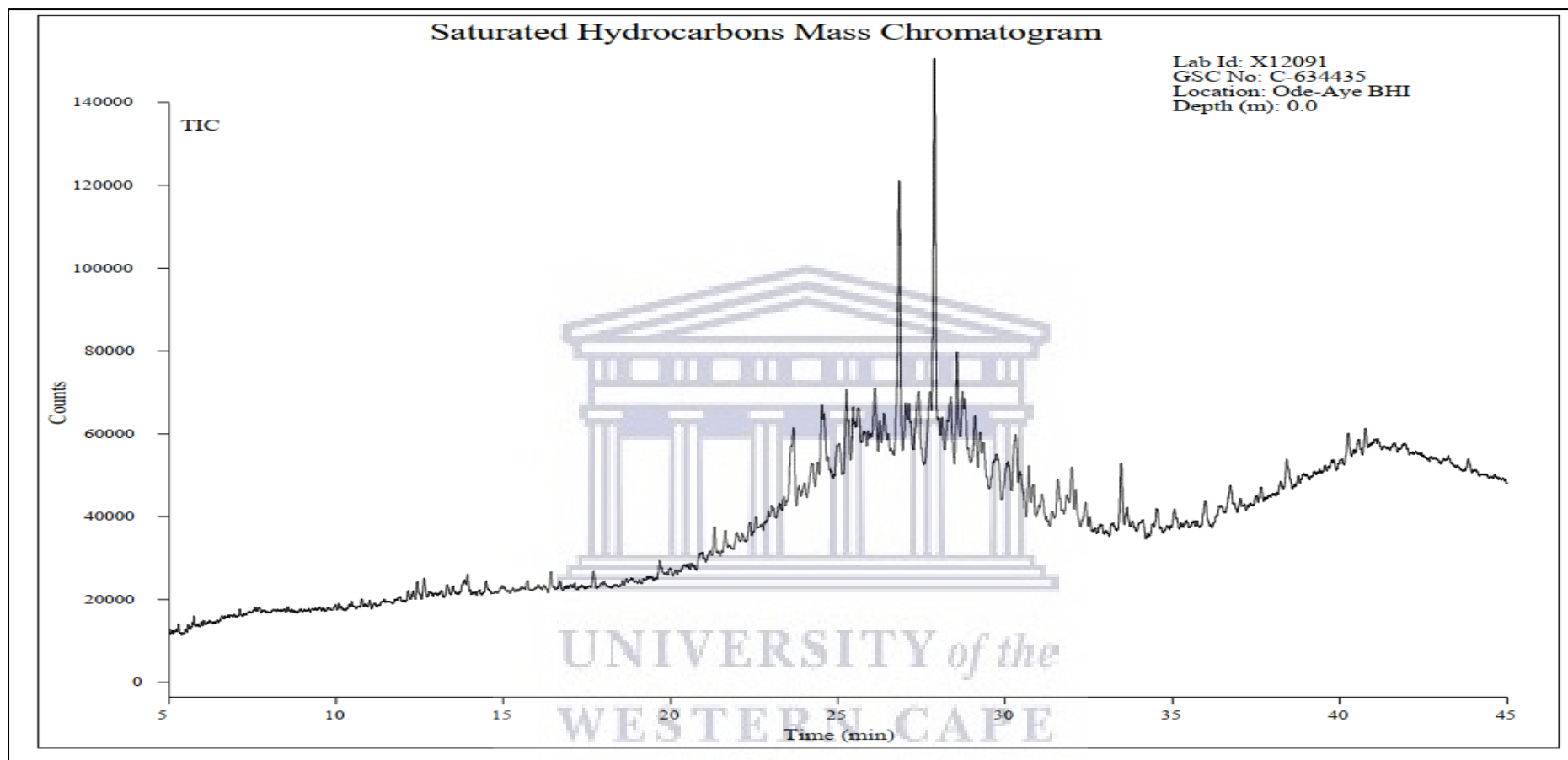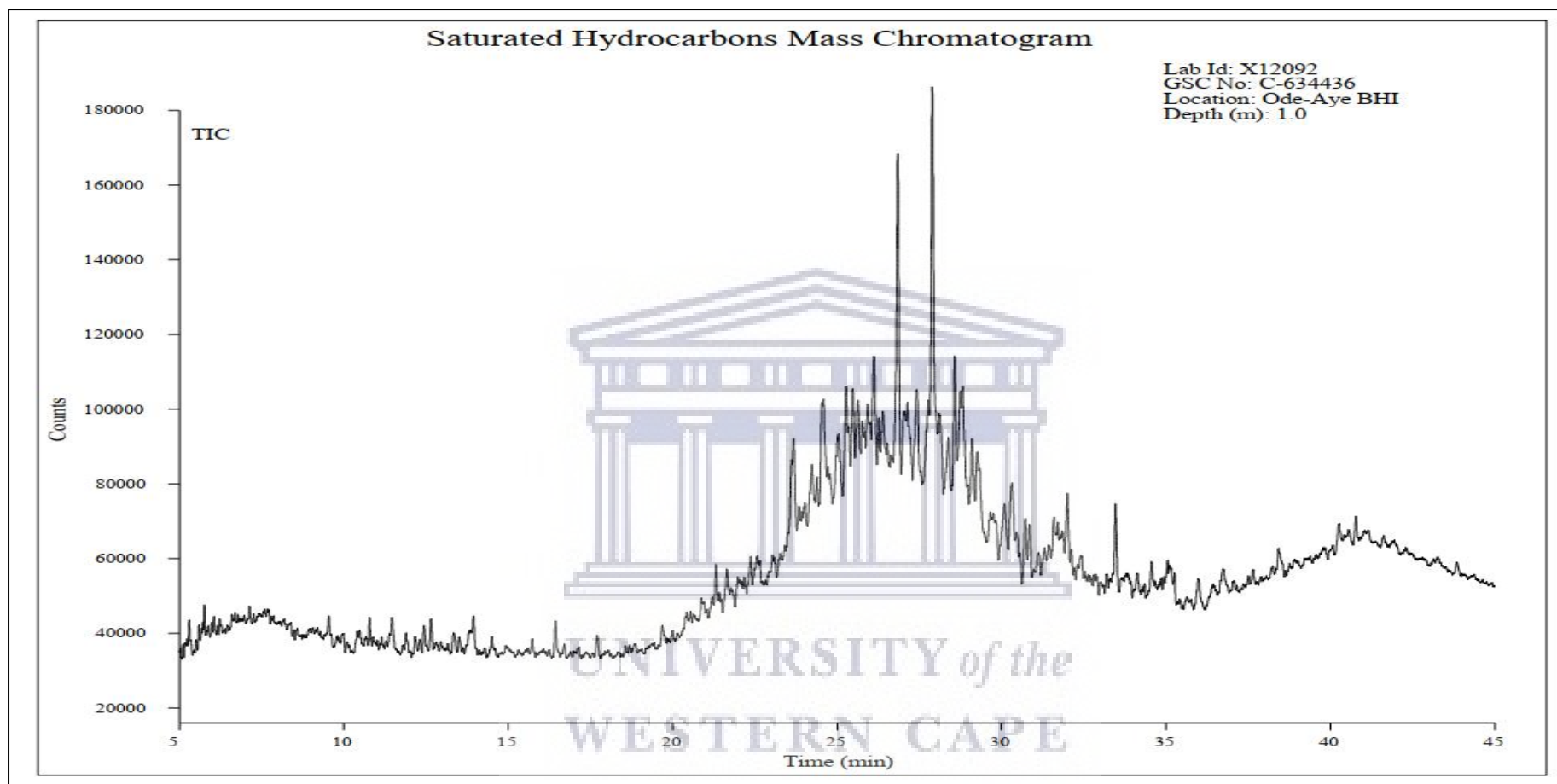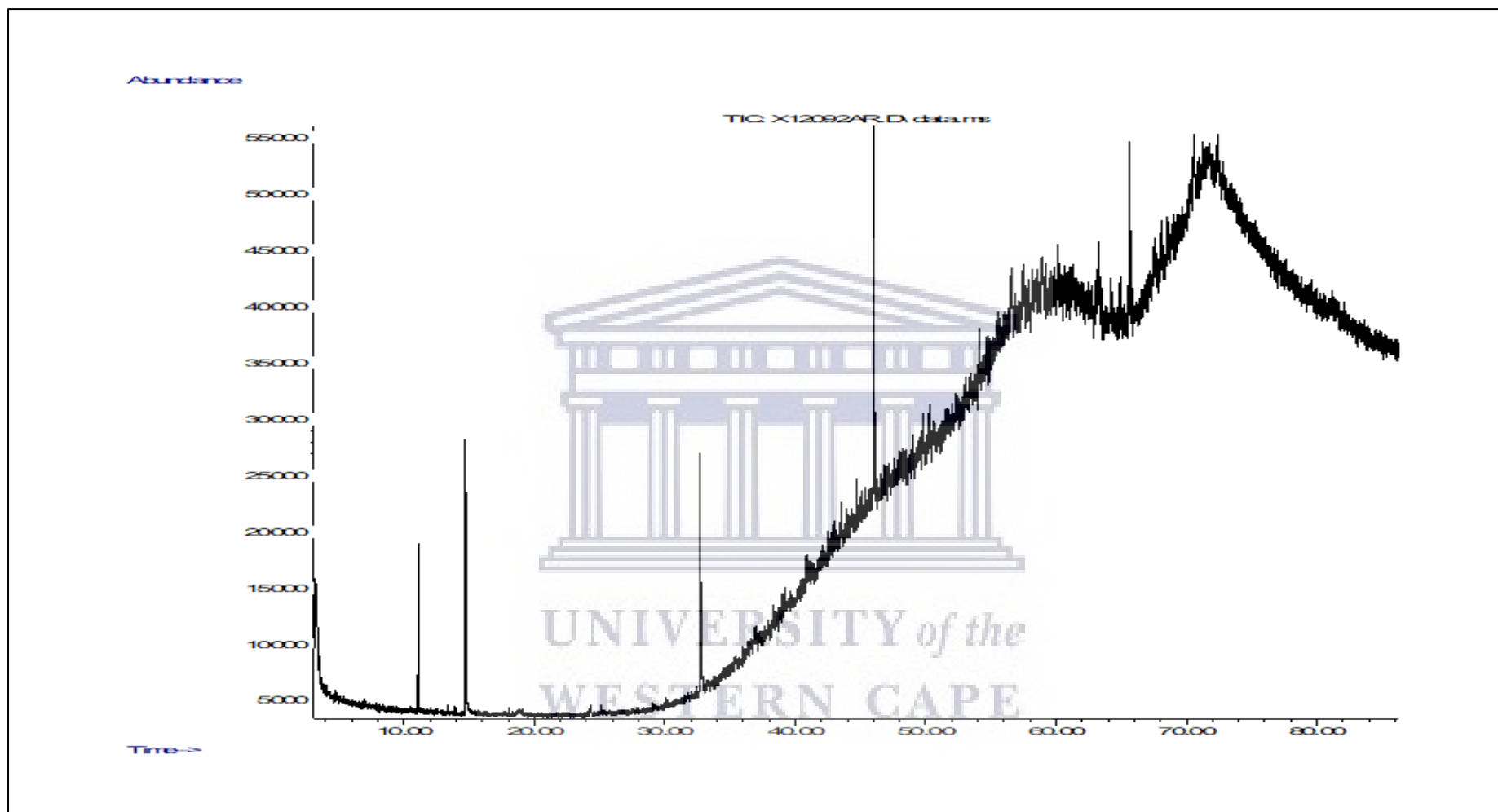
*Figure 111: Display of total ion chromatogram of the aromatic fraction for Ode-Aye oil sand at a depth of 1.0 m.*
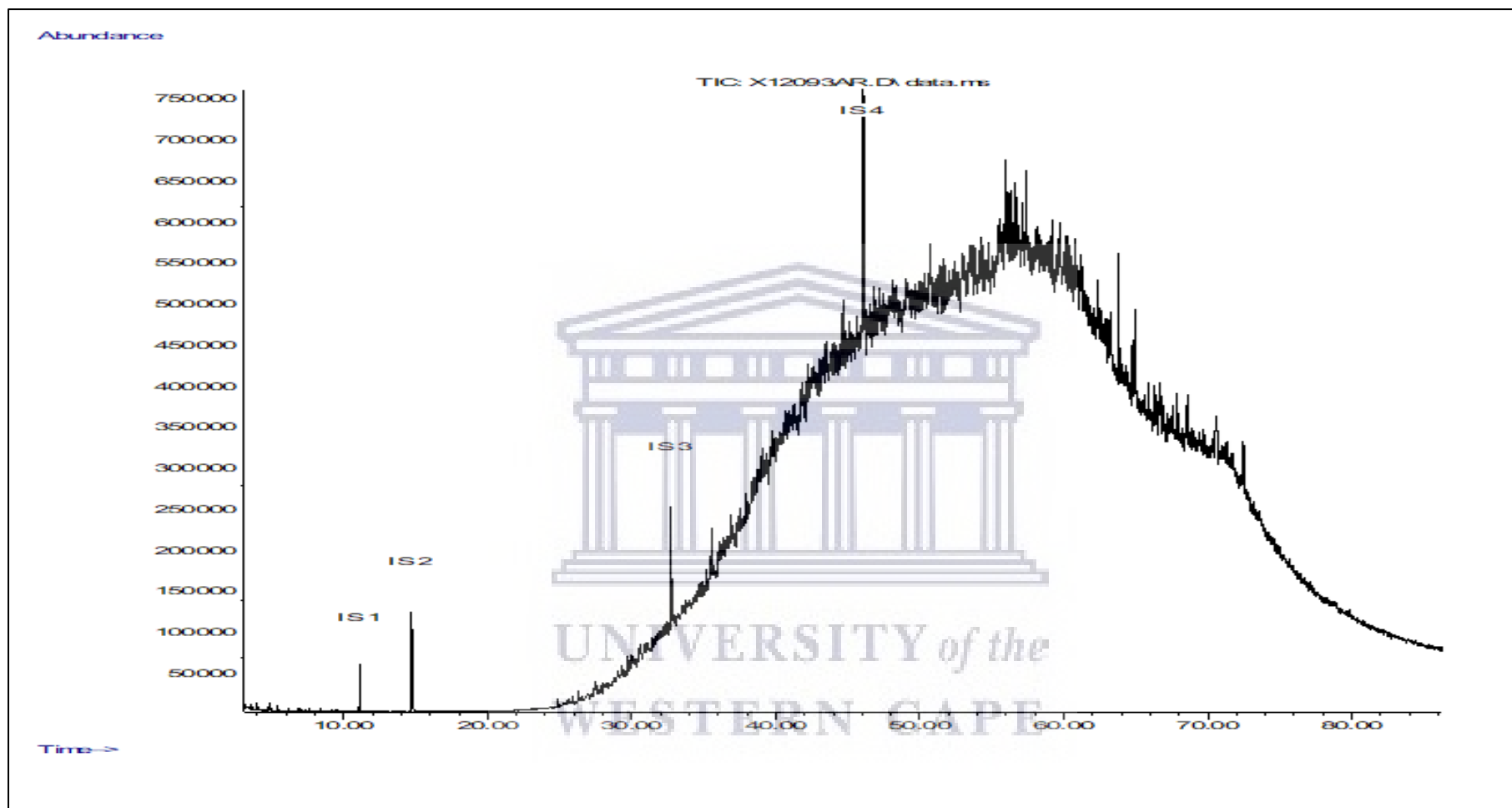
*Figure 112: Display of total ion chromatogram of Ode-Aye oil sand at a depth of 4.1 m.*

Gas Chromatography-Mass Spectrometry was carried out using selected ion monitoring (SIM). The SIM allows a single ion to be monitored at a time, enabling one class of compounds to be separated and analyzed separately from all the others. The mass spectrums for ions 191, and 217 are shown in Figures 113 to 120. In contrast, the mass spectrums for ions 231, and 253 are displayed in Figures 121 to 128. Both ions 191, 217 were obtained from the saturate fractions to analyze for the presence of triterpanes, bicadinanes, tricyclic diterpanes, sterane and bicadinanes compounds. Ions 231 and 253 were derived from the aromatic fractions to monitor the presence of triaromatic and monoaromatic steroid compounds. The results of the selected ion monitoring indicated that it was not possible to identify and quantify any of these compounds, possibly due to their scanty contents resulting from their removal and alteration.
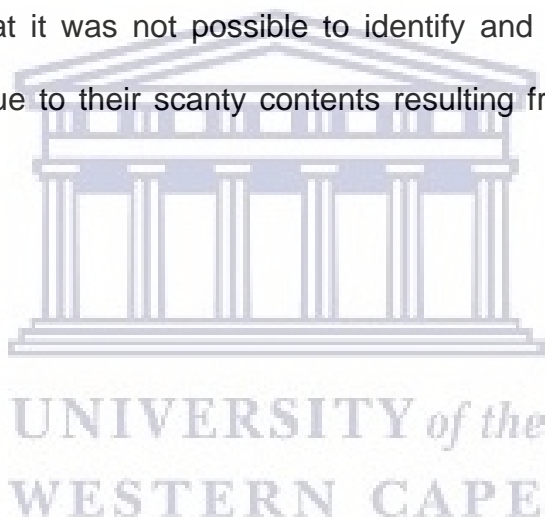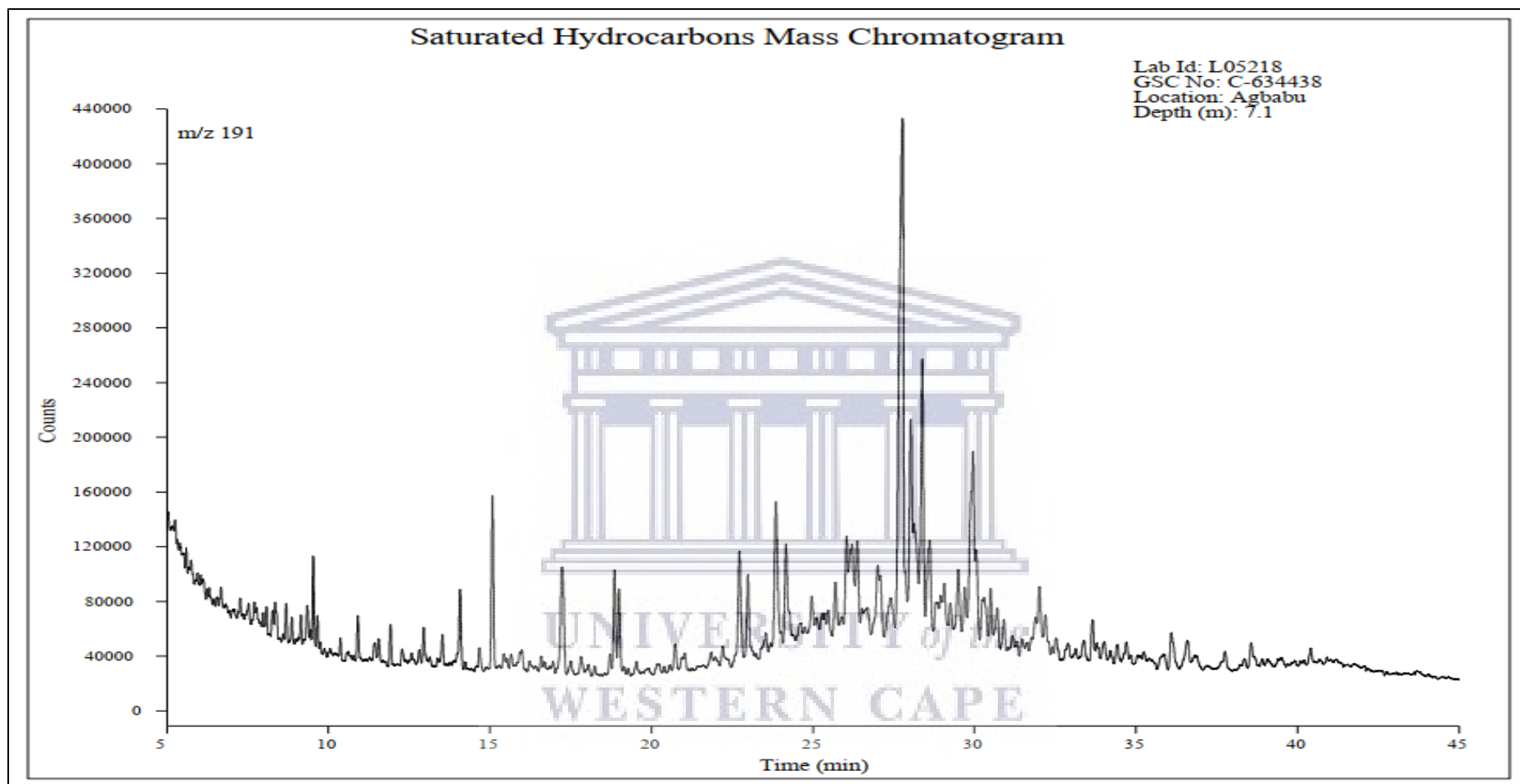
*Figure 113: Mass chromatogram of m/z 191 for the saturate fraction of Agbabu heavy oil.*
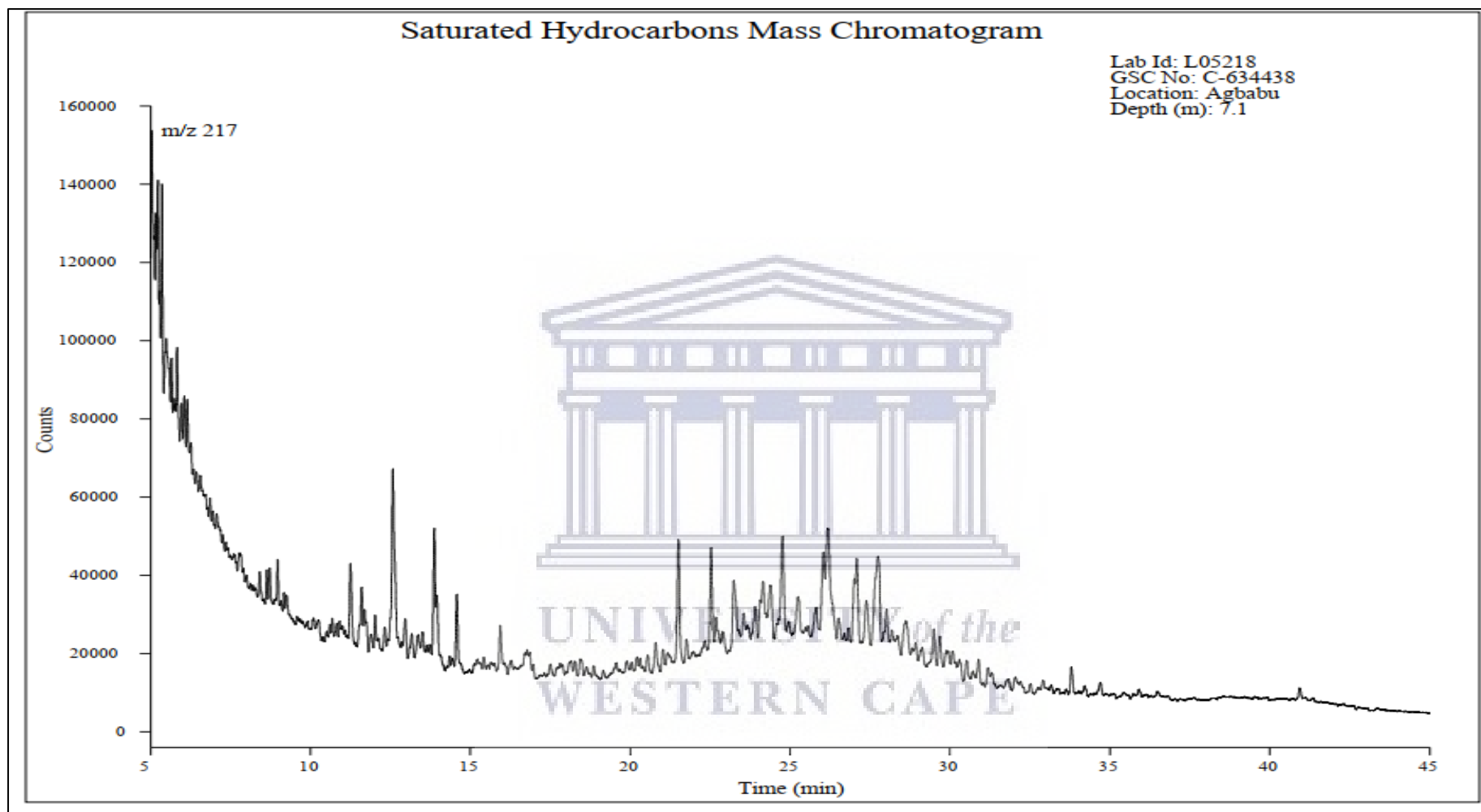
*Figure 114: Mass chromatogram of m/z 217 for the saturate fraction of Agbabu heavy oil.*

*Figure 115: Mass chromatogram of m/z 191 for the saturate fraction of Ode-Aye oil sand at a depth of 0.0 m.*

*Figure 116: Mass chromatogram of m/z 217 for the saturate fraction of Ode-Aye oil sand at a depth of 0.0 m.*

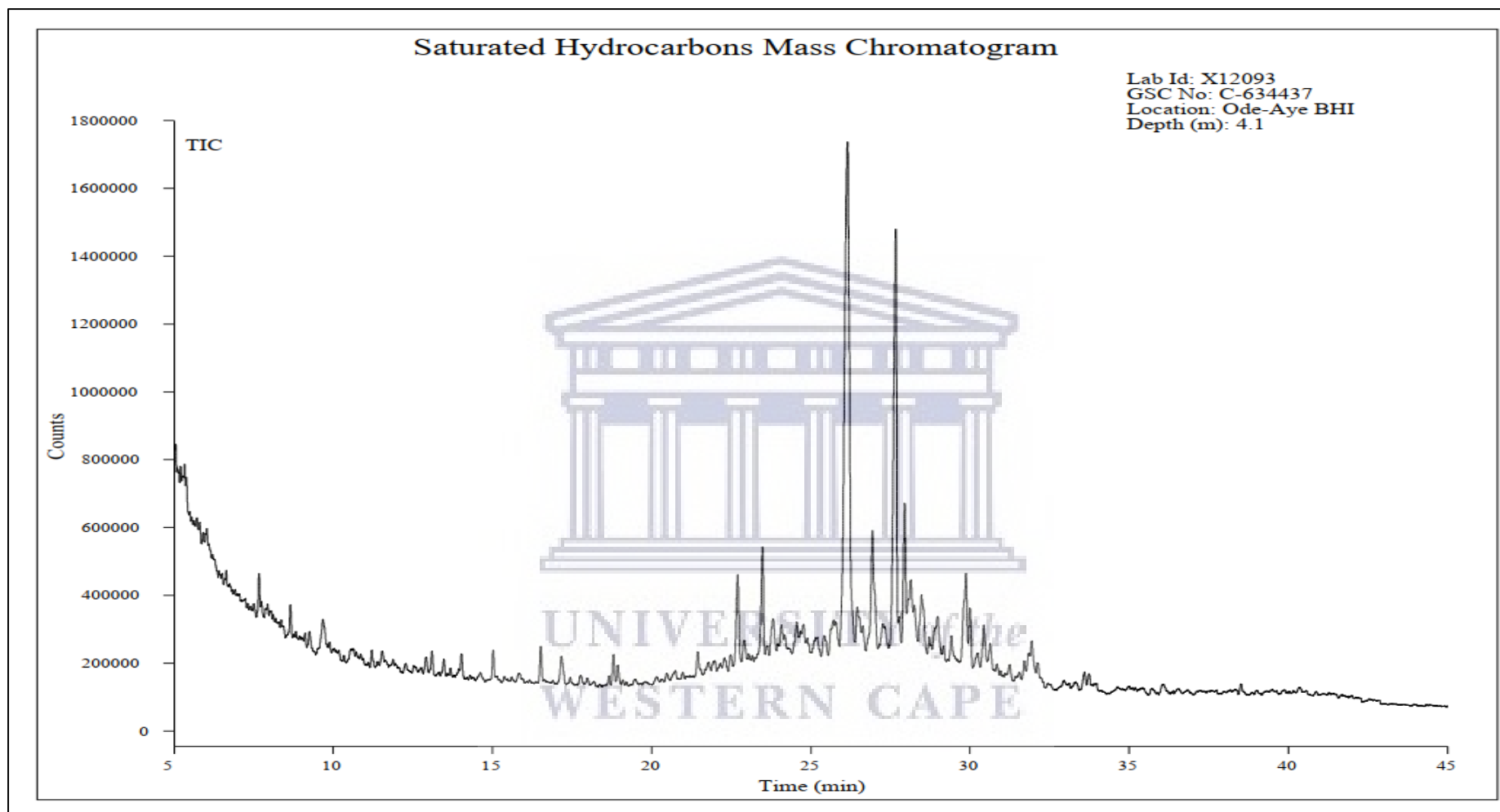*Figure 117: Mass chromatogram of m/z 191 for the saturate fraction of Ode-Aye oil sand at a depth of 1.0 m.*

*Figure 118: Mass chromatogram of m/z 217 for the saturate fraction of Ode-Aye oil sand at a depth of 1.0 m.*
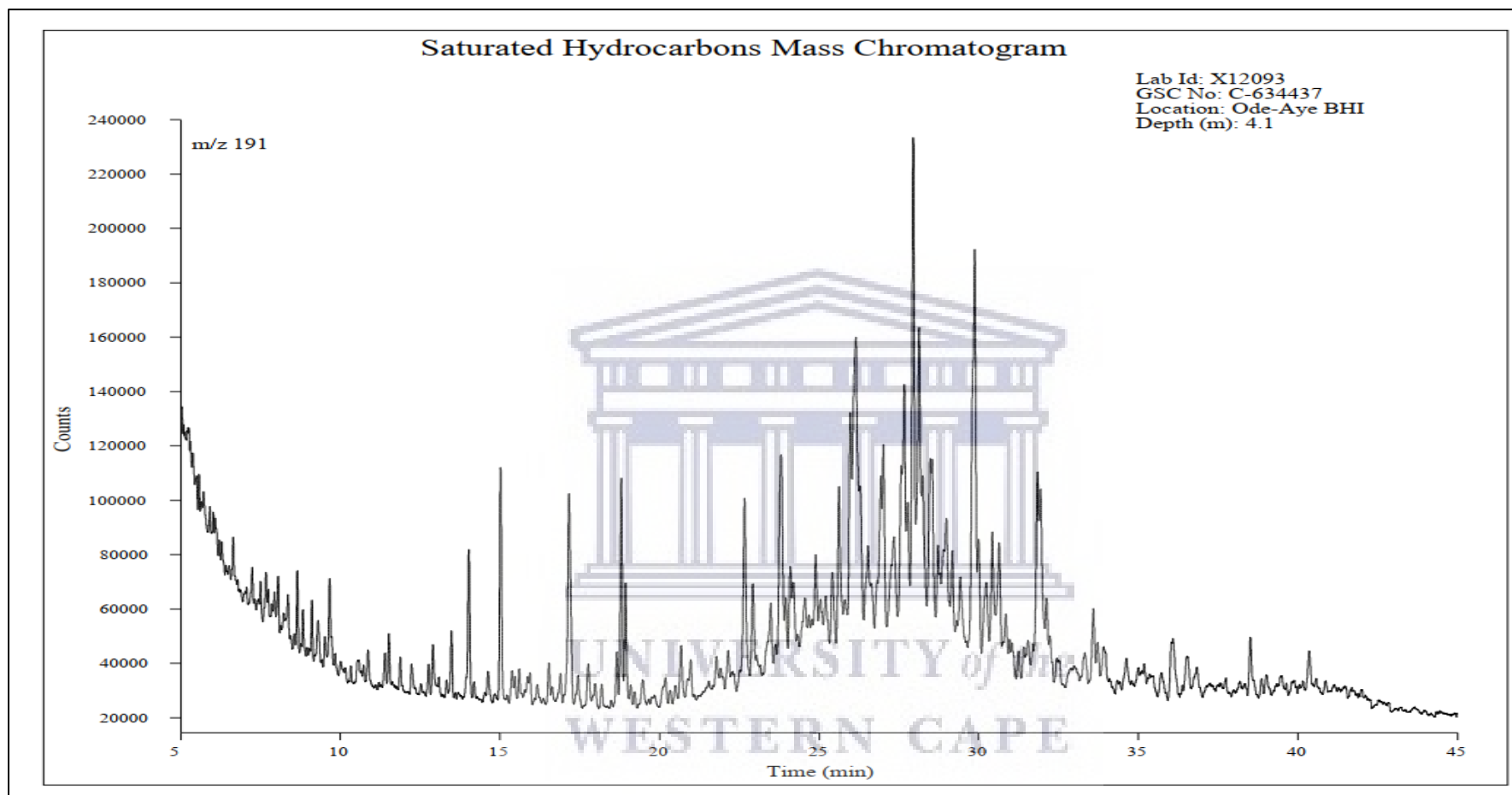
*Figure 119: Mass chromatogram of m/z 191 for the saturate fraction of Ode-Aye oil sand at a depth of 4.1 m.*
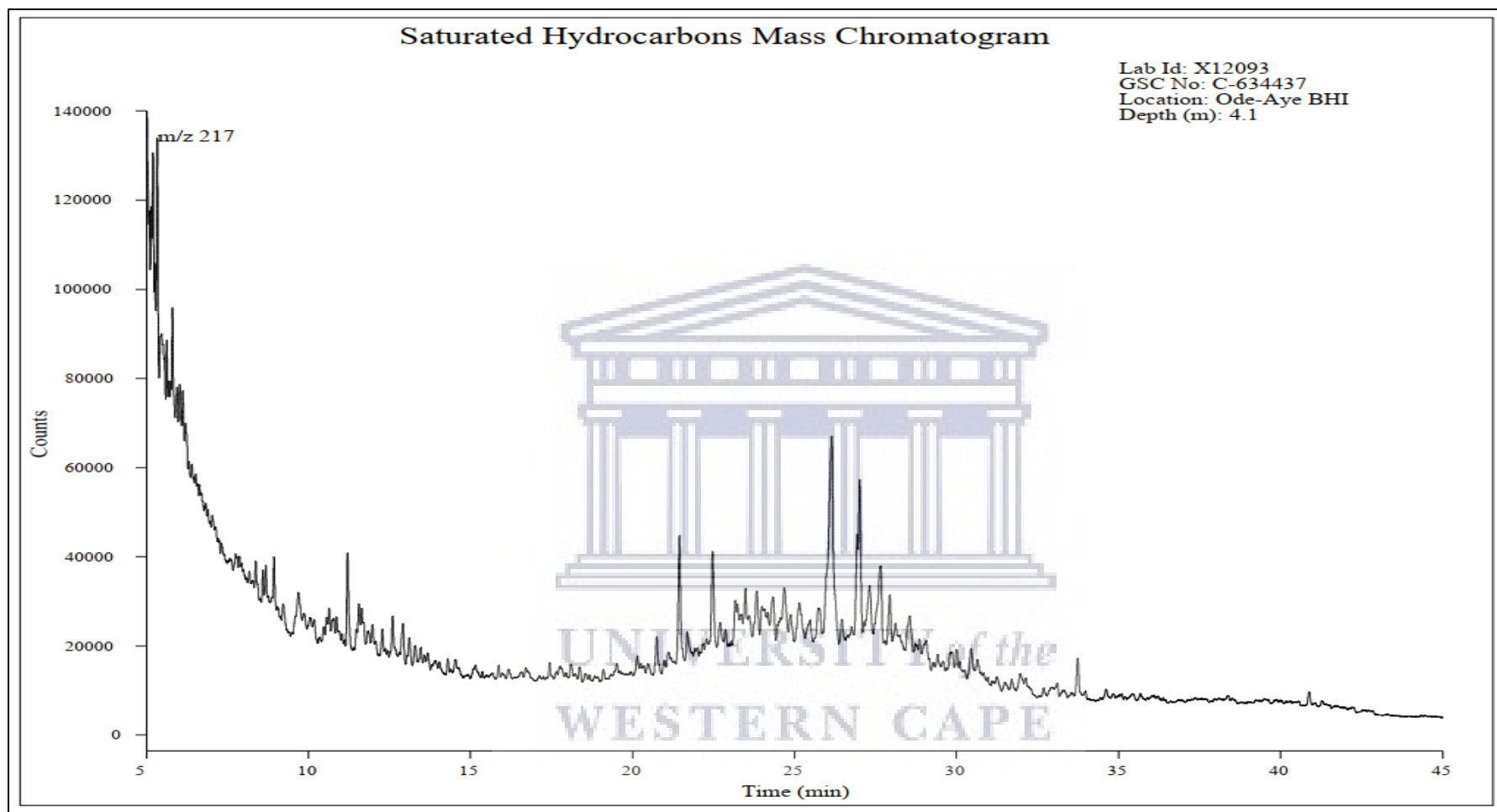
*Figure 120: Mass chromatogram of m/z 217 for the saturate fraction of Ode-Aye oil sand at a depth of 4.1 m.*
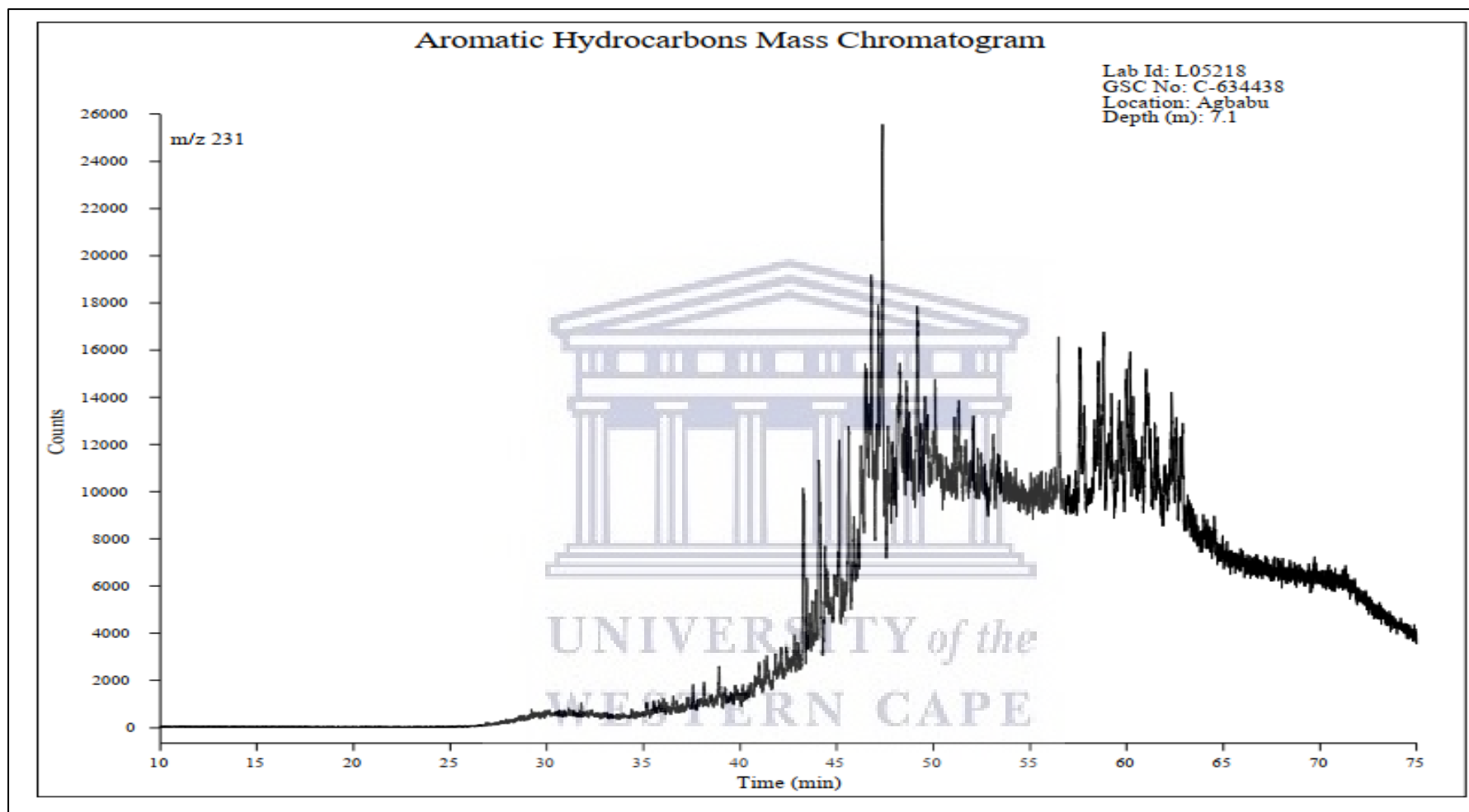
*Figure 121: Mass chromatogram of m/z 231 for the aromatic fraction of Agbabu heavy oil.*
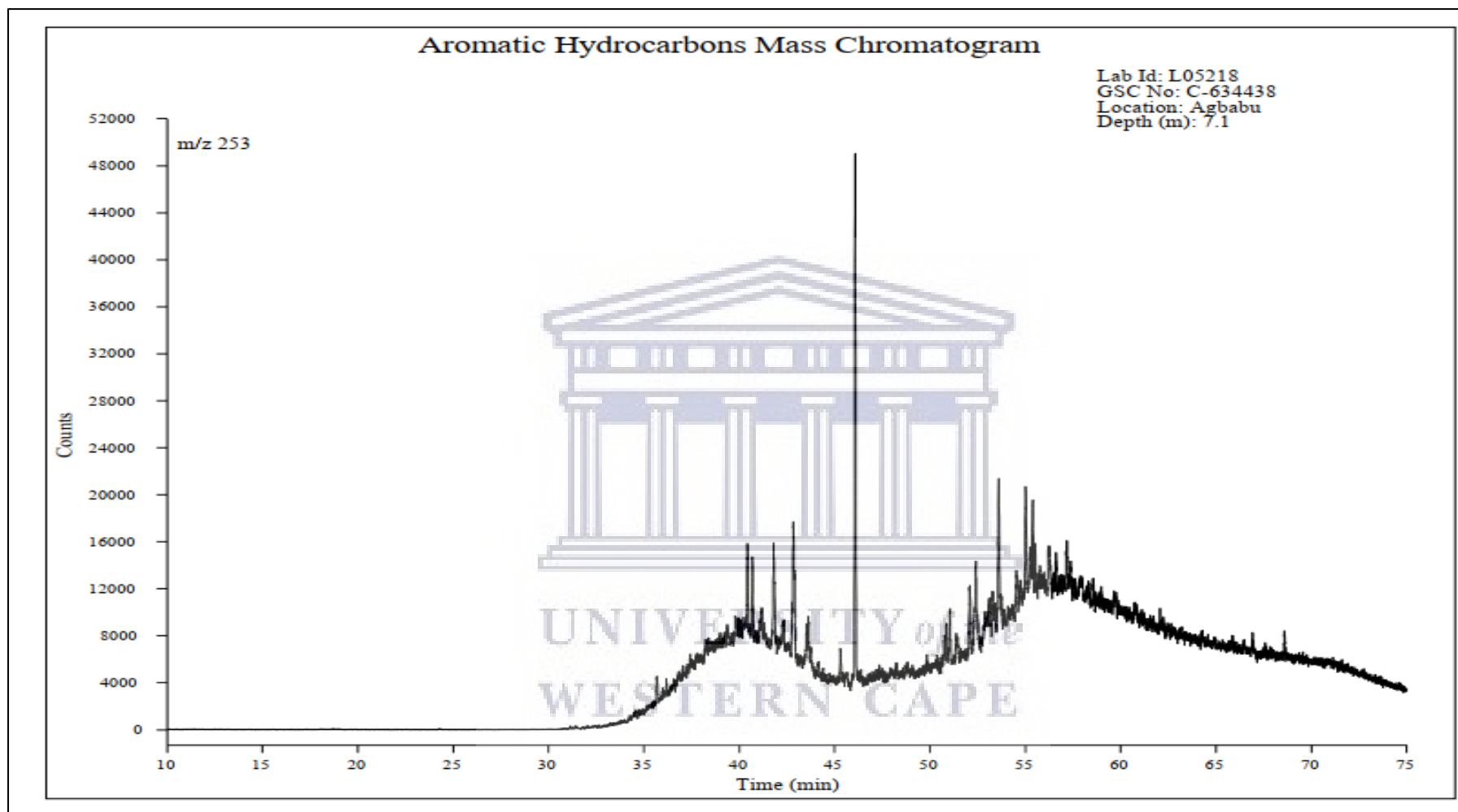
*Figure 122: Mass chromatogram of m/z 253 for the aromatic fraction of Agbabu heavy oil.*

216
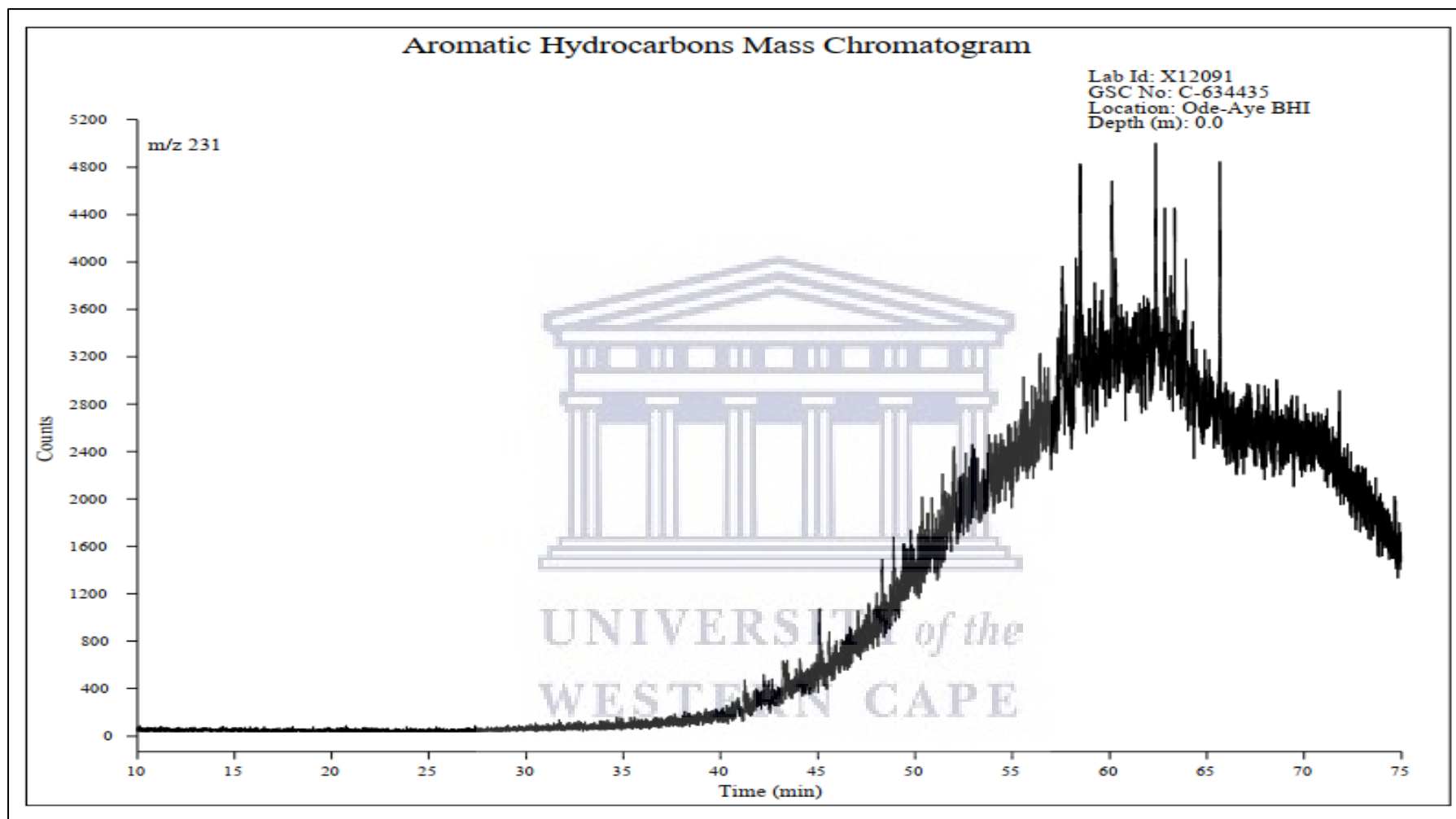
*Figure 123: Mass chromatogram of m/z 231 for the aromatic fraction of Ode-Aye oil sand at a depth of 0.0 m.*
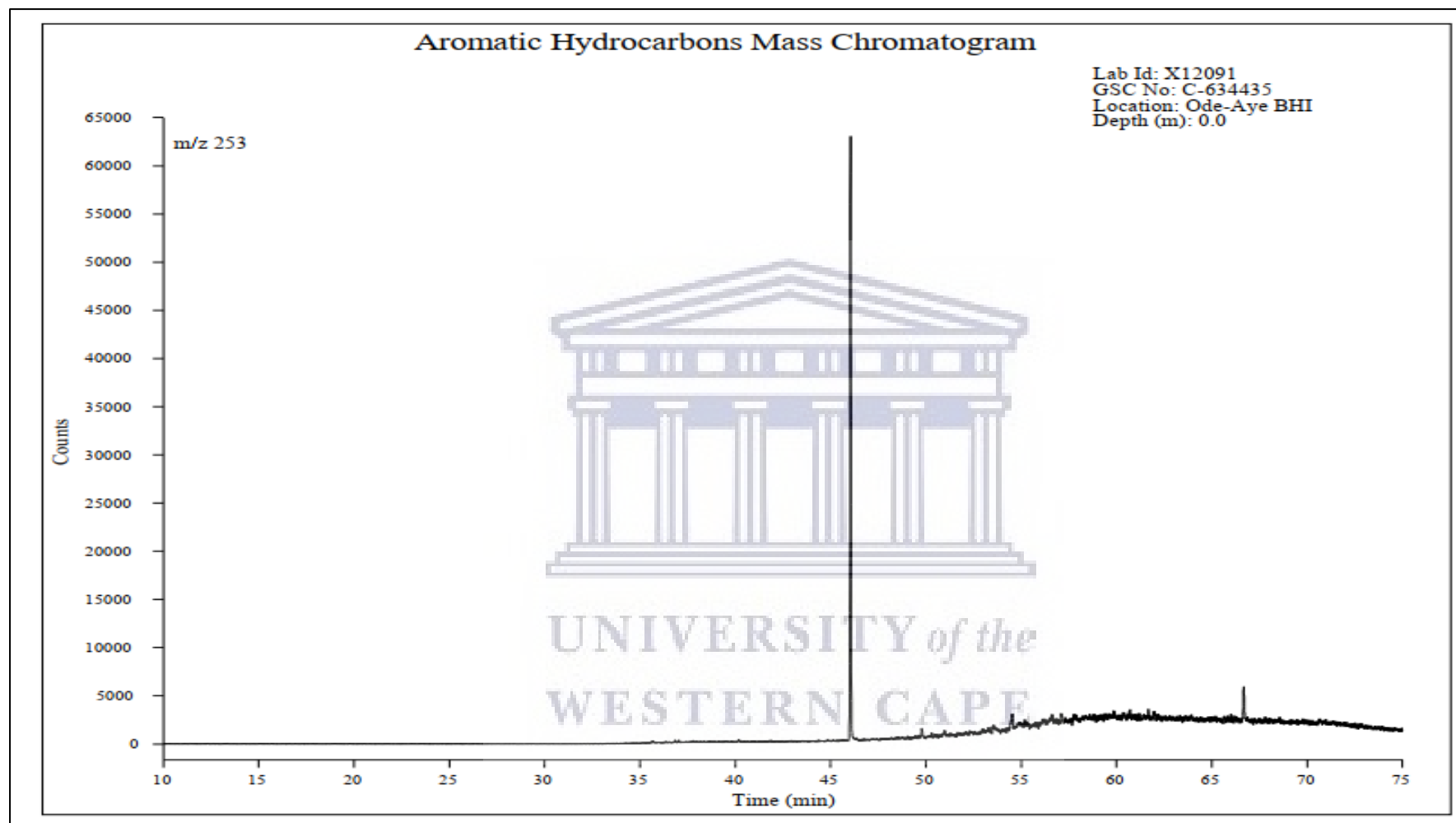
*Figure 124: Mass chromatogram of m/z 253 for the aromatic fraction of Ode-Aye oil sand at a depth of 0.0 m.*
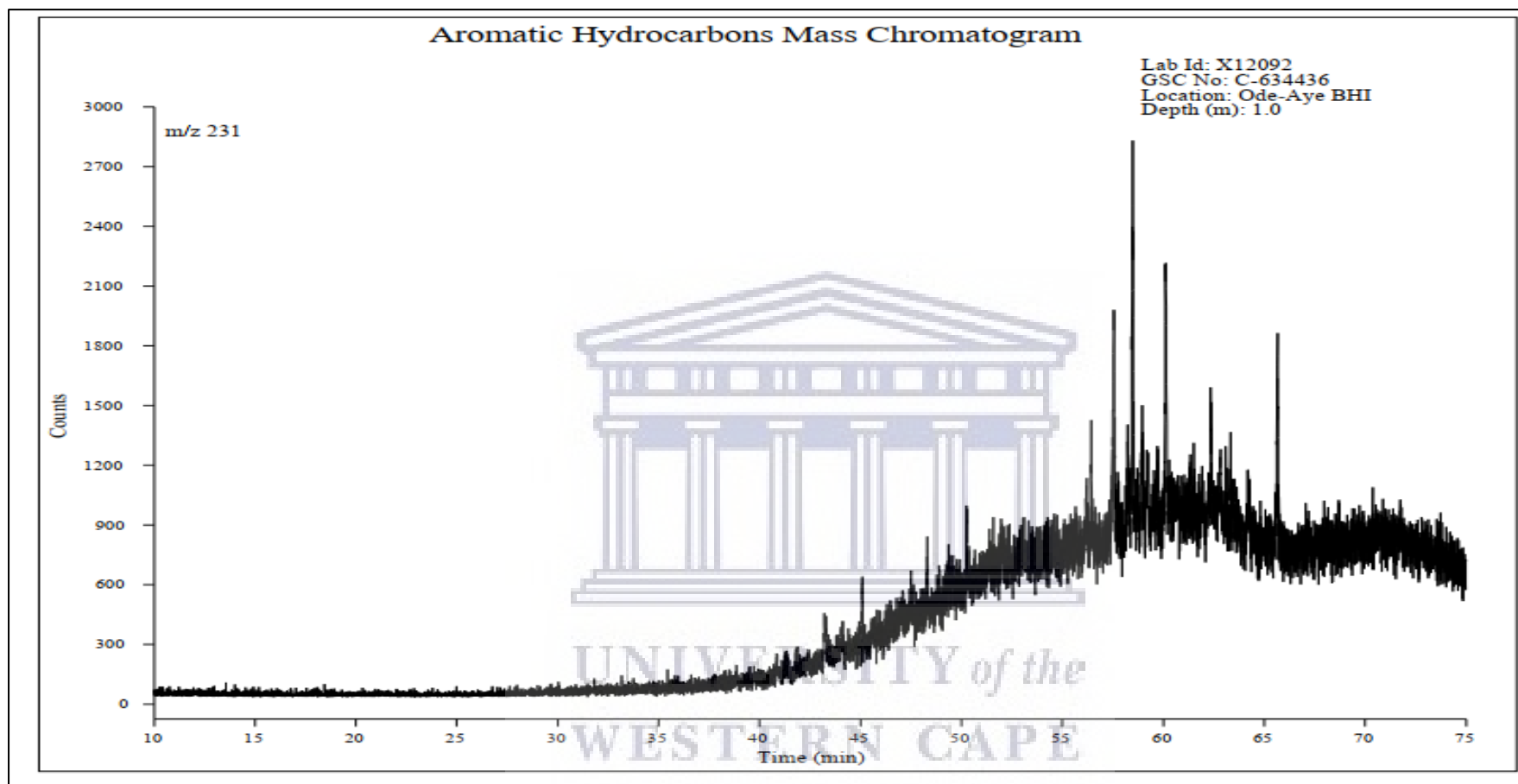
*Figure 125: Mass chromatogram of m/z 231 for the aromatic fraction of Ode-Aye oil sand at a depth of 1.0 m.*
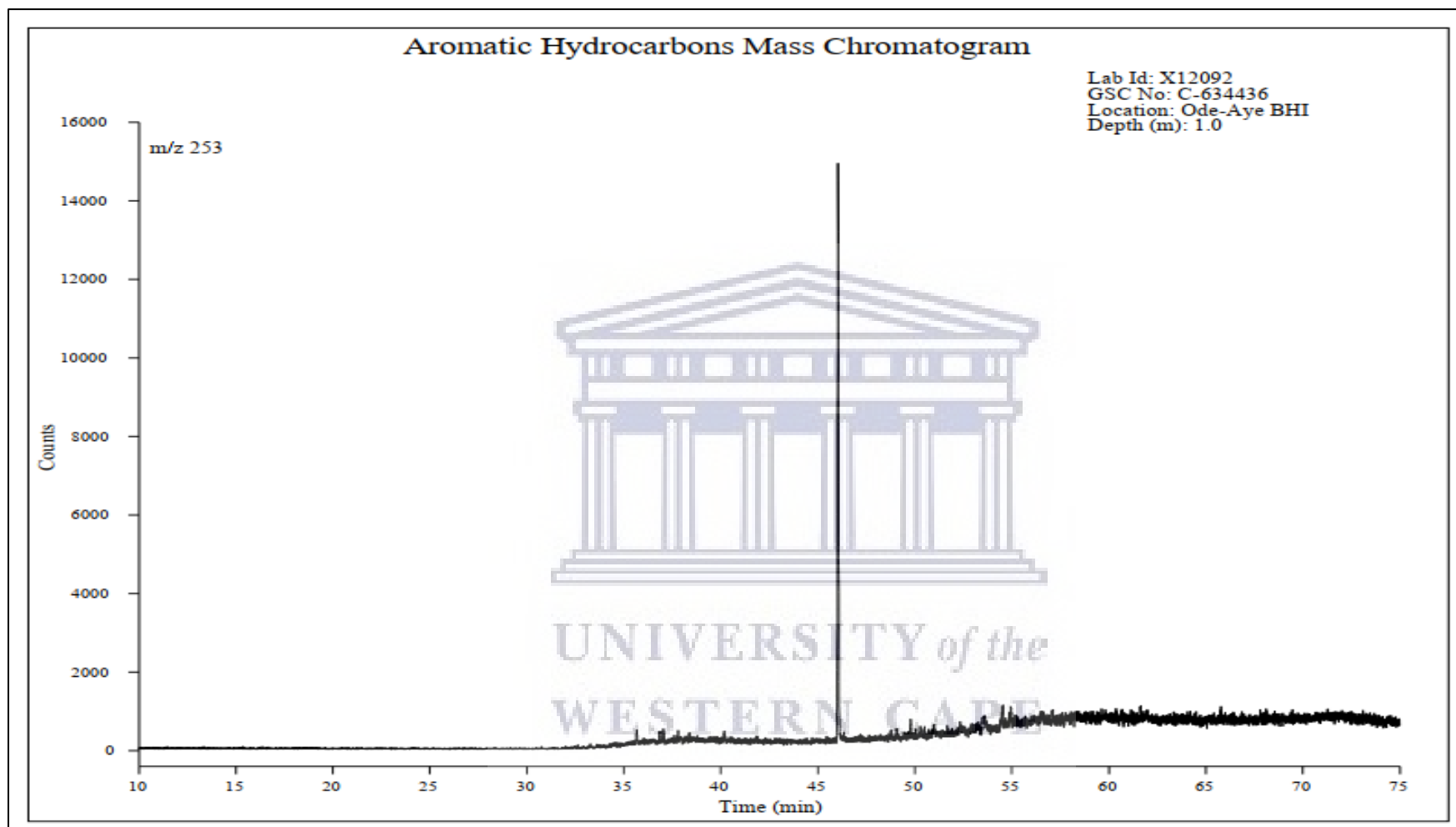
*Figure 126: Mass chromatogram of m/z 253 for the aromatic fraction of Ode-Aye oil sand at a depth of 1.0 m.*

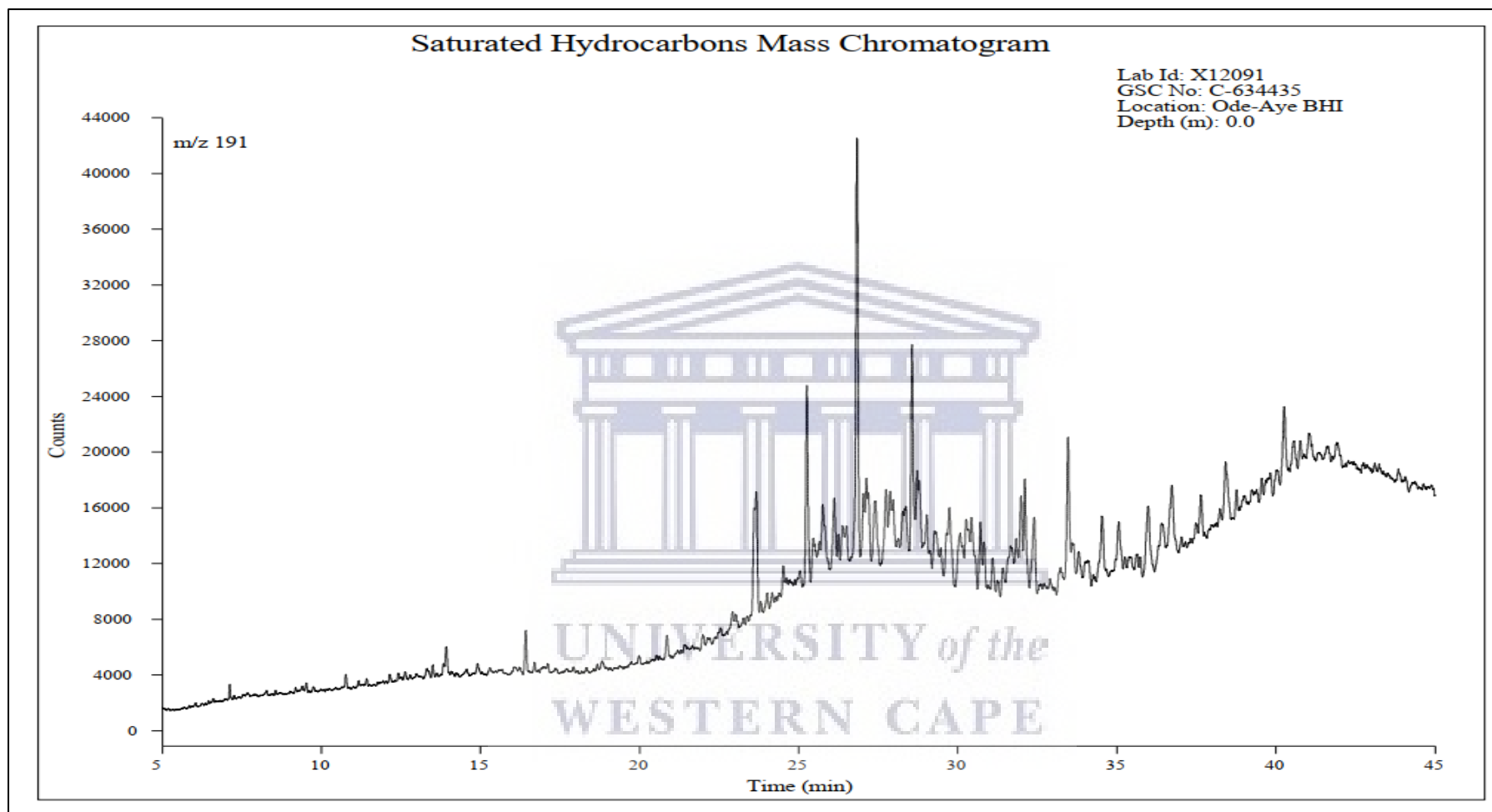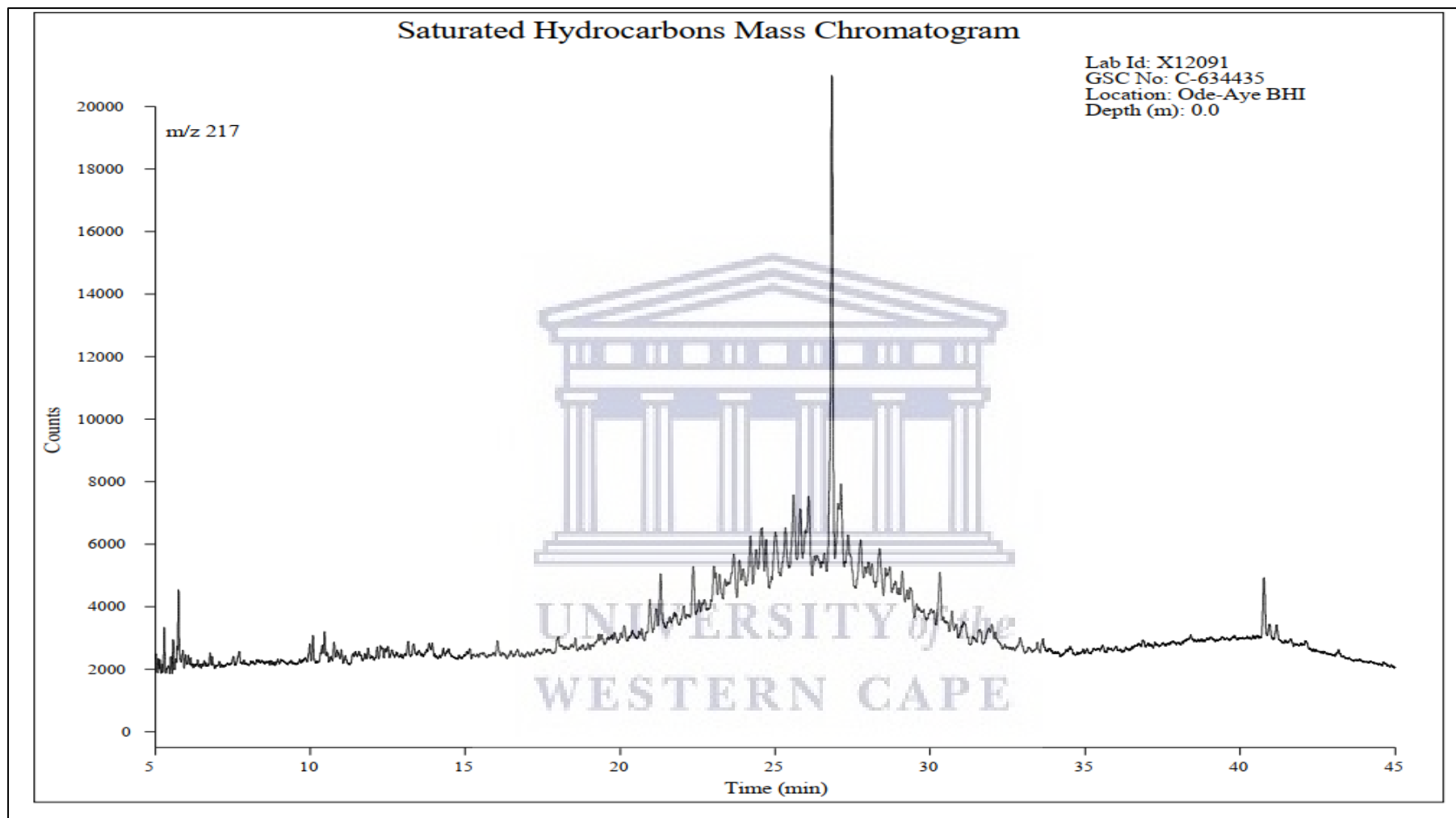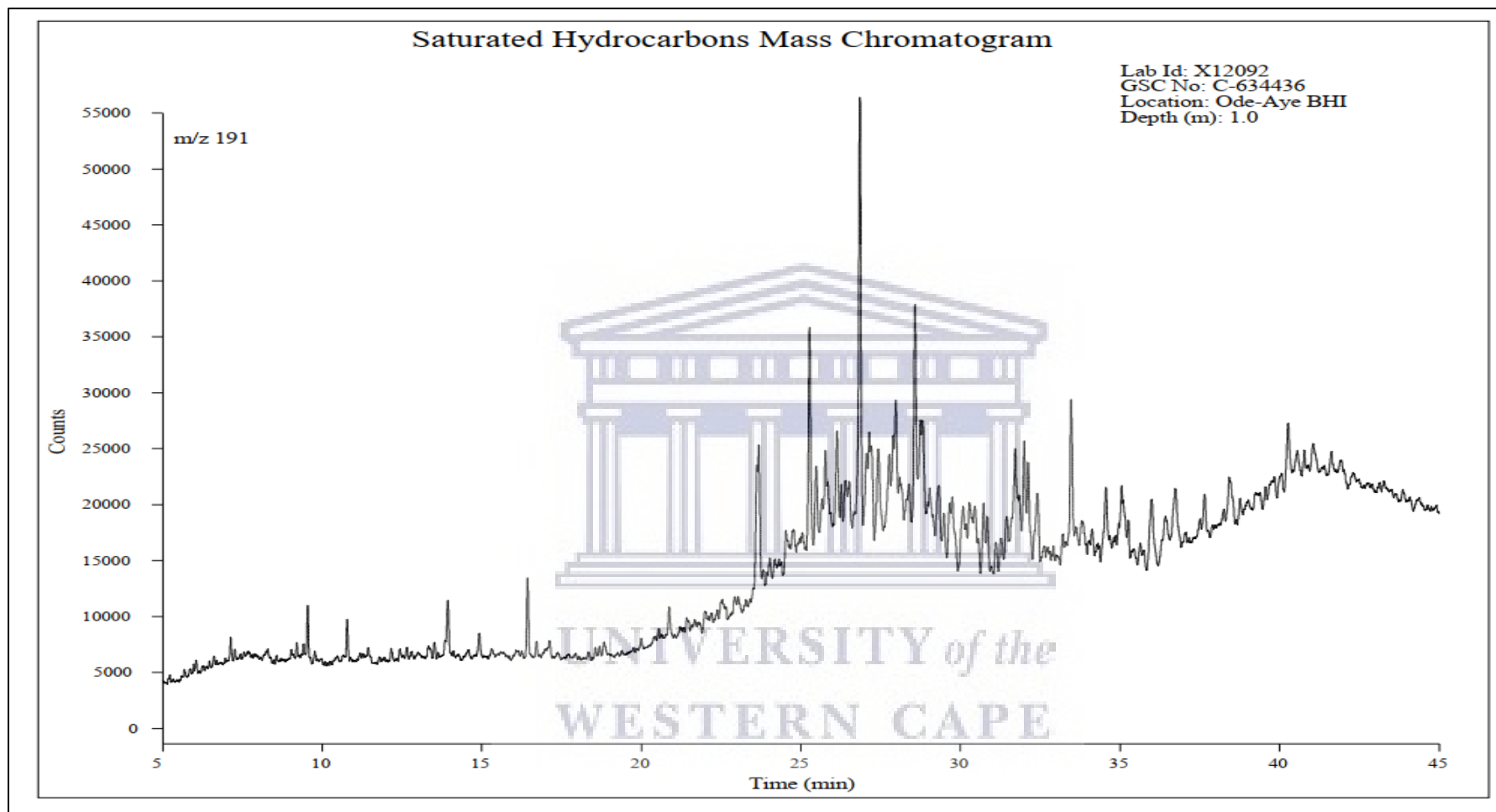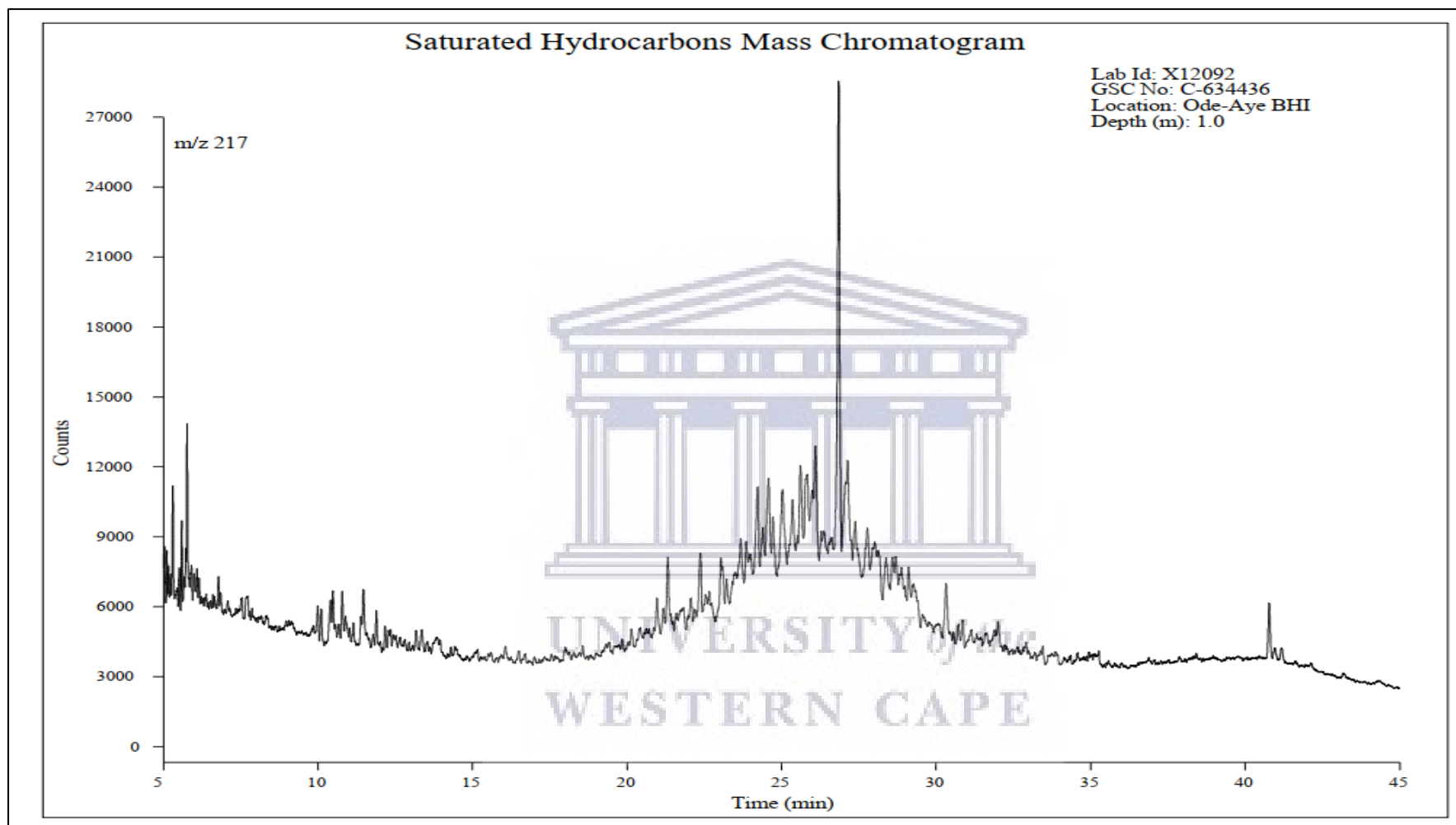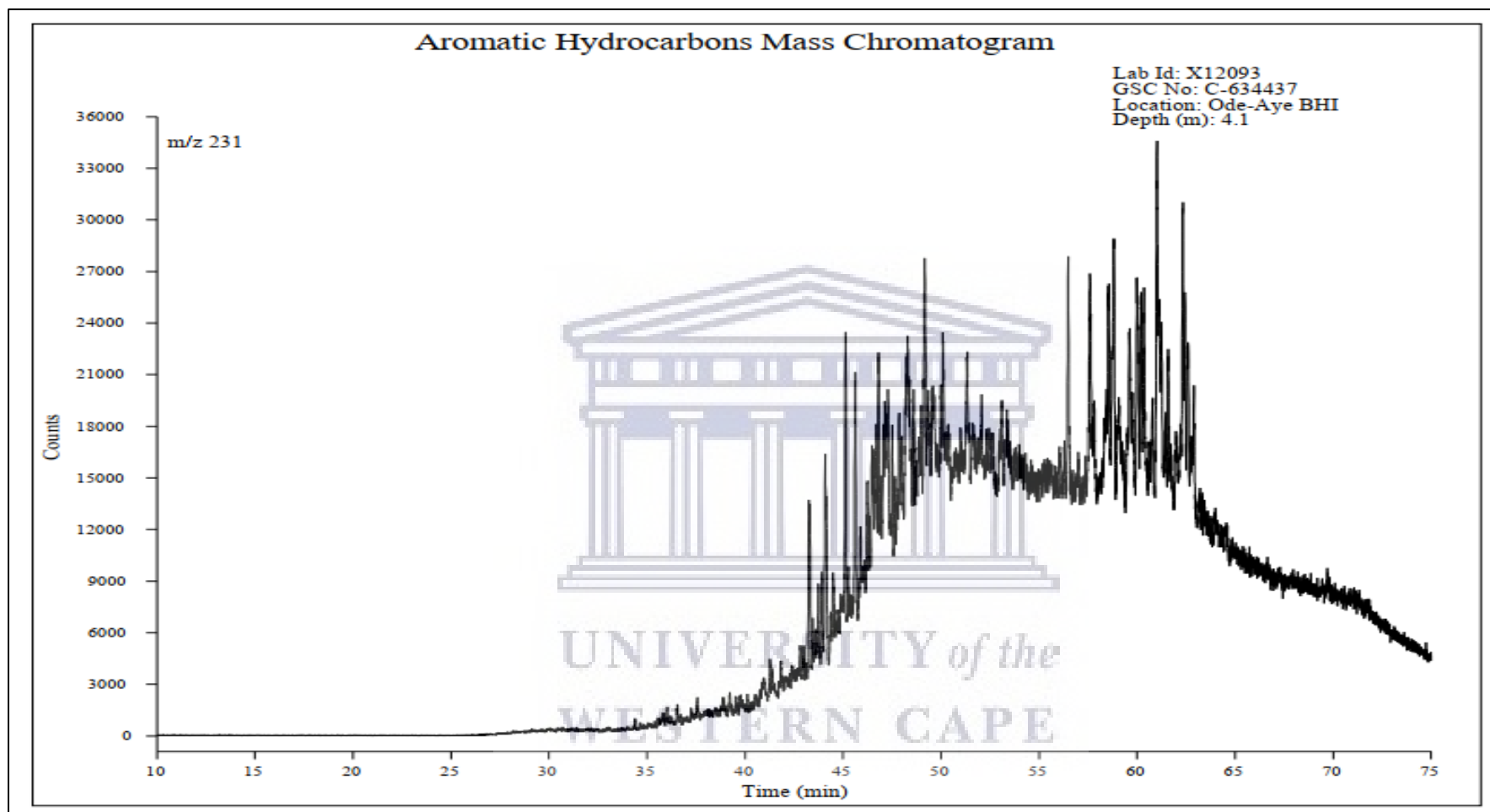*Figure 127: Mass chromatogram of m/z 231 for the aromatic fraction of Ode-Aye oil sand at a depth of 4.1 m.*
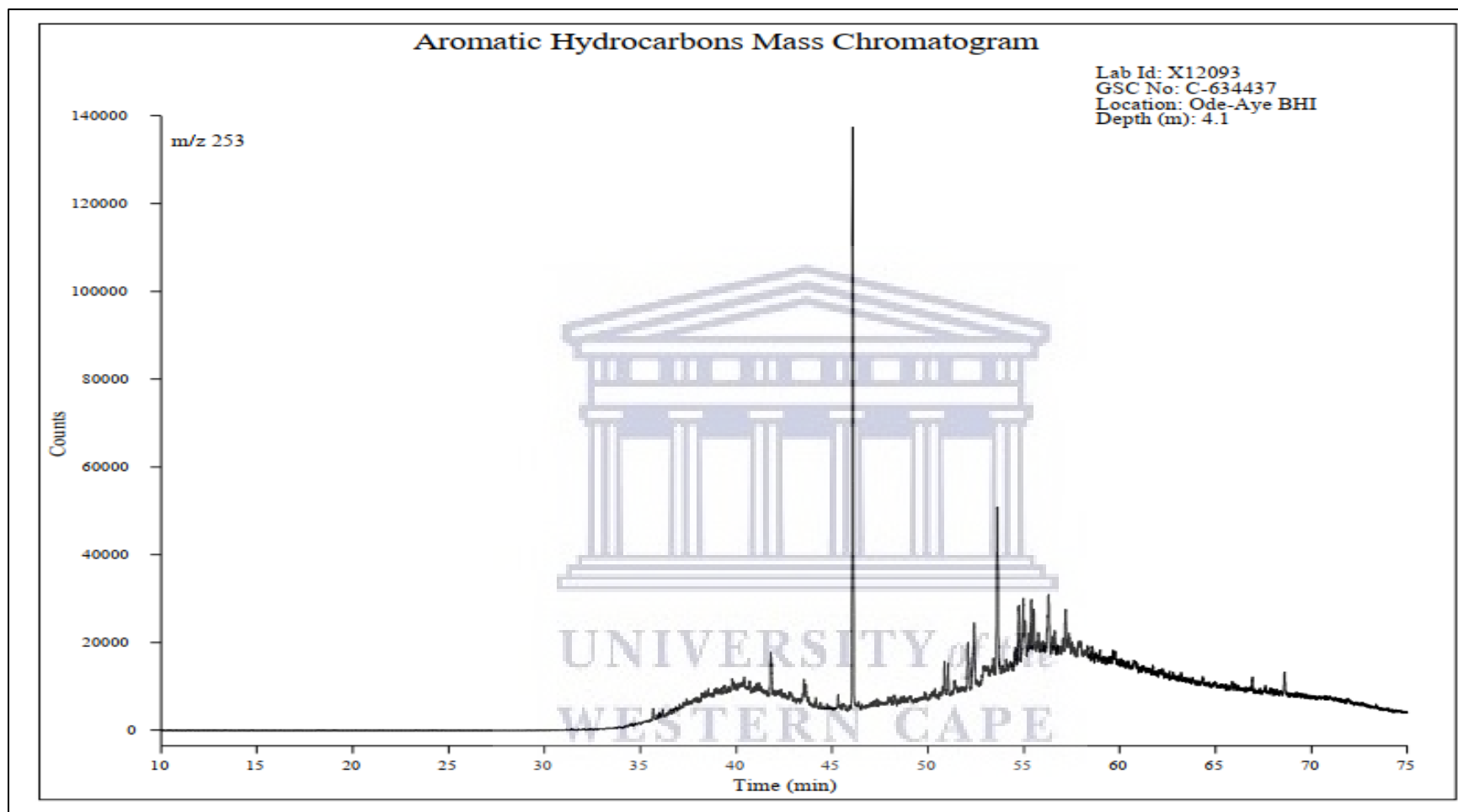
*Figure 128: Mass chromatogram of m/z 253 for the aromatic fraction of Ode-Aye oil sand at a depth of 4.1 m.*

The chemical composition of crude oils in the reservoirs may be significantly altered by processes such as biodegradation and water washing (Milner et al., 1977). Biodegradation of crude oil leads to a serial removal of n-alkanes (normal alkanes), isoprenoid, and other branched alkanes, and ultimately some cyclic alkanes (Bailey et al., 1973; Wardroper et al., 1984). Within a class of compounds, the lower molecular weight compounds are selectively depleted. As degradation progresses, saturated hydrocarbons outside of the initial range, as well as the phytane, and pristane are selectively removed, either by microbial degradation or by water washing (Palmer, 1983). The progressive decrease in the amount of resolved compounds usually occurs with an increase in the chromatographic baseline hump of the unresolved complex mixture (UCM). Based on the amounts of polar compounds and asphaltenes that are present initially in non-degraded petroleum, the UCM may account for nearly all to less than half of the total Mass of a highly degraded oil (Peters et al., 2005). The chromatograms (Figures 101 to 104) showed features consistent with severely biodegraded oils.

Biodegradation can be a stepwise process, and saturated and aromatic biomarkers are biodegraded only after depletion of n-alkanes, simple branched alkanes, and some of the alkylated benzenes (Moldowan et al., 1992; Seifert and Moldowan, 1979). The class of compounds that can be identified and quantified from ions 191, 217, 231, and 253 are resistant to biodegradation. The noisy chromatograms (Figures 113 – 128) and the absence of these compounds indicates that the oil sands and heavy oil are severely biodegraded. The severity of the degradation may have been accelerated by the combined effects of microbial action, water washing, low temperature, and salinity, an abundant supply of nutrients  (Head et al., 2003; Larter et al., 2006b; Mille et al., 1991) and their shallow depth of occurrence  (Alexander et al., 1983).

The oil sands and heavy oil evaluated in this study are found at shallow depths within the rain forest. The heavy seasonal rainfall appears to have contributed to the degradation of the crude oils.

# CHAPTER SEVEN

## CONCLUSION AND RECOMMENDATIONS

Petroleum has the source rock as its origin, and the viability of a petroleum system is hinged on the organic matter component of the source rock. The source rocks control the geography and distribution of both conventional and unconventional hydrocarbon plays. The hydrocarbon types that are generated by petroleum source rocks throughout its evolutionary pathway are influenced by the quantity/quality of organic matter and organic maturation temperature.

The Geochemical evaluation of the source rock potential of the Afowo Formation has been carried out to determine its hydrocarbon generating potential. The assessments made use of a multi-parameter method that incorporated rock-evaluation pyrolysis, organic petrography, thermogravimetric analysis, gas chromatography, and loss on ignition, and they provided comprehensive datasets for the evaluation. The multi-parameter approach required that more than one analytical method was used to appraise the source rocks to establish a high degree of confidence in the results. Prior studies to evaluate the hydrocarbon generating potential of the Afowo Formation in the Eastern Dahomey Basin relied chiefly on rock-evaluation pyrolysis alone.

Besides, the oil sands and heavy oil of the Eastern Dahomey Basin were characterized to assess their quality and possible origin. The characterization utilized several measurements that included the petroleum assessment method, carbon isotopes, crude oil assay, gas chromatography-mass spectrometry, thermal desorption-gas chromatography, inductively coupled plasma-mass spectrometry, ASTM and CHNS analysis. These analyses provided data that were used to determine the hydrocarbon composition, refining characteristics, metal content, API gravities, sulfur content, total acid number, viscosity, boiling point distribution, extent of biodegradation, and the

likelihood of mixed petroleum source beds. The results are envisioned to be used in the extraction, processing, refining of the oil sand, and heavy oil to diversify the economy and create jobs for the teeming population. Previous works were limited to the oil sands and did not include the heavy oil. Neither were they aimed at determining the quality of the oil sands with assessments to exploiting the resources.

The research adds to the body of knowledge and elucidate the geochemistry of the hydrocarbon resources of the Eastern Dahomey Basin (Dahomey Embayment). It is envisaged that the results of this research will serve as a guide on geochemical evaluations of the petroliferous Afowo Formation.

The novelty of this study dwells on primary data, a multi-parameter method to characterize and assess the hydrocarbon generating potential of the petroleum source rocks. Also, the oil sands and heavy oils were categorized using several techniques. The primary data included samples that were acquired from boreholes that were drilled in different parts of the basin as part of the research endeavor. It also comprised of outcrop samples of oil sands, source rock, and oil seeps that were acquired during the fieldwork. In addition, it comprised of the core samples that were provided by an agency of the Ministry of Solid Minerals, Federal Government of Nigeria, for which I am deeply grateful.

The overwhelming body of evidence from the source rock assessment suggests that the source rock that underlies the oil sands is rich in total organic carbon with the potential to generate oil and gas at higher maturation temperature. The organic matter types ranged from Type II to Type II/III and Type III. The Tmax for the source rocks sampled in this study are all below 435 $^{\circ}$C and the vitrinite reflectance are below 0.6 **%**$R_o$ with a dominance of liptinite maceral.

Multiple data from trace metal analysis and carbon isotopes indicated the possibilities of mixed petroleum source beds in the basin, implying that deeper reservoirs hold potential for oil and gas discoveries. The crude oils evaluated in this study may be products of a long distant migration, possibly along a zone of unconformity, fault plane, or from deeper reservoirs of poor cap rock integrity.

The highlights of the study include the following amongst others:

1) A multi-parameter method that included Rock-Eval Pyrolysis, Organic Petrography, Gas Chromatography-Mass Spectrometry, Thermogravimetric Analysis, and Loss on Ignition was used for source rock assessments. The results indicated an abundance of organic matter with liptinite macerals. These organic matters have not attained the thermal maturity to generate hydrocarbons. The hydrocarbons investigated in this study were, therefore, produced by other source rocks within the basin at deeper burial depths and higher maturation temperature.

2) Thermal Desorption- Gas Chromatography (TD-GC), Gas Chromatography (GC), and Gas Chromatography-Mass Spectrometry (GC-MS) results showed that the crude oils are severely biodegraded with missing lightweight molecular components and complete absence of pristane and phytane. It was not possible to identify and quantify both the saturated and aromatic biomarkers due to the extensive nature of the biodegradation.

3) The API gravities, total acid number, sulfur, and metal content, are consistent with biodegraded oils. It is envisaged that the data can be utilized for the extraction, processing, transportation, and refining of the oil sands and heavy oil.

4) The boiling point distribution data from the study indicated a dominance of

middle and heavy distillates. The Nigerian crude oil from the Niger Delta Basin is light, and the country currently imports heavy oils for blending purposes. The imperative is to exploit the Eastern Dahomey Basin's heavy crude oil to cut down on the imports of heavy oils, conserve foreign reserves, and create jobs.

5) Carbon Isotopes and Inductively Coupled Plasma-Mass Spectrometry data suggested that the oils were possibly generated from mixed petroleum source rocks. The oil sands and heavy oils were encountered at shallow depths and are biodegraded. Therefore, it can be inferred that deeper reservoirs represent better prospects for oil and gas discoveries in the Eastern Dahomey Basin.

## 7.1: RECOMMENDATIONS

The paradigm shifts to diversify the economy, increase petroleum reserves, and create jobs for the teeming population, requires that a comprehensive evaluation of the hydrocarbon resources of the Eastern Dahomey Basin be carried out. The scarcity of data drives the current estimates of reserves of about 58 billion of oil equivalent in the basin. Based on the results of this study, I recommend the following:

1) Acquire 3-dimensional seismic data to define structures and potential reservoirs to exploit.

2) It is recommended that some in-depth exploration wells with full suite logging are sited at oil sand outcrops and locations of heavy oil deposits; these wells should penetrate the basement rocks. For these wells, I recommend acquiring cores, mud logging, measurement-while-drilling, logging-while-drilling, wireline, and formation pressure data for comprehensive petrophysical and geochemical evaluation. A suite of spectral gamma-ray, density, neutron, caliper, resistivity,

image, sonic, and borehole seismic should be run in these wells. The borehole seismic data is needed for well to seismic tie and for reservoir studies. The data from these wells will assist in the interpretation of the surface seismic data, leading to successful exploration and field development.

3) A strong partnership with the indigenous communities should be established to avoid or minimize community unrest, such as the ones being experienced in the Niger Delta Basin. Decades of oil exploration and exploitation in the Niger Delta Basin have created a sense of apathy, tension, poverty, disturbances, oil spills, kidnapping, and destruction of infrastructures in the region. The communities can be stakeholders in the projects by which the members can be given employment, invest in the company's stocks, or some stocks allotted to their communities. Besides, there should be a functional corporate social responsibility to address fundamental issues such as potable drinking water, roads, and electricity. A seamless engagement with the chiefs, elders, and youth organizations of the communities is also recommended.

4) An environmental impact assessment should be carried out with clear guidelines and emphasis on ecology; these resources are found in the pristine rain forest where economic trees are grown, and farming is the indigenous people's dominant occupation.

5) Finally, drawing on my experience, research such as the current one should be funded. Efforts to secure funding from the government were not successful, and promises for funding were not kept leading to a severe drain of personal resources.

**REFERENCES**

Abrakasa, S., & Nwankwoala, H. O. (2019). Distribution of Some Diamondoids in
Crude Oils from Niger Delta Basin. *Petroleum and Chemical Industry
International*, *2*(2), 1–5. https://doi.org/10.33140/pcii.02.02.04

Adekeye, O.A., Akande, S.O, Adeoye, J. A. (2019). The assessment of potential
source rocks of Maastrichtian Araromi formation in Araromi and Gbekebo wells
Dahomey Basin, southwestern Nigeria. *Heliyon*, 1–9.
https://doi.org/10.1016/j.heliyon.2019.e01561

Akaegbobi, I.M., Nwachukwu, J.I., Schmitt, M. (2000). Aromatic hydrocarbon
distribution and calculation of oil and gas volumes in post-Santonian shale and
coal, Anambra Basin, Nigeria. *AAPG Memoir (American Association of
Petroleum Geologists)*, (73), 233–245.

Akande, S. O., Adekeye, O. A., Adeoye, J. A., Jacob, N., & Lufadeju, G. (2012).
Paleoecologic and organic geochemical assessment of Cretaceous hydrocarbon
source rocks in the Gulf of Guinea: new insights from eastern Dahomey and
Benue rift basins with implications for the Cenomanian – Coniacian petroleum
system. *AAPG Bulletin (American Association of Petroleum Geologists)*.

Akinlua, A., Torto, N., Ajayi, T. R., & Oyekunle, J. A. O. (2007). Trace metals
characterisation of Niger delta kerogens. *Fuel*, *86*(10–11), 1358–1364.

Akinmosin, A., Omosanya, K.O; Olawole, A.O. (2015). Hydrocarbon Potential of
Some Afowo Shale Deposits in Part of South Western Nigeria. *International
Journal of African and Asian Studies*, *11*, 1–22.

Akinmosin, A.A., Omosanya, K.O., Ige, T. (2013). The occurence of Tar Sands at

Ijebu-Itele, Eastern Dahomey Basin, SW, Nigeria. *ARPN Journal of Science and Technology*, *3 (1)*, 98–105.

Al-Selwi, A.; Joshi, M. (2015). Source Rock Evaluation using Total Organic Carbon (TOC) and the Loss- On-Ignition (LOI) Techniques. *Oil & Gas Research*, *1*(1), 1–5. https://doi.org/10.4172/2472-0518.1000105

Alexander, R., Kagi, R. I., Woodhouse, G. W., & Volkman, J. K. (1983). Geochemistry of Some Biodegraded Australian Oils. *Australian Petroleum Exploration Association*, *23*(1), 53–63. https://doi.org/10.1071/aj82006

Amigun, J. O., Adelusi, A. O., & Ako, B. D. (2012). The application of integrated geophysical methods in oil sand exploration in Agbabu area of Southwestern. *International Research Journal of Geology and Mining*, *2*(November), 243–253.

ASTM. (2009). *ASTM D70-09, Standard Test Method for Density of Semi-Solid Bituminous Materials (Pycnometer Method)*. ASTM International West Conshohocken, PA.

ASTM. (2010). *ASTM D5291: standard test methods for instrumental determination of carbon, hydrogen and nitrogen in petroleum products and lubricants*.

ASTM. (2011a). *ASTM D7169-2011. Standard test method for boiling point distribution of samples with residues such as crude oils and atmospheric and vacuum residues by high temperature gas chromatography*. ASTM International West Conshohocken, PA.

ASTM. (2011b). Standard TEST method for water in crude oils by potentiometric Karl Fischer titration. *Annual Book of ASTM Standards*, *5*.

Austrich, A. J., Buenrostro-Gonzalez, E., & Lira-Galeana, C. (2015). ASTM D-5307

and ASTM D-7169 SIMDIS standards: A comparison and correlation of methods. *Petroleum Science and Technology*, *33*(6), 657–663. https://doi.org/10.1080/10916466.2015.1004345

Bailey, N. J. L., Jobson, A. M., & Rogers, M. A. (1973). Bacterial degradation of crude oil: comparison of field and experimental data. *Chemical Geology*, *11*(3), 203–221.

Bailey, N. J. L., Krouse, H. R., Evans, C. R., & Rogers, M. A. (1973). Alteration of crude oil by waters and bacteria—evidence from geochemical and isotope studies. *AAPG Bulletin*, *57*(7), 1276–1290.

Barker, C. (1974). Pyrolysis techniques for Source-Rock Evaluation. *AAPG Bulletin (American Association of Petroleum Geologists), 58*(11), 2349–2361.

Barker, C. E., & Pawlewicz, M. J. (1993). An empirical determination of the minimum number of measurements needed to estimate the mean random vitrinite reflectance of disseminated organic matter. *Organic Geochemistry*, *20*(6), 643–651.

Bertrand, R. (1993). Standardization of solid bitumen reflectance to vitrinite in some Paleozoic sequences of Canada. *Energy Sources*, *15*, 269–288.

Billman, H.G. (1992). Offshore Stratigraphy and Paleontology of the Dahomey Embayment, West African. *Nigerian Association of Petroleum Explorationists Bulletin*, *7*(2), 121–130.

Boduszynski, M. M. (1987). Composition of heavy petroleums. 1. Molecular weight, hydrogen deficiency, and heteroatom concentration as a function of atmospheric equivalent boiling point up to 1400. degree. F (760. degree. C). *Energy & Fuels*,

*1*(1), 2–11.

Bostick, N. H. (1979). *Microscopic measurement of the level of catagenesis of solid organic matter in sedimentary rocks to aid exploration for petroleum and to determine former burial temperatures—a review*.

Bray, E. E., & Evans, E. D. (1965). Hydrocarbons in non-reservoir-rock source beds. *AAPG Bulletin*, *49*(3), 248–257.

Brongersma-Sanders, M., & others. (1951). On conditions favouring the preservation of chlorophyll in marine sediments. *3rd World Petroleum Congress*.

Brooks, J. D., Gould, K., & Smith, J. W. (1969). Isoprenoid hydrocarbons in coal and petroleum. *Nature*, Vol. 222, pp. 257–259. https://doi.org/10.1038/222257a0

Brownfield, M. . E., & Charpentier, R. E. (2006). Geology and total petroleum systems of the Gulf of Guinea Province of West Africa. *USGS Bulletin*, 32. Retrieved from http://pubs.usgs.gov/bul/2207/C/

Brunnock J. V., Duckworth D. F., S. G. G. (1968). Analysis of beach pollutants. *J. Inst. Petrol*, *54*, 310–325.

Carvajal-Ortiz, H., Gentzis, T. (2015). Critical considerations when assessing hydrocarbon plays using Rock-Eval pyrolysis and organic petrology data: data quality revisited. *International Journal of Coal Geology*, *152*, 113-122.

Chappe, B., Albrecht, P., & Michaelis, W. (1982). Polar lipids of archaebacteria in sediments and petroleums. *Science*, *217*(4554), 65–66. https://doi.org/10.1126/science.217.4554.65

Chung, H. M., Rooney, M. A., Toon, M. B., & Claypool, G. E. (1992). Carbon isotope composition of marine crude oils. *AAPG Bulletin*, *76*(7), 1000–1007.

Clifford, A. C. (1986). Africa oil - past, present, and future. *AAPG Memoir (American Association of Petroleum Geologists)*, *40*, 339–372.

Coker, S. J. L. (2002). *Field excursion guide to tar sand outcrops.* Nigerian Association of Petroleum Explorationists.

Coker, S.J., Ejedawe, J.E. and Oshiorienua, J. A. (1983). Hydrocarbon source potentials of Cretaceous rocks of Okitipupa Uplift, Nigeria. *Nigeria Journal of Mining and Geology*, *22*, 163–169.

Connan, J. (1984). Biodegradation of crude oils in reservoirs. In *Advances in petroleum geochemistry* (J. Brooks, Vol. 1, pp. 229–335). London: Academy Press.

Constantinides, G., Arich, G., & Lomi, C. (1959). Detection and behavior of porphyrin aggregates in petroleum residues and bitumens. *Proc. 5th World Petrol. Cong., SCc*, 131–142.

Cook, A. C., & Sherwood, N. R. (1991). Classification of oil shales, coals and other organic-rich rocks. *Organic Geochemistry*, *17*(2), 211–222.

Corcoran, D. V, & Doré, A. G. (2005). A review of techniques for the estimation of magnitude and timing of exhumation in offshore basins. *Earth-Science Reviews*, *72*(3–4), 129–168.

Coursey, D. G. Hubbard, F. H., Hitch, L. S. and F. I. of I. R. (1963). *Preliminary observations on the tar sand deposits of Western Nigeria* (p. 3). p. 3. Federal Ministry of Commerce and Industry.

Craig, H. (1957). Isotopic standards for carbon and oxygen and correction factors for mass-spectrometric analysis of carbon dioxide. *Geochimica et Cosmochimica*

*Acta*, *12*(1–2), 133–149.

Crocket, L. O., & Wescott, B. C. (1954). Asphalt samples from West Africa. *Extract from Report*, Vol. 17617, pp. 1–6.

Curiale, J. A. (1984). Distribution and Occurrence of Metals in Heavy Crude Oils and Solid Bitumens — Implications for Petroleum Exploration. In R. F. Meyer (Ed.), *AAPG Studies in Geology #25* (pp. 207–219). Santa Maria, California: AAPG.

Curtis, C., Kopper, R., Decoster, E., Guzmán-Garcia, A., Huggins, C., Knauer, L., … Waite, M. (2002). Heavy-oil reservoirs. *Oilfield Review*, *14*(3), 30-51+70.

d'Almeida, G. A. F., Kaki, C., & Adeoye, J. A. (2016). Benin and Western Nigeria Offshore Basins: A Stratigraphic Nomenclature Comparison. *International Journal of Geosciences*, *07*(02), 177–188. https://doi.org/10.4236/ijg.2016.72014

Daly, A.R., Edman, J. D. (1987). Loss of organic carbon from source rocks during thermal maturation. *American Association of Petroleum Geologists*, (71), 546.

Davis S. J. and Gibbs C. F. (1975). The effect of weathering on a crude oil residue exposed at sea. *Water Research*, *9*(3), 275–285.

Dembicki, H. (2009). Three common source rock evaluation errors made by geologists during prospect or play appraisals. *AAPG Bulletin*, *93*(3), 341–356. https://doi.org/10.1306/10230808076

Dembicki, H. J. (2017). *Practical Petroleum Geochemistry for Exploration and Production*. Elsevier.

Deroo, G., Tissot, B., McCrossan, R. G., & Der, F. (1974). *Geochemistry of the Heavy Oils of Alberta. 3*(1974), 148–167. Can Soc of Pet Geol.

Didyk, B. M., Simoneit, B. R. T., Brassell, S. C. t, & Eglinton, G. (1978). Organic geochemical indicators of palaeoenvironmental conditions of sedimentation. *Nature*, *272*(5650), 216–222.

Drozdova, T. V, & Gorskiy, Y. N. (1972). Conditions of preservation of chlorophyll, pheophytin and humic matter in Black Sea sediments. *Geokhimiya*, *3*, 323–334.

Durham, K. N., & Pickett, C. R. (1966). Oil Mining Lease 47, Lekki Corehole Programm, Rep. *Tennessee Nigeria Inc*.

Elueze, A.A., Nton, M. E. (2004). Organic geochemical appraisal of limestone and shales in part of eastern Dahomey Basin, southwestern Nigeria. *Nigeria Journal of Mining and Geology*, *40 (1)*, 29–40.

Emery, K. O., & Uchupi, E. (2012). *The geology of the Atlantic Ocean*. Springer Science & Business Media.

Emmanuel, E., & Ajibade, O. M. (2014). Elemental composition and geochemistry of heavy oil in parts of eastern Dahomey Basin, southwestern Nigeria. *Journal of Environment and Earth Science*, *4*(12), 18–23.

Enu, E.I. (1987). The paleoenvironment of deposition of Late Maastrichtian to Paleocene black shales in the eastern Dahomey Basin. *Geol. Mijnbouw*, *66*, 15–20.

Enu, E. I. (1985). Textural characteristic of the Nigerian Tar Sands. *Sedimentary Geology*, *44*, 65–81.

Enu, E. I. (1990). Nature and occurrence of tar sands in Nigeria. In Ako, B.D. and Enu, E.I. (Ed.), *Occurrence, utilization and economics of tar sands*. Nigeria Mining and Geosciences Society.

Erickson, R. L., Myers, A. T., Horr, C. A. (1954). Association of uranium and other metals with crude oil, asphalt, and petroliferous rock. *AAPG Bulletin (American Association of Petroleum Geologists)*, *38*(10), 2211–2218.

Espitalie, J., Madec, M., Tissot, B. (1980). Role of mineral matrix in kerogen pyrolysis: Influence on petroleum generation and migration. *AAPG Bulletin (American Association of Petroleum Geologists)*, *64*, 59–66.

Espitalie, J., Marquis, F., Barsony, I. (1984). *Geochemical logging- Analytical Pyrolysis - Techniques and Applications*. Butterworth, Boston: Voorhees, K.J.

Espitalié, J. (1986). Use of Tmax as a maturation index for different types of organic matter: comparison with vitrinite reflectance. *Collection Colloques et Séminaires-Institut Français Du Pétrole*, (44), 475–496.

Espitalié, J., Deroo, G., & Marquis, F. (1985). La pyrolyse Rock-Eval et ses applications. Deuxième partie. *Revue de l'Institut Français Du Pétrole*, *40*(6), 755–784.

Espitalie, J., Madec, M., Tissot, B., Mennig, J. J., & Leplat, P. (1977). Source rock characterization method for petroleum exploration. *Proceedings of the Annual Offshore Technology Conference*. https://doi.org/10.4043/2935-ms

Fabianńska, M. J., Bzowska, G., Matuszewska, A., Racka, M., & Skr\ket, U. (2003). Gas chromatography-mass spectrometry in geochemical investigation of organic matter of the Grodziec beds (Upper Carboniferous), Upper Silesian coal basin, Poland. *Geochemistry*, *63*(1), 63–91.

Faboya, O. L., Sonibare, O. O., Liao, Z., Ekundayo, O., & Tian, Y. (2015). Oil-source Rock Correlation and Distributions of Pyrrolic Nitrogen Compounds in Oils from

the Niger Delta, Nigeria. *Petroleum Science and Technology*, *33*(11), 1253–1266. https://doi.org/10.1080/10916466.2015.1050505

Farrington, J. W., & Quinn, J. G. (2015). "Unresolved Complex Mixture" (UCM): A brief history of the term and moving beyond it. *Marine Pollution Bulletin*, *96*(1–2), 29–31. https://doi.org/10.1016/j.marpolbul.2015.04.039

Filby, R. (1975). The nature of metals in petroleum. In *The Role of Trace Elements in Petroleum.* (Yen, T.F., pp. 31–58). Ann Arbor: Ann Arbor Science Publishers Inc.

Fuex, A. N. (1977). The use of stable carbon isotopes in hydrocarbon exploration. *Journal of Geochemical Exploration*, *7*, 155–188.

Goossens, H. d, De Leeuw, J. W., Schenck, P. A., & Brassell, S. C. (1984). Tocopherols as likely precursors of pristane in ancient sediments and crude oils. *Nature*, *312*(5993), 440–442.

Gorham, E., & Sanger, J. (1967). Plant pigments in woodland soils. *Ecology*, *48*(2), 306–308.

Hackley, P. C., Araujo, C. V., Borrego, A. G., Bouzinos, A., Cardott, B. J., Cook, A. C., … Valentine, B. J. (2015). Standardization of reflectance measurements in dispersed organic matter: Results of an exercise to improve interlaboratory agreement. *Marine and Petroleum Geology*, *59*, 22–34. https://doi.org/10.1016/j.marpetgeo.2014.07.015

Hackley, P. C., Araujo, C. V, Borrego, Á. G., Cardott, B. J., Cook, A. C., Hámor-Vidó, M., … others. (2011). *New ASTM Standard Test MEthod D7708-11 for Determination of the Reflectance of Vitrinite Dispersed in Sedimentary Rocks.*

Harry Dembicki, J. (2017). *Practical Petroleum Geochemistry for Exploration and Production*. Retrieved from www.elsevier.com

Head, I. M., Jones, D. M., & Larter, S. R. (2003). Biological activity in the deep subsurface and the origin of heavy oil. *Nature*, *426*(6964), 344–352. https://doi.org/10.1038/nature02134

Hein, F. J. (2006). Heavy oil and oil (tar) sands in North America: An overview & summary of contributions. *Natural Resources Research*, *15*(2), 67–84. https://doi.org/10.1007/s11053-006-9016-3

Hoefs, J. (1973). *Applied stable isotope geochemistry. Minerals, rocks and inorganic materials, Vol. 9*. Berlin-Heidelberg-New York: Springer.

Horvath, Z., & Jackson, K. S. (1981). *Procedure for the Isolation of Kerogen from Sedimentary Rocks (BMR Record 1981/62)*.

Hunt, J. M. (1979). *Petroleum geochemistry and geology*. W. H. Freeman and Co.: San Francisco, Calif., United States.

Hunt, J. M. (1996). Petroleum geology and geochemistry. In *Freeman, New York* (second edi). W.H Freeman and Company.

International, C. for C., & Petrology. (1998). The new vitrinite classification (ICCP System 1994). *Fuel*, *77*(5), 349–358.

Jacob, H. (1989). Classification, structure, genesis and practical importance of natural solid oil bitumen ("migrabitumen"). *International Journal of Coal Geology*, *11*(1), 65–79.

Jarvie, D. M., Morelos, A., & Han, Z. (2001). Detection of Pay Zones and Pay Quality, Gulf of Mexico: Application of Geochemical Techniques. *Gulf Coast*

*Association of Geological Societies Transactions*, *LI*, 151–160.
https://doi.org/10.1306/8626CED3-173B-11D7-8645000102C1865D

Jones, H.A., Hockey, R. D. (1964). The geology of part of southwestern Nigeria.
*Geological Survey of Nigeria, Bulletin 31,101*.

Jones, D. M., Head, I. M., Gray, N. D., Adams, J. J., Rowan, A. K., Aitken, C. M., …
others. (2008). Crude-oil biodegradation via methanogenesis in subsurface
petroleum reservoirs. *Nature*, *451*(7175), 176–180.

Jones H.A. and Hockey R.D. (1964). *The Geology of part of Southwestern Nigeria.
Bull. Geol. Surv. Nig. 31*, 101.

Jozanikohan, G., Sahabi, F., Norouzi, G. H., & Memarian, H. (2015). Thermal
Analysis: A Complementary Method to Study the Shurijeh Clay Minerals. *Ijmge*,
*49*(1), 33–45.

Kaki, C., d'Almeida, G. A. F., Yalo, N., & Amelina, S. (2013). Géologie et système
pétrolier du bassin offshore du Benin (Benin). *Oil and Gas Science and
Technology*, *68*(2), 363–381. https://doi.org/10.2516/ogst/2012038

Katz, B. J., & Elrod, L. W. (1983). Organic geochemistry of DSDP Site 467, offshore
California, Middle Miocene to Lower Pliocene strata. *Geochimica et
Cosmochimica Acta*, *47*(3), 389–396. https://doi.org/10.1016/0016-
7037(83)90261-2

Kayukawa, T., Aoyama, H., Fujimoto, T., & others. (2017). Optimum Transportation
Method for Development of Extra Heavy Crude Oil. *22nd World Petroleum
Congress*.

Kingston, D.R., Dishroon, C.P. and Williams P.A. (1983). Global basin classification

system. *AAPG Bulletin (American Association of Petroleum Geologists)*, *67*(12), 2175–2193.

Kjemperud, A., Agbesinyale, W., Agdestein, T., Gustafsson, C., Yukler A. (1992). Tectono-stratigraphic history of the Keta Basin, Ghana with emphasis on late erosional episodes. *Bulletin Des Centres de Recherches Exploration-Production Elf-Aquitaine. Mémoire*, (13), 55–69.

Klemme, H.D. (1975). Geothermal gradient, heat flow and hydrocarbon recovery. In *Petroleum and global tectonics* (Fischer, A). Princeton University Press.

Klett, T. R., Ahlbrandt, T. S., Schmoker, J. W., & Dolton, G. L. (1997). *Ranking of the world's oil and gas provinces by known petroleum volumes*. USGS Open File Report

Koyama T. and Tomino T. (1967). Decomposition process of organic carbon and nitrogen in lake water. *Geochem. J.*, *1*(3), 109–124.

Krevelen, D. W. van. (1961). Coal. *Elsevier, Amsterdam*, *5*, 14.

Krumbein, W. C., & Garrels, R. M. (1952). Origin and classification of chemical sediments in terms of pH and oxidation-reduction potentials. *The Journal of Geology*, *60*(1), 1–33.

Kuuskraa, V. A., Hammershaimb, E. C., & Paque, M. (1987). Major Tar Sand and Heavy-Oil Deposits of the United States: Section I. Regional Resources. *AAPG Special Volumes*. Retrieved from http://search.datapages.com/data/specpubs/methodo2/data/a081/a081/0001/0100/0123.htm

Landis, C. R., & Castaño, J. R. (1995). Maturation and bulk chemical properties of a

suite of solid hydrocarbons. *Organic Geochemistry*, *22*(1), 137–149.

Larter, S., Huang, H., Adams, J., Bennett, B., Jokanola, O., Oldenburg, T., …
Fowler, M. (2006a). The controls on the composition of biodegraded oils in the
deep subsurface: Part II—Geological controls on subsurface biodegradation
fluxes and constraints on reservoir-fluid property prediction: Part I of this study
was published in Organic Chemistry in . *AAPG Bulletin*, *90*(6), 921–938.

Larter, S., Huang, H., Adams, J., Bennett, B., Jokanola, O., Oldenburg, T., …
Fowler, M. (2006b). The controls on the composition of biodegraded oils in the
deep subsurface: Part II - Geological controls on subsurface biodegradation
fluxes and constraints on reservoir-fluid property prediction. *AAPG Bulletin*,
*90*(6), 921–938. https://doi.org/10.1306/01270605130

Levinson, A.A. (1974). *Introduction to Geochemical Exploration* (Second). Wilmette,
Illinois: Applied Publishing Ltd.

Lewan, M. D. (1980). *Geochemistry of vanadium and nickel in organic matter of
sedimentary rocks*. University of Cincinnati.

Lewan, M .D. (1984). Factors controlling the proportionality of vanadium to nickel in
crude oils. *Geochimica et Cosmochimica Acta*, *48*(11), 2231–2238.

Lewan, M. D., & Maynard, J. B. (1982). Factors controlling enrichment of vanadium
and nickel in the bitumen of organic sedimentary rocks. *Geochimica et
Cosmochimica Acta*, *46*(12), 2547–2560. https://doi.org/10.1016/0016-
7037(82)90377-5

López, L., Mónaco, S.L. (2017). Vanadium, nickel and sulfur in crude oils and source
rocks and their relationship with biomarkers: Implications for the origin of crude

oils in Venezuelan basins. *Organic Geochemistry*, *104*, 53–68. https://doi.org/10.1016/j.orggeochem.2016.11.007

MacGregor, D. S., Robinson, J., & Spear, G. (2003). Play fairways of the Gulf of Guinea transform margin. *Geological Society, London, Special Publications*, *207*(1), 131–150.

Maende, A. (2016). *Application Note ( 181017-1 ) Assessment of Oil Mobility , Evaluation of Evaporative Loss and Correlation of Reservoir Compartments using HAWK Petroleum Assessment Method ( HAWK-PAM )*. Humble.

Maende, Albert, Pepper, A. S., Jarvie, D. M., & Weldon, W. D. (2017). Advanced pyrolysis data and interpretation methods to identify unconventional reservoir sweet spots in fluid phase saturation and fluid properties (API gravity) from drill cuttings and cores. *Search and Discovery*, *80596*(80596), 1–23. https://doi.org/10.15530/urtec-2016-2433439.Maende

Mallakh, R. El. (1983). *Heavy Versus Light Oil: Technical Issues and Economic Considerations*. Boulder, CO: International Research Center for Energy and Economic Development.

McCarthy, K., Rojas, K., Niemann, M., Palrnowski, D., Peters, K., Stankiewicz, A. (2011). Basic petroleum geochemistry for source rock evaluation. *Oilfield Review*, *23*(2), 32–43.

Meyer, R.F., Attanasi, E.D., Freeman, P.A. (2007). Natural Bitumen Resources in Geological Basins of the World. *US Geological Survey*, *1084*, 1–36. Retrieved from http://pubs.usgs.gov/of/2007/

Mille, G., Almallah, M., Bianchi, M., van Wambeke, F., & Bertrand, J. C. (1991).

Effect of salinity on petroleum biodegradation. *Fresenius' Journal of Analytical Chemistry*, *339*(10), 788–791. https://doi.org/10.1007/BF00321746

Milner, C. W. D., Rogers, M. A., & Evans, C. R. (1977). Petroleum transformations in reservoirs. *Journal of Geochemical Exploration*, *7*, 101–153.

Ministry of Mines and Steel Development (MMSD). (2009). *Tarsands & Bitumen Investment Opportunities In Nigeria*.

Mohammed, S., Opuwari, M., & Titinchi, S. (2020). Source rock evaluation of Afowo clay type from the Eastern Dahomey Basin , Nigeria : insights from different measurements. *Scientific Reports*, 1–13. https://doi.org/10.1038/s41598-020-68918-y

Moldowan, J.M., Lee, C.Y., Sundararaman, P. (1992). Source correlation and maturity assessment of select oils and rocks from the Central Adriatic Basin (Italy and Yugoslavia). In Moldowan, J.M., Albrecht, P., and Philp, R.P. (Ed.), *Biological Markers in Sediments and Petroleum* (pp. 370–401). Eaglewood Cliffs, NJ: Prentice Hall.

Moldowan, J. M., Albrecht, P., & Philp, R. P. (1992). *Biological markers in sediments and petroleum*. Englewood Cliffs, NJ (United States); Prentice Hall.

Moldowan, J. M., Sundararaman, P., & Schoell, M. (1986). Sensitivity of biomarker properties to depositional environment and/or source input in the Lower Toarcian of SW-Germany. *Organic Geochemistry*, *10*(4–6), 915–926.

National Energy Board, C. (2004). *Canada's Oil Sands: Opportunities and Challenges to 2015, An Energy Market Assessment*.

Ndukwe, V. A., Ogunyinka, B. O., & Abrakasa, S. (2015). Some Aspects of the

Petroleum Geochemistry of Tarsand Deposits in Western Nigeria. *Pyrex Journal of Geology and Mining Research*, *1*(1), 1–6.

Nton, M. E., Eze, F.P., Elueze, A. A. (2005). Aspects of Source Rock Evaluation and Diagenetic History of the Akinbo Shale, Eastern Dahomey Basin, Southwestern Nigeria. *Nigerian Association of Petroleum Explorationists*, *19*, 35–49.

Nton, M.E. (2001). *Sedimentological and geochemical studies of rock units in the eastern Dahomey basin, south western Nigeria,*. University of Ibadan.

Nton, M. E., Ikhane, P. R., & Tijani, M. N. (2009). Aspect of rock-eval studies of the maastrichtian-eocene sediments from subsurface, in the eastern Dahomey basin southwestern Nigeria. *European Journal of Scientific Research*, *25*(3), 417–427.

Nwajide, C.S. (2013). *Geology of Nigeria's Sedimentary Basins*. Lagos: CSS Bookshops Limited.

Obaje, N.G. (2009). *Geology and Mineral Resources of Nigeria*. Berlin Heidelberg: Springer-Verlag.

Odunaike, R. K., Laoye, J. A., Fasunwon, O. O., Ijeoma, G. C., & Akinyemi, L. P. (2010). *Geophysical mapping of the occurrence of shallow oil sands in Idiopopo at Okitipupa area , South-western Nigeria*. African Journal of Environmental Science and Technology, *4*(1), 34–44

Ogala, J.E., Akaegbobi, I. M. (2014). Using aromatic biological markers as a tool for assessing thermal maturity of source rocks in the Campano-Maastrichtian Mamu Formation, southeastern Nigeria. *Earth Sciences Research Journal*, *18(1)*, 51–62.

Ogala, J. E., Kalaitzidis, S., Christanis, K., Omo-Irabor, O. O., Akinmosin, A., Yusuf, C. U., … Papaefthymiou, H. (2019). Geochemical and organic petrological study of bituminous sediments from Dahomey Basin, SW Nigeria. *Marine and Petroleum Geology*, *99*(October 2018), 577–595. https://doi.org/10.1016/j.marpetgeo.2018.10.033

Ogbe, F. G. A. (1972a). Stratigraphy of strata exposed in the Ewekoro quarry, Western Nigeria. In *African Geology* (Dessauvagi, pp. 305–322). University Press, Nigeria.

Ogbe, F. G. A. (1972b). Stratigraphy of Strata Exposed in the Ewekoro Quarry, Western Nigeria. In *African Geology* (pp. 305–322). University Press, Nigeria.

Okosun, E. A. (1998). Review of the Early Tertiary Stratigraphy of southwestern Nigeria. *Nigeria Journal of Mining and Geology*, *34*(1), 27–35.

Olabode, S. O. (2015). Subsidence patterns in the Nigerian sector of Benin (Dahomey) Basin: Evidence from three offshore wells. *Ife Journal of Science*, *17*(2), 455-475–475.

Oli, I.C., Okeke, O.C., Abiahu C.M.G., Anifowose, F, A., Fagorite, V. I. (2019). A Review of the Geology and Mineral Resources of Dahomey Basin, Southwestern Nigeria. *International Journal of Environmental Sciences & Natural Resources*, *21*(1), 1–5. https://doi.org/10.19080/ijesnr.2019.21.556055

Omatsola, M. E., and Adegoke, O.S. (1981). Tectonic Evolution and Cretaceous Stratigraphy of the Dahomey Basin. *Nigeria Journal of Mining and Geology*, *18*, 130–137.

Onwe-Moses, F. D., Eze, S. O., Okoro, A. U., & Aghamelu, O. P. (2019). Organic geochemical evaluation and hydrocarbon prospects of the Coniacian Awgu Formation, southern Benue Trough, Nigeria. *Arabian Journal of Geosciences*, *12*(3). https://doi.org/10.1007/s12517-019-4238-y

Orr, W. L. (1986). Kerogen/asphaltene/sulfur relationships in sulfur-rich Monterey oils. *Organic Geochemistry*, (10), 499–516.

Palmer, S. E. (1983). Porphyrin distributions in degraded and nondegraded oils from Colombia. *Abstracts of Papers of the American Chemical Society*, *186*(AUG), 23--GEOC.

Persits, F., Ahlbrandt, T., Tuttle, M., Charpentier, R., Brownfield, M., & Takahashi, K. (2002). Map showing geology, oil and gas fields, and geological provinces of Africa, Ver. 2.0. In *US Geol Surv Open-File Rep*.

Peters, K.E., Walters, C.C., Moldowan, J. M. (2005a). *The Biomarker Guide Volume 1, Biomarkers and Isotopes in the Environment and Human History* (Second Edition). Cambridge University Press.

Peters, K.E., Walters, C.C., Moldowan, J. M. (2005b). *The Biomarker Guide Volume 2 , Biomarkers and Isotopes in Petroleum Exploration and Earth History* (Second Edition). New York: Cambridge University Press.

Peters, K.E. and Moldowan, J. M. (1993). *The Biomarker Guide: Interpreting molecular fossils in petroleum and ancient and recent sediments*. Englewood Cliffs, NJ, United States: Prentice Hall.

Peters, K. E. (1986). Guidelines for evaluting petroleum source rock using programmed pyrolysis. *American Association of Petroleum Geologists Bulletin*, *70*(3), 318–329. https://doi.org/10.1306/94885688-1704-11d7-8645000102c1865d

Peters K.E., Walters, C. and Moldowan, J. M. (2005). *The Biomarker Guide Volume 2; Biomarkers and Isotopes in Petroleum Exploration and Earth History* (2nd ed.). New York: Cambridge University Press.

Peters, K.E., & Cassa, M. R. (1994). *Applied source rock geochemistry: Chapter 5: Part II. Essential elements*. AAPG Special Volumes.

Pettijohn, F. J. (1975). *Sedimentary Rocks* (Third). New York: Harper & Row, Publishers, Inc.

Pickel, W., Kus, J., Flores, D., Kalaitzidis, S., Christanis, K., Cardott, B. J., … Wagner, N. (2017). Classification of liptinite – ICCP System 1994. *International Journal of Coal Geology*, *169*, 40–61. https://doi.org/10.1016/j.coal.2016.11.004

Powell, T. G., & McKirdy, D. M. (1973). Relationship between ratio of pristane to phytane, crude oil composition and geological environment in Australia. *Nature Physical Science*, *243*(124), 37–39.

Rahimi, P. (2019). Properties of Canadian Bitumen and Bitumen-Derived Crudes, and Their Impacts on Refinery Processing. In *Chemistry Solutions to Challenges in the Petroleum Industry* (pp. 223–240). ACS Publications.

Revill, A. T., Volkman, J. K., O'Leary, T., Summons, R. E., Boreham, C. J., Banks, M. R., & Denwer, K. (1994). Hydrocarbon biomarkers, thermal maturity, and depositional setting of tasmanite oil shales from Tasmania, Australia.

Geochimica et Cosmochimica Acta, 58(18), 3803–3822.
https://doi.org/10.1016/0016-7037(94)90365-4

Ronov, A. B. (1958). Organic carbon in sedimentary rocks (in relation to the presence of petroleum). *Geochemistry*, *5*, 497–509.

Rowland, S. J. (1990). Production of acyclic isoprenoid hydrocarbons by laboratory maturation of methanogenic bacteria. *Organic Geochemistry*, *15*(1), 9–16. https://doi.org/10.1016/0146-6380(90)90181-X

Santos, A. C. (1991). Geology of the experimental production project BEP 0--16 Cerro Negro area, Orinoco Belt. *5th UNITAR International Conference on Heavy Crude and Tar Sands—Hydrocarbons for the 21st Century, Proceedings*, *1*, 321–356. Caracas, Venezuela.

Scalan, E. S., & Smith, J. E. (1970). An improved measure of the odd-even predominance in the normal alkanes of sediment extracts and petroleum. *Geochimica et Cosmochimica Acta*, *34*(5), 611–620.

Schoell, M. (1984). Stable isotopes in petroleum research: Advances in Petroleum Geochemistry. In *Organic Geochemistry* (J. Brooks, Vol. 1). London: Academy Press.

Seifert, W. K., & Moldowan, J. M. (1979). The effect of biodegradation on steranes and terpanes in crude oils. *Geochimica et Cosmochimica Acta*, *43*(1), 111–126.

Seifert, W. K., Moldowan, J. M., & Demaison, G. J. (1984). Source correlation of biodegraded oils. *Organic Geochemistry*, *6,* 633–643.

Silverman, S. R., & Epstein, S. (1958). Carbon isotopic compositions of petroleums and other sedimentary organic materials. *AAPG Bulletin*, *42*(5), 998–1012.

Skinner, D. A. (1952). Chemical state of vanadium in Santa Maria Valley crude oil. *Industrial & Engineering Chemistry*, *44*(5), 1159–1165.

Sofer, Z. (1984). Stable carbon isotope compositions of crude oils: application to source depositional environments and petroleum alteration. *AAPG Bulletin*, *68*(1), 31–49.

Sonibare, O., Alimi, H., Jarvie, D., & Ehinola, O. A. (2008). Origin and occurrence of crude oil in the Niger delta, Nigeria. *Journal of Petroleum Science and Engineering*, *61*(2–4), 99–107. https://doi.org/10.1016/j.petrol.2008.05.002

Stach, E., Mackowsky, M.-T., Teichmüller, M., Taylor, G. H., Chandra, D., & Teichmüller, R. (1982). *Textbook of Coal Petrology*. Berlin-Stuttgart: Gebrüder Borntraeger.

Stach, Erich, Mackowsky, M. T., Teichmuller, M., Taylor, G. H., Chandra, D., & Teichmuller, R. (1982). Stach's textbook of coal petrology, 535 p. In *Gebruder, Borntraeger, Berlin*.

Stahl, W. J. (1977). Carbon and nitrogen isotopes in hydrocarbon research and exploration. *Chemical Geology*, *20*(2), 121–149.

Staplin, F. L. (1969). Sedimentary organic matter, organic metamorphism, and oil and gas occurrence. *Bulletin of Canadian Petroleum Geology*, *17*(1), 47–66.

Storey, B. C. (1995). The role of mantle plumes in continental breakup: Case Histories from Gondwanaland. *Nature*, *377*(6547), 301–308.

Taylor, G.H., Teichmuller, M., Davis, A.,  et al. (1998). *Organic Petrology*. Berlin: Gebruder Borntraeger.

Taylor, G. H., Liu, S. Y., & Teichmüller, M. (1991). Bituminite—a TEM view.

*International Journal of Coal Geology*, *18*(1–2), 71–85.

Teichmüller, M. (1974). Generation of petroleum-like substances in coal seams as seen under the microscope. In F. Tissot, B., and Bienner (Ed.), *Advances in Organic Geochemistry* (Editions T, pp. 379–405). Paris.

Teichmüller, M. (1982). Application of coal petrological methods in geology including oil and natural gas prospecting. In E. Stach, M.-T. Mackowsky, M. Teichmüller, G. H. Taylor, D. Chandra, & R. Teichmüller (Eds.), *Stach's textbook of coal petrology* (pp. 381–413). Berlin: Gebrüder Borntraeger.

Teichmüller, M. (1989). The genesis of coal from the viewpoint of coal petrology. *International Journal of Coal Geology*, (12), 1–87.

Teichmüller, Marlies. (1987). Recent advances in coalification studies and their application to geology. *Geological Society, London, Special Publications*, *32*(1), 127–169.

Ten Haven, H. L., De Leeuw, J. W., Rullkötter, J., & Damsté, J. S. S. (1987). Restricted utility of the pristane/phytane ratio as a palaeoenvironmental indicator. *Nature*, *330*(6149), 641–643. https://doi.org/10.1038/330641a0

Tissot, B.P., Welte, D.H. (1984). *Petroleum Formation and Occurrence*. New York: Springer-Verlag Heidelberg.

Tissot, B., Durand, B., Espitalie, J., & Combaz, A. (1974). Influence of nature and diagenesis of organic matter in formation of petroleum. *Aapg Bulletin*, *58*(3), 499–506.

Treibs, A. (1934). Chlorophyll-und Häminderivate in bituminösen Gesteinen, Erdölen, Erdwachsen und Asphalten. Ein Beitrag zur Entstehung des Erdöls. *Justus*

*Liebigs Annalen Der Chemie, 510*(1), 42–62.

Udo, O.T., Ekweozor, C. M. (1990). Significance of oleanane occurrence in shales of Opuama channel complex, Niger Delta. *Energy and Fuels*, *4 (3)*, 248–254.

Udo, O.T., Ekwere, S., Abrakasa, S. (1992). Some trace metals in selected Niger Delta crude oils: application in oil-oil correlation studies. *Mining Geol*, *28*, 289–291.

Uzoegbu, U. M., Agbadamashi, M. O., & Ugbome, C. (2016). Hydrocarbon Geochemical Characteristics and Depositional Environment of Tertiary Tar Sand from Ondo, SW Nigeria. *IOSR Journal of Applied Geology and Geophysics*, *4*(5), 37–45. https://doi.org/10.9790/0990-0405013745

Wardroper, A., Hoffmann, C., Maxwell, J., Barwise. A., Goodwin, N., Park, P. (1984). Crude oil biodegradation under simulated and natural conditions -II. Aromatic steroid hydrocarbons. *Organic Geochemistry, 6*, 605–617.

Whiteman, A. J. (1982). *Nigeria: Its Petroleum Geology, Resources and Potential*. London: Graham and Trotman.

Zhao, B., & Shaw, J. M. (2007). Composition and size distribution of coherent nanostructures in Athabasca bitumen and Maya crude oil. *Energy & Fuels*, *21*(5), 2795–2804.

Zobell C. E. (1946). *Marine Microbiology*. Waltham: Chronica Botanica Company.